Topological structure of quantum graph and its applications

井上，奉紀

(Degree)
博士（理学）
(Date of Degree)
2023-03-25
(Date of Publication)
2024-03-01
(Resource Type)
doctoral thesis
(Report Number)
甲第8581号
(URL)
https://hdl.handle.net/20.500.14094/0100482329

Doctoral Dissertation

Topological structure of quantum graph and its applications

(量子グラフのトポロジカルな構造とその応用)

January 2023

Graduate School of Science, Kobe University

Tomonori Inoue
(井上 奉紀)

Abstract

A quantum graph is a one-dimensional circuit-like quantum system composed of edges and vertices. Despite its simple composition, it has emerged as a research subject in various fields due to its diverse shapes. In this dissertation, we study Dirac fermions on a five-dimensional spacetime with a quantum graph called a rose graph as a one-dimensional extra dimension. The rose graph is a graph with some loops of edge on a single vertex that can be transformed into a wide variety of shapes by changing the boundary conditions at the vertex. In an extra-dimensional model, higher-dimensional fields are expanded by the mass eigenfunctions of the four-dimensional part of the field, which is called the Kaluza–Klein expansion. The expansion of the five-dimensional Dirac fermions is given by the product of the four-dimensional chiral fermions and the mode function in the extra dimension direction. The degeneracy and eigenvalues of the Kaluza–Klein modes are determined by the boundary conditions on the graph. For the above setup, we study three major things by focusing on the topological structure of the boundary conditions.

The first thing is the possibility of solving the remaining problems of the Standard Model. In particular, it has the potential to explain three problems: the generation number problem, the fermion mass hierarchy problem, and the origin of flavor mixing and *CP* phases.

The second thing is that by focusing on the Kaluza–Klein zero mode, instanton configurations can be constructed as Berry's connections in the parameter space of boundary conditions. Likewise, the Atiyah–Drinfeld–Hitchin–Manin construction method can be applied to these constructions.

The third thing is that there is a non-trivial correspondence between matrices specifying boundary conditions at the vertex of the quantum graphs and zero-dimensional Hamiltonians in gapped free-fermion systems. Based on the correspondence, we provide a complete topological classification of the boundary conditions in terms of non-interacting fermionic topological phases. Furthermore, the topological numbers of each class correspond to the number of four-dimensional chiral zero modes.

Acknowledgments

This dissertation and the research presented here benefited substantially from Prof. Makoto Sakamoto, whose supervision I gratefully acknowledge. His guidance and openness toward discussing have been crucial to the progress of my research. I am grateful to my collaborators Yukihiro Fujimoto, Masatoshi Sato, Kazunori Takenaga, and Inori Ueba for tackling problems together in various stages of my studies and for their patience in answering my questions. During my PhD, I was supported by the Particle Theory Group and Cosmology group. My time at the Kobe university was made precious and fruitful by numerous wonderful people. In addition to the ones already named, Hidenori Sonoda, Toshifumi Noumi, Jiro Soda, Pedro Hugo Tanaka, Toshiaki Takeuchi, Kaishu Saito, Hibiki Satake, Maki Takeuchi, and Kimihiro Nomura. Finally, I would like to show my greatest appreciation to my family for their support during the graduate course.

Publication list

[1] Y. Fujimoto, T. Inoue, M. Sakamoto, K. Takenaga and I. Ueba, "5d Dirac fermion on quantum graph," J. Phys. A **52** no. 45, (2019) 455401, arXiv:1904.12458 [hep-th].

[2] T. Inoue, M. Sakamoto and I. Ueba, "Instantons and Berry's connections on quantum graph," J. Phys. A **54** no. 35, (2021) 355301, arXiv:2104.02311 [hep-th].

[3] T. Inoue, M. Sakamoto, M. Sato and I. Ueba, "Correspondence of topological classification between quantum graph extra dimension and topological matter," Phys. Rev. D **106** no. 8, (2022) 085006 , arXiv:2204.03834 [hep-th].

Contents

1 Introduction **1**
- 1.1 Why quantum graph . . . 1
- 1.2 Why topological structure . . . 2
- 1.3 The three themes addressed in this dissertation . . . 3
  - 1.3.1 Application to beyond the Standard Model . . . 3
  - 1.3.2 Instantons as Berry's connections . . . 5
  - 1.3.3 Topological classification of boundary conditions . . . 6
- 1.4 Outline . . . 7

2 Quantum graphs and boundary conditions **8**
- 2.1 Quantum graphs . . . 8
- 2.2 Simple example . . . 8
- 2.3 Summary . . . 11

3 5d fermion on quantum graph **12**
- 3.1 Setup and Kaluza–Klein expansion . . . 13
- 3.2 Boundary conditions and zero-modes . . . 15
  - 3.2.1 Boundary conditions . . . 15
  - 3.2.2 Zero-mode degeneracy . . . 17
- 3.3 Perspectives on SUSY quantum mechanics . . . 20
- 3.4 Application to beyond the Standard Model . . . 22
  - 3.4.1 Generation number problem . . . 22
  - 3.4.2 Fermion mass hierarchy and flavor mixing . . . 23
  - 3.4.3 *CP* phase . . . 24
- 3.5 Summary and discussion . . . 25

4 Instantons and Berry's connections on quantum graph **26**
- 4.1 Brief review of instanton . . . 26
- 4.2 ADHM construction . . . 27
  - 4.2.1 Notations . . . 27
  - 4.2.2 Procedures for the ADHM construction . . . 28
  - 4.2.3 Some concrete examples . . . 29
- 4.3 Application to quantum graph extra dimensional model . . . 34
  - 4.3.1 Setup . . . 34
  - 4.3.2 Berry's connection in our model . . . 36

4.3.3 How to apply . . . 38
4.4 Results . . . 40
4.4.1 The case of $(N, k, l) = (4, 2, 2)$ . . . 40
4.4.2 The case of $(N, k, l) = (5, 2, 2)$ . . . 42
4.4.3 The case of $(N, k, l) = (6, 4, 4)$ . . . 43
4.5 Summary and discussion . . . 44

5 Correspondence between quantum graph extra dimension and AZ classes 46
5.1 Setup . . . 46
5.2 Topological classification of gapped free-fermion system . . . 47
5.3 Correspondence to zero-dimensional Hamiltonian . . . 49
5.4 Transformations in the y-direction . . . 49
5.4.1 Permutation S_y . . . 50
5.4.2 Half-reflection R_y . . . 51
5.4.3 Composite transformation $Q_y = -iR_yS_y$ . . . 51
5.4.4 Parity in the y-direction P_y . . . 52
5.5 Correspondence to time-reversal symmetry . . . 53
5.5.1 Time-reversal $\mathcal{T}_+$ . . . 53
5.5.2 Time-reversal $\mathcal{T}_-$ . . . 55
5.6 Correspondence to particle-hole symmetry . . . 56
5.6.1 Charge conjugation C_- . . . 56
5.6.2 Charge conjugation C_+ . . . 58
5.7 Correspondence to chiral symmetry . . . 59
5.7.1 Chiral symmetry Γ_+ . . . 59
5.7.2 Chiral symmetry Γ_- . . . 60
5.8 Summary of correspondence to AZ symmetry class . . . 61
5.9 Index and zero modes in each symmetry class . . . 62
5.9.1 Witten index and classifying space . . . 63
5.9.2 $\mathbb{Z}_2$ index . . . 78
5.10 Summary and discussion . . . 82

6 Summary and discussion 85

A Details of Calculation 87
A.1 't Hooft instanton . . . 87

B Structure of the ADHM construction 89
B.1 Instanton side settings . . . 89
B.2 ADHM data side settings . . . 95
B.3 ADHM data $\rightarrow$ Instanton . . . 101
B.3.1 Gauge group . . . 103
B.3.2 Pure gauge condition . . . 105
B.3.3 Anti-self duality of $F_{\mu\nu}$ . . . 105
B.3.4 Instanton number . . . 105
B.3.5 Invertibility of D^2 . . . 106

B.4 Instanton $\to$ ADHM data . . . 107
B.4.1 Constructing the ADHM data from instanton . . . 107
B.4.2 Satisfying the ADHM equation . . . 108
B.4.3 Invertibility of $\Delta^\dagger\Delta$ . . . 112
B.5 Completeness: ADHM data $\to$ Instanton $\to$ ADHM data . . . 113
B.5.1 Constructing ψ from V . . . 114
B.5.2 Satisfying the normalization condition . . . 115
B.5.3 Equivalence to the original ADHM data . . . 116
B.6 Uniqueness: Instaton $\to$ ADHM data $\to$ Instanton . . . 118
B.6.1 Constructing V from ψ . . . 119
B.6.2 Satisfying the 0d Dirac equation . . . 121
B.6.3 Satisfying the normalization condition . . . 122
B.6.4 Equivalence to the original ADHM data . . . 123

C Topological insulator and superconductor **124**
C.1 Classification of Hamiltonians based on symmetry . . . 125
C.1.1 Time-reversal symmetry . . . 125
C.1.2 Particle-hole symmetry . . . 125
C.1.3 Chiral symmetry . . . 127
C.1.4 Symmetry classes of Hamiltonians . . . 127
C.1.5 Classification table for topological insulators and superconductors . . . 128
C.2 Some examples of topological insulators . . . 129
C.2.1 The 1d class AIII polyacetylene . . . 129
C.2.2 2d topological insulators . . . 131
C.3 Some examples of topological superconductor . . . 132
C.3.1 The 1d class D p-wave superconductor . . . 132
C.3.2 The 2d class D chiral p-wave superconductor . . . 133
C.3.3 The 3d class DIII ^{3}He-B . . . 134

Bibliography **135**

Chapter 1

Introduction

1.1 Why quantum graph

A quantum graph is a one-dimensional (1d) graph that consists of edges and vertices connected to each other with differential operators on each edge. For example, the graph shown in the Fig. 1.1 consists of six edges and five vertices. Unlike the simple 1d systems treated in quantum mechanics textbooks, quantum graphs can take many different forms. Because of this property, it has been studied in various research areas, e.g.,

- **Scattering theory on 1d graphs** [1–4]: It is a study that is based on mathematical interest and its application as a pass filter to amplify or attenuate wave functions has been proposed.
- **Quantum chaos** [5, 6]: Quantum graphs are being studied as a toy model for quantum chaos.
- **Supersymmetric quantum mechanics** [7–9]: It was proposed that supersymmetry can be extended by introducing symmetries such as swapping the edges that compose the graph.
- **Berry's phases** [10–12]: Wave functions on the graph can keep the degrees of freedom of edge connection at the vertices. Therefore, it is shown that nontrivial Berry's phases can be computed for the wave functions.
- **Extra-dimensional models** [13–19]: Unlike simple one-dimensional quantum mechanical systems, quantum graphs can realize multiple degeneracies to zero modes. Some studies have applied this property to extra-dimensional models.

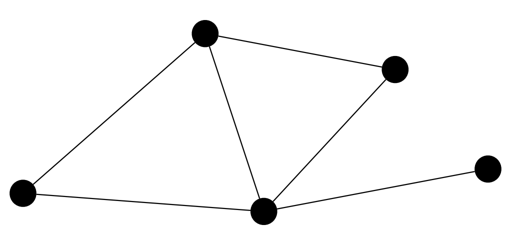

Figure 1.1: Quantum graph consisting of six edges and five vertices.

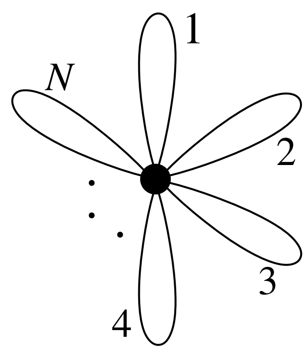

Figure 1.2: Rose graph consisting of N edges (or called loops) and single vertex.

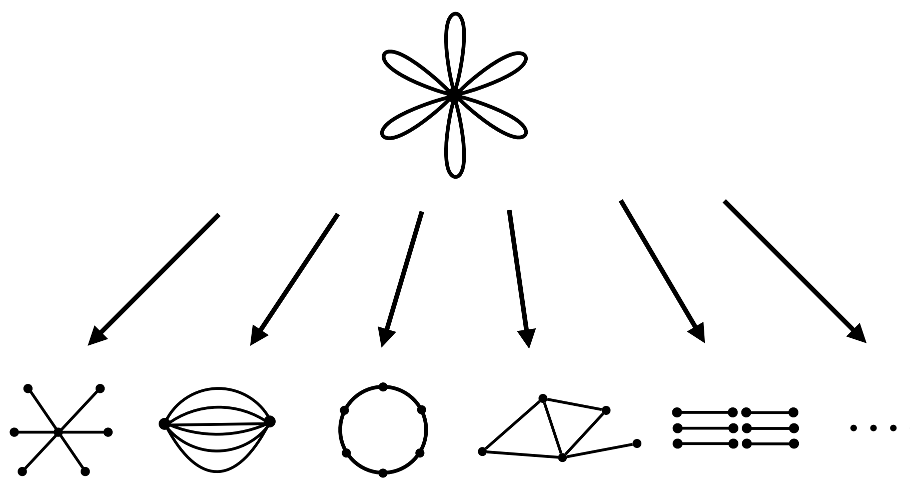

Figure 1.3: Decompositions of the rose graph with six edges. A variety of graphs can be obtained by changing the boundary conditions at the vertex of the rose graph.

As can be seen from the above studies, the quantum graph is the research subject in physics on a wide range of energy scales. Thus, we believe that pushing forward the study of quantum graphs will have an impact on physics at various energy scales and reveal new connections between them.

1.2 Why topological structure

In this dissertation, we focus on applying quantum graphs to the extra space of 5d fermions, that is, 5d fermions with the extra space given by the quantum graph. Specifically, we consider a master graph called a rose graph as shown in Fig. 1.2. This graph consists of N edges and a single vertex. All edges are connected at both ends and are also called loops. However, for example, if we consider $N = 6$, the graph can be transformed into various shapes by changing the boundary condition at the vertex (see Fig. 1.3). Therefore, by using the rose graph in Fig. 1.2 as the extra dimension, it is possible to analyze 1d extra-dimensional models of arbitrary shape.

Boundary conditions at the vertex of the rose graph can be written down as edge connection conditions containing parameters. Since the rose graph contains graphs of arbitrary shape, their parameter degrees of freedom are complicated. Consequently, it is difficult to examine each and every one of those degrees of freedom. To avoid these difficulties, we consider the space formed by all of these parameters and focus on its topological structure. The topological structure is preserved under continuous deformation of the boundary conditions, thus systematic and comprehensive analysis of the boundary condition is possible.

1.3 The three themes addressed in this dissertation

We analyze such the parameter space of boundary conditions and clarify the following three contents.

1. It is possible to solve the problem of the number of generations in the Standard Model (SM). At the same time, it may explain the fermion mass hierarchy, and the origin of flavor mixing of fermions and the *CP* phase. Notably, the number of generations is given as a topological quantity of boundary conditions in our model.

2. Various boundary conditions at the vertex of the rose graph can be written down using parameters. As a consequence of the topological structure of the parameter space, instanton configurations can be constructed as Berry's connections by applying the Atiyah–Drinfeld–Hitchin–Manin (ADHM) construction method.

3. The boundary conditions are classified into ten symmetry classes by considering time reversal, charge conjugation, and extra spatial symmetries in 5d Dirac fermions. Surprisingly, the classification of the boundary conditions has a complete correspondence to the topological classification of $(1 + 0)$-d gapped free-fermion systems.

These results cover not only the discussion in the high-energy region beyond the scale of the Standard Model but also the discussion in the low-energy region of topological classification of physical systems. Therefore, the analysis of quantum graphs can have a significant impact on physics at various energy scales and reveal mutual relationships.

In the following Subsections, we provide a more detailed introduction to the above three themes.

1.3.1 Application to beyond the Standard Model

Adopting the rose graph as an extra dimension, we construct a theory that goes beyond the SM. We explain the problems with the SM that we are trying to solve in this study. Furthermore, we show the mechanism of the resolution of those problems.

1.3.1.1 Problems in the Standard Model

The SM successfully describes the behavior of elementary particles. However, some things remain unexplained, and various new theories have been proposed to solve these problems. We attempt to solve the following three problems.

- **Generation number problem:**
  In the SM, fermions have a structure called a generation, where the particles between generations have the same charge and spin, except for their masses. From the Kobayashi–Maskawa

theory [20], those generations must be more than three generations. However, the current observations seem to confirm that generation is three, not four or five. The fact that there is no theoretical origin of the three-generation structure is called the generation number problem.

- **Fermion mass hierarchy problem:**
The masses of the particles between generations take exponentially different values. Taking the up-type quark sectors as an example, $m_u : m_c : m_t = 0.00001 : 0.07 : 1$. This means that the strength of the coupling between fermions and Higgs, which is known as the Yukawa coupling, takes exponentially different values. In the SM, however, the Yukawa couplings are free parameters and are determined through experiment. The fact that these coupling constants take on unnaturally hierarchical values is called the fermion mass hierarchy problem.

- **Origin of the flavor mixing and the *CP*-violating phase:**
Particles from different generations mix through weak interactions. The degrees of mixing are determined by the values of the off-diagonal components of the Cabibbo–Kobayashi–Maskawa (CKM) matrix and the Pontecorvo–Maki–Nakagawa–Sakata (PMNS) matrix. Furthermore, the complex phases of the CKM matrix and the PMNS matrix are called the *CP*-violating phases. However, these components and phases are determined through experiment, and there is no theoretical explanation for their origin. This fact is one of the remaining problems with the SM.

If we can theoretically explain these problems in a natural way, we will have a theory that goes beyond the SM. If phenomenological predictions are proposed and then confirmed by experiment, our model is regarded as the correct theory.

1.3.1.2 Resolution of the Problems in the Standard Model

The extra-dimensional model is a promising candidate as a theory beyond the SM. In this study, we also consider extra-dimensional models and attempt to solve the above problems in the SM. The most notable feature of the extra-dimensional model is the appearance of an infinite number of particles with various masses in the 4d low-energy effective theory due to the Kaluza–Klein (KK) expansion of higher-dimensional fields. In general, the masses of those particles are inversely proportional to the radius of the extra dimension. Previous high-energy experiments have found no direct evidence for the existence of extra dimensions, and there is an upper bound to the radius of the extra dimension. Since the radius of the extra dimension is small enough, the massive modes are very heavy. Therefore, if the extra-dimensional model describes the world, then we are currently observing KK zero modes with zero mass as elementary particles.

There are two major steps to solve the problems. First, we consider a 5d spacetime whose extra dimension is a rose graph that can take various shapes as an 1d extra dimension. Second, the 5d field is KK expanded and its KK zero modes are analyzed.

- **Generation number problem:**
The difference between the right- and left-handed chiral zero modes of the 5d Dirac fermions, which is called Witten index, is invariant under continuous deformation of the boundary conditions. Also, right- and left-handed pairs generally disappear from zero modes as massive modes through interactions with gauge and scalar fields. Since KK zero modes are regarded as the SM particles, the difference of the number of right- and left-chiral zero modes, which is

an invariant quantity in our model, can be regarded as the number of generation of fermions. Therefore, in our model, the generation number problem can be explained by the geometry of the extra dimension as follows. First, we prepare 5d Dirac fermions with the same quantum numbers as the SM, but for only one generation instead of three. Note now that the extra dimension has a geometric structure such that the Witten index is three. Next, we investigate the 4d low-energy effective theory of this model. As a result, the SM is naturally obtained from the 4d low-energy effective theory of our model.

- **Fermion mass hierarchy problem:**
  In our model, mass matrix m_{ij} between the i-th generation and the j-th one of the fermions will be of the form
  $$m_{ij} = g_{\mathrm{Y}} v \int dy \left(f_0^{(i)}(y)\right)^* g_0^{(j)}(y),$$
  where g_{Y} is a 5d Yukawa coupling constant with the same value in all generations, v is a vacuum expectation value of the Higgs field, $\int dy$ denotes the integral over the extra dimension, and $f_0^{(i)}(y)$ ($g_0^{(j)}(y)$) is the profile of the i-th (j-th) generation of the 4d massless chiral zero modes. Zero-mode profiles are localized, and the values of their overlap integrals can also achieve exponential differences. Therefore, the fermion mass hierarchy in the SM can be naturally explained in our model. It should be noted that unlike the SM, the Yukawa coupling g_Y is common parameter throughout all generations in our model.

- **Origin of flavor mixing and *CP*-violating phase:**
  The m_{ij} that appeared in the above is regarded as the CKM matrix or the PMNS matrix itself. Therefore, if the $f_0^{(i)}(y)$ and $g_0^{(j)}(y)$ profiles are realized such that the m_{ij} $(i, j = 1, 2, 3)$ take values suggested by the SM, then our model naturally explains the origin of flavor mixing. Furthermore, since zero-mode functions are genuine complex functions, m_{ij} can have a complex phase, which can also explain the origin of the *CP* phase. Since the components and the complex phase of the CKM matrix are determined by the form of the extra dimension, these problems can be naturally explained by assuming that the extra dimension exists and has appropriate boundary conditions.

1.3.2 Instantons as Berry's connections

Berry's phase and Berry's connection are interesting phenomena that appear in quantum systems when model parameters are adiabatically driven along a closed loop on the parameter space. For example, a spin-1/2 free particle interacting with a magnetic field can be described as $H = -\vec{B} \cdot \vec{\sigma}$. Let the magnetic field $\vec{B}$ be parametrized by an angle in space that can be controlled. Then, if we adiabatically vary the parameters to closed path in space, we can obtain nontrivial Berry's phases and Berry's connections. This result reflects the topological structure of the parameter space with angles as variables, and Berry's connection is nothing but a Dirac monopole. Therefore, when nontrivial Berry's phases or Berry's connections are obtained for a theory with parameter degrees of freedom, it can be revealed that there is an interesting topological structure hidden behind it.

If the energy eigenstates are degenerate and there are multiple parameters in the model, one can obtain a non-Abelian Berry's phase or a non-Abelian Berry's connection. These objects also reflect the topological structure of the parameter space [10, 11].

Rose graphs can be transformed into graphs of various shapes by changing the boundary conditions at the vertex. We consider the Dirac fermions on 5d space-time with the rose graph as a 1d extra dimension. The boundary conditions can be characterized by an N-dimensional unitary Hermitian matrix with 1_N squared, and the mode functions on the graph can be expressed in a form that is dependent on the parameter of the boundary conditions. The mode functions are now eigenfunctions with various 4d masses obtained in the KK expansion of the 5d Dirac field.

A major feature of quantum graphs is that they generally have multiple degeneracies in the zero modes. Also, through the boundary conditions, our model has multiple parameters. Therefore, it is possible to compute the non-Abelian Berry's connection. In previous studies, authors have shown that one can consider boson-like particles on a quantum graph of simple form and obtain Abelian geometric phase [21] and non-Abelian geometric phase [10–12]. In addition to these, they have shown that $U(1)$ monopoles and Bogomolny–Prasad–Sommerfield monopoles can be obtained as Berry's connections.

In this study, we show that instanton configuration can be obtained as Berry's connection in the parameter space of boundary conditions. Surprisingly, we find that the ADHM construction method [22] can be applied to the calculation of Berry's connections. The ADHM construction is a method for constructing arbitrary instantons. Therefore, it is revealed that arbitrary instanton configurations can be constructed as Berry's connections in the parameter space of boundary conditions. These results imply that the topological structure of the boundary conditions of quantum graphs is diverse.

1.3.3 Topological classification of boundary conditions

The parameter space of the boundary conditions of the rose graph increases as N in Fig. 1.2 is increased. To understand the structure of the parameter space of the boundary conditions, we systematically investigate them. A hint of the strategy is that we obtained 4d chiral zero modes localized at the vertices depending on the topological structure of the parameter space of the boundary conditions. This reminds us of topological insulators and superconductors, where gapless states appear on the boundaries by the topology in bulk from the bulk-boundary correspondence. These topological matters are classified into ten symmetry classes by the presence or absence of time-reversal, particle-hole, and chiral symmetries [23–25]. For gapped free-fermion systems, since the second quantized Hamiltonian can be written in a quadratic form as $\hat{H} = \sum_{i,j} \hat{\psi}_i H_{ij} \hat{\psi}_j$, this system can be described by the matrix H. This H has a dependence on the momentum $\boldsymbol{k}$ in the Brillouin zone and is classified according to symmetry.

In this study, we perform a topological classification of the boundary conditions for 5d Dirac fermions on quantum graphs. The boundary conditions are classified into ten symmetry classes by considering time reversal, charge conjugation, and extra spatial symmetries in 5d Dirac fermions. Remarkably, it is shown that this classification has a complete correspondence to the topological classification of the $(1+0)$-d gapped free-fermion system. Specifically, the classification of the Hermitian matrix that specifies the boundary conditions corresponds to the classification of the Hamiltonian H for $\dim(\boldsymbol{k}) = 0$ with the Altland–Zirnbauer symmetries. Furthermore, we obtain the topological numbers $\mathbb{Z}$, $\mathbb{Z}_2$, $2\mathbb{Z}$ for each symmetry class of the boundary conditions in the same manner as those of topological insulators and superconductors. Importantly, these numbers predict the number of 4d massless fields localized at the vertex of quantum graphs, i.e., the $\mathbb{Z}$ and $2\mathbb{Z}$ indices are equal to the number of KK chiral zero modes, and the $\mathbb{Z}_2$ index coincides with the even/odd parity of the number of Dirac zero modes. These zero modes would be regarded as gapless boundary states of topological phases. A similar relation between boundary conditions and (1 + 1)-d symmetry-protected topological (SPT) phases [26] or (1 + 2)-d SPT phases [27] has been known in the boundary conformal field theories. In this study, we reveal for the first time the relation between the boundary conditions on quantum graphs and (1 + 0)-d SPT phases.

1.4 Outline

This dissertation is organized as follows. In the next chapter, we explain how the boundary conditions of a quantum graph are obtained through a simple example. In Chap. 3, we consider a Dirac fermion on 5d spacetime with the rose graph as an extra dimension and analyze its zero modes. It becomes clear that the difference between chiral zero modes is a quantity that is invariant under continuous deformation of the boundary conditions. We will also illustrate applications of this invariant to explain the generation number problem, the mass hierarchy of fermions, the origin of flavor mixing and the CP-violating phase. These results are based on the publication paper [28]. In Chap. 4, the ADHM construction method is explained, and then the instanton configuration as the Berry's connections are constructed. This study is based on publication paper [29]. In Chap. 5, we show that boundary conditions are classified into ten symmetry classes by considering time reversal, charge conjugation, and extra spatial symmetries in 5d Dirac fermions. These classification have a nontrivial correspondence with the (1 + 0)-d SPT phase. These discussions are based on the publication paper [30]. Chap. 6 is devoted to summary and discussion.

Chapter 2

Quantum graphs and boundary conditions

We consider quantum mechanics on a graph composed of vertices and edges. The quantum graph describes quantum mechanics on a one-dimensional (1d) graph and has been paid attention to since we can obtain attractive physics caused by the degrees of freedom in boundary conditions for wave functions imposed at vertices from the requirement of current conservation. In this chapter, through a simple example, we will illustrate how the boundary conditions at the vertices of a quantum graph are obtained.

2.1 Quantum graphs

In order to describe the behavior of a particle by quantum mechanics, the Hamiltonian on the system must be Hermitian. This Hermitian condition is equivalent to the condition for the probability density of the particle or the current to be conserved in the system [1]. As we will explain later through a concrete example, the condition for conservation of the current can be replaced by a boundary condition at the vertex where the current flows in. A quantum graph is a 1d quantum mechanical system with a general form that satisfies these conditions.

For example, considering the case of a 1d circuit as shown in Fig. 2.1, the conservation law of current is the condition that the sum of $j_1, j_2, \cdots, j_6$ flowing into the center is zero. Let us consider that the current is conserved in $\{j_1, j_2, j_3\}$ and $\{j_4, j_5, j_6\}$ independently. In this case, a total of six segments form an independent graph connected by three segments each (See Fig. 2.1). The current conservation and the boundary conditions at the vertices are closely related.

2.2 Simple example

We will explain that the boundary conditions are derived from the current conservation law. As the simplest example, we consider one free bosonic particle on the graph shown in Fig. 2.2 connecting the endpoints of an edge. The method of deriving the boundary conditions here is based on the paper [21].

For this graph to be a quantum graph, the current on it must be conserved. In the present case, the probability density flow must be conserved, i.e.,

$$j(+0) = j(-0), \quad j(x) \equiv -i\left[\varphi^* \frac{d\varphi}{dx} - \frac{d\varphi^*}{dx}\varphi\right](x) \tag{2.2.1}$$

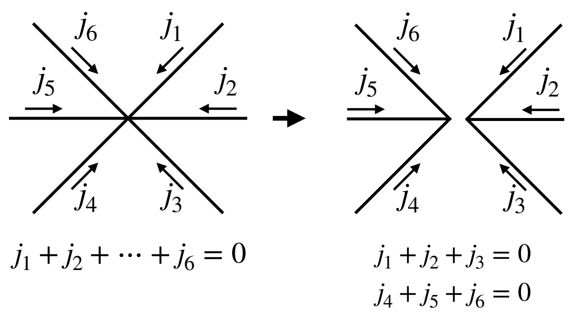

Figure 2.1: Diagram of six edges connected by a single point. The current is preserved by adding all of them together, but changes to the form on the right when $\{j_1, j_2, j_3\}$ and $\{j_4, j_5, j_6\}$ are requested to be preserved independently of each other.

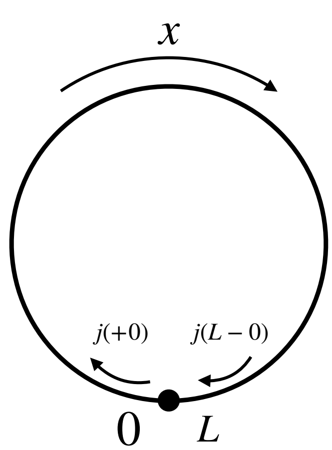

Figure 2.2: Example of the simplest quantum graph. This graph can be constructed by connecting the endpoints of the edge. In this operation, the boundary condition is non-trivial and described by $U(2)$ parameters.

must hold at the $x = 0$. In the above equation, the natural unit is adopted. Since derivatives cannot be defined in general just at the vertex ($x = 0$), e.g., consider the case of δ-function type potential, we wrote the conditions for current conservation excluding that point. If we introduce a new 2-component complex vectors

$$\Phi \equiv \begin{pmatrix} \varphi(+0) \\ \varphi(L-0) \end{pmatrix}, \quad \Phi' \equiv \begin{pmatrix} \varphi'(+0) \\ -\varphi'(L-0) \end{pmatrix}, \tag{2.2.2}$$

we can rewrite (2.2.1) to

$$|\Phi - iL_0\Phi'|^2 = |\Phi + iL_0\Phi|^2 \,, \tag{2.2.3}$$

where L_0 is an arbitrary nonzero constant with a dimension of length for dimension matching. Since the Eq. (2.2.3) implies that the norms of the two-dimensional complex vectors are equal, we can remove the square,

$$|\Phi - iL_0\Phi'| = |\Phi + iL_0\Phi| \,. \tag{2.2.4}$$

With a rotation matrix U in a two-dimensional complex vector space, Eq. (2.2.4) can be replaced by

$$\Phi - iL_0\Phi' = U\,(\Phi + iL_0\Phi) \quad (U \in U(2)) \tag{2.2.5}$$

or

$$(1_2 - U)\Phi = iL_0\,(1_2 + U)\,\Phi' \quad (U \in U(2)). \tag{2.2.6}$$

It is important to note that U is included as degrees of freedom. In particular, in the case of Fig. 2.2, the boundary condition is specified by $U(2)$ parameters. In the following, we discuss some of the boundary conditions that can be obtained by choosing specific values for these parameters.

As a first example, we consider $U = \pm 1_2$. In this case, Eq. (2.2.6) becomes

$$U = 1_2 : \Phi' = 0 \Longleftrightarrow \begin{cases} \varphi'(+0) = 0, \\ \varphi'(-0) = 0, \end{cases} \tag{2.2.7}$$

$$U = -1_2 : \Phi = 0 \Longleftrightarrow \begin{cases} \varphi(+0) = 0, \\ \varphi(-0) = 0, \end{cases} \tag{2.2.8}$$

which are the Neumann boundary condition ($U = 1_2$) and the Dirichlet boundary condition ($U = -1_2$), respectively. As a next example, we consider

$$U = \begin{pmatrix} 0 & 1 \\ 1 & 0 \end{pmatrix}. \tag{2.2.9}$$

In this case, Eq. (2.2.6) becomes

$$\varphi(+0) = \varphi(-0), \quad \varphi'(+0) = \varphi'(-0), \tag{2.2.10}$$

which is nothing but a periodic boundary condition. As a final example, we consider

$$U = \frac{1}{2}\begin{pmatrix} e^{i\theta} - 1 & e^{i\theta} + 1 \\ e^{i\theta} + 1 & e^{i\theta} - 1 \end{pmatrix}, \tag{2.2.11}$$

leaving parameter $\theta \in [0, 2\pi)$. In this case, Eq. (2.2.6) becomes

$$\varphi(+0) = \varphi(-0), \tag{2.2.12}$$

$$\varphi'(+0) - \varphi'(-0) = \frac{2i}{L_0} \tan \frac{\theta}{2} \cdot \varphi(+0). \tag{2.2.13}$$

This is the boundary condition for the case of a delta-function type potential, which often appears in quantum mechanics textbooks.

From the above discussion, we were able to derive the boundary conditions from the conservation condition of current. The derived boundary conditions were found to contain parameters.

2.3 Summary

For a simple example, we derived the boundary conditions that a quantum graph must satisfy. We show that these boundary conditions include not only the well-known boundary conditions in quantum mechanics but also various types of boundary conditions. The diversity of boundary conditions is the reason we focus on quantum graphs. In the following chapter, we consider models with quantum graphs as extra dimensions and discuss applications of their topological structure and their classification.

Chapter 3

5d fermion on quantum graph

The extra-dimensional model is promising as a theory of beyond the Standard Model (SM). Various extra-dimensional models have been proposed, but we will focus here on studies that attempt to solve the generation number problem of the SM. In the extra-dimensional model, particles with various masses emerge as a four-dimensional (4d) theory by expanding the extra-dimensional directions with eigenfunctions of 4d fields. Their masses are given by the inverse of the radius of the extra dimension, but in general the size of the extra dimension is so small that only massless modes can be observed in current experiments. The degeneracy of the massless modes depends on the geometry of the extra dimension. Therefore, if there exists an extra-dimensional geometry that achieves threefold degeneracy, the three-generation structure of the SM can be explained by that geometry in the extra-dimensional model.

As an extra dimension, we consider in particular a 1d model. In this case, are there a 1d extra-dimensional geometry that achieves zero-mode three-fold degeneracy? To answer this question, we analyze a model that the quantum graph, which has the most general geometry as 1d space, is the extra-dimension. As a result, we can identify boundary conditions for quantum graphs for which three-fold degeneracy is feasible. It also shows the possibility of simultaneously explaining not only the generation number problem, but also the mass hierarchy problem of fermions and the origin of flavor mixing and *CP* phases.

This chapter is organized as follows: In the next Section, we explain our setup and derive boundary conditions on quantum graphs from current conservation law. In Sec. 3.2, first, the boundary conditions are rewritten in terms of mode functions. Solving the eigenfunctions under the boundary conditions yields the spectrum, degeneracy of the eigenvalues, and shape of the zero modes. Therefore, we next perform an exhaustive analysis of the degeneracy of zero modes for various boundary conditions. In the extra-dimensional model, degeneracy generally appears in the massive mode of fermions. This phenomenon is understood from the standpoint of supersymmetric quantum mechanics, and we will briefly explain in Sec. 3.3 that this is also the case in our model. In Sec. 3.4, we show that our model can simultaneously explain the generation number problem of the SM, the mass hierarchy problem of fermions, and the origin of flavor mixing and *CP* phases.

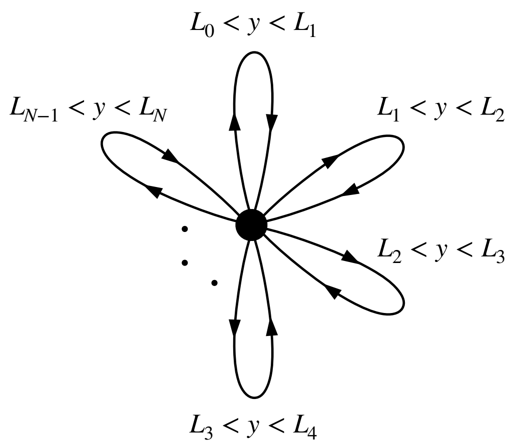

Figure 3.1: Rose graph with N edges (or called loops) and one vertex

3.1 Setup and Kaluza–Klein expansion

We consider a Dirac fermion on 5d spacetime, which is constructed with 4d Minkowski spacetime and quantum graph as an extra dimension. Especially we chose a quantum graph like Fig. 3.1. This graph consists of one vertex and N edges (or called loops). Since varying the boundary conditions at the vertex can transform the graph into various shapes (see Fig. 1.3), a rose graph like Fig. 3.1 is the master graph. Now we consider the 5d Dirac fermion on a 5d spacetime with the rose graph as an extra dimension. The action is given by

$$S = \int d^4x \sum_{a=1}^{N} \int_{L_{a-1}}^{L_a} dy\, \overline{\Psi}(x,y) \left[i\gamma^\mu \partial_\mu + i\gamma^y \partial_y + M \right] \Psi(x,y), \tag{3.1.1}$$

where x^μ ($\mu = 0,1,2,3$) are the coordinates of the 4d Minkowski spacetime and y is the coordinate of the quantum graph. $\Psi(x,y)$ represents a 4-component Dirac fermion and the Dirac conjugate $\overline{\Psi}$ is defined by $\overline{\Psi} = \Psi^\dagger \gamma^0$. γ^A ($A = 0,1,2,3,y$) are defined as 4×4 gamma matrices satisfying the Clifford algebra:

$$\{\gamma^A, \gamma^B\} = -2\eta^{AB}, \quad \eta^{AB} = \mathrm{diag}(-,+,+,+,+), \tag{3.1.2}$$

and especially chose γ^y as $\gamma^y = -i\gamma^5$ ($\gamma^5 = i\gamma^0\gamma^1\gamma^2\gamma^3$). M denotes the bulk mass.

In this chapter, we consider the quantum graph shown in Fig. 3.1, which consists of one vertex and N edges, each of which forms a loop with $L_{a-1} < y < L_a\,(a = 1,2,\cdots,N)$. N loops are connected with appropriate boundary conditions. These conditions are derived in several ways: (1) the current conservation law on the vertex, (2) Hermiticity of the action, (3) the request that the equation of motion for $\overline{\Psi}$ can be obtained from the variational principle for Ψ. Now we chose the first way[1].

The current is given by the ordinary form

$$j^M(x,y) = \overline{\Psi}(x,y)\gamma^M\Psi(x,y) \quad (M = \mu, y). \tag{3.1.3}$$

$j^\mu(x,y)$ trivially conserves on 4d Minkowski spacetime, on the other hand, $j^y(x,y)$ can only conserve on the quantum graph with appropriate boundary conditions. To obtain boundary conditions,

[1]There are some calculations and discussions in the paper [31].

we request the current conservation law on the quantum graph

$$\sum_{a=1}^{N}\left[\overline{\Psi}(x,y)\gamma^5\Psi(x,y)\right]_{y=L_{a-1}+\varepsilon}^{y=L_a-\varepsilon}=0, \tag{3.1.4}$$

where ε is an infinitesimal positive constant. We shift from the vertices with ε because there are singular in general and the derivative ∂_y is not well-defined at there points.

If the current is conserved in the system, the equation of motion of 5d Dirac fermion $\Psi(x,y)$ is obtained by the action principle $\delta S = 0$. In fact, if we use the variational principle for $\overline{\Psi}$, then we can obtain

$$\left[i\gamma^\mu\partial_\mu+\gamma^5\partial_y+M\right]\Psi(x,y)=0. \tag{3.1.5}$$

Since we consider a compact quantum graph (see Fig. 3.1) as an extra dimension, the 5d Dirac fermion $\Psi(x,y)$ can be expanded with 4d chiral fermions $\psi^{(i)}_{\mathrm{R/L},n}(x)$ and mode functions $f^{(i)}_n(y)$, $g^{(i)}_n(y)$:

$$\Psi(x,y)=\sum_i\sum_{n=0}^{\infty}\psi^{(i)}_{\mathrm{R},n}(x)f^{(i)}_n(y)+\sum_i\sum_{n=0}^{\infty}\psi^{(i)}_{\mathrm{L,n}}(x)g^{(i)}_n(y), \tag{3.1.6}$$

$$\gamma^5\psi^{(i)}_{\mathrm{R/L},n}(x)=\pm\psi^{(i)}_{\mathrm{R/L},n}(x), \tag{3.1.7}$$

where n indicates the n-th level of Kaluza–Klein modes and i denotes the index that distinguishes the degeneracy (if it exists). The mode functions $f^{(i)}_n(y)$, $g^{(i)}_n(y)$ are the mass eigenstates of 4d Dirac fermions and satisfy the complete orthonormal relations

$$\sum_{a=1}^{N}\int_{L_{a-1}}^{L_a}dy\,\left(f^{(i)}_n(y)\right)^* f^{(j)}_m(y)=\delta_{nm}\delta^{ij}, \tag{3.1.8}$$

$$\sum_{a=1}^{N}\int_{L_{a-1}}^{L_a}dy\,\left(g^{(i)}_n(y)\right)^* g^{(j)}_m(y)=\delta_{nm}\delta^{ij}. \tag{3.1.9}$$

Since the 4d chiral fermions $\psi^{(i)}_{\mathrm{R/L},n}(x)$ with mass m_n obeys the equations

$$i\gamma^\mu\partial_\mu\psi^{(i)}_{\mathrm{R},n}(x)+m_n\psi^{(i)}_{\mathrm{L,n}}(x)=0, \tag{3.1.10}$$

$$i\gamma^\mu\partial_\mu\psi^{(i)}_{\mathrm{L},n}(x)+m_n\psi^{(i)}_{\mathrm{R,n}}(x)=0, \tag{3.1.11}$$

substituting the KK expansion (3.1.6) into the 5d Dirac equation (3.1.5), we obtain

$$\begin{aligned}
0&=\left[i\gamma^\mu\partial_\mu+i\gamma^y\partial_y+M\right]\Psi(x,y)\\
&=\sum_i\sum_n\left[i\gamma^\mu\partial_\mu+\gamma^5\partial_y+M\right]\psi^{(i)}_{\mathrm{R},n}(x)f^{(i)}_n(y)\\
&\quad+\sum_i\sum_n\left[i\gamma^\mu\partial_\mu+\gamma^5\partial_y+M\right]\psi^{(i)}_{\mathrm{L},n}(x)g^{(i)}_n(y)\\
&=\sum_i\sum_n\left[-m_nf^{(i)}_n(y)+(-\partial_y+M)g^{(i)}_n(y)\right]\psi^{(i)}_{\mathrm{L},n}(x)\\
&\quad+\sum_i\sum_n\left[-m_ng^{(i)}_g(y)+(\partial_y+M)f^{(i)}_n(y)\right]\psi^{(i)}_{\mathrm{R},n}(x).
\end{aligned} \tag{3.1.12}$$

Then, $\psi^{(i)}_{\mathrm{R/L},n}(x)$ are independently transformed under the Lorentz transformation and independent with respect to the label n, we can obtain

$$(\partial_y + M) f^{(i)}_n(y) = m_n g^{(i)}_n(y), \tag{3.1.13}$$
$$(-\partial_y + M) g^{(i)}_n(y) = m_n f^{(i)}_n(y). \tag{3.1.14}$$

These equations are called SUSY relations because it gives the relationship between $f^{(i)}_n$ and $g^{(i)}_n$. To obtain the eigenequations according to $f^{(i)}_n$ and $g^{(i)}_n$, multiply by $(-\partial_y + M)$ and $(\partial_y + M)$ from the left of both sides of the above equations, respectively, then we can obtain

$$(-\partial_y^2 + M^2) f^{(i)}_n(y) = m_n^2 f^{(i)}_n(y), \tag{3.1.15}$$
$$(-\partial_y^2 + M^2) g^{(i)}_n(y) = m_n^2 g^{(i)}_n(y). \tag{3.1.16}$$

3.2 Boundary conditions and zero-modes

We rewrite the current conservation law into boundary conditions at the vertices of the rose graph and classify the boundary conditions in terms of the zero-mode degeneracy.

3.2.1 Boundary conditions

First, we rewrite the current conservation law in terms of boundary conditions at the vertices.

Substituting the expansion (3.1.6) into the current conservation law (3.1.4), we get

$$\begin{aligned}
0 &= \sum_{a=1}^{N} \left[\overline{\Psi}(x,y)\gamma^5 \Psi(x,y) \right]_{y=L_{a-1}+\varepsilon}^{y=L_a-\varepsilon} \\
&= -\sum_{i,j}\sum_{n,m} \overline{\psi}^{(i)}_{\mathrm{R},n}(x)\psi^{(j)}_{\mathrm{L},m}(x) \sum_{a=1}^{N} \left[\left(f^{(i)}_n(y) \right)^* g^{(j)}_m(y) \right]_{y=L_{a-1}+\varepsilon}^{y=L_a-\varepsilon} \\
&\quad + \sum_{i,j}\sum_{n,m} \overline{\psi}^{(i)}_{\mathrm{L},n}(x)\psi^{(j)}_{\mathrm{R},m}(x) \sum_{a=1}^{N} \left[\left(g^{(i)}_n(y) \right)^* f^{(j)}_m(y) \right]_{y=L_{a-1}+\varepsilon}^{y=L_a-\varepsilon}.
\end{aligned} \tag{3.2.1}$$

Since $\overline{\psi}^{(i)}_{\mathrm{R},n}$ and $\overline{\psi}^{(i)}_{\mathrm{L},n}$ transform independently under the 4d Lorentz transformation and are independent with respect to n, Eq. (3.2.1) reduces to

$$\sum_{a=1}^{N} \left[\left(f^{(i)}_n(y) \right)^* g^{(j)}_m(y) \right]_{y=L_{a-1}+\varepsilon}^{y=L_a-\varepsilon} = 0, \tag{3.2.2}$$
$$\sum_{a=1}^{N} \left[\left(g^{(i)}_n(y) \right)^* f^{(j)}_m(y) \right]_{y=L_{a-1}+\varepsilon}^{y=L_a-\varepsilon} = 0. \tag{3.2.3}$$

In the following, we will analyze only (3.2.2), because the above two equations are in a complex conjugate relationship.

To simplify the classification of boundary conditions, we introduce two $2N$-dimensional complex vectors whose components are the values of the mode functions near the vertex:

$$\vec{F}_n^{(i)} \equiv \begin{pmatrix} f_n^{(i)}(L_0+\varepsilon) \\ f_n^{(i)}(L_1-\varepsilon) \\ \vdots \\ f_n^{(i)}(L_{a-1}+\varepsilon) \\ f_n^{(i)}(L_a-\varepsilon) \\ \vdots \\ f_n^{(i)}(L_{N-1}+\varepsilon) \\ f_n^{(i)}(L_N-\varepsilon) \end{pmatrix}, \quad \vec{G}_m^{(j)} \equiv \begin{pmatrix} g_n^{(i)}(L_0+\varepsilon) \\ -g_n^{(i)}(L_1-\varepsilon) \\ \vdots \\ g_n^{(i)}(L_{a-1}+\varepsilon) \\ -g_n^{(i)}(L_a-\varepsilon) \\ \vdots \\ g_n^{(i)}(L_{N-1}+\varepsilon) \\ -g_n^{(i)}(L_N-\varepsilon) \end{pmatrix}. \tag{3.2.4}$$

The boundary condition (3.2.2) can be rewritten as

$$\vec{F}_n^{(i)\dagger}\vec{G}_m^{(j)} = 0 \quad (\forall i, j, n, m). \tag{3.2.5}$$

Now, to solve the Eqs. (3.1.15) and (3.1.16) and determine the mass eigenvalues m_n, we want to obtain $4N$ boundary conditions in total, since the graph has $2N$ boundaries $y = L_0+\varepsilon,\ L_1 \pm \varepsilon, \cdots, L_{N-1}\pm\varepsilon,\ L_N - \varepsilon$ for $f_n^{(i)}$ and $g_m^{(j)}$. However, the SUSY relations (3.1.13) and (3.1.14) imply that the massive mode functions $f_{n\neq 0}^{(i)}$ and $g_{m\neq 0}^{(j)}$ are related with each other (except for the zero mode functions which obey the first differential equations). Thus, we should require that the conditions (3.2.5) provide $2N$ constraints in total, otherwise, the system is undetermined or overdetermined. For example, we impose $4N$ constraints with the condition

$$f_n^{(i)}(y) = g_m^{(j)}(y) = 0 \quad \text{at} \quad y = L_0+\varepsilon,\ L_1 \pm \varepsilon, \cdots, L_{N-1}\pm\varepsilon,\ L_N-\varepsilon. \tag{3.2.6}$$

Then, we can obtain the additional boundary conditions

$$f_n^{(i)}(y) = 0 \Longrightarrow -\partial_y g_m^{(j)}(y) = 0, \tag{3.2.7}$$

$$g_m^{(j)}(y) = 0 \Longrightarrow \partial_y f_m^{(j)}(y) = 0, \tag{3.2.8}$$

from the SUSY relations (3.1.13), (3.1.14). Since now the mode functions should satisfy both the Dirichlet and Neumann boundary conditions, we can conclude that there are no non-trivial solutions which satisfy boundary conditions (3.2.6). It follows from this observation that Eq. (3.2.5) is replaced by the boundary conditions

$$(1_{2N} - U_{\mathrm{B}})\vec{F}_n^{(i)} = 0, \quad (1_{2N} + U_{\mathrm{B}})\vec{G}_m^{(j)} = 0 \quad (\forall i, j, n, m), \tag{3.2.9}$$

where U_{B} is a $2N \times 2N$ Hermitian unitary matrix

$$U_{\mathrm{B}}^2 = 1_{2N}, \quad U_{\mathrm{B}}^\dagger = U_{\mathrm{B}}. \tag{3.2.10}$$

The conditions for U_{B} are the constraints to make $2N$ boundary conditions in total.

The Hermitian matrix U_{B} can be diagonalized using a unitary matrix, whose eigenvalues are ± 1 since $U_{\mathrm{B}}^2 = 1_{2N}$. In this chapter, we will classify the boundary conditions by the number of -1

eigenvalues. Therefore, the boundary conditions can be classified into $2N + 1$, and let "Type($2N - k, k$)" be the class with k eigenvalues of -1:

$$\text{Type}(2N-k,k) : U_{\mathrm{B}} = V \begin{pmatrix} 1_{2N-k} & \mathbf{0} \\ \mathbf{0} & -1_k \end{pmatrix} V^\dagger \quad (V \in U(2N), \quad 0 \leq k \leq 2N). \tag{3.2.11}$$

Classes with different values of k do not connect each other under continuous deformations in the parameter space of U_{B}. In this sense, we say that Type($2N - k, k$) and Type($2N - k', k'$) belong to topologically distinct classes if $k \neq k'$.

3.2.2 Zero-mode degeneracy

Various degeneracies can occur in the 4d mass spectrum considering the quantum graph as an extra dimension. This is a feature that does not appear in open 1d quantum mechanical systems of infinite length. In this chapter, we will not focus on the massive modes, but only on the degeneracy of the zero modes. Furthermore, we perform an exhaustive analysis of the degeneracy of zero modes for various boundary conditions

Substituting $m_n = 0$ into the right-hand side of Eqs. (3.1.13) and (3.1.14) yields the zero mode equations

$$(\partial_y + M) f_0^{(i)}(y) = 0, \tag{3.2.12}$$

$$(-\partial_y + M) g_0^{(j)}(y) = 0. \tag{3.2.13}$$

Since they need not to be continuous in general at the boundaries $y = L_0 + \varepsilon$, $L_1 \pm \varepsilon, \cdots, L_{N-1} \pm \varepsilon$, $L_N - \varepsilon$, these equations lead to

$$f_0^{(i)}(y) = \begin{cases} A_1^{(i)} C_1 e^{-My} & (L_0 < y < L_1), \\ A_2^{(i)} C_2 e^{-My} & (L_1 < y < L_2), \\ \vdots & \\ A_N^{(i)} C_N e^{-My} & (L_{N-1} < y < L_N), \end{cases} \tag{3.2.14}$$

$$g_0^{(j)}(y) = \begin{cases} B_1^{(j)} C'_1 e^{My} & (L_0 < y < L_1), \\ B_2^{(j)} C'_2 e^{My} & (L_1 < y < L_2), \\ \vdots & \\ B_N^{(j)} C'_N e^{My} & (L_{N-1} < y < L_N), \end{cases} \tag{3.2.15}$$

where $A_a^{(i)}$, $B_a^{(j)}$ are complex constants determined to satisfy the boundary conditions and C_a, C'_a are constants independent of degeneracy i, j, which are determined immediately follow. Using the Heaviside step function $\theta(y)$, they can be rewritten in simple forms,

$$f_0^{(i)}(y) = \sum_{a=1}^{N} \theta(y - L_{a-1})\theta(L_a - y) A_a^{(i)} C_a e^{-My}, \tag{3.2.16}$$

$$g_0^{(j)}(y) = \sum_{a=1}^{N} \theta(y - L_{a-1})\theta(L_a - y) B_a^{(j)} C'_a e^{My}. \tag{3.2.17}$$

To find the degeneracy of the zero modes, we have to count the number of independent $f_0^{(i)}$, $g_0^{(j)}$ in each case under the boundary conditions.

There exists a convenient basis for counting zero-mode degeneracy, which we define as

$$\vec{\mathcal{F}}_a \equiv C_a(\underbrace{0,\cdots,0}_{2(a-1)}, e^{-M(L_{a-1}+\varepsilon)}, e^{-M(L_a-\varepsilon)}, \underbrace{0,\cdots,0}_{2(N-a)})^\top, \tag{3.2.18}$$

$$\vec{\mathcal{G}}_a \equiv C'_a(\underbrace{0,\cdots,0}_{2(a-1)}, e^{M(L_{a-1}+\varepsilon)}, -e^{M(L_a-\varepsilon)}, \underbrace{0,\cdots,0}_{2(N-a)})^\top, \tag{3.2.19}$$

where C_a, C'_a $(a = 1, 2, \cdots, N)$ are coefficients to normalize the basis and are given by

$$|C_a| = \frac{1}{\sqrt{\vec{\mathcal{F}}_a^\dagger \vec{\mathcal{F}}_a}} = \frac{1}{\sqrt{e^{-2M(L_{a-1}+\varepsilon)} + e^{-2M(L_a-\varepsilon)}}}, \tag{3.2.20}$$

$$|C'_a| = \frac{1}{\sqrt{\vec{\mathcal{G}}_a^\dagger \vec{\mathcal{G}}_a}} = \frac{1}{\sqrt{e^{+2M(L_{a-1}+\varepsilon)} + e^{+2M(L_a-\varepsilon)}}}. \tag{3.2.21}$$

As you can see from the direct calculations, these bases satisfy orthonormal relations:

$$\vec{\mathcal{F}}_a^\dagger \vec{\mathcal{F}}_b = \vec{\mathcal{G}}_a^\dagger \vec{\mathcal{G}}_b = \delta_{ab} \quad (a, b = 1, 2, \cdots, N), \tag{3.2.22}$$

$$\vec{\mathcal{F}}_a^\dagger \vec{\mathcal{G}}_b = \vec{\mathcal{G}}_a^\dagger \vec{\mathcal{F}}_b = 0 \quad (a, b = 1, 2, \cdots, N). \tag{3.2.23}$$

Expanding $\vec{F}_0^{(i)}$ and $\vec{G}_0^{(j)}$ in the introduced basis yields

$$\vec{F}_0^{(i)} = A_1^{(i)}\vec{\mathcal{F}}_1 + A_2^{(i)}\vec{\mathcal{F}}_2 + \cdots + A_N^{(i)}\vec{\mathcal{F}}_N, \tag{3.2.24}$$

$$\vec{G}_0^{(j)} = B_1^{(j)}\vec{\mathcal{G}}_1 + B_2^{(j)}\vec{\mathcal{G}}_2 + \cdots + B_N^{(j)}\vec{\mathcal{G}}_N. \tag{3.2.25}$$

Also, the unitary matrix V in the Eq. (3.2.11) can be expressed by using complex orthonormal vectors $\vec{v}_p$ $(p = 1, 2, \cdots, 2N)$ as

$$V = (\vec{v}_1, \vec{v}_2, \cdots, \vec{v}_{2N}), \quad \vec{v}_p^\dagger \vec{v}_q = \delta_{pq} \quad (p, q = 1, 2, \cdots, 2N), \tag{3.2.26}$$

and $\vec{v}_p$ can be expanded in terms of $\vec{\mathcal{F}}_a$ and $\vec{\mathcal{G}}_a$, as follows

$$\vec{v}_p = \sum_{a=1}^{N} \alpha_{p,a}\vec{\mathcal{F}}_a + \sum_{a=1}^{N} \beta_{p,a}\vec{\mathcal{G}}_a \quad (p = 1, 2, \cdots, 2N). \tag{3.2.27}$$

On the above basis, we can rewrite the original boundary conditions (3.2.9) as

$$
\begin{aligned}
0 &= \left[1_{2N} - V \begin{pmatrix} 1_{2N-k} & 0 \\ 0 & -1_k \end{pmatrix} V^\dagger \right] \vec{F}_0^{(i)} \\
&= 2V \begin{pmatrix} 0_{2N-k} & 0 \\ 0 & -1_k \end{pmatrix} \begin{pmatrix} \vec{v}_1^\dagger \\ \vdots \\ \vec{v}_{2N}^\dagger \end{pmatrix} \vec{F}_0^{(i)} \\
&= -2V \begin{pmatrix} \vec{0}^\dagger \\ \vdots \\ \vec{0}^\dagger \\ \vec{v}_{2N-k+1}^\dagger \vec{F}_0^{(i)} \\ \vdots \\ \vec{v}_{2N}^\dagger \vec{F}_0^{(i)} \end{pmatrix} \qquad (3.2.28)\\
&\Longrightarrow \sum_{a=1}^{N} \alpha_{p,a}^* A_a^{(i)} = 0 \quad (p = 2N-k+1, \cdots, 2N), \qquad (3.2.29)\\
0 &= \left[1_{2N} + V \begin{pmatrix} 1_{2N-k} & 0 \\ 0 & -1_k \end{pmatrix} V^\dagger \right] \vec{G}_0^{(j)} \\
&= 2V \begin{pmatrix} \vec{v}_1^\dagger \vec{G}_0^{(j)} \\ \vdots \\ \vec{v}_{2N-k}^\dagger \vec{G}_0^{(j)} \\ \vec{0} \\ \vdots \\ \vec{0} \end{pmatrix} \qquad (3.2.30)\\
&\Longrightarrow \sum_{a=1}^{N} \beta_{p,a}^* B_a^{(j)} = 0 \quad (p = 1, \cdots, 2N-k). \qquad (3.2.31)
\end{aligned}
$$

Or, by using vectors defined by

$$
\boldsymbol{\alpha}_p \equiv (\alpha_{p,1}, \alpha_{p,2}, \cdots, \alpha_{p,N})^\top, \quad \boldsymbol{\beta}_p \equiv (\beta_{p,1}, \beta_{p,2}. \cdots, \beta_{p,N})^\top, \qquad (3.2.32)
$$

$$
\boldsymbol{A}^{(i)} \equiv (A_1^{(i)}, A_2^{(i)}, \cdots, A_N^{(i)})^\top, \quad \boldsymbol{B}^{(j)} \equiv (B_1^{(j)}, B_2^{(j)}, \cdots, B_N^{(j)})^\top, \qquad (3.2.33)
$$

we can rewrite the boundary conditions as

$$
\boldsymbol{\alpha}_{2N-k+1}^\dagger \boldsymbol{A}^{(i)} = \boldsymbol{\alpha}_{2N-k+2}^\dagger \boldsymbol{A}^{(i)} = \cdots = \boldsymbol{\alpha}_{2N}^\dagger \boldsymbol{A}^{(i)} = 0, \qquad (3.2.34)
$$

$$
\boldsymbol{\beta}_1^\dagger \boldsymbol{B}^{(j)} = \boldsymbol{\beta}_2^\dagger \boldsymbol{B}^{(j)} = \cdots = \boldsymbol{\beta}_{2N-k}^\dagger \boldsymbol{B}^{(j)} = 0. \qquad (3.2.35)
$$

The above boundary conditions are regarded as conditions on the zero mode coefficients $A_a^{(i}$, $B_a^{(j)}$ ($a = 1, 2 \cdots, N$) in Eqs. (3.2.16), (3.2.17). Also, changing the boundary conditions at the vertices of the quantum graph is nothing more than changing $\boldsymbol{\alpha}_p$ or $\boldsymbol{\beta}_p$. To calculate the degeneracy of the zero modes under a certain boundary condition, it is sufficient to determine how many linearly independent $\boldsymbol{A}^{(i)}$ or $\boldsymbol{B}^{(j)}$ exsit when $\boldsymbol{\alpha}_p$ and $\boldsymbol{\beta}_p$ are given. From Eqs. (3.2.28), (3.2.30), $\vec{G}_0^{(j)}$ can be

Table 3.1: The number of the zero mode solutions of $f_0^{(i)}(y)$ and $g_0^{(j)}(y)$ for the type$(2N-k,k)$ BC. The l denotes the maximal number of the linearly independent vectors $\boldsymbol{\alpha}_q$ $(q = 2N-k+1, \cdots, 2N)$ in Eq. (3.2.34). N_{f_0} (N_{g_0}) is the number of the zero mode solutions of $f_0^{(i)}(y)$ $(g_0^{(j)}(y))$. We can find that $N_{f_0} - N_{g_0}$ is independent of l, though both of N_{f_0} and N_{g_0} depend of l.

k	l	N_{f_0}	N_{g_0}	$N_{f_0} - N_{g_0}$
	0	N	k	$N-k$
	1	$N-1$	$k-1$	$N-k$
$0 \leq k \leq N$	$\vdots$	$\vdots$	$\vdots$	$\vdots$
	$k-1$	$N-k+1$	1	$N-k$
	k	$N-k$	0	$N-k$
	$k-N$	$2N-k$	N	$N-k$
	$k-N+1$	$2N-k-1$	$N-1$	$N-k$
$N \leq k \leq 2N$	$\vdots$	$\vdots$	$\vdots$	$\vdots$
	$N-1$	1	$k-N+1$	$N-k$
	N	0	$k-N$	$N-k$

represented by a linear combination of $\{\vec{v}_q \mid q = 2N-k+1, \cdots, 2N\}$. Therefore, determining the number of linearly independent vectors in $\boldsymbol{\alpha}_p$ $(p = 2N-k+1, \cdots, 2N)$ also determines the number of linearly independent vectors in $\boldsymbol{B}^{(j)}$.

Now, let us suppose that the maximal number of the linear independent vectors for $\{\boldsymbol{\alpha}_q \mid q = 2N-k+1, \cdots, 2N\}$ is l. Then it turns out that there exist $N-l$ linearly independent solutions of $\boldsymbol{A}^{(i)}$ $(i = 1, 2, \cdots, N-l)$ to Eq. (3.2.34). This immediately implies that there are $N-l$ linearly independent solutions $f_0^{(i)}(y)$ $(i = 1, 2, \cdots, N-l)$. On the other hand, the number of the linearly independent vectors for $\{\boldsymbol{\beta}_p \mid p = 1, 2, \cdots, 2N-k\}$ is $k-l$ in this case. This means that there exist $k-l$ linearly independent solutions of $\boldsymbol{B}^{(j)}$ $(j = 1, 2, \cdots, k-l)$. Therefore, for the type$(2N-k,k)$ BC, we can conclude that the degeneracy of zero mode $f^{(i)}(y)$ is given by $N_{f_0} = N-l$, and that of zero mode $g_0^{(i)}(y)$ is given by $N_{g_0} = k-l$. The degeneracies N_{f_0} and N_{g_0} for each boundary condition are shown in Table 3.1.

3.3 Perspectives on SUSY quantum mechanics

In the previous Sections, we have clarified the number of zero-modes under each of the boundary conditions. The number of zero modes in each chirality varies by changing $l\,(\leq k)$. However, for a class of Type$(2N-k,k)$ with fixed N and k, the difference between right- and left-handed chiral zero modes is invariant. In this Section, we explain that there is a topological reason behind this fact in terms of supersymmetric quantum mechanics [32].

Supersymmetric quantum mechanics is a theory that describes quantum systems for which there exist operators satisfying a minimal supersymmetry algebra. A minimal supersymmetry algebra is defined as

$$H = Q^2, \tag{3.3.1}$$

$$(-1)^F Q = -Q(-1)^F, \tag{3.3.2}$$

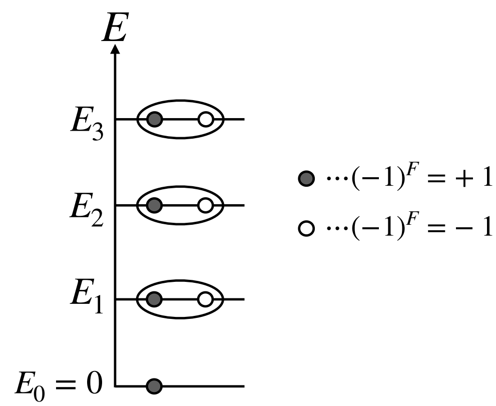

Figure 3.2: Typical energy spectrum. There are three properties: (1) The energy eigenvalues are non-negative, $E \geq 0$; (2) The bosonic state $|E, +\rangle$ and the fermionic state $|E, -\rangle$ form a supermultiplet in the positive energy level; (3) Zero energy states do not necessarily form pairs.

$$\left[(-1)^F\right]^2 = 1 \tag{3.3.3}$$

where H is the Hamiltonian, Q is the supercharge, and $(-1)^F$ is the fermion number operator, all of which are Hermitian operators. Note that the fermion number operator is an operator that returns eigenvalue $+1$ for "bosonic" states and eigenvalue -1 for "fermionic" states, but each state need not be a state with spin degrees of freedom. Now, three properties always appear in the energy spectrum of this system. (1) The energy eigenvalues are non-negative, $E \geq 0$. (2) The bosonic state $|E, +\rangle$ and the fermionic state $|E, -\rangle$ form a supermultiplet in the positive energy level. (3) Zero energy states do not necessarily form pairs. A typical spectrum that well represents these properties is shown in Fig. 3.2. Due to the properties (2) and (3), the difference in the number of zero-energy states between bosonic and fermionic states is invariant, which is called Witten index.

Considering our model again, we find that the following three Hermitian operators satisfy the minimal supersymmetry algebra:

$$H = Q^2, \quad Q = \begin{pmatrix} 0 & -\partial_y + M \\ \partial_y + M & 0 \end{pmatrix}, \quad (-1)^F = \begin{pmatrix} 1 & 0 \\ 0 & -1 \end{pmatrix}. \tag{3.3.4}$$

In addition, the states in which these operators act are

$$|m_n^2, +\rangle = \begin{pmatrix} f_n^{(i)}(y) \\ 0 \end{pmatrix}, \quad |m_n^2, -\rangle = \begin{pmatrix} 0 \\ g_n^{(i)}(y) \end{pmatrix}. \tag{3.3.5}$$

From the general discussion of supersymmetric quantum mechanics, the difference between the number of $|0, +\rangle$ and $|0, -\rangle$ is called the Witten index and is a topologically invariant quantity. Thus, the reason why the difference between the number of chiral zero modes is invariant in our model is explained from the perspective on supersymmetric quantum mechanics.

3.4 Application to beyond the Standard Model

In this Section, we explain how to construct a phenomenological model using the results obtained in the previous Sections. Since the model construction is not yet complete, we will only discuss how to apply it.

In 5d theories, there exist an infinite number of particles with different masses when viewed in 4d. Therefore, in the low-energy region, where zero-mode behavior becomes important, the 5d theory must reproduce the 4d theory with which we are familiar. Now, the 1d extra dimension is taken to be the quantum graph described so far, and the 4d spacetime is taken to be the Minkowski spacetime. As matter particles, we prepare 5d Dirac fermion of one generation of the Standard Model (SM), a 5d Higgs field of the $SU(2)$ doublet, a 5d gauge fields of $SU(3)$, and a 5d gauge field of $SU(2) \times U(1)_Y$. For simplicity, we discuss only the quark sector in the following, but the lepton sector can be discussed in the same way. Furthermore, we do not discuss the kinetic terms of the gauge fields in detail.

3.4.1 Generation number problem

The SM contains three generations of particles with the same spin and charge, but there is no reason for the number to be three, which is called the generation number problem. In our model, one generation of 5d Dirac fermions is prepared first, and three generations of chiral fermions appear naturally in the 4d low-energy effective theory. The reason for this is that the extra dimension of a quantum graph generally causes a degeneracy in the chiral zero modes.

For a more specific discussion, we consider the action of the starting point in the following.

$$\begin{aligned} S_{\text{fermion}} = \int d^4x \sum_{a=1}^{N} \int_{L_{a-1}}^{L_a} dy \Big[&\overline{Q}_d(i\gamma^\mu \partial_\mu + \gamma^5 \partial_y + M_Q) Q_d \\ &+ \overline{U}_s(i\gamma^\mu \partial_\mu + \gamma^5 \partial_y + M_U) U_s + \overline{D}_s(i\gamma^\mu \partial_\mu + \gamma^5 \partial_y + M_D) D_s \Big], \end{aligned} \tag{3.4.1}$$

$$S_{\text{Yukawa}} = \int d^4x \sum_{a=1}^{N} \int_{L_{a-1}}^{L_a} dy \left[g'_Y \overline{Q}_d H D_s + g_Y \overline{Q}_d \widetilde{H} U_s + \text{h.c.} \right], \tag{3.4.2}$$

where Q_d is 5d Dirac fermion of $SU(2)$ doublet, U_s and D_s are 5d Dirac fermion of $SU(2)$ singlet, H is 5d Higgs of $SU(2)$ doublet, $\widetilde{H}$ is defined as $\widetilde{H} = i\sigma_2 H^*$, and g_Y, g'_Y are the Yukawa coupling. These actions correspond to the usual kinetic term of fermion and Yukawa interaction terms in the quark sector of the SM. We now adopt a quantum graph as the extra-dimensional direction that satisfies the following boundary conditions for each field (see Fig. 3.3).

$$Q_d : \text{Type}(N-3, N+3), \tag{3.4.3}$$

$$U_s, D_s : \text{Type}(N+3, N-3). \tag{3.4.4}$$

Higgs is subjected to a suitable boundary condition in which only one zero mode appears, independently of the fermions. In general, a pair of right- and left-handed chiral zero modes could become massive due to quantum corrections from the Yukawa interaction and the interaction with the gauge field. Therefore, three left-handed chiral zero-modes remain from Q_d and three right-handed chiral zero-modes from U_s, D_s as the low-energy effective theory, which are nothing but of three generations of fermions in the SM.

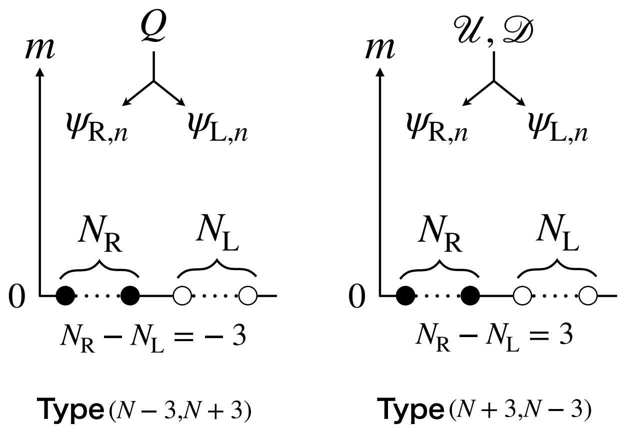

Figure 3.3: Witten index under each boundary condition.

This study is not the first approach to solving the generation problem that applies zero-mode degeneracy. In the 2000s, it was proposed that the number of generations could be reproduced by using vortex and magnetic flux [33–39]. In the 2010s, it was shown that this could be explained by using boundary conditions [15–18]. Our study extends the latter to the case of more diverse extra-dimensional forms.

3.4.2 Fermion mass hierarchy and flavor mixing

In the SM, the generational masses have a hierarchical structure, and particles belonging to different generations interact with each other. There is no theoretical explanation from the SM for these masses or the strength of the interaction. On the other hand, our model is naturally able to explain by using the mechanism proposed in the paper [40].

To explain how this mechanism works, we derive the mass matrix in our model. Under the boundary conditions (3.4.3), (3.4.4), Q_d, U_s and D_s can be expanded as

$$Q_d(x,y) = \sum_{i=1}^{3} \begin{pmatrix} u_{i\mathrm{L}}(x) \\ d_{i\mathrm{L}}(x) \end{pmatrix} g_0^{(i)}(y) + (\text{massive modes}), \tag{3.4.5}$$

$$D_s(x,y) = \sum_{i=1}^{3} d_{i\mathrm{R}}(x) \widetilde{f}_0^{(i)}(y) + (\text{massive modes}), \tag{3.4.6}$$

$$U_s(x,y) = \sum_{i=1}^{3} u_{i\mathrm{R}}(x) f_0^{(i)}(y) + (\text{massive modes}), \tag{3.4.7}$$

where the subscript R/L for a 4d part is a chirality index and all modes with $n > 0$ are denoted as "(massive modes)". It should be noted that the degeneracy of 3 in the above equations is the key consequence of our model. In other words, the generation number problem in the SM is naturally reproduced based on the geometry of the extra dimension.

If the Higgs H has a vacuum expectation value like $\langle H \rangle = (0, v)^\top$, then the action (3.4.2) is written by

$$
\begin{aligned}
S_{\text{Yukawa}} &= \int d^4x \sum_{a=1}^{N} \int_{L_{a-1}}^{L_a} dy \left[g'_Y \overline{Q}_d \langle H \rangle D_s + g_Y \overline{Q}_d \langle \widetilde{H} \rangle U_s + \text{h.c.} \right] \\
&\overset{\text{B.C.}}{\to} \int d^4x \sum_{a=1}^{N} \int_{L_{a-1}}^{L_a} dy\, g'_Y \sum_{i,j=1}^{3} \left(\overline{u_{i\mathrm{L}}}(x), \overline{d_{i\mathrm{L}}}(x) \right) g_0^{(i)*}(y) \begin{pmatrix} 0 \\ v \end{pmatrix} d_{j\mathrm{R}}(x) \widetilde{f}_0^{(j)}(y) + \text{h.c.} \\
&\quad + \int d^4x \sum_{a=1}^{N} \int_{L_{a-1}}^{L_a} dy g_Y \sum_{i,j=1}^{3} \left(\overline{u_{i\mathrm{L}}}(x), \overline{d_{i\mathrm{L}}}(x) \right) g_0^{(i)*}(y) \begin{pmatrix} v \\ 0 \end{pmatrix} u_{j\mathrm{R}}(x) f_0^{(j)}(y) + \text{h.c.} \\
&\quad + \int d^4x \sum_{a=1}^{N} \int_{L_{a-1}}^{L_a} dy\, (\text{massive modes} + \text{h.c.}) \\
&= \int d^4x \sum_{i,j=1}^{3} \left[g'_Y v \sum_{a=1}^{N} \int_{L_{a-1}}^{L_a} dy\, g_0^{(i)*}(y) \widetilde{f}_0^{(j)}(y) \right] \overline{d_{i\mathrm{L}}}(x) d_{j\mathrm{R}}(x) + \text{h.c.} \\
&\quad + \int d^4x \sum_{i,j=1}^{3} \left[g_Y v \sum_{a=1}^{N} \int_{L_{a-1}}^{L_a} dy\, g_0^{(i)*}(y) f_0^{(j)}(y) \right] \overline{u_{i\mathrm{L}}}(x) u_{j\mathrm{R}}(x) + \text{h.c.} \\
&\quad + \int d^4x \sum_{a=1}^{N} \int_{L_{a-1}}^{L_a} dy\, (\text{massive modes} + \text{h.c.}) \\
&= \int d^4x \sum_{i,j=1}^{3} \left[m_{ij} \overline{u_{i\mathrm{L}}}(x) u_{j\mathrm{R}}(x) + \widetilde{m}_{ij} \overline{d_{i\mathrm{L}}}(x) d_{j\mathrm{R}}(x) + \text{h.c.} \right] + (\text{massive modes} + \text{h.c.}), \quad (3.4.8)
\end{aligned}
$$

where m_{ij}, $\widetilde{m}_{ij}$ are defined as

$$
m_{ij} = g_Y v \sum_{a=1}^{N} \int_{L_{a-1}}^{L_a} dy\, g_0^{(i)*}(y) f_0^{(j)}(y), \quad (3.4.9)
$$

$$
\widetilde{m}_{ij} = g'_Y v \sum_{a=1}^{N} \int_{L_{a-1}}^{L_a} dy\, g_0^{(i)*}(y) \widetilde{f}_0^{(j)}(y). \quad (3.4.10)
$$

The zero-mode solutions are given by (3.2.16), (3.2.17). Therefore, if $f_0^{(i)}(y)$ and $g_0^{(j)}$ take the profile shown in Fig. 3.4, for example, fermion mass hierarchy is also naturally realized, i.e., $m_{11} \ll m_{22} \ll m_{33}$ is feasible. The same applies to $\widetilde{m}_{ij}$. In addition, the mass matrix m_{ij}, $\widetilde{m}_{ij}$ now also have off-diagonal components, and the value of flavor mixing can be naturally explained by the profile of zero-modes. It is noted that m_{13} can have a nonzero value since $y = L_0$ and $y = L_{10}$ are identified and $f_0^{(3)}$, $g_0^{(1)}$ overlap. By the above mechanism, our model can theoretically explain not only the number of generations but also the fermion mass hierarchy and the flavor mixing.

3.4.3 *CP* phase

CP phases are complex only of the Cabibbo–Kobayashi–Maskawa matrix and Pontecorvo–Maki–Nakagawa–Sakata (PMNS) matrix in the SM. In our model, we obtain (3.4.9) and (3.4.10) as mass

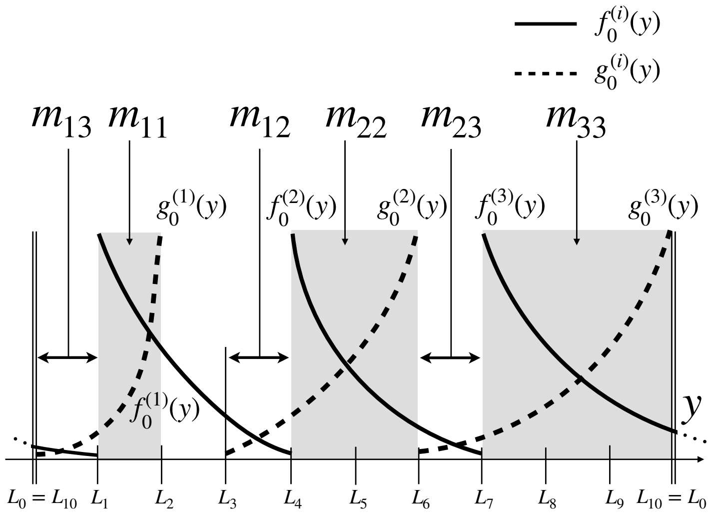

Figure 3.4: Relationship between zero-mode profiles and mass matrix. By applying the exponential localization of zero modes, masses with a hierarchical structure can be realized. The double lines at $y = L_0,\ L_{10}$ represent the same point.

matrices at low energies, which can be complex matrices since $f_0^{(i)}(y)$, $g_0^{(j)}(y)$ are genuine complex functions. When constructing the phenomenological model, it is necessary to change the phases for three generations of quarks and calculate complex phases that will eventually remain in the mass matrix.

3.5 Summary and discussion

In this chapter, we have investigated the KK decomposition of the 5d Dirac fermion on the rose graph which consists of one vertex and N loops (see Fig. 3.1). We have succeeded in classifying the allowed boundary conditions on the rose graph into the type$(2N-k, k)$ BC with $0 \le k \le 2N$ and finding the number of the zero mode solutions for each type of the boundary conditions.

Using the present results, for models with type$(N-3, N+3)$ or type$(N+3, N-3)$ boundary conditions imposed, only the chiral zero modes, either right-handed or left-handed, is threefold degenerate. Therefore, we explained the possibility of simultaneously solving the three remaining problems of the SM: the generation number problem, the mass hierarchy problem of fermions, and the origin of flavor mixing and CP phases. However, since the SM includes gauge fields as dynamical fields, additional boundary conditions on the gauge fields must be considered when quantitatively evaluating the solvability of the above problems. It is important to note that the boundary conditions must not break gauge symmetry. This means that the boundary conditions for gauge fields are more restrictive than those for fermions derived in this Chapter.

It would be of great interest to note that the rose graph has nontrivial geometry and that the parameter space of the boundary conditions has been found to possess a rich structure. For instance, if we take the length of all bonds to be equal ($L = L_a - L_{a-1}$ for $a = 1, 2, \cdots, N$) and choose the boundary conditions appropriately, we will have higher degeneracy in the 4d mass spectrum and then extended supersymmetries might appear in the spectrum [7, 8].

Chapter 4

Instantons and Berry's connections on quantum graph

Berry's phases and Berry's connections are interesting phenomena that appear in quantum systems when model parameters are adiabatically driven along a closed path on a parameter space. Once a nontrivial Berry's phase or Berry's connection is obtained, it is known that the parameter space under consideration has a nontrivial topological structure.

We consider a Dirac fermion on a 5-dimensional (5d) spacetime with a quantum graph as an extra dimension. As clarified in Chap. 3, the mode functions on quantum graph have a parameter dependence on the boundary conditions. Furthermore, zero modes generally have many degeneracies. Therefore, the parameter space of the boundary conditions may have a nontrivial topological structure, resulting in a nontrivial non-Abelian Berry's connection. In this chapter, we show that the ADHM construction method can be applied to construct instanton solutions as Berry's connections in the parameter space of boundary conditions.

This chapter is organized as follows: In Secs. 4.1 and 4.2, we briefly review the basics of instantons and the ADHM construction method. In Sec. 4.3, we reiterate our setup and explain how the ADHM construction method is applied. In Sec. 4.4, applying the ADHM construction method, we construct the instanton solution as a Berry's connection.

4.1 Brief review of instanton

Before going into the content of this study, we briefly review instanton. An instanton on 4d Euclidean spacetime is a configuration of gauge fields that satisfies the 4d (anti-)self-dual equation and makes the Yang–Mills action finite. This equation of $SU(N)$ Yang–Mills theory is given by

$$F_{\mu\nu} = \pm\widetilde{F}_{\mu\nu} \quad (\mu, \nu = 1, 2, 3, 4), \tag{4.1.1}$$

where the field strength $F_{\mu\nu}$ and its Hodge dual $\widetilde{F}_{\mu\nu}$ are defined as

$$F_{\mu\nu} = \partial_\mu A_\nu - \partial_\nu A_\mu + [A_\mu, A_\nu], \tag{4.1.2}$$

$$\widetilde{F}_{\mu\nu} = \frac{1}{2}\epsilon_{\mu\nu\rho\sigma}F_{\rho\sigma}, \tag{4.1.3}$$

and the gauge field A_μ is defined as an $n \times n$ anti-Hermitian matrix. In Eq. (4.1.1), + means self dual and − means anti-self dual. The (anti-)self-dual equation gives the minimum value of the Yang-Mills action. Completing the square of the action yields

$$\begin{aligned} S_{\mathrm{YM}} &= -\frac{1}{2g_{\mathrm{YM}}^2}\int d^4x\,\mathrm{Tr}\,(F_{\mu\nu}F_{\mu\nu}) \\ &= -\frac{1}{4g_{\mathrm{YM}}^2}\int d^4x\,\mathrm{Tr}\,(F_{\mu\nu}F_{\mu\nu}+\widetilde{F}_{\mu\nu}\widetilde{F}_{\mu\nu}) \\ &= -\frac{1}{4g_{\mathrm{YM}}^2}\int d^4x\,\mathrm{Tr}\left[(F_{\mu\nu}\pm\widetilde{F}_{\mu\nu})^2\mp 2F_{\mu\nu}\widetilde{F}_{\mu\nu}\right] \\ &= -\frac{1}{4g_{\mathrm{YM}}^2}\int d^4x\,\mathrm{Tr}\,(F_{\mu\nu}\pm\widetilde{F}_{\mu\nu})^2 \pm \frac{8\pi^2}{g_{\mathrm{YM}}^2}\left[\frac{-1}{16\pi^2}\int d^4x\,\mathrm{Tr}\,(F_{\mu\nu}\widetilde{F}_{\mu\nu})\right], \end{aligned} \tag{4.1.4}$$

and the condition that the first term be zero is nothing but (anti-)self-dual equation (4.1.1). The second term in the above equation can be expressed as

$$\pm\frac{8\pi^2}{g_{\mathrm{YM}}^2}\left[\frac{-1}{16\pi^2}\int d^4x\,\mathrm{Tr}\,(F_{\mu\nu}\widetilde{F}_{\mu\nu})\right] = \frac{8\pi^2}{g_{\mathrm{YM}}^2}|Q| \tag{4.1.5}$$

with a topological charge Q. The Q takes integer values. To take finite values for $|Q|$, the field strength must satisfy $F_{\mu\nu} = 0$ (called pure gauge) at infinity. Under these conditions, the integer value Q is called the instanton number. Solutions with $Q = k$ are called k-instantons, solutions with $Q > 1$ are called multi-instantons, and solutions with $Q < 0$ are called anti-instantons.

Instanton solutions are described by a certain number of parameters, which is called the moduli space, except for the degrees of freedom that are transferred by the gauge transformation. The dimension of the moduli space of the k-instanton of the gauge group $SU(N)$ is known to be

$$\dim \mathcal{M}_{N,k} = \begin{cases} 4Nk - N^2 + 1 & (N \le 2k), \\ 4k^2 + 1 & (N > 2k). \end{cases} \tag{4.1.6}$$

4.2 ADHM construction

The ADHM construction method was discovered by Atiyah, Drinfeld, Hitchin, and Manin[22]. The idea is to construct a solution by focusing on the moduli space of ADHM data, which is dual to the moduli space of instantons and following appropriate procedures. Since there is a one-to-one correspondence between the moduli spaces of each other, arbitrary instanton solutions can be constructed using the ADHM construction method.

In this section, we describe the ADHM construction procedure and construct some well-known instanton solutions as examples.

4.2.1 Notations

In this subsection, we summarize the notation of the symbols used in this chapter.

First, we introduce 2×2 matrices

$$e_\mu = (-i\sigma^i,\ 1), \quad \bar{e}_\mu = (i\sigma^i,\ 1) \qquad (\mu = 1,2,3,4) \tag{4.2.1}$$

where σ^i $(i = 1, 2, 3)$ are Pauli matrices.

Second, the 't Hooft matrix is defined by

$$\eta^{(\pm)}_{\mu\nu} = \eta^{a(\pm)}_{\mu\nu}\sigma_a, \tag{4.2.2}$$

where $\eta^{a(\pm)}_{\mu\nu}$ is called the 't Hoot symbol and given by

$$\eta^{a(\pm)}_{\mu\nu} = \epsilon_{a\mu\nu 4} \pm (\delta_{a\mu}\delta_{\nu 4} - \delta_{a\nu}\delta_{\mu 4}) \quad (a = 1, 2, 3). \tag{4.2.3}$$

These are useful for constructing instanton solutions. Matrices (4.2.1) and the 't Hooft matrix (4.2.2) satisfy the following relationship.

$$\bar{e}_\mu e_\nu = \delta_{\mu\nu} + i\eta^{(+)}_{\mu\nu}, \qquad e_\mu \bar{e}_\nu = \delta_{\mu\nu} + i\eta^{(-)}_{\mu\nu}, \tag{4.2.4}$$

$$e_\mu \bar{e}_\nu + e_\nu \bar{e}_\mu = 2\delta_{\mu\nu}, \qquad \bar{e}_\mu e_\nu + \bar{e}_\nu e_\mu = 2\delta_{\mu\nu}, \tag{4.2.5}$$

$$e_\mu \bar{e}_\nu e_\mu = -2e_\nu, \qquad \bar{e}_\mu e_\nu \bar{e}_\mu = -2\bar{e}_\nu. \tag{4.2.6}$$

Some useful relations satisfied by the 't Hooft matrix $\eta^{(\pm)}_{\mu\nu}$ are

$$\begin{aligned}
\eta^{(\pm)}_{\mu\nu}\eta^{(\pm)}_{\lambda\rho} &= (\delta_{\mu\lambda}\delta_{\nu\rho} - \delta_{\mu\rho}\delta_{\nu\lambda} \pm \epsilon_{\mu\nu\lambda\rho}) \cdot 1 \\
&\quad + i\left(\delta_{\mu\lambda}\eta^{(\pm)}_{\nu\rho} - \delta_{\mu\rho}\eta^{(\pm)}_{\nu\lambda} + \delta_{\nu\rho}\eta^{(\pm)}_{\mu\lambda} - \delta_{\nu\lambda}\eta^{(\pm)}_{\mu\rho}\right), && (4.2.7) \\
\left[\eta^{(\pm)}_{\mu\nu}, \eta^{(\pm)}_{\lambda\rho}\right] &= 2i\left(\delta_{\mu\lambda}\eta^{(\pm)}_{\nu\rho} - \delta_{\nu\lambda}\eta^{(\pm)}_{\mu\rho} + \delta_{\mu\rho}\eta^{(\pm)}_{\lambda\nu} - \delta_{\nu\rho}\eta^{(\pm)}_{\lambda\mu}\right), && (4.2.8) \\
\epsilon_{\mu\nu\lambda\rho}\eta^{(\pm)}_{\sigma\rho} &= \pm\left(\delta_{\mu\sigma}\eta^{(\pm)}_{\nu\lambda} + \delta_{\lambda\sigma}\eta^{(\pm)}_{\mu\nu} + \delta_{\nu\sigma}\eta^{(\pm)}_{\lambda\mu}\right), && (4.2.9) \\
\mathrm{Tr}\,\eta^{(\pm)}_{\mu\nu}\eta^{(\pm)}_{\lambda\rho} &= 2\left(\delta_{\mu\lambda}\delta_{\nu\rho} - \delta_{\mu\rho}\delta_{\nu\lambda} \pm \epsilon_{\mu\nu\lambda\rho}\right), && (4.2.10) \\
\mathrm{Tr}\,\eta^{(\pm)}_{\mu\nu}\eta^{(\pm)}_{\mu\rho} &= 6\delta_{\nu\rho}, && (4.2.11) \\
\mathrm{Tr}\,\eta^{(\pm)}_{\mu\nu}\eta^{(\pm)}_{\mu\nu} &= 24. && (4.2.12)
\end{aligned}$$

The relations satisfied by the 't Hooft symbol $\eta^{a(\pm)}_{\mu\nu}$ are

$$\begin{aligned}
\eta^{i(\pm)}_{\mu\nu}\eta^{j(\pm)}_{\lambda\rho} &= (\delta_{\mu\lambda}\delta_{\nu\rho} - \delta_{\mu\rho}\delta_{\nu\lambda} \pm \epsilon_{\mu\nu\lambda\rho})\delta_{ij} \\
&\quad + \frac{1}{2}\epsilon_{ijk}\left(\delta_{\mu\lambda}\eta^{k(\pm)}_{\nu\rho} - \delta_{\mu\rho}\eta^{k(\pm)}_{\nu\lambda} + \delta_{\nu\rho}\eta^{k(\pm)}_{\mu\lambda} - \delta_{\nu\lambda}\eta^{k(\pm)}_{\mu\rho}\right), && (4.2.13) \\
\eta^{i(\pm)}_{\mu\nu}\eta^{j(\pm)}_{\mu\rho} &= \delta_{\nu\rho}\delta_{ij} + \epsilon_{ijk}\eta^{k(\pm)}_{\nu\rho}, && (4.2.14) \\
\eta^{a(-)}_{\mu\nu} &= -\frac{i}{2}\mathrm{Tr}\,\sigma^a\bar{e}_\mu e_\nu, && (4.2.15) \\
\eta^{a(-)}_{\mu\nu} &= -\frac{i}{2}\mathrm{Tr}\,\sigma^a e_\mu \bar{e}_\nu. && (4.2.16)
\end{aligned}$$

To specify the size of an $m \times n$ matrix M, we write $M_{[m]\times[n]}$ with [...] as a subscript.

4.2.2 Procedures for the ADHM construction

We explain the construction of $SU(N)$ anti-self dual instanton solutions for the instanton number $-k$ using the ADHM construction method. If one wants to construct self-dual instanton solutions instead of anti-self dual, $\bar{e}_\mu$ is replaced to e_μ in the following procedures.

First, we introduce the following matrix called the 0d Dirac operator:

$$\Delta(x)_{[N+2k]\times[2k]} = \begin{pmatrix} S_{[N]\times[2k]} \\ e_\mu \otimes (x_\mu 1_k - (T_\mu)_{[k]\times[k]}) \end{pmatrix}, \tag{4.2.17}$$

$$\Delta^\dagger(x)_{[2k]\times[N+2k]} = \begin{pmatrix} S^\dagger_{[2k]\times[N]} & \bar{e}_\mu \otimes (x_\mu 1_k - (T_\mu)_{[k]\times[k]}) \end{pmatrix}, \tag{4.2.18}$$

where x_μ ($\mu = 1, 2, 3, 4$) are the coordinates of the 4d Euclid spacetime, the matrix S is defined by

$$S_{[N]\times[2k]} = \begin{pmatrix} I^\dagger_{[N]\times[k]} & J_{[N]\times[k]} \end{pmatrix} \tag{4.2.19}$$

with $N \times k$ complex constant matrices $I^\dagger$, J, and T_μ is $k \times k$ constant Hermitian matrix. We will see later that the matrix sizes k and N correspond to the instanton number and the size of the gauge group, respectively. The matrices I, J, T_μ are not arbitrary and must satisfy the ADHM equations

$$[T_1, T_2] + [T_3, T_4] - \frac{i}{2}(II^\dagger - J^\dagger J) = 0, \tag{4.2.20}$$

$$[T_1, T_3] - [T_2, T_4] - \frac{1}{2}(IJ - J^\dagger J^\dagger) = 0, \tag{4.2.21}$$

$$[T_1, T_4] + [T_2, T_3] - \frac{i}{2}(IJ + J^\dagger J^\dagger) = 0. \tag{4.2.22}$$

In addition, $\Delta^\dagger\Delta$ must be invertible. This invertibility implies that the $2k$ column vectors in

$$\Delta(x) = \left(\vec{\Delta}_1, \vec{\Delta}_2, \cdots, \vec{\Delta}_{2k}\right), \quad \vec{\Delta}_i = (\vec{\Delta}_i)_{[N+2k]\times[1]} \tag{4.2.23}$$

are linearly independent of each other.

In the second step, we find the normalized solution V that satisfies the equation

$$\Delta^\dagger(x)_{[2k]\times[N+2k]} V_{[N+2k]\times[N]} = 0, \quad V^\dagger V = 1_N. \tag{4.2.24}$$

In the final step, using the derivative ∂_μ with respect to the coordinate x_μ in 4d Euclid space, we can compute

$$(\mathcal{A}_\mu)_{[N]\times[N]} = V^\dagger \partial_\mu V \tag{4.2.25}$$

to obtain the desired instanton configuration.

See Appendix B for a more detailed description of the ADHM construction method.

4.2.3 Some concrete examples

We show how the ADHM construction method works through specific examples. In the following, $SU(2)$ BPST instanton, $SU(N)$ one-instanton, and $SU(2)$ 't Hooft instanton are presented as examples.

4.2.3.1 $SU(2)$ BPST instanton

We construct $SU(2)$ Belavin–Polyakov–Schwartz–Tyupkin (BPST) instanton [41] by the ADHM construction. This is an $SU(2)$ anti-self dual instanton solution with instanton number -1.

First, we determine the constant complex matrices $I^\dagger_{[N]\times[k]}$, $J_{[N]\times[k]}$ and the constant Hermitian matrix $(T_\mu)_{[k]\times[k]}$ that satisfy the ADHM Eqs. (4.2.20)-(4.2.22). Since $k = 1$, T_μ is a real constant rather than a Hermitian matrix. And $I^\dagger$, J are two dimensional complex vectors because of $N = 2$. Therefore, Eqs. (4.2.20)-(4.2.22) break down to

$$-\frac{i}{2}(II^\dagger - J^\dagger J) = 0, \tag{4.2.26}$$

$$-\frac{1}{2}(IJ - J^\dagger I^\dagger) = 0, \tag{4.2.27}$$

$$-\frac{i}{2}(IJ + J^\dagger I^\dagger) = 0, \tag{4.2.28}$$

The general two dimensional complex vectors $I^\dagger$, J satisfying the above equations are given by

$$I^\dagger = \begin{pmatrix} i_1 \\ i_2 \end{pmatrix}, \quad J = \begin{pmatrix} i_2^* \\ -i_1^* \end{pmatrix} \quad (i_1, i_2 \in \mathbb{C}). \tag{4.2.29}$$

To simplify the computation, we transform the matrices $I^\dagger$ and J using the ADHM transformation as follows:

$$I^\dagger \to QI^\dagger R = \begin{pmatrix} \sqrt{|i_1|^2 + |i_2|^2} \\ 0 \end{pmatrix} \equiv \begin{pmatrix} \rho \\ 0 \end{pmatrix}, \tag{4.2.30}$$

$$J \to QJR = \begin{pmatrix} 0 \\ \sqrt{|i_1|^2 + |i_2|^2} \end{pmatrix} \equiv \begin{pmatrix} 0 \\ \rho \end{pmatrix}, \tag{4.2.31}$$

where ρ is a real constant and Q, R are given by

$$Q = \frac{1}{\sqrt{|i_1|^2 + |i_2|^2}} \begin{pmatrix} i_1^* & i_2^* \\ i_2 & -i_1 \end{pmatrix} \in SU(2), \quad R = e^{-i\pi/2} \in U(1). \tag{4.2.32}$$

See Appendix B.2 for a detailed description of ADHM trasnformation. The real constants T_μ are denoted by

$$T_\mu = b_\mu \in \mathbb{R} \quad (\mu = 1, 2, 3, 4). \tag{4.2.33}$$

Next, we consider the 0d Dirac operator (4.2.24) and construct its solution $V_{[N+2k]\times[N]}$. In this case, the 0d Dirac operator is given by

$$\Delta(x)_{[4]\times[2]} = \begin{pmatrix} \begin{pmatrix} (I^\dagger) & (J) \end{pmatrix}_{[2]\times[2]} \\ e_\mu(x_\mu - b_\mu) \end{pmatrix} = \begin{pmatrix} \rho & 0 \\ 0 & \rho \\ \multicolumn{2}{c}{e_\mu(x_\mu - b_\mu)} \end{pmatrix}, \tag{4.2.34}$$

$$\Delta^\dagger(x)_{[2]\times[4]} = \begin{pmatrix} \begin{matrix} \rho & 0 \\ 0 & \rho \end{matrix} & \bar{e}_\mu(x_\mu - b_\mu) \end{pmatrix}, \tag{4.2.35}$$

so the normalized solution can be obtained as

$$\begin{aligned} V_{[4]\times[2]} &= \frac{1}{\sqrt{(x-b)^2 + \rho^2}} \begin{pmatrix} \multicolumn{2}{c}{\bar{e}_\mu(x_\mu - b_\mu)} \\ -\rho & 0 \\ 0 & -\rho \end{pmatrix} \\ &= \frac{1}{\sqrt{(x-b)^2 + \rho^2}} \begin{pmatrix} ix_3 - ib_3 + x_4 - b_4 & ix_1 - ib_1 - x_2 - b_2 \\ ix_1 - ib_1 - x_2 + b_2 & -ix_3 + ib_3 + x_4 - b_4 \\ -\rho & 0 \\ 0 & -\rho \end{pmatrix} \end{aligned} \tag{4.2.36}$$

from Eq. (4.2.24).

Finally, by computing (4.2.25), we can obtain

$$
\begin{aligned}
(\mathcal{A}_\mu)_{[2]\times[2]} &= V^\dagger \partial_\mu V \\
&= -\frac{(x-b)_\mu}{(x-b)^2+\rho^2} + \frac{1}{(x-b)^2+\rho^2} e_\nu \bar{e}_\mu (x-b)_\nu \\
&= -\frac{(x-b)_\mu}{(x-b)^2+\rho^2} + \frac{1}{(x-b)^2+\rho^2} \left(\delta_{\mu\nu} + i\eta^{(-)}_{\mu\nu}\right)(x-b)_\nu \quad (\because (4.2.4)) \\
&= -i\eta^{(-)}_{\mu\nu} \frac{(x-b)_\nu}{(x-b)^2+\rho^2}.
\end{aligned} \tag{4.2.37}
$$

This solution is the $SU(2)$ BPST instanton, where b_μ is the position of the instanton and ρ is the parameter corresponding to its size of it.

4.2.3.2 $SU(N)$ one-instanton

$SU(N)$ one-instanton is the solution with $SU(2)$ BPST instantons in the 2×2 part of the $N \times N$ matrix.

First, we determine the complex constant matrices $I^\dagger_{[N]\times[k]}$, $J_{[N]\times[k]}$ and the constant Hermitian matrix $(T_\mu)_{[k]\times[k]}$ that satisfy the ADHM equations (4.2.20)-(4.2.22). Since $k = 1$, the $I^\dagger$, J are complex constant vectors and as general solutions given by

$$
I^\dagger = \begin{pmatrix} i_1 \\ i_2 \\ \vdots \\ i_N \end{pmatrix}, \quad J = \begin{pmatrix} j_1 \\ j_2 \\ \vdots \\ j_N \end{pmatrix}, \quad I^\dagger J = 0, \quad |I|^2 = |J|^2. \tag{4.2.38}
$$

To simplify the computation, we transform the vectors $I^\dagger$ and J using the ADHM transformation as follows:

$$
I^\dagger = \begin{pmatrix} \sqrt{|i_1|^2 + \cdots + |i_N|^2} \\ 0 \\ \vdots \\ 0 \end{pmatrix} \equiv \begin{pmatrix} \rho \\ 0 \\ \vdots \\ 0 \end{pmatrix}, \tag{4.2.39}
$$

$$
J = \begin{pmatrix} 0 \\ \sqrt{|i_1|^2 + \cdots + |i_N|^2} \\ \vdots \\ 0 \end{pmatrix} \equiv \begin{pmatrix} 0 \\ \rho \\ \vdots \\ 0 \end{pmatrix}, \tag{4.2.40}
$$

where ρ is real constant. The real constant T_μ are represented by

$$
T_\mu = b_\mu \in \mathbb{R} \quad (\mu = 1, 2, 3, 4) \tag{4.2.41}
$$

as the previous example.

Next, we consider the 0d Dirac operator (4.2.24) and construct its solution $V_{[N+2]\times[N]}$. In this case, the 0d Dirac operator is given by

$$\Delta(x)_{[N+2]\times[2]} = \begin{pmatrix} \rho & 0 \\ 0 & \rho \\ \vec{0} & \vec{0} \\ \multicolumn{2}{c}{e_\mu(x_\mu - b_\mu)} \end{pmatrix}, \tag{4.2.42}$$

$$\Delta^\dagger(x)_{[2]\times[N+2]} = \begin{pmatrix} \rho & 0 & \vec{0}^\top & \bar{e}_\mu(x_\mu - b_\mu) \\ 0 & \rho & \vec{0}^\top & \end{pmatrix}, \tag{4.2.43}$$

so the normalized solution can be obtained

$$V_{[N+2]\times[N]} = \frac{1}{\sqrt{(x-b)^2+\rho^2}} \left(\begin{array}{cc|ccc} \multicolumn{2}{c|}{\bar{e}_\mu(x_\mu - b_\mu)} & 0 & \cdots & 0 \\ & & 0 & \cdots & 0 \\ \hline 0 & 0 & & & \\ \vdots & \vdots & & c1_{N-2} & \\ 0 & 0 & & & \\ \hline -\rho & 0 & 0 & \cdots & 0 \\ 0 & -\rho & 0 & \cdots & 0 \end{array}\right),$$

$$c \equiv \sqrt{(x-b)^2+\rho^2}, \tag{4.2.44}$$

Finally, by computing (4.2.25), we can obtain

$$(\mathcal{A}_\mu)_{[N]\times[N]} = \begin{pmatrix} \mathcal{A}_\mu^{SU(2)} & 0_{[2]\times[N-2]} \\ 0_{[N-2]\times[2]} & 0_{[N-2]\times[N-2]} \end{pmatrix}, \tag{4.2.45}$$

$$\left(\mathcal{A}_\mu^{SU(2)}\right)_{[2]\times[2]} = -i\eta^{(-)}_{\mu\nu}\frac{(x-b)_\nu}{(x-b)^2+\rho^2}. \tag{4.2.46}$$

This solution is a $SU(N)$ one-instanton with the $SU(2)$ BPST instanton solution in the 2×2 part of the $N\times N$ matrix.

4.2.3.3 $SU(2)$ 't Hooft instanton

The 't Hooft instanton is the $SU(2)$ anti-self dual instanton with instanton number $-k$. Therefore, we consider the case $N = 2$ and $k > 1$ and apply the ADHM construction.

To simplify the solution of the ADHM equation, we restrict T_μ to be of the form

$$(T_\mu)_{[k]\times[k]} = \begin{pmatrix} b^1_\mu & & & \mathbf{0} \\ & b^2_\mu & & \\ & & \ddots & \\ \mathbf{0} & & & b^k_\mu \end{pmatrix} \quad (b^1_\mu, b^2_\mu, \cdots, b^k_\mu \in \mathbb{R},\ k > 1). \tag{4.2.47}$$

Under this restriction, we determine the complex constant matrices $I^\dagger_{[2]\times[k]}$, $J_{[2]\times[k]}$ that satisfy the

ADHM equations

$$-\frac{i}{2}(II^\dagger - J^\dagger J) = 0, \tag{4.2.48}$$
$$-\frac{1}{2}(IJ - J^\dagger I^\dagger) = 0, \tag{4.2.49}$$
$$-\frac{i}{2}(IJ + J^\dagger I^\dagger) = 0. \tag{4.2.50}$$

The general solutions of $I^\dagger_{[2]\times[k]}$, $J_{[2]\times[k]}$ satisfying these equations are given by

$$I^\dagger = \begin{pmatrix} i_{11} & i_{12} & \cdots & i_{1k} \\ i_{21} & i_{22} & \cdots & i_{2k} \end{pmatrix}, \quad J = \begin{pmatrix} j_{11} & j_{12} & \cdots & j_{1k} \\ j_{21} & j_{22} & \cdots & j_{2k} \end{pmatrix}, \quad I^\dagger J = 0, \quad |I|^2 = |J|^2 = 1. \tag{4.2.51}$$

To simplify the computation, we transform the matrices $I^\dagger$ and J using the ADHM transformation

$$I^\dagger \to QI^\dagger R, \quad J \to QJR \quad (Q \in SU(2),\, R \in U(k)). \tag{4.2.52}$$

First, the R transformation sets the lower component to 0, leaving one component, and then the Q transformation transforms the remaining vertical vector into the form $(i''_{11}, 0)^\top$.

$$\begin{pmatrix} i_{11} & i_{12} & \cdots & i_{1k} \\ i_{21} & i_{22} & \cdots & i_{2k} \end{pmatrix} \xrightarrow{R} \begin{pmatrix} i'_{11} & i'_{12} & \cdots & i'_{1k} \\ i'_{21} & 0 & \cdots & 0 \end{pmatrix} \xrightarrow{Q} \begin{pmatrix} i''_{11} & i'_{12} & \cdots & i'_{1k} \\ 0 & 0 & \cdots & 0 \end{pmatrix} \tag{4.2.53}$$

Therefore, we can obtain

$$I^\dagger \to \begin{pmatrix} \rho_1 & \rho_2 & \cdots & \rho_k \\ 0 & 0 & \cdots & 0 \end{pmatrix}, \quad J \to \begin{pmatrix} 0 & 0 & \cdots & 0 \\ \rho_1 & \rho_2 & \cdots & \rho_k \end{pmatrix} \quad (\rho_1, \rho_2, \cdots, \rho_k \in \mathbb{R}), \tag{4.2.54}$$

where the transformation of J is obtained from Eq. (4.2.51).

Next, we consider the 0d Dirac operator (4.2.24) and construct its solution $V_{[2+2k]\times[2]}$. In this case, the 0d Dirac operator is given by

$$\begin{aligned} \Delta(x)_{[2+2k]\times[2k]} &= \begin{pmatrix} S_{[2]\times[2k]} \\ \left(e_\mu \otimes \left[x_\mu 1_k - (T_\mu)_{[k]\times[k]}\right]\right)_{[2k]\times[2k]} \end{pmatrix} \\ &= \begin{pmatrix} \begin{pmatrix} \rho_1 & \cdots & \rho_k & 0 & \cdots & 0 \\ 0 & \cdots & 0 & \rho_1 & \cdots & \rho_k \end{pmatrix}_{[2]\times[2k]} \\ \left(e_\mu \otimes \left[x_\mu 1_k - (T_\mu)_{[k]\times[k]}\right]\right)_{[2k]\times[2k]} \end{pmatrix}, \end{aligned} \tag{4.2.55}$$

$$\Delta^\dagger(x)_{[2k]\times[2+2k]} = \left(S^\dagger_{[2k]\times[2]} \quad \left(\bar{e}_\mu \otimes \left[x_\mu 1_k - (T_\mu)_{[k]\times[k]}\right]\right)\right), \tag{4.2.56}$$

where $S_{[2]\times[2k]} \equiv \left((I^\dagger)\ (J)\right)_{[2]\times[2k]}$. Therefore the normalized solution can be obtained

$$V_{[2+2k]\times[2]} = \frac{1}{\sqrt{\phi}} \begin{pmatrix} 1_2 \\ -\left(\bar{e}_\mu \otimes \left(x_\mu 1_k - T_\mu\right)\right)^{-1} S^\dagger \end{pmatrix}, \tag{4.2.57}$$

where

$$\left(\bar{e}_\mu \otimes \left(x_\mu 1_k - T_\mu\right)\right)^{-1} = e_\mu \otimes \begin{pmatrix} \frac{(x-b^1)_\mu}{(x-b^1)^2} & & & 0 \\ & \frac{(x-b^2)_\mu}{(x-b^2)^2} & & \\ & & \ddots & \\ 0 & & & \frac{(x-b^k)_\mu}{(x-b^k)^2} \end{pmatrix}_{[k]\times[k]}, \tag{4.2.58}$$

$$\phi = 1 + \sum_{i=1}^{k} \frac{\rho_i^2}{(x-b^i)^2}. \tag{4.2.59}$$

Finally, by computing (4.2.25), we can obtain

$$\begin{aligned}(\mathcal{A}_\mu)_{[2]\times[2]} &= V^\dagger \partial_\mu V \\ &= -i\eta^{(+)}_{\mu\alpha} \frac{\sum_{i=1}^{k} \rho_i^2 \frac{(x-b_i)^\alpha}{(x-b_i)^2}}{1 + \sum_{i=1}^{k} \frac{\rho_i^2}{(x-b_i)^2}}.\end{aligned} \tag{4.2.60}$$

See the Appendix A for details of calculations. This is nothing but the 't Hooft instanton solution.

4.3 Application to quantum graph extra dimensional model

We consider a 5d Dirac fermion on the 5d spacetime with a quantum graph as an extra dimension. In such the case, the 5d Dirac fermion expanded as the KK expansion and mode functions on the quantum graph direction depend on boundary condition of the quantum graph. Now, it is possible to compute the non-Abelian Berry's connection for the parameter space of boundary conditions. In this Section, the setup is summarized again to illustrate the application of the ADHM construction method.

4.3.1 Setup

The same setup is considered throughout Chap. 3, 4 and 5 in this dissertation. In this Subsection, we brief summarize the setup again. See Chap. 3 for more details.

We consider the quantum graph shown in Fig. 4.1, which consists of N loops and a vertex. At the vertex, $2N$ lines are connected with appropriate boundary conditions for the current to be conserved.

The Dirac zero modes on the quantum graph satisfy the eigenequations

$$(\partial_y + M) f_0^{(i)}(y) = 0, \tag{4.3.1}$$

$$(-\partial_y + M) g_0^{(j)}(y) = 0, \tag{4.3.2}$$

and the general solution is given by

$$f_0^{(i)}(y) = \sum_{a=1}^{N} \theta(y - L_{a-1})\theta(L_a - y) A_a^{(i)} C_a e^{-My} \quad \left(C_a \equiv \sqrt{\frac{1}{e^{-2M(L_{a-1}+\varepsilon)} + e^{-2M(L_a-\varepsilon)}}} \right), \tag{4.3.3}$$

$$g_0^{(j)}(y) = \sum_{a=1}^{N} \theta(y - L_{a-1})\theta(L_a - y) B_a^{(j)} C'_a e^{My} \quad \left(C'_a \equiv \sqrt{\frac{1}{e^{2M(L_{a-1}+\varepsilon)} + e^{2M(L_a-\varepsilon)}}} \right), \tag{4.3.4}$$

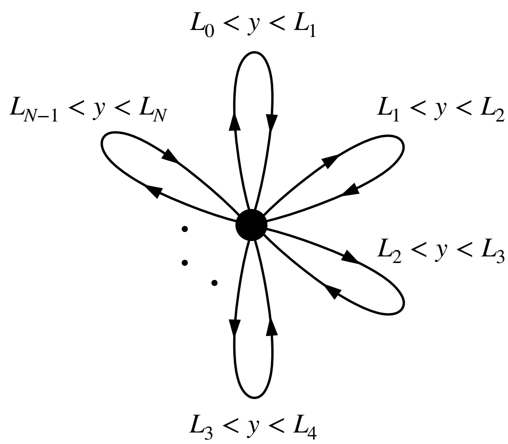

Figure 4.1: Rose graph consisting of N edges and single vertex.

where $A_a^{(i)}$, $B_a^{(j)}$ are determined by boundary conditions. The boundary conditions are given by

$$(I_{2N} - U_{\rm B})\,\vec{F}_n^{(i)} = 0, \quad (I_{2N} + U_{\rm B})\,\vec{G}_m^{(j)} = 0, \tag{4.3.5}$$

$$(U_{\rm B}^2 = 1_{2N}, \quad U_{\rm B}^\dagger = U_{\rm B}), \tag{4.3.6}$$

where $\vec{F}_n^{(i)}$, $\vec{G}_m^{(j)}$ are defined by

$$\vec{F}_n^{(i)} \equiv \begin{pmatrix} f_n^{(i)}(L_0+\varepsilon) \\ f_n^{(i)}(L_1-\varepsilon) \\ \vdots \\ f_n^{(i)}(L_{N-1}+\varepsilon) \\ f_n^{(i)}(L_N-\varepsilon) \end{pmatrix}, \qquad \vec{G}_m^{(j)} \equiv \begin{pmatrix} g_m^{(j)}(L_0+\varepsilon) \\ -g_m^{(j)}(L_1-\varepsilon) \\ \vdots \\ g_m^{(j)}(L_{N-1}+\varepsilon) \\ -g_m^{(j)}(L_N-\varepsilon) \end{pmatrix}. \tag{4.3.7}$$

Since the matrix $U_{\rm B}$ is a $2N \times 2N$ Hermitian matrix with eigenvalues of ± 1, it can be diagonalized into the form

$$\text{Type}(2N-k, k) : U_{\rm B} = V \begin{pmatrix} 1_{2N-k} & \mathbf{0} \\ \mathbf{0} & -1_k \end{pmatrix} V^\dagger \quad (k = 0, 1, \cdots, 2N) \tag{4.3.8}$$

using the unitary matrix V.

We introduce a new orthonormal basis in which the number of independent zero-modes can be easily counted.

$$\vec{\mathcal{F}}_a \equiv C_a(\underbrace{0, \ldots, 0}_{2(a-1)}, e^{-M(L_{a-1}+\varepsilon)}, e^{-M(L_a-\varepsilon)}, 0, \cdots, 0)^\top, \tag{4.3.9}$$

$$\vec{\mathcal{G}}_a \equiv C'_a(\underbrace{0, \ldots, 0}_{2(a-1)}, e^{M(L_{a-1}+\varepsilon)}, -e^{M(L_a-\varepsilon)}, 0, \cdots, 0)^\top. \tag{4.3.10}$$

In these bases, boundary vectors $\vec{F}_0^{(i)}$ and $\vec{G}_0^{(j)}$ are expanded as

$$\vec{F}_0^{(i)} = \sum_{a=1}^{N} A_a^{(i)} \vec{\mathcal{F}}_a, \tag{4.3.11}$$

$$\vec{G}_0^{(j)} = \sum_{a=1}^{N} B_a^{(j)} \vec{\mathcal{G}}_a. \tag{4.3.12}$$

Also, the unitary matrix V in Eq. (4.3.8) is expressed using column vectors as

$$V = (\vec{v}_1, \vec{v}_2, \cdots, \vec{v}_{2N}), \quad \vec{v}_p^\dagger \vec{v}_q = \delta_{pq} \quad (p, q = 1, 2, \cdots, 2N), \tag{4.3.13}$$

and $\vec{v}_p$ are expanded as follows

$$\vec{v}_p = \sum_{a=1}^{N} \alpha_{p,a} \vec{\mathcal{F}}_a + \sum_{a=1}^{N} \beta_{p,a} \vec{\mathcal{G}}_a \quad (p = 1, 2, \cdots, 2N). \tag{4.3.14}$$

Therefore, the boundary conditions (4.3.5) are also rewritten as

$$\boldsymbol{\alpha}_q^\dagger \vec{A}^{(i)} = 0 \quad (q = 2N - k + 1, \cdots, 2N), \tag{4.3.15}$$

$$\boldsymbol{\beta}_p^\dagger \vec{B}^{(j)} = 0 \quad (p = 1, 2, \cdots, 2N - k), \tag{4.3.16}$$

where $\boldsymbol{\alpha}_q \equiv (\alpha_{q,1}, \alpha_{q,2}, \cdots, \alpha_{q,N})^\top$, $\boldsymbol{\beta}_p \equiv (\beta_{p,1}, \beta_{p,2}, \cdots, \beta_{p,N})^\top$.

From the discussion in Subsec. 3.2.2, if l of $\{\boldsymbol{\alpha}_q \mid q = 2N - k + 1, \cdots, 2N\}$ are linearly independent, we obtain $N - l$ right-handed chiral zero modes and $k - l$ left-handed chiral zero modes. The chiral zero modes obtained in the case of Type$(2N - k, k)$ boundary conditions are summarized in the Table 4.1.

4.3.2 Berry's connection in our model

We consider Berry's connections in the parameter space of the boundary conditions. Since the mode functions $f_0^{(i)}(y)$ and $g_0^{(j)}(y)$ are not mixed with each other under changing boundary conditions, the Berry's connection for each can be computed independently. In this study, we focus only on the Berry's connection for zero modes, for which the solution can be easily obtained.

Throughout the boundary conditions (4.3.15), (4.3.16), the mode functions $f_0^{(i)}(y)\,(i = 1, 2, \cdots, N - l)$ and $g_0^{(j)}(y)\,(j = 1, 2, \cdots, k - l)$ depend on the parameters $\boldsymbol{\alpha}_q\,(q = 2N - k + 1, \cdots, 2N)$ and $\boldsymbol{\beta}_p\,(p = 1, \cdots, 2N - k)$, respectively. Therefore, to express the parameter dependence, we write $f_0^{(i)}(y, \boldsymbol{\alpha}_q)$ and $g_0^{(j)}(y, \boldsymbol{\beta}_p)$. Here, we consider the situation that the parameters of the boundary condition $\boldsymbol{\alpha}_q\,(q = 2N - k + 1, \cdots, 2N)$ and $\boldsymbol{\beta}_p\,(p = 1, \cdots, 2N - k)$ in the type$(2N - k, k)$ boundary condition with l fixed are time-dependent, and externally driven along a closed path. Let $0 \le t \le 1$ be the parameter along the closed path, then the final state $f_0^{(i)}(y, \boldsymbol{\alpha}_q(t = 1))$ $(g_0^{(j)}(y, \boldsymbol{\beta}_p(t = 1))$ are given as linear combinations of the degenerate initial states $f_0^{(i')}(y, \boldsymbol{\alpha}_q(t = 0))$ $(g_0^{(j')}(y, \boldsymbol{\beta}_p(t = 0))$ $(i', j' = 1, 2, \cdots, N - l)$:

$$f_0^{(i)}(y, \boldsymbol{\alpha}_q(t = 1)) = \sum_{i'=1}^{N-l} f_0^{(i')}(y, \boldsymbol{\alpha}_q(t = 0)) \left(\Gamma_f[C_f]\right)_{i'i} \quad (i = 1, 2, \cdots, N - l), \tag{4.3.17}$$

$$g_0^{(j)}(y, \boldsymbol{\beta}_p(t = 1)) = \sum_{j'=1}^{k-l} g_0^{(j')}(y, \boldsymbol{\beta}_p(t = 0)) \left(\Gamma_g[C_g]\right)_{j'j} \quad (j = 1, 2, \cdots, N - l), \tag{4.3.18}$$

Table 4.1: The number of the zero mode solutions of $f_0^{(i)}(y)$ and $g_0^{(j)}(y)$ for the type$(2N-k,k)$ BC. The l denotes the maximal number of the linearly independent vectors $\boldsymbol{\alpha}_q$ $(q = 2N-k+1, \cdots, 2N)$ in Eq. (4.3.15). N_{f_0} (N_{g_0}) is the number of the zero mode solutions of $f_0^{(i)}(y)$ ($g_0^{(j)}(y)$). We can find that $N_{f_0} - N_{g_0}$ is independent of l, though both of N_{f_0} and N_{g_0} depend of l.

k	l	N_{f_0}	N_{g_0}	$N_{f_0} - N_{g_0}$
$0 \le k \le N$	0	N	k	$N-k$
	1	$N-1$	$k-1$	$N-k$
	$\vdots$	$\vdots$	$\vdots$	$\vdots$
	$k-1$	$N-k+1$	1	$N-k$
	k	$N-k$	0	$N-k$
$N \le k \le 2N$	$k-N$	$2N-k$	N	$N-k$
	$k-N+1$	$2N-k-1$	$N-1$	$N-k$
	$\vdots$	$\vdots$	$\vdots$	$\vdots$
	$N-1$	1	$k-N+1$	$N-k$
	N	0	$k-N$	$N-k$

where C_f and C_g are closed paths on the parameter spaces of $\boldsymbol{\alpha}_q$ $(q = 2N-k+1, \cdots, 2N)$ and $\boldsymbol{\beta}_p$ $(p = 1, \cdots, 2N-k)$ with l fixed, respectively. The matrices $\Gamma_f[C_f]$ and $\Gamma_g[C_g]$ are called the non-Abelian Berry's phases and given as the path-ordered exponential

$$\Gamma_f[C_f] = P\exp\left(-\oint_{C_f} A^{(f)}\right), \tag{4.3.19}$$

$$\Gamma_g[C_g] = P\exp\left(-\oint_{C_g} A^{(g)}\right). \tag{4.3.20}$$

$A^{(f)}$ and $A^{(g)}$ are anti-Hermitian matrices of 1-forms defined by

$$(A^{(f)})_{i'i} \equiv \int dy\, f_0^{(i')\dagger}(y, \boldsymbol{\alpha}_q) d f_0^{(i)}(y, \boldsymbol{\alpha}_q) \quad (i, i' = 1, 2, \cdots, N-l), \tag{4.3.21}$$

$$(A^{(g)})_{j'j} \equiv \int dy\, g_0^{(j')\dagger}(y, \boldsymbol{\beta}_p) d g_0^{(j)}(y, \boldsymbol{\beta}_p) \quad (j, j' = 1, 2, \cdots, k-l) \tag{4.3.22}$$

with the exterior derivative d for the parameter space of the boundary condition Type$(2N-k,k)$ with l fixed. These 1-forms are transformed as connections. On the other hand, the non-Abelian Berry's phase is transformed as the Wilson line. Indeed, $A^{(f)}$ and $A^{(g)}$ or $\Gamma_f[C_f]$ and $\Gamma_g[C_g]$ are transformed as

$$A^{(f)} \to A^{(f)\prime} = U_f^{-1} A^{(f)} U_f + U_f^{-1} dU_f \quad (U_f \in U(N-l)), \tag{4.3.23}$$

$$A^{(g)} \to A^{(g)\prime} = U_g^{-1} A^{(g)} U_g + U_g^{-1} dU_g \quad (U_g \in U(k-l)), \tag{4.3.24}$$

$$\Gamma_f[C_f] \to \Gamma'_f[C_f] = U_f^{-1} \Gamma_f[C_f] U_f, \tag{4.3.25}$$

$$\Gamma_g[C_g] \to \Gamma'_g[C_g] = U_g^{-1} \Gamma_g[C_g] U_g, \tag{4.3.26}$$

under the unitary transformation for the zero-modes

$$f_0^{(i)}(y,\boldsymbol{\alpha}_q) \to \sum_{i'=1}^{N-l} f_0^{(i')}(y,\boldsymbol{\alpha}_q)(U_f)_{i'i} \quad (i=1,2,\cdots,N-l), \tag{4.3.27}$$

$$g_0^{(j)}(y,\boldsymbol{\beta}_q) \to \sum_{j'=1}^{k-l} g_0^{(j')}(y,\boldsymbol{\beta}_p)(U_g)_{j'j} \quad (j=1,2,\cdots,k-l). \tag{4.3.28}$$

Note that $A^{(f)}$ and $A^{(g)}$ are regarded as non-abelian gauge filed from the transformations (4.3.23), (4.3.24).

For later convenience, we denote the Berry's connection by the expression which is integrated with respect to y. To obtain this expression, we introduce the normalized matrices

$$\widetilde{F}(\boldsymbol{\alpha}_q) \equiv \left(N_1\vec{A}^{(1)},\ N_2\vec{A}^{(2)},\cdots,N_{N-l}\vec{A}^{(N-l)}\right), \quad \widetilde{G}(\boldsymbol{\beta}_p) \equiv \left(N_1\vec{B}^{(1)},\ N_2\vec{B}^{(2)},\cdots,N_{k-l}\vec{B}^{(k-l)}\right), \tag{4.3.29}$$

$$N_a \equiv \sqrt{\frac{\tanh M(L_a-L_{a-1})}{2M}} \quad (a=1,2,\cdots), \tag{4.3.30}$$

where $\vec{A}^{(i)}$ and $\vec{B}^{(j)}$ are N dimensional vectors composed of the coefficients of zero mode functions (4.3.3), (4.3.4), respectively. Then, $A^{(f)}$ and $A^{(g)}$ can be rewritten as

$$A^{(f)} = \widetilde{F}^\dagger(\boldsymbol{\alpha}_q)d\widetilde{F}(\boldsymbol{\alpha}_q), \tag{4.3.31}$$

$$A^{(g)} = \widetilde{G}^\dagger(\boldsymbol{\beta}_p)d\widetilde{G}(\boldsymbol{\beta}_p). \tag{4.3.32}$$

These are matrix forms of the non-Abelian Berry's connection in our setup. In the following, this form is used as the Berry's connection in our setup.

4.3.3 How to apply

The ADHM construction requires a Dirac operator $\Delta^\dagger(x)$ consisting of a matrix satisfying the ADHM equations and its solution $V(x)$. In this Subsection, we identify counterparts in our setup and explain how to apply the ADHM construction to our model.

We consider the boundary condition Type$(2N-k,k)$ with l is fixed and the case that all the edges in the rose graph have the same length, i.e., $L_1-L_0=\cdots=L_N-L_{N-1}=L$[1]. In this case, $\widetilde{F}(\boldsymbol{\alpha}_q)$ and $\widetilde{G}(\boldsymbol{\beta}_p)$ introduced above have parameters dependent through boundary conditions

$$\alpha^\dagger_{[l]\times[N]}\widetilde{F}(\boldsymbol{\alpha}_q)_{[N]\times[N-l]} = 0, \tag{4.3.33}$$

$$\beta^\dagger_{[N-k+l]\times[N]}\widetilde{G}(\boldsymbol{\beta}_p)_{[N]\times[k-l]} = 0, \tag{4.3.34}$$

[1]For simplicity, we imposed $L_1-L_0=\cdots=L_N-L_{N-1}=L$ in the dissertation and the paper [29]. However, there are looser conditions. The minimum condition that must be satisfied is that there exists a matrix $K_{[l]\times[l]}$ satisfying

$$\begin{pmatrix} N_1 & & 0 \\ & \ddots & \\ 0 & & N_N \end{pmatrix}\alpha_{[N]\times[l]} = \alpha_{[N]\times[l]}K_{[l]\times[l]}.$$

where $\alpha_{[N]\times[l]}$ is an $N \times l$ matrix whose column vectors are given by linear combinations of the vectors $\{\boldsymbol{\alpha}_q \mid q = 2N - k + 1, \cdots, 2N\}$ and independent with each other, and $\beta_{[N-k]\times[N]}$ is also an $N \times (N - k + l)$ matrix whose column vectors are given by linear combinations of the vectors $\{\boldsymbol{\beta}_p \mid p = 1, \cdots, 2N - k\}$ and independent of each other.

Here, comparing (4.3.16) and (4.3.33),(4.3.34), we see the following correspondence

$$\Delta(x)_{[2k']\times[N'+2k']} \Longleftrightarrow \alpha^{\dagger}_{[l]\times[N]}, \qquad \Delta(x)_{[2k'']\times[N''+2k'']} \Longleftrightarrow \beta^{\dagger}_{[N-k]\times[N]}, \tag{4.3.35}$$

$$V_{[N'+2k']\times[N']}(x) \Longleftrightarrow \widetilde{F}(\boldsymbol{\alpha})_{[N]\times[N-l]}, \qquad V_{[N''+2k'']\times[N'']}(x) \Longleftrightarrow \widetilde{G}(\boldsymbol{\beta})_{[N]\times[k-l]}. \tag{4.3.36}$$

Furthermore, the Berry's connections calculated using $\widetilde{F}$ and $\widetilde{G}$ are given by (4.3.31), (4.3.32), which also corresponds to the instanton configuration that can be constructed using the ADHM construction (4.2.25).

While the ADHM construction method focuses on a 4d Euclidean spacetime E^4, our system focuses on a parameter space of boundary conditions. Therefore, three things should be noted when applying the ADHM construction to our model. First, the correspondence revealed above is well-defined when l is even. Second, the parameter space of boundary conditions is generally larger than S^4 or E^4. This means that when applying the ADHM construction method, it is necessary to fix all but the x^μ ($\mu = 1, 2, 3, 4$) degrees of freedom as

$$\alpha_{[N]\times[l]} = \Delta(x)_{[N]\times[l]} \quad \text{or} \quad \beta_{[N-k]\times[N]} = \Delta(x)_{[N-k]\times[N]}. \tag{4.3.37}$$

Third, the nontrivial solution constructed by applying the ADHM construction is that it reflects the topological structure of the parameter space, rather than the instantons usually treated in a quantum field theory.

In the following discussion, l is restricted to even numbers. In addition, we will discuss only $f_0^{(i)}(y)$ in detail, but the same can apply to $g_0^{(j)}(y)$. We summarize the procedure of applying the ADHM construction method to our model to construct the instanton coordination as Berry's connection. The first step, from the correspondence in (4.3.35), we focus on the boundary condition

$$\alpha^{\dagger}_{[l]\times[N]}\widetilde{F}(\boldsymbol{\alpha})_{[N]\times[N-l]} = 0.$$

At this time, the boundary condition is parameterized to display $\Delta^{\dagger}(x)_{[l]\times[N]}$ corresponding to the instanton solution to be constructed. The second step, we find the normalized solution $\widetilde{F}(\boldsymbol{\alpha})$ that satisfies the above boundary condition. Finally, computing

$$A^{(f)}_{\mu}(x) = \widetilde{F}(\boldsymbol{\alpha}_q)\partial_\mu \widetilde{F}(\boldsymbol{\alpha}_q) \tag{4.3.38}$$

yields the instanton solution, where ∂_μ is the derivative with respect to 4d Euclidean spacetime. This solution has an instanton number $l/2$ and the gauge group is $SU(N - l)$.

Summarizing the above discussion, the following correspondences were obtained:

Boundary condition $\alpha^{\dagger}_{[l]\times[N]}\widetilde{F}(\boldsymbol{\alpha})_{[N]\times[N-l]} = 0$	$\Longleftrightarrow$	Zero mode equation $\Delta^{\dagger}(x)_{[l]\times[N]}V_{[N]\times[N-l]} = 0$
Normalization condition $\widetilde{F}^{\dagger}\widetilde{F} = 1_{N-l}$	$\Longleftrightarrow$	Normalization condition $V^{\dagger}V = 1_{N-l}$
Berry's connection $A^{(f)} = \widetilde{F}^{\dagger}(\boldsymbol{\alpha})d\widetilde{F}(\boldsymbol{\alpha})$	$\Longleftrightarrow$	Instanton solution $A = V^{\dagger}(x)dV(x)$

In the following, by applying the ADHM construction method, we specifically construct the instanton solution as the Berry's connection in the parameter space of boundary conditions.

4.4 Results

Our results are shown in Table 4.2. Some specific derivations are given below. Other cases can be calculated in the same way.

4.4.1 The case of $(N, k, l) = (4, 2, 2)$

We consider the boundary conditions specified by $(N, k, l) = (4, 2, 2)$. In this case, the number of independent zero modes for $f_0^{(i)}(y)$ and $g_0^{(j)}(y)$ is 2 and 0, respectively (see Table 4.1). Therefore, we apply the ADHM construction method to construct $SU(2)$ instanton with the topological charge $Q = \pm 1$ as the Berry's connections (4.3.38).

Boundary conditions of $f_0^{(i)}(y, \boldsymbol{\alpha})$ are given by

$$0 = \alpha^\dagger_{[2]\times[4]} \widetilde{F}_{[4]\times[2]} = \begin{pmatrix} \boldsymbol{\alpha}_1'^\dagger \\ \boldsymbol{\alpha}_2'^\dagger \end{pmatrix}_{[2]\times[4]} \begin{pmatrix} N_1 \vec{A}^{(1)} & N_2 \vec{A}^{(2)} \end{pmatrix}_{[4]\times[2]}, \tag{4.4.1}$$

where $\{\boldsymbol{\alpha}_1', \boldsymbol{\alpha}_2'\}$ are generally given by a linear combination of $\boldsymbol{\alpha}_7$ and $\boldsymbol{\alpha}_8$, but for simplicity, we chose

$$\boldsymbol{\alpha}_1' \propto \boldsymbol{\alpha}_7, \quad \boldsymbol{\alpha}_2' \propto \boldsymbol{\alpha}_8. \tag{4.4.2}$$

Here we parameterize them as

$$\begin{aligned} \alpha_{[4]\times[2]} &= \begin{pmatrix} \sqrt{\rho^2 + (x-b)^2}\boldsymbol{\alpha}_7 & \sqrt{\rho^2 + (x-b)^2}\boldsymbol{\alpha}_8 \end{pmatrix} \\ &= \begin{pmatrix} \rho & 0 \\ 0 & \rho \\ x^4 - b^4 - i(x^3 - b^3) & -(x^2 - b^2) - i(x^1 - b^1) \\ x^2 - b^2 - i(x^1 - b^1) & x^4 - b^4 + i(x^3 - b^3) \end{pmatrix} \\ &= \begin{pmatrix} \rho & 0 \\ 0 & \rho \\ \multicolumn{2}{c}{e_\mu (x^\mu - b^\mu)} \end{pmatrix}, \end{aligned} \tag{4.4.3}$$

where b^μ ($\mu = 1, 2, 3, 4$) and ρ are real constants. Then, the matrix $\widetilde{F}_{[4]\times[2]}$ is given by

$$\widetilde{F}(x)_{[4]\times[2]} = \frac{1}{\sqrt{\rho^2 + (x-b)^2}} \begin{pmatrix} \multicolumn{2}{c}{e^\dagger_\mu (x^\mu - b^\mu)} \\ -\rho & 0 \\ 0 & -\rho \end{pmatrix} \tag{4.4.4}$$

through the boundary condition (4.4.1). If we explicitly calculate the Berry's connection that can

Table 4.2: The gauge groups of instantons and topological charges in the case of $N = 4, 5, 6$. The symbol "–" indicates that the instanton does not exist. The cases without the instantons for both $A^{(f)}$ and $A^{(g)}$ are not listed in this table.

			for $f_0^{(i)}(y)$		for $g_0^{(j)}(y)$	
			gauge group	topological charge	gauge group	topological charge
N	k	l	$SU(N-l)$	$\lvert Q\rvert = l/2$	$SU(k-l)$	$\lvert Q\rvert = (N-k+l)/2$
	2	0	–	–	$SU(2)$	1
	2	2	$SU(2)$	1	–	–
	3	1	–	–	$SU(2)$	1
	3	2	$SU(2)$	1	–	–
4	4	2	$SU(2)$	1	$SU(2)$	1
	5	2	$SU(2)$	1	–	–
	5	3	–	–	$SU(2)$	1
	6	2	$SU(2)$	1	–	–
	6	4	–	–	$SU(2)$	1
	2	2	$SU(3)$	1	–	–
	3	0	–	–	$SU(3)$	1
	3	2	$SU(3)$	1	–	–
	4	1	–	–	$SU(3)$	1
	4	2	$SU(3)$	1	–	–
5	5	2	$SU(3)$	1	$SU(3)$	1
	6	2	$SU(3)$	1	–	–
	6	3	–	–	$SU(3)$	1
	7	2	$SU(3)$	1	–	–
	7	4	–	–	$SU(3)$	1
	8	5	–	–	$SU(3)$	1
	2	0	–	–	$SU(2)$	2
	2	2	$SU(4)$	1	–	–
	3	1	–	–	$SU(2)$	2
	3	2	$SU(4)$	1	–	–
	4	0	–	–	$SU(4)$	1
	4	2	$SU(4)$	1	$SU(2)$	2
6	4	4	$SU(2)$	2	–	–
	5	1	–	–	$SU(4)$	1
	5	2	$SU(4)$	1	–	–
	5	3	–	–	$SU(2)$	2
	5	4	$SU(2)$	2	–	–
	6	2	$SU(4)$	1	$SU(4)$	1
	6	4	$SU(2)$	2	$SU(2)$	2
	$\vdots$	$\vdots$	$\vdots$	$\vdots$	$\vdots$	$\vdots$

be computed using $\widetilde{F}(x)_{[4]\times[2]}$, we obtain

$$\begin{aligned}(A_\mu^{(f)})_{[2]\times[2]} &= \widetilde{F}^\dagger(x)_{[2]\times[4]}\partial_\mu \widetilde{F}(x)_{[4]\times[2]} \\ &= -\frac{(x-b)_\mu}{(x-b)^2+\rho^2} + \frac{1}{(x-b)^2+\rho^2} e_\nu \bar{e}_\mu (x-b)_\nu \\ &= -\frac{(x-b)_\mu}{(x-b)^2+\rho^2} + \frac{1}{(x-b)^2+\rho^2}\left(\delta_{\mu\nu} + i\eta_{\mu\nu}^{(-)}\right)(x-b)_\nu \\ &= -i\eta_{\mu\nu}^{(-)} \frac{(x-b)_\nu}{\rho^2+(x-b)^2}. \end{aligned} \tag{4.4.5}$$

This connection is well known as the $SU(2)$ BPST instanton and has the topological charge -1.

4.4.2 The case of $(N, k, l) = (5, 2, 2)$

We consider the boundary conditions specified by $(N, k, l) = (5, 2, 2)$. In this case, the number of independent zero modes for $f_0^{(i)}(y)$ and $g_0^{(j)}(y)$ is 3 and 0, respectively (see Table 4.1). Therefore, $SU(3)$ one-instanton solution can be obtained as the Berry's connection by the ADHM construction.

Boundary conditions of $f_0^{(i)}(y, \boldsymbol{\alpha})$ are given by

$$0 = \alpha^\dagger_{[2]\times[5]}\widetilde{F}_{[5]\times[3]} = \begin{pmatrix} \boldsymbol{\alpha}_1'^\dagger \\ \boldsymbol{\alpha}_2'^\dagger \end{pmatrix}_{[2]\times[5]} \begin{pmatrix} N_1\vec{A}^{(1)} \; N_2\vec{A}^{(2)} \; N_3\vec{A}^{(3)} \end{pmatrix}_{[5]\times[3]}, \tag{4.4.6}$$

where $\{\boldsymbol{\alpha}_1', \boldsymbol{\alpha}_2'\}$ are generally given by a linear combination of $\boldsymbol{\alpha}_9$ and $\boldsymbol{\alpha}_{10}$, but for simplicity, we chose

$$\boldsymbol{\alpha}_1' \propto \boldsymbol{\alpha}_9, \quad \boldsymbol{\alpha}_2' \propto \boldsymbol{\alpha}_{10}. \tag{4.4.7}$$

Here we parameterize them as

$$\begin{aligned}\alpha_{[5]\times[2]} &= \begin{pmatrix} \sqrt{\rho^2+(x-b)^2}\boldsymbol{\alpha}_9 & \sqrt{\rho^2+(x-b)^2}\boldsymbol{\alpha}_{10} \end{pmatrix} \\ &= \begin{pmatrix} \rho & 0 \\ 0 & \rho \\ 0 & 0 \\ x^4-b^4-i(x^3-b^3) & -(x^2-b^2)-i(x^1-b^1) \\ x^2-b^2-i(x^1-b^1) & x^4-b^4+i(x^3-b^3) \end{pmatrix} \\ &= \begin{pmatrix} \rho \quad 0 \\ 0 \quad \rho \\ 0 \quad 0 \\ e_\mu(x^\mu - b^\mu) \end{pmatrix}, \end{aligned} \tag{4.4.8}$$

where b^μ $(\mu = 1, 2, 3, 4)$ and ρ are real constants. Then, the matrix $\widetilde{F}_{[5]\times[3]}$ is given by

$$\widetilde{F}_{[5]\times[3]} = \frac{1}{\sqrt{(x-b)^2+\rho^2}} \left(\begin{array}{cc|c} \multicolumn{2}{c|}{\bar{e}_\mu(x_\mu-b_\mu)} & \vec{0} \\ \hline 0 & 0 & 1 \\ -\rho & 0 & 0 \\ 0 & -\rho & 0 \end{array}\right), \quad \vec{0} = \begin{pmatrix} 0 \\ 0 \end{pmatrix} \tag{4.4.9}$$

through the boundary condition (4.4.6). If we explicitly calculate the Berry's connection that can be computed using $\widetilde{F}(x)_{[5]\times[2]}$, we obtain

$$(A_\mu^{(f)})_{[3]\times[3]} = \widetilde{F}^\dagger(x)_{[5]\times[2]}\partial_\mu \widetilde{F}(x)_{[2]\times[5]} = \begin{pmatrix} \mathcal{A}_\mu^{SU(2)} & \vec{0} \\ \vec{0}^\top & 0 \end{pmatrix}, \tag{4.4.10}$$

$$\mathcal{A}_\mu^{SU(2)} = -i\eta_{\mu\nu}^{(-)}\frac{(x-b)_\nu}{(x-b)^2+\rho^2}. \tag{4.4.11}$$

This connection is well known as the $SU(3)$ one-instanton and has the topological charge -1.

4.4.3 The case of $(N,k,l) = (6,4,4)$

We consider the boundary conditions specified by $(N,k,l) = (6,4,4)$. In this case, the number of independent zero modes for $f_0^{(i)}(y)$ and $g_0^{(j)}(y)$ is 2 and 0, respectively (see Table 4.1). Therefore, we apply the ADHM construction method to construct the $SU(2)$ instanton with the topological charge $Q = \pm 2$ as the Berry's connections (4.3.3).

Boundary conditions of $f_0^{(i)}(y,\boldsymbol{\alpha})$ are given by

$$0 = \alpha^\dagger_{[4]\times[6]}\widetilde{F}_{[6]\times[2]} = \begin{pmatrix} \boldsymbol{\alpha}_1'^\dagger \\ \boldsymbol{\alpha}_2'^\dagger \\ \boldsymbol{\alpha}_3'^\dagger \\ \boldsymbol{\alpha}_4'^\dagger \end{pmatrix}_{[4]\times[6]} \begin{pmatrix} N_1\vec{A}^{(1)} & N_2\vec{A}^{(2)} \end{pmatrix}_{[6]\times[2]}, \tag{4.4.12}$$

where $\{\boldsymbol{\alpha}_1', \boldsymbol{\alpha}_2', \cdots, \boldsymbol{\alpha}_4'\}$ are generally given by a linear combination of $\boldsymbol{\alpha}_9$, $\boldsymbol{\alpha}_{10}$, $\boldsymbol{\alpha}_{11}$ and $\boldsymbol{\alpha}_{12}$, but for simplicity, we chose

$$\boldsymbol{\alpha}_1' \propto \boldsymbol{\alpha}_9, \quad \boldsymbol{\alpha}_2' \propto \boldsymbol{\alpha}_{10}, \quad \boldsymbol{\alpha}_3' \propto \boldsymbol{\alpha}_{11}, \quad \boldsymbol{\alpha}_4' \propto \boldsymbol{\alpha}_{12}. \tag{4.4.13}$$

Here we parameterize them as

$$\boldsymbol{\alpha}_9 = \frac{1}{\sqrt{\rho_1^2+(x-b_1)^2}}\begin{pmatrix} \rho_1 \\ 0 \\ x^4-b_1^4-i(x^3-b_1^3) \\ 0 \\ x^2-b_1^2-i(x^1-b_1^1) \\ 0 \end{pmatrix}, \quad \boldsymbol{\alpha}_{10} = \frac{1}{\sqrt{\rho_2^2+(x-b_2)^2}}\begin{pmatrix} \rho_2 \\ 0 \\ 0 \\ x^4-b_2^4-i(x^3-b_2^3) \\ 0 \\ x^2-b_2^2-i(x^1-b_2^1) \end{pmatrix}, \tag{4.4.14}$$

$$\boldsymbol{\alpha}_{11} = \frac{1}{\sqrt{\rho_1^2+(x-b_1)^2}}\begin{pmatrix} 0 \\ \rho_1 \\ -(x^2-b_1^2)-i(x^1-b_1^1) \\ 0 \\ x^4-b_1^4+i(x^3-b_1^3) \\ 0 \end{pmatrix}, \quad \boldsymbol{\alpha}_{12} = \frac{1}{\sqrt{\rho_2^2+(x-b_2)^2}}\begin{pmatrix} 0 \\ \rho_2 \\ 0 \\ -(x^2-b_2^2)-i(x^1-b_2^1) \\ 0 \\ x^4-b_2^4+i(x^3-b_2^3) \end{pmatrix}, \tag{4.4.15}$$

where ρ_i, $b_i^\mu = (b_i^1, b_i^2, b_i^3, b_i^4)$ $(i = 1, 2)$ are real constants. And we take

$$
\begin{aligned}
\alpha_{[5]\times[2]} &= (\boldsymbol{\alpha}_9\, \boldsymbol{\alpha}_{10}\, \boldsymbol{\alpha}_{11}\, \boldsymbol{\alpha}_{12}) \cdot \left[1_2 \otimes \begin{pmatrix} \sqrt{\rho_1^2 + (x - b_1)^2} & 0 \\ 0 & \sqrt{\rho_2^2 + (x - b_2)^2} \end{pmatrix} \right] \\
&= \begin{pmatrix} \rho_1 \quad \rho_2 \quad 0 \quad 0 \\ 0 \quad 0 \quad \rho_1 \quad \rho_2 \\ e_\mu \otimes (x^\mu 1 - T^\mu)_{[2]\times[2]} \end{pmatrix},
\end{aligned}
\tag{4.4.16}
$$

where $T^\mu_{[2]\times[2]} = \mathrm{diag}\,(b_1^\mu,\, b_2^\mu)$. Then, the matrix $\widetilde{F}_{[6]\times[2]}$ is given by

$$
\widetilde{F}(x)_{[6]\times[2]} = \frac{1}{\sqrt{\phi}} \begin{pmatrix} 1_2 \\ -e_\mu \otimes \left(\rho_1 \frac{(x-b_1)^\mu}{(x-b_1)\cdot(x-b_1)},\ \rho_2 \frac{(x-b_2)^\mu}{(x-b_2)\cdot(x-b_2)} \right)^\dagger \end{pmatrix},
\tag{4.4.17}
$$

$$
\phi \equiv 1 + \sum_{i=1}^{2} \frac{\rho_i^2}{(x - b_i)^\mu (x - b_i)_\mu}
\tag{4.4.18}
$$

through the boundary condition (4.4.12). If we explicitly calculate the Berry's connection that can be computed using $\widetilde{F}(x)_{[6]\times[2]}$, we obtain

$$
(A_\mu^{(f)})_{[2]\times[2]} = \widetilde{F}^\dagger(x)_{[2]\times[6]} \partial_\mu \widetilde{F}(x)_{[6]\times[2]} = -i\eta^{(+)}_{\mu\alpha} \frac{\sum_{i=1}^2 \rho_i^2 \frac{(x-b_i)^\alpha}{(x-b_i)^2}}{1 + \sum_{i=1}^2 \frac{\rho_i^2}{(x-b_i)^2}}
\tag{4.4.19}
$$

This connection is well known as the $SU(2)$ 't Hooft instanton and has the topological charge -2.

4.5 Summary and discussion

In this chapter, we have considered the Dirac zero modes on the quantum graph and revealed the parameter space which gives the $SU(N)$ instantons as the Berry's connections due to the structure of the ADHM construction. The constructions for the $O(N)$ and $Sp(N)$ instantons are known and will be applied to this system in the same manner. The reason we were able to construct various instanton solutions is that the parameter space in which the boundary conditions of the quantum graph are very rich.

Higher dimensional extension of ADHM construction is proposed [42–44]. This method can construct instantons on more than 4d spacetime. We are interested in applying these construction to our models.

While there have been several studies that monopole solutions are constructed as Berry's connection in a simple quantum graph system [10–12, 21], this study is the first to construct instanton solutions as Berry's connections. Since we have restricted the parameter space, other topological configurations such as monopoles, vortices and so on may appear in the other parameter spaces. Especially, the method for constructing general Bogomolny–Prasad–Sommerfield (BPS) monopole solutions is known as the Nahm construction and applied to the Berry's connection of $SU(2)$ monopoles in various models, e.g., supersymmetric quantum mechanics [45], Weyl semimetal [46] and furthermore, 1d quantum mechanics with point interactions which belongs to a class of the quantum graph [11]. The systematic construction of such a Berry's connection is also discussed in [12]. Since the general quantum graph has a wide parameter space, we can expect that the structure of the Nahm construction is also hidden and other BPS monopoles appear as the Berry's connection on the boundary condition.

Chapter 5

Correspondence between quantum graph extra dimension and AZ classes

A gapped free-fermion system is known to be classified by symmetry, and classes with nontrivial topological numbers are considered to correspond to topological insulators and superconductors. A. Altland and M. R. Zirnbauer have shown that the gapped free-fermion system can be classified into 10 symmetries classes by considering time-reversal symmetry, particle-hole symmetry and chiral symmetry [47]. This is known as the Altland–Zirnbauer (AZ) classification.

In this chapter, we show nontrivial correspondence between the AZ classification of (1 + 0)-d gapped free-fermion system and a classification of boundary conditions on quantum graphs. Similar to the previous chapters, the quantum graph is the rose graph with N segments, and the Dirac fermions on it are considered.

This chapter is organized as follows: In the next Section, we summarize our setup. In Sec. 5.2 and Sec. 5.3, we briefly review the AZ classification and show the counterpart of (1 + 0)-d gapped free-fermion Hamiltonian in our model. In Sec. 5.4–Sec. 5.8, by corresponding to the time-reversal symmetry, particle-hole symmetry, and chiral symmetry in the AZ classification, we construct three transformations in our model. The AZ classification gives a topological number for each of the 10 classes. In Sec. 5.9, we identify its counterparts.

5.1 Setup

The same setup is considered throughout Chap. 3, 4 and 5 in this dissertation. In this Section, we briefly summarize the setup again. See Chap. 3 for more details.

We consider a Dirac fermion on a 5-dimensional (5d) spacetime with 1d extra dimension of the quantum graph. The action is given by

$$S = \int d^4x \sum_{a=1}^{N} \int_{L_{a-1}}^{L_a} dy\, \overline{\Psi}(x,y)[i\gamma^\mu \partial_\mu + i\gamma^y \partial_y + M]\Psi(x,y). \tag{5.1.1}$$

After separating the variables in the 4d part and the quantum graph direction, the function in the quantum graph direction is expanded in the complete set of the mass eigenstates of the 4d field:

$$\Psi(x,y) = \sum_i \sum_{n=0}^{\infty} \left[\psi^{(i)}_{\mathrm{R},n}(x) f^{(i)}_n(y) + \psi^{(i)}_{\mathrm{L},n}(x) g^{(i)}_n(y)\right]. \tag{5.1.2}$$

This expansion is called the Kaluza–Klein (KK) expansion. The eigenfunctions to be satisfied by the mode function are

$$(-\partial_y^2 + M^2) f^{(i)}_n(y) = m_n^2 f^{(i)}_n(y), \tag{5.1.3}$$

$$(-\partial_y^2 + M^2) g^{(i)}_n(y) = m_n^2 g^{(i)}_n(y), \tag{5.1.4}$$

where $f^{(i)}_n(y)$ and $g^{(i)}_n(y)$ are related each other through the supersymmetric relations

$$(\partial_y + M) f^{(i)}_n(y) = m_n g^{(i)}_n(y), \tag{5.1.5}$$

$$(-\partial_y + M) g^{(i)}_n(y) = m_n f^{(i)}_n(y). \tag{5.1.6}$$

In the y-direction, appropriate boundary conditions

$$(1_{2N} - U_{\mathrm{B}}) \vec{F}^{(i)}_n = 0, \tag{5.1.7}$$

$$(1_{2N} + U_{\mathrm{B}}) \vec{G}^{(j)}_m = 0, \tag{5.1.8}$$

$$U_{\mathrm{B}}^2 = 1_{2N}, \quad U_{\mathrm{B}}^\dagger = U_{\mathrm{B}}, \tag{5.1.9}$$

are imposed. Let Type$(2N-k,k)$ denote the boundary condition where the number of -1 eigenvalues of U_{B} is k. In this class, the number of chiral zero modes and the Witten index are given by

$$N_{f_0} = N - l, \quad N_{g_0} = k - l, \tag{5.1.10}$$

$$\Delta_{\mathrm{W}} = N_{f_0} - N_{g_0} = N - k, \tag{5.1.11}$$

respectively.

5.2 Topological classification of gapped free-fermion system

In this Section, we review well-known topological classifications in condensed matter systems. For gapped free-fermion systems, since the second quantized Hamiltonian can be written in a quadratic form as $\hat{H} = \sum_{i,j} \hat{\psi}_i H_{ij} \hat{\psi}_j$, this system can be described by the matrix H. The Altland–Zirnbauer (AZ) symmetries determine the space of H based on the symmetry of the system. However, if a unitary symmetry exists and there exists a unitary matrix commutative with H, then H is block diagonalized and one block is considered to be H. In other words, we assume that no matrix is commutative with H. Then, the matrix H is allowed to have discrete anti-unitary and chiral symmetries and is classified into 10 symmetry classes corresponding to its existence or absence [47]. These symmetry classes are composed of three symmetries, time-reversal symmetry (TRS), particle-hole symmetry (PHS), and chiral symmetry (CS). If each symmetry exists, then the Hamiltonian matrix H satisfies

$$\mathrm{TRS}: TH(\boldsymbol{k})T^{-1} = H(-\boldsymbol{k}) \quad (T^2 = \pm 1), \tag{5.2.1}$$

$$\mathrm{PHS}: CH(\boldsymbol{k})C^{-1} = H(-\boldsymbol{k}) \quad (C^2 = \pm 1), \tag{5.2.2}$$

$$\mathrm{CS}: \Gamma H(\boldsymbol{k})\Gamma^{-1} = H(\boldsymbol{k}) \quad (\Gamma^2 = 1), \tag{5.2.3}$$

where $\boldsymbol{k}$ is momentum taking values in the Brillouin zone. Since the system is invariant when TRS or PHS acts twice, we know that $T^2 = \pm 1$ and $C^2 = \pm 1$. On the other hand, CS is given by the product $\Gamma = TC$ up to a phase and taken as $\Gamma^2 = 1$. Furthermore, when discussing the topological classification of Hamiltonians, it is convenient to consider the following normalized form called flatted Hamiltonian:

$$H^2(\boldsymbol{k}) = 1, \quad H^\dagger(\boldsymbol{k}) = H(\boldsymbol{k}). \tag{5.2.4}$$

The use of a flatted Hamiltonian simplifies the analysis of $H(\boldsymbol{k})$ because the eigenvalues can be set to ± 1. Since the normalizing can be performed in a continuous deformation without closing the energy gap, the flatted Hamiltonian fully preserves the topological structure of the original $H(\boldsymbol{k})$.

The results of the classification of AZ symmetric classes are known to be as shown in Table 5.1. For each class, the squared value of T, C and Γ is listed if present, or 0 if not present. V_d refers to the classifying space of $H(\boldsymbol{k})$ (see Table 5.2 for details). $\pi_0(V_d)$ describe the zeroth homotopy groups of the classifying space obtained for each class, which are called topological number. In condensed matter physics, classes with nontrivial topological numbers are considered to correspond to superconductors or topological insulators.

Table 5.1: Tenfold classification of topological insulators and superconductors. The class A, AIII, AI, BDI, $\cdots$ represent the ten AZ symmetry classes of the Hamiltonian. The signs +1 in the chiral symmetry Γ and ± 1 in the time-reversal T and the particle-hole C mean the presence of those symmetries and also they denote the squares of corresponding symmetries, while 0 indicates the absence of the symmetries. d is the spatial dimension of the system and V_d denotes the classifying space in each class for the d dimensional space given in Table 5.4. $\mathbb{Z}$, $\mathbb{Z}_2$, $2\mathbb{Z}$ and 0 in the other entries mean the presence or absence of nontrivial topological insulators or superconductors. The class A and AIII are called the complex AZ symmetry classes and have twofold periodicity, while the other classes are referred to the real AZ symmetry classes and have eightfold periodicity. These periodicities are known as the Bott periodicity, which are related to the structure of the K-theory and Clifford algebra.

class	T	C	Γ	V_d	$\pi_0(V_0)$	$\pi_0(V_1)$	$\pi_0(V_2)$	$\pi_0(V_3)$	$\pi_0(V_4)$	$\pi_0(V_5)$	$\pi_0(V_6)$	$\pi_0(V_7)$
A	0	0	0	C_{0+d}	$\mathbb{Z}$	0	$\mathbb{Z}$	0	$\mathbb{Z}$	0	$\mathbb{Z}$	0
AIII	0	0	1	C_{1+d}	0	$\mathbb{Z}$	0	$\mathbb{Z}$	0	$\mathbb{Z}$	0	$\mathbb{Z}$
AI	+1	0	0	R_{0+d}	$\mathbb{Z}$	0	0	0	$2\mathbb{Z}$	0	$\mathbb{Z}_2$	$\mathbb{Z}_2$
BDI	+1	+1	1	R_{1+d}	$\mathbb{Z}_2$	$\mathbb{Z}$	0	0	0	$2\mathbb{Z}$	0	$\mathbb{Z}_2$
D	0	+1	0	R_{2+d}	$\mathbb{Z}_2$	$\mathbb{Z}_2$	$\mathbb{Z}$	0	0	0	$2\mathbb{Z}$	0
DIII	−1	+1	1	R_{3+d}	0	$\mathbb{Z}_2$	$\mathbb{Z}_2$	$\mathbb{Z}$	0	0	0	$2\mathbb{Z}$
AII	−1	0	0	R_{4+d}	$2\mathbb{Z}$	0	$\mathbb{Z}_2$	$\mathbb{Z}_2$	$\mathbb{Z}$	0	0	0
CII	−1	−1	1	R_{5+d}	0	$2\mathbb{Z}$	0	$\mathbb{Z}_2$	$\mathbb{Z}_2$	$\mathbb{Z}$	0	0
C	0	−1	0	R_{6+d}	0	0	$2\mathbb{Z}$	0	$\mathbb{Z}_2$	$\mathbb{Z}_2$	$\mathbb{Z}$	0
CI	+1	−1	1	R_{7+d}	0	0	0	$2\mathbb{Z}$	0	$\mathbb{Z}_2$	$\mathbb{Z}_2$	$\mathbb{Z}$

Table 5.2: Classifying spaces and 0th homotopy groups. The integers p and q are related to the number of empty bands and occupied bands, respectively. Here, taking the limit of p means that there are an infinite number of empty bands and we focus on the stable classification which is independent of the addition of empty bands. From the viewpoint of the K-theory, this limit results from the property of the so-called stable equivalence.

ℓ mod 2	Complex classifying space C_ℓ	$\pi_0(C_\ell)$
$\ell = 0$	$C_0 = \bigcup_q \lim_{p\to\infty} \dfrac{U(p+q)}{U(p)\times U(q)}$	$\mathbb{Z}$
$\ell = 1$	$C_1 = \lim_{p\to\infty} U(p)$	0

ℓ mod 8	Real classifying space	$\pi_0(R_\ell)$
$\ell = 0$	$R_0 = \bigcup_q \lim_{p\to\infty} \dfrac{O(p+q)}{O(p)\times O(q)}$	$\mathbb{Z}$
$\ell = 1$	$R_1 = \lim_{p\to\infty} O(p)$	$\mathbb{Z}_2$
$\ell = 2$	$R_2 = \lim_{p\to\infty} \dfrac{O(2p)}{U(p)}$	$\mathbb{Z}_2$
$\ell = 3$	$R_3 = \lim_{p\to\infty} \dfrac{U(2p)}{Sp(p)}$	0
$\ell = 4$	$R_4 = \bigcup_q \lim_{p\to\infty} \dfrac{Sp(p+q)}{Sp(p)\times Sp(q)}$	$2\mathbb{Z}$
$\ell = 5$	$R_5 = \lim_{p\to\infty} Sp(p)$	0
$\ell = 6$	$R_6 = \lim_{p\to\infty} \dfrac{Sp(p)}{U(p)}$	0
$\ell = 7$	$R_7 = \lim_{p\to\infty} \dfrac{U(p)}{O(p)}$	0

5.3 Correspondence to zero-dimensional Hamiltonian

Let us focus on the zero-dimensional Hamiltonian, which has no momentum dependence. In this case, it consists of only a mass term and is given by a constant Hermitian matrix. Now we can aware that this condition is the same as Eq. (5.1.9) and the flattened Hamiltonian correspond to boundary matrix U_B:

$$H^2 = 1, \quad H^\dagger = H \Longleftrightarrow U_\mathrm{B}^2 = 1, \quad U_\mathrm{B}^\dagger = U_\mathrm{B}. \tag{5.3.1}$$

Thus, it is expected that the classification of the zero-dimensional Hamiltonian can be applied to that of the boundary conditions in our model.

To show the correspondence of the classification, we need symmetries which correspond to the TRS, PHS and CS in the zero-dimensional gapped free Hamiltonian. In the following Sections, we introduce the time-reversal and charge conjugation symmetries combined with some extra-spatial symmetries in our model and show that these provide restrictions for the boundary matrix U_B consistent with the conditions (5.2.1)–(5.2.3).

5.4 Transformations in the y-direction

First of all, we introduce transformations that act only in the extra dimensional direction, i.e., y-direction. Specifically, we consider permutation, half-reflection, and their combination, and parity transformation in the y-direction.

For later convenience, we introduce

$$D_a = \{y \mid L_{a-1} < y < L_a\}, \quad (a = 1, 2, \cdots, N) \tag{5.4.1}$$

to denote the region representing the a-th interval.

5.4.1 Permutation S_y

We first introduce a permutation S_y that exchanges the a-segments to the $(N/2 + a)$-segments ($a = 1, 2, \cdots, N/2$). This permutation is well-defined when the a-segment and the $(N/2 + a)$-segment have the same length

$$L_a - L_{a-1} = L_{a+N/2} - L_{a-1+N/2} \quad (a = 1, 2, \cdots, N/2)$$

and the number of segment N is even. The mode functions $\varphi(y) = \{f_n^{(i)}(y) \,\text{or}\, g_n^{(i)}(y)\}$ on D_a are transformed as

$$(S_y\varphi)(y) = \begin{cases} \varphi(y + L_{a-1+N/2} - L_{a-1}) & (y \in D_a,\ a = 1, 2, \cdots, N/2), \\ \varphi(y + L_{a-1-N/2} - L_{a-1}) & (y \in D_a,\ a = N/2 + 1, \cdots, N). \end{cases} \tag{5.4.2}$$

As can be seen from this transformation, S_y is Hermitian operator, and it can also be regarded as a transformation that translates $N/2$ intervals rather than a permutation. The S_y transformation is shown in Fig. 5.1.

Under the S_y transformation, the boundary vectors are transformed as

$$\vec{F}_n^{(i)} \xrightarrow{S_y} \begin{pmatrix} f_n^{(i)}(L_{N/2} + \varepsilon) \\ f_n^{(i)}(L_{N/2+1} - \varepsilon) \\ \vdots \\ f_n^{(i)}(L_{N-1} + \varepsilon) \\ f_n^{(i)}(L_N - \varepsilon) \\ \hline f_n^{(i)}(L_0 + \varepsilon) \\ f_n^{(i)}(L_1 - \varepsilon) \\ \vdots \\ f_n^{(i)}(L_{N/2-1} + \varepsilon) \\ f_n^{(i)}(L_{N/2} - \varepsilon) \end{pmatrix} = \begin{pmatrix} 0 & 1_N \\ 1_N & 0 \end{pmatrix} \begin{pmatrix} f_n^{(i)}(L_0 + \varepsilon) \\ f_n^{(i)}(L_1 - \varepsilon) \\ \vdots \\ f_n^{(i)}(L_{N/2-1} + \varepsilon) \\ f_n^{(i)}(L_{N/2} - \varepsilon) \\ \hline f_n^{(i)}(L_{N/2} + \varepsilon) \\ f_n^{(i)}(L_{N/2+1} - \varepsilon) \\ \vdots \\ f_n^{(i)}(L_{N-1} + \varepsilon) \\ f_n^{(i)}(L_N - \varepsilon) \end{pmatrix} = (\sigma_1 \otimes 1_N)\vec{F}_n^{(i)}, \tag{5.4.3}$$

$$\vec{G}_m^{(j)} \xrightarrow{S_y} \begin{pmatrix} g_m^{(j)}(L_{N/2} + \varepsilon) \\ -g_m^{(j)}(L_{N/2+1} - \varepsilon) \\ \vdots \\ g_m^{(j)}(L_{N-1} + \varepsilon) \\ -g_m^{(j)}(L_{N/2+1} - \varepsilon) \\ \hline g_m^{(j)}(L_0 + \varepsilon) \\ -g_m^{(j)}(L_1 - \varepsilon) \\ \vdots \\ g_m^{(j)}(L_{N/2-1} + \varepsilon) \\ -g_m^{(j)}(L_{N/2} - \varepsilon) \end{pmatrix} = \begin{pmatrix} 0 & 1_N \\ 1_N & 0 \end{pmatrix} \begin{pmatrix} g_m^{(j)}(L_0 + \varepsilon) \\ -g_m^{(j)}(L_1 - \varepsilon) \\ \vdots \\ g_m^{(j)}(L_{N/2-1} + \varepsilon) \\ -g_m^{(j)}(L_{N/2} - \varepsilon) \\ \hline g_m^{(j)}(L_{N/2} + \varepsilon) \\ -g_m^{(j)}(L_{N/2+1} - \varepsilon) \\ \vdots \\ g_m^{(j)}(L_{N-1} + \varepsilon) \\ -g_m^{(j)}(L_N - \varepsilon) \end{pmatrix} = (\sigma_1 \otimes 1_N)\vec{G}_m^{(j)}. \tag{5.4.4}$$

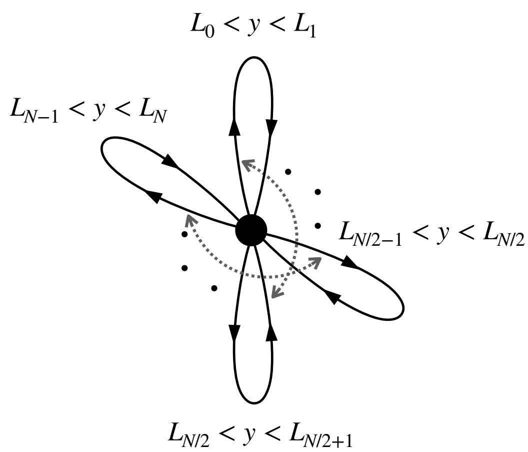

Figure 5.1: Permutation S_y that exchanges the a-th edge for the $(N/2 + a)$-th edge ($a = 1, 2, \cdots, N/2$).

5.4.2 Half-reflection R_y

Next, we introduce a half-reflection R_y that multiplies the mode function on D_a ($a = N/2 + 1, \cdots, 2N$) by -1. The name "half-reflection" comes from the fact that the coefficients of the mode function on half D_a ($a = N/2 + 1, \cdots, 2N$) of the N intervals are inverted like a mirror. This transformation is well-defined only if the number of intervals is even.

The mode function $\varphi(y) = \{f_n^{(i)}(y) \text{ or } g_n^{(i)}(y)\}$ on D_a ($a = 1, 2, \cdots, N$) are transformed as

$$(R_y\varphi)(y) = \begin{cases} \varphi(y) & (y \in D_a,\ a = 1, 2, \cdots, N/2), \\ -\varphi(y) & (y \in D_a,\ a = N/2 + 1, \cdots, N). \end{cases} \tag{5.4.5}$$

Half-reflection R_y is a Hermitian operator. Since this transformation changes the coefficients of the mode function, the boundary vector is also transformed as

$$\vec{F}_n^{(i)} \xrightarrow{R_y} (\sigma_3 \otimes 1_N)\vec{F}_n^{(i)}, \tag{5.4.6}$$

$$\vec{G}_m^{(j)} \xrightarrow{R_y} (\sigma_3 \otimes 1_N)\vec{G}_m^{(j)}. \tag{5.4.7}$$

Fig. 5.2 schematically shows the R_y transformation. In the Figure, the coefficients of the mode function are not changed in the interval marked +, and only the sign of the mode function in the interval marked − is multiplied by -1.

5.4.3 Composite transformation $Q_y = -iR_yS_y$

Furthermore, we define the transformation Q_y which is given by the product of S_y and R_y

$$Q_y = -iR_yS_y, \tag{5.4.8}$$

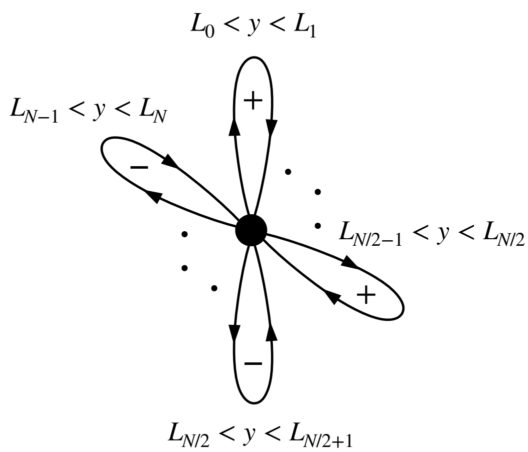

Figure 5.2: Half-reflection R_y that multiplies the mode functions on D_a ($a = N/2 + 1, \cdots, 2N$) by -1.

where we suppose that S_y acts on the mode function first, and then R_y acts on it[1]. R_y and S_y are anticommuting but by adding an imaginary unit i to the whole, Q_y is defined as a Hermitian operator.

The mode functions $\varphi(y) = \{f_n^{(i)}(y) \text{ or } g_n^{(i)}(y)\}$ on D_a ($a = 1, 2, \cdots, N$) are transformed as

$$(Q_y\varphi)(y) = \begin{cases} -i\varphi(y + L_{a-1+N/2} - L_{a-1}) & (y \in D_a,\ a = 1, 2, \cdots, N/2), \\ i\varphi(y + L_{a-1-N/2} - L_{a-1}) & (y \in D_a,\ a = N/2 + 1, \cdots, N). \end{cases} \tag{5.4.9}$$

In addition, the boundary vector also transforms as in

$$\vec{F}_n^{(i)} \xrightarrow{Q_y} (\sigma_2 \otimes 1_N)\vec{F}_n^{(i)}, \tag{5.4.10}$$

$$\vec{G}_m^{(j)} \xrightarrow{Q_y} (\sigma_2 \otimes 1_N)\vec{G}_m^{(j)}. \tag{5.4.11}$$

5.4.4 Parity in the y-direction P_y

Finally, we introduce the parity P_y that inverts the coordinates in each segment described in Fig. 5.3. Under this transformation, the mode functions $\varphi(y) = \{f_n^{(i)}(y) \text{ or } g_n^{(i)}(y)\}$ on D_a ($a = 1, 2, \cdots, N$) are transformed as

$$(P_y\varphi)(y) = \varphi(L_a - y + L_{a-1}) \quad (y \in D_a,\ a = 1, 2, \cdots, N). \tag{5.4.12}$$

We find that the P_y is a Hermitian operator and the boundary vectors are transformed as

$$\vec{F}_n^{(i)} \xrightarrow{P_y} (1_N \otimes \sigma_1)\vec{F}_n^{(i)}, \tag{5.4.13}$$

$$\vec{G}_m^{(j)} \xrightarrow{P_y} -(1_N \otimes \sigma_1)\vec{G}_m^{(j)}. \tag{5.4.14}$$

[1] It is worth noting that the operators Q_y, R_y and S_y form the $SU(2)$ algebra and that operators $(O_1, O_2, O_3) = (Q_y, R_y, S_y)$ satisfy the following relations:

$$\{O_i, O_j\} = 2\delta_{ij}, \quad [O_i, O_j] = 2i\epsilon_{ijk}O_k \quad (i, j = 1, 2, 3),$$

where ϵ_{ijk} is a completely antisymmetric tensor.

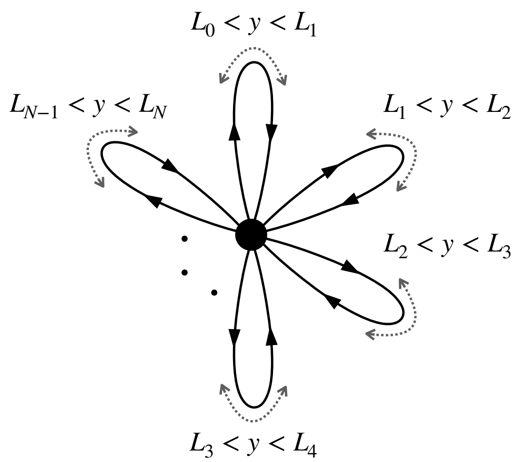

Figure 5.3: Parity in the y-direction P_y that inverts the coordinates in each edge.

5.5 Correspondence to time-reversal symmetry

We construct a transformation corresponding to the time-reversal symmetry (TRS) of AZ symmetry in our model. The time-reversal that appears in ordinary quantum field theory corresponds to $\mathcal{T}_+$, but we can construct a transformation corresponding to $\mathcal{T}_-$ by combining the Q_y transformations.

5.5.1 Time-reversal $\mathcal{T}_+$

First, we define the time-reversal transformation $\mathcal{T}_+$ and derive the boundary conditions for the system to be invariant under this transformation.

The time-reversal transformation $\mathcal{T}_+$ is acted on the 5d Dirac fermion as

$$\Psi(x, y) \xrightarrow{\mathcal{T}_+} \Psi^{\mathcal{T}_+}(x, y) = U_T \mathcal{K} \Psi(-x^0, x^i, y) = U_T \Psi^*(-x^0, x^i, y), \tag{5.5.1}$$

where $\mathcal{K}$ is a complex conjugate operator that acts like $\mathcal{K} z \mathcal{K}^{-1} = z^*$ on the complex number z and U_T is given by a 4×4 unitary matrix that satisfies the equations

$$U_T (\gamma^A)^* U_T^{-1} = \begin{cases} \gamma^0 & (A = 0), \\ -\gamma^i & (A = i = 1, 2, 3), \\ -\gamma^y & (A = y). \end{cases} \tag{5.5.2}$$

The action is invariant under the time-reversal $\mathcal{T}_+$. Indeed, the action can be transformed as

$$\begin{aligned} S \xrightarrow{\mathcal{T}_+} & \int d^4x \sum_{a=1}^{N} \int_{L_{a-1}}^{L_a} dy\, \overline{\Psi^{\mathcal{T}_+}}(x, y) \left[i\gamma^\mu \partial_\mu + i\gamma^y \partial_y + M \right] \Psi^{\mathcal{T}_+}(x, y) \\ = & \int d^4x \sum_{a=1}^{N} \int_{L_{a-1}}^{L_a} dy\, \Psi^\dagger(-x^0, x^i, y) \mathcal{K}^{-1} U_T^{-1} \gamma^0 \left[i\gamma^\mu \partial_\mu + i\gamma^y \partial_y + M \right] U_T \mathcal{K} \Psi(-x^0, x^i, y) \\ = & \int d^4x \sum_{a=1}^{N} \int_{L_{a-1}}^{L_a} dy\, \Psi^\dagger(-x^0, x^i, y) \gamma^0 \mathcal{K}^{-1} U_T^{-1} \left[i\gamma^0 \partial_0 + i\gamma^i \partial_i + i\gamma^y \partial_y + M \right] U_T \mathcal{K} \Psi(-x^0, x^i, y) \end{aligned}$$

$$
\begin{aligned}
&(\because (5.5.2),\ \mathcal{K}^{-1}(\gamma^0)^* = \gamma^0\mathcal{K}^{-1})\\
&= \int d^4x \sum_{a=1}^{N}\int_{L_{a-1}}^{L_a} dy\, \Psi^\dagger(x^0,x^i,y)\gamma^0\mathcal{K}^{-1}\underbrace{U_T^{-1}U_T}_{=1}\Big[i(\gamma^0)^*(-\partial_0) - i(\gamma^i)^*\partial_i - i(\gamma^y)^*\partial_y + M\Big]\mathcal{K}\Psi(x^0,x^i,y)\\
&(\because (5.5.2),\ x^0 \to -x^0)\\
&= \int d^4x \sum_{a=1}^{N}\int_{L_{a-1}}^{L_a} dy\, \overline{\Psi}(x,y)\Big[i\gamma^\mu\partial_\mu + i\gamma^y\partial_y + M\Big]\Psi(x,y)\\
&(\because (\gamma^A)^*\mathcal{K} = \mathcal{K}\gamma^A,\ i\mathcal{K} = -\mathcal{K}i)\\
&= S. && (5.5.3)
\end{aligned}
$$

In the case of free Dirac fermions on an ordinary flat 4d spacetime, we conclude from this invariance that they have the time-reversal symmetry. On the other hand, the boundary conditions are generally not invariant under the time-reversal. This is because the transformed 5d Dirac fermion $\Psi^{\mathcal{T}_+}(x,y)$ generally does not satisfy the same boundary conditions for $\Psi(x,y)$ on the quantum graph.

To obtain additional conditions for the BCs to be invariant under the time-reversal $\mathcal{T}_+$, we substitute the KK expansion (5.1.2) into (5.5.1) to obtain

$$
\begin{aligned}
&\sum_i\sum_n\Big[\psi^{(i)}_{\mathrm{R},n}(x)f^{(i)}_n(y) + \psi^{(i)}_{\mathrm{L},n}(x)g^{(i)}_n(y)\Big]\\
&\xrightarrow{\mathcal{T}_+} \sum_i\sum_n U_T\psi^{(i)*}_{\mathrm{R},n}(-x^0,x^i)f^{(i)*}_n(y) + \sum_i\sum_n U_T\psi^{(i)*}_{\mathrm{L},n}(-x^0,x^i)g^{(i)*}_n(y). \qquad (5.5.4)
\end{aligned}
$$

Then, taking account of the chirality in four dimensions, we obtain the transformations for the 4d fields $\psi^{(i)}_{\mathrm{R/L},n}(x)$ and the mode functions $f^{(i)}_n(y)$, $g^{(i)}_n(y)$ as

$$
\psi^{(i)}_{\mathrm{R/L},n}(x) \xrightarrow{\mathcal{T}_+} U_T\psi^{(i)*}_{\mathrm{R/L},n}(-x^0,x^i),\quad f^{(i)}_n(y) \xrightarrow{\mathcal{T}_+} f^{(i)*}_n(y),\quad g^{(i)}_n(y) \xrightarrow{\mathcal{T}_+} g^{(i)*}_n(y). \qquad (5.5.5)
$$

Focusing only on the 4d part, it is a time-reversal of the usual 4d Dirac fermions, which are always symmetric in a system of free Dirac fermions. On the other hand, the requirement that the transformed field $\Psi^{\mathcal{T}_+}(x,y)$ satisfies the original boundary conditions yields

$$
(1_{2N} - U_{\mathrm{B}})\vec{F}^{(i)*}_n = 0, \qquad (5.5.6)
$$
$$
(1_{2N} + U_{\mathrm{B}})\vec{G}^{(j)*}_m = 0. \qquad (5.5.7)
$$

To rewrite the condition for U_{B}, comparing these relations with the complex conjugate of the original boundary conditions leads to

$$
T_+U_{\mathrm{B}}T_+^{-1} = U_{\mathrm{B}},\quad T_+ \equiv \mathcal{K}. \qquad (5.5.8)
$$

Since T_+ is anti-unitary and satisfies

$$
T_+^2 = 1, \qquad (5.5.9)
$$

Eq. (5.5.8) implies that T_+ corresponds to the TRS with $T^2 = 1$ in the AZ symmetry classes.

5.5.2 Time-reversal $\mathcal{T}_-$

Next, we define the time-reversal transformation $\mathcal{T}_-$ and derive the boundary conditions for the system to be invariant under this transformation.

Let us consider a symmetry which leads to the restriction corresponds to the TRS with $T^2 = -1$ in the AZ symmetry classes. This symmetry can be achieved by combining the transformation of Q_y to T_+ introduced above. The 5d Dirac fermion is transformed as

$$\Psi(x,y) \xrightarrow{\mathcal{T}_-} \Psi^{\mathcal{T}_-}(x,y) = Q_y U_T \Psi^*(-x^0, x^i, y) = Q_y U_T \mathcal{K}\Psi(-x^0, x^i, y), \tag{5.5.10}$$

under the $\mathcal{T}_-$ transformation. Q_y acts as in (5.4.9) for the mode functions in the y direction and U_T is a unitary matrix satisfying (5.5.2). The transformation by Q_y does not affect the 5d Dirac equation described on each edge and then the 5d Dirac equation is also invariant for the transformation. However, the transformed field should satisfy the same boundary condition as the original one in order for $\mathcal{T}_-$ to be a symmetry.

To obtain additional conditions, we substitute the KK expansion (5.1.2) into (5.5.10) to obtain

$$\begin{aligned}&\sum_i \sum_n \left[\psi^{(i)}_{\mathrm{R},n}(x) f^{(i)}_n(y) + \psi^{(i)}_{\mathrm{L},n}(x) g^{(i)}_n(y)\right]\\ &\xrightarrow{\mathcal{T}_-} \sum_i \sum_n U_T \psi^{(i)*}_{\mathrm{R},n}(-x^0, x^i) Q_y f^{(i)*}_n(y) + \sum_i \sum_n U_T \psi^{(i)*}_{\mathrm{L},n}(-x^0, x^i) Q_y g^{(i)*}_n(y).\end{aligned} \tag{5.5.11}$$

If we compare the 4d chirality in the same way, we obtain the transformation $\mathcal{T}_+$ for the 4d fields, and the mode functions as

$$\psi^{(i)}_{\mathrm{R/L},n}(x) \xrightarrow{\mathcal{T}_-} U_T \psi^{(i)*}_{\mathrm{R/L},n}(-x^0, x^i), \quad f^{(i)}_n(y) \xrightarrow{\mathcal{T}_-} Q_y f^{(i)*}_n(y), \quad g^{(i)}_n(y) \xrightarrow{\mathcal{T}_-} Q_y g^{(i)*}_n(y). \tag{5.5.12}$$

Then, in order for our model to have the time-reversal symmetry $\mathcal{T}_-$, we obtain the relations

$$(1_{2N} - U_\mathrm{B})(\sigma_2 \otimes 1_N)\vec{F}^{(i)*}_n = 0, \tag{5.5.13}$$

$$(1_{2N} + U_\mathrm{B})(\sigma_2 \otimes 1_N)\vec{G}^{(j)*}_m = 0. \tag{5.5.14}$$

To rewrite the condition for U_B, comparing these relations with the complex conjugate of the original boundary conditions leads to

$$T_- U_\mathrm{B} T_-^{-1} = U_\mathrm{B}, \quad T_- \equiv (i\sigma_2 \otimes 1_N)\mathcal{K}. \tag{5.5.15}$$

Note that T_- is defined by inserting the imaginary number i. Since T_- is anti-unitary and satisfies

$$T_-^2 = -1, \tag{5.5.16}$$

Eq. (5.5.15) implies that T_- corresponds to the TRS with $T^2 = -1$ in the AZ symmetry classes. In the AZ symmetry classes, the $T^2 = -1$ symmetry causes a double degeneracy in the ground state, called the Kramers degeneracy. Surprisingly, we will see later that the above restricted matrix U_B induces a double degeneracy in the chiral zero modes.

As can be seen from the present discussion, Q_y inverts the positive and negative of the square of the transformation. In other words, $\mathcal{T}_+$ combined with Q_y results in a transformation whose square is negative, $\mathcal{T}_-$. This property will be used in the next Section.

5.6 Correspondence to particle-hole symmetry

The AZ symmetry classes include particle-hole symmetry. This symmetry restricts the gapped free-fermion Hamiltonian as $CHC^{-1} = -H$. In this Section, we construct two types of charge conjugations with extra-spatial transformations similar to the time-reversal symmetries and show those provide the restrictions for U_{B}.

5.6.1 Charge conjugation C_-

First, we define the charge conjugation C_- and derive the boundary conditions for the system to be invariant under this transformation.

We introduce a transformation that combined usual the charge conjugation on the 4d Minkowski spacetime and the parity in the y-direction P_y. The 5d Dirac fermion is transformed as

$$\Psi(x,y) \xrightarrow{C_-} \Psi^{C_-}(x,y) = P_y U_C \overline{\Psi}^{\top}(x,y) = P_y U_C (\gamma^0)^{\top} \mathcal{K} \Psi(x,y), \tag{5.6.1}$$

where U_C is the usual 4d charge conjugation matrix defined by

$$U_C (\gamma^{\mu})^{\top} U_C^{-1} = -\gamma^{\mu}, \quad U_C^{\top} = -U_C. \tag{5.6.2}$$

From the above relations, the gamma matrix γ^y $(\equiv -i\gamma^5)$ satisfies

$$U_C (\gamma^y)^{\top} U_C^{-1} = \gamma^y. \tag{5.6.3}$$

This definition of the charge conjugation is different from a usual the 5d charge conjugation in 5d Minkowski spacetime. Indeed, a 5d massless free Dirac fermion is transformed as

$$\Psi(x,y) \to U_{C'} \overline{\Psi}^{\top}(x,y) \tag{5.6.4}$$

by the 5d charge conjugation, where the matrix $U_{C'}$ satisfies

$$U_{C'} (\gamma^A)^{\top} U_{C'} = \gamma^A, \quad U_{C'}^{\top} = -U_{C'}. \tag{5.6.5}$$

For the purpose that constructs a symmetry corresponding to a particle-hole symmetry, we choose the former definition.

Now, the action is invariant under C_-:

$$
\begin{aligned}
S \xrightarrow{C_-} &\int d^4x \sum_{a=1}^{N} \int_{L_{a-1}}^{L_a} dy\, \overline{\Psi^{C_-}}(x,y) \left[i\gamma^\mu \partial_\mu + i\gamma^y \partial_y + M \right] \Psi^{C_-}(x,y) \\
= &\int d^4x \sum_{a=1}^{N} \int_{L_{a-1}}^{L_a} dy\, \Psi^\top(x,y) \underbrace{(\gamma^0)^* U_C^{-1}}_{=-U_C^{-1}(\gamma^0)^\dagger} P_y \gamma^0 \left[i\gamma^\mu \partial_\mu + i\gamma^y \partial_y + M \right] P_y U_C (\gamma^0)^\top \Psi^*(x,y) \\
= &\int d^4x \sum_{a=1}^{N} \int_{L_{a-1}}^{L_a} dy\, \Psi^\top(x,y) (-U_C^{-1}) \left[i\gamma^\mu \partial_\mu + i\gamma^y (-\partial_y) + M \right] U_C (\gamma^0)^\top \Psi^*(x,y) \\
&(\because \partial_y P_y = -P_y \partial_y,\ (\gamma^0)^\dagger = \gamma^0,\ (\gamma^0)^2 = 1) \\
= &\int d^4x \sum_{a=1}^{N} \int_{L_{a-1}}^{L_a} dy\, \Psi^\top(x,y) \left[i(\gamma^\mu)^\top \partial_\mu + i(\gamma^y)^\top \partial_y - M \right] (\gamma^0)^\top \Psi^*(x,y) \\
&(\because (5.6.2), (5.6.3)) \\
= &\int d^4x \sum_{a=1}^{N} \int_{L_{a-1}}^{L_a} dy\, \overline{\Psi}(x,y) \left[-i\gamma^\mu \overleftarrow{\partial}_\mu - i\gamma^y \overleftarrow{\partial}_y + M \right] \Psi(x,y) \\
&(\because \text{overall transposition}) \\
= &\int d^4x \sum_{a=1}^{N} \int_{L_{a-1}}^{L_a} dy\, \overline{\Psi}(x,y) \left[i\gamma^\mu \partial_\mu + i\gamma^y \partial_y + M \right] \Psi(x,y) \\
&(\because \text{integration by parts}) \\
= &\, S.
\end{aligned}
\tag{5.6.6}
$$

Even if the action is invariant, the transformed field does not always satisfy the some boundary conditions as the original field.

To obtain additional conditions, we substitute the KK expansion (5.1.2) into (5.6.1) to obtain

$$
\begin{aligned}
&\sum_i \sum_n \left[\psi^{(i)}_{\mathrm{R},n}(x) f^{(i)}_n(y) + \psi^{(i)}_{\mathrm{L},n}(x) g^{(i)}_n(y) \right] \\
&\xrightarrow{C_-} \sum_i \sum_n U_C \overline{\psi^{(i)}_{\mathrm{R},n}}^\top(x) P_y f^{(i)*}_n(y) + \sum_i \sum_n U_C \overline{\psi^{(i)}_{\mathrm{L},n}}^\top(x) P_y g^{(i)*}_n(y).
\end{aligned}
\tag{5.6.7}
$$

Comparing the chirality in four dimensions, we obtain the transformation C_- for the 4d fields and the mode functions as

$$
\psi^{(i)}_{\mathrm{R/L},n}(x) \xrightarrow{C_-} U_C \overline{\psi^{(i)}_{\mathrm{L/R},n}}^\top(x), \quad f^{(i)}_n(y) \xrightarrow{C_-} P_y g^{(i)*}_n(y), \quad g^{(i)}_n(y) \xrightarrow{C_-} P_y f^{(i)*}_n(y).
\tag{5.6.8}
$$

Note that the overall chirality of $\overline{\psi^{(i)}_{\mathrm{L/R},n}}^\top$ is R/L, respectively. This is because $\overline{\psi^{(i)}_{\mathrm{R/L},n}}^\top \left(= (\gamma^0)^\top \psi^{(i)*}_{\mathrm{R/L},n}\right)$ contains γ^0 and thus is anti-commutative with the chiral projection operator. It can be seen that as the chirality of the 4d field is inverted, the mode functions $f^{(i)}_n$ and $g^{(i)}_n$ are also interchanged. Therefore, if there exist zero mode functions $f^{(i)}_0$, zero modes $g^{(i)}_0$ should also exist and they can be given by

$$
g^{(i)}_0(y) = P_y f^{(i)}_0(y).
\tag{5.6.9}
$$

By this property, a class with C_- symmetry has an equal number of $f_0^{(i)}$ and $g_0^{(i)}$, i.e., the Witten index is zero. For massive modes ($n \neq 0$), since the SUSY relations connect $f_n^{(i)}$ with $g_n^{(i)}$ and vice versa, $P_y g_n^{(i)*}$ ($P_y f_n^{(i)}$) should be given by linear combinations of $f_n^{(i)}$ ($g_n^{(i)}$).

The boundary vectors are transformed as

$$\vec{F}_n^{(i)} \xrightarrow{C_-} -(1_N \otimes i\sigma_2)\vec{G}_n^{(i)*}, \tag{5.6.10}$$

$$\vec{G}_m^{(j)} \xrightarrow{C_-} (1_N \otimes i\sigma_2)\vec{F}_m^{(j)*}, \tag{5.6.11}$$

under the charge conjugation C_- and the following relations must hold:

$$(1_{2N} - U_{\mathrm{B}})(1_N \otimes i\sigma_2)\vec{G}_n^{(i)*} = 0, \tag{5.6.12}$$

$$(1_{2N} + U_{\mathrm{B}})(1_N \otimes i\sigma_2)\vec{F}_m^{(j)*} = 0. \tag{5.6.13}$$

To rewrite the condition for U_{B}, comparing these relations with the complex conjugate of the original boundary conditions leads to

$$C_- U_{\mathrm{B}} C_-^{-1} = -U_{\mathrm{B}}, \quad C_- \equiv (1_N \otimes i\sigma_2)\mathcal{K}. \tag{5.6.14}$$

Since C_- is anti-unitary and satisfies

$$C_-^2 = -1, \tag{5.6.15}$$

then we can construct the symmetry that corresponds to PHS with $C^2 = -1$ in the AZ symmetry classes.

5.6.2 Charge conjugation C_+

Next, we define the charge conjugation C_+ and derive the boundary conditions for the system to be invariant under this transformation.

We construct a transformation C_+ which correspond to PHS with $C^2 = 1$ in the AZ symmetry classes. To do this, we can follow the same procedure as the construction of $\mathcal{T}_-$ from $\mathcal{T}_+$. Consider a transformation that combines C_- with the Q_y transformation. This transformation acts on the 5d Dirac fermion as

$$\Psi(x,y) \xrightarrow{C_+} \Psi^{C_+}(x,y) = Q_y P_y U_C (\gamma^0)^\top \mathcal{K} \Psi(x,y), \tag{5.6.16}$$

where U_C is defined by Eqs. (5.6.2), (5.6.3). Since the action is invariant under the transformation of Q_y alone, it is also invariant under the transformation of C_+.

The matrix U_{B} must satisfy an additional condition for the C_+ symmetry to hold. Now, the transformations for the 4d fields and the mode functions are given by

$$\psi_{\mathrm{R/L},n}^{(i)}(x) \xrightarrow{C_+} U_C \overline{\psi_{\mathrm{L/R},n}^{(i)}}^\top(x), \quad f_n^{(i)}(y) \xrightarrow{C_+} Q_y P_y g_n^{(i)*}(y), \quad g_n^{(i)}(y) \xrightarrow{C_+} Q_y P_y f_n^{(i)*}(y). \tag{5.6.17}$$

The only difference from the C_- case is the insertion of the Q_y transformation for the mode functions. As a result, the boundary vectors $\vec{F}_n^{(i)}$, $\vec{G}_n^{(i)}$ are transformed as

$$\vec{F}_n^{(i)} \xrightarrow{C_+} -(\sigma_2 \otimes 1_{N/2} \otimes i\sigma_2)\vec{G}_n^{(i)*}, \tag{5.6.18}$$

$$\vec{G}_m^{(j)} \xrightarrow{C_+} (\sigma_2 \otimes 1_{N/2} \otimes i\sigma_2)\vec{F}_m^{(j)*}. \tag{5.6.19}$$

Therefore, the following relations must hold:

$$(1_{2N} - U_{\mathrm{B}})(\sigma_2 \otimes 1_{N/2} \otimes i\sigma_2)\vec{G}_n^{(i)*} = 0, \tag{5.6.20}$$
$$(1_{2N} + U_{\mathrm{B}})(\sigma_2 \otimes 1_{N/2} \otimes i\sigma_2)\vec{F}_n^{(j)*} = 0. \tag{5.6.21}$$

To rewrite the condition for U_{B}, comparing these relations with the original boundary conditions leads to

$$C_+ U_{\mathrm{B}} C_+^{-1} = -U_{\mathrm{B}}, \quad C_+ \equiv (i\sigma_2 \otimes 1_{N/2} \otimes i\sigma_2)\mathcal{K}. \tag{5.6.22}$$

Note the additional insertion of the imaginary number i. From the direct computation, C_+ is found to satisfy

$$C_+^2 = 1. \tag{5.6.23}$$

Thus, we can find that C_+ corresponds to the PHS with $C^2 = 1$ in the AZ symmetry classes.

5.7 Correspondence to chiral symmetry

There exists a symmetry under the transformation defined as the product of TRS and PHS in the AZ symmetries, called chiral symmetry (CS). A system with both TRS and PHS symmetry automatically has CS as well. However, even when both symmetries are broken, only the CS can exist.

Here we construct the transformation of the product of the time-reversal and the charge-conjugation constructed above, corresponding to the definition of the CS in the AZ symmetry class. In addition, we show that these symmetries lead to same restriction for U_{B} and correspond to the CS in the AZ symmetry classes.

5.7.1 Chiral symmetry Γ_+

First, we define the chiral symmetry Γ_+ and derive the boundary conditions for the system to be invariant under this transformation.

We consider the transformation of the product $\mathcal{T}_+ C_+$ or $\mathcal{T}_- C_-$. The order of the two transformations is such that $C_\pm$ acts first, then $\mathcal{T}_\pm$. From Eqs. (5.5.1), (5.6.16) or Eqs. (5.5.10), (5.6.1), the 5d Dirac fermion is transformed as

$$\Psi(x, y) \xrightarrow{\mathcal{T}_+ C_+} (\Psi^{C_+}(x, y))^{\mathcal{T}_+} = -Q_y P_y U_T U_C^* \gamma^0 \Psi(-x^0, x^i, y), \tag{5.7.1}$$
$$\Psi(x, y) \xrightarrow{\mathcal{T}_- C_-} (\Psi^{C_-}(x, y))^{\mathcal{T}_-} = +Q_y P_y U_T U_C^* \gamma^0 \Psi(-x^0, x^i, y), \tag{5.7.2}$$

under $\mathcal{T}_\pm C_\pm$ transformations. As can be seen from the above transformations, $\mathcal{T}_+ C_+$ and $\mathcal{T}_- C_-$ transformations are equivalent up to the sign. Since the action is invariant under both $\mathcal{T}_\pm$ and $C_\pm$ transformations, it is also invariant under the transformation of their product. However, additional conditions are derived for the matrix U_{B} since the transformed fields do not in general satisfy the boundary conditions.

We substitute the KK expansion (5.1.2) into (5.7.1) and (5.7.2) to obtain

$$\begin{aligned}
&\sum_i \sum_n \left[\psi^{(i)}_{\mathrm{R},n}(x) f^{(i)}_n(y) + \psi^{(i)}_{\mathrm{L},n}(x) g^{(i)}_n(y)\right] \\
&\xrightarrow{\mathcal{T}_\pm \mathcal{C}_\pm} \sum_i \sum_n U_T U_C^* \gamma^0 \psi^{(i)}_{\mathrm{R},n}(-x^0, x^i)(\mp 1) Q_y P_y f^{(i)}_n(y) \\
&\qquad + \sum_i \sum_n U_T U_C^* \gamma^0 \psi^{(i)}_{\mathrm{L},n}(-x^0, x^i)(\mp 1) Q_y P_y g^{(i)}_n(y).
\end{aligned} \tag{5.7.3}$$

Comparing the chirality in 4d, we obtain the transformations for the 4d fields and the mode functions as

$$\psi^{(i)}_{\mathrm{R/L},n}(x) \xrightarrow{\mathcal{T}_\pm \mathcal{C}_\pm} U_T U_C^* \gamma^0 \psi^{(i)}_{\mathrm{L/R},n}(-x^0, x^i), \tag{5.7.4}$$

$$f^{(i)}_n(y) \xrightarrow{\mathcal{T}_\pm \mathcal{C}_\pm} \mp Q_y P_y g^{(i)}_n(y), \tag{5.7.5}$$

$$g^{(i)}_n(y) \xrightarrow{\mathcal{T}_\pm \mathcal{C}_\pm} \mp Q_y P_y f^{(i)}_n(y). \tag{5.7.6}$$

Note that the mode functions $f^{(i)}_n$ and $g^{(i)}_n$ are interchanged since the chirality of the entire 4d field is reversed. As a result, the boundary vectors $\vec{F}^{(i)}_n$, $\vec{G}^{(i)}_n$ are transformed as

$$\vec{F}^{(i)}_n \xrightarrow{\mathcal{T}_\pm \mathcal{C}_\pm} \pm(\sigma_2 \otimes 1_{N/2} \otimes i\sigma_2)\vec{G}^{(i)}_n, \tag{5.7.7}$$

$$\vec{G}^{(j)}_m \xrightarrow{\mathcal{T}_\pm \mathcal{C}_\pm} \mp(\sigma_2 \otimes 1_{N/2} \otimes i\sigma_2)\vec{F}^{(j)}_m. \tag{5.7.8}$$

Therefore, these indicate that the relations

$$(1_{2N} - U_{\mathrm{B}})(\sigma_2 \otimes 1_{N/2} \otimes i\sigma_2)\vec{G}^{(i)}_n = 0, \tag{5.7.9}$$

$$(1_{2N} + U_{\mathrm{B}})(\sigma_2 \otimes 1_{N/2} \otimes i\sigma_2)\vec{F}^{(j)}_n = 0 \tag{5.7.10}$$

must hold in order for $\mathcal{T}_\pm \mathcal{C}_\pm$ to be symmetry.

To rewrite the condition for U_{B}, comparing these relations with the original boundary conditions leads to

$$\Gamma_+ U_{\mathrm{B}} \Gamma_+^{-1} = -U_{\mathrm{B}}, \quad \Gamma_+ \equiv i\sigma_2 \otimes 1_{N/2} \otimes i\sigma_2. \tag{5.7.11}$$

Note the additional insertion of the imaginary number i in order to make the sign of the square positive. From the direct computation, Γ_+ is unitary and we can find that Γ_+ corresponds to the CS in the AZ symmetry classes. In terms of operators that act on U_{B}, we can confirm the relation

$$\Gamma_+ = T_\pm C_\pm. \tag{5.7.12}$$

5.7.2 Chiral symmetry Γ_-

Next, we define the chiral symmetry Γ_- and derive the boundary conditions for the system to be invariant under this transformation.

We consider the transformation of the product $\mathcal{T}_+\mathcal{C}_-$ or $\mathcal{T}_-\mathcal{C}_+$. The order of the two transformations is such that $\mathcal{C}_\mp$ acts first, then $\mathcal{T}_\pm$.

$$\Psi(x,y) \xrightarrow{\mathcal{T}_\pm\mathcal{C}_\mp} (\Psi^{\mathcal{C}_\mp}(x,y))^{\mathcal{T}_\pm} = \pm P_y U_T U_C^* \gamma^0 \Psi(-x^0, x^i, y) \tag{5.7.13}$$

From Eqs. (5.5.1), (5.6.1) and Eqs. (5.5.10), (5.6.16), the 5d Dirac fermion is transformed as

$$\psi^{(i)}_{\mathrm{R/L},n}(x) \xrightarrow{\mathcal{T}_\pm\mathcal{C}_\mp} U_T U_C^* \gamma^0 \psi^{(i)}_{\mathrm{L/R},n}(-x^0, x^i), \tag{5.7.14}$$

$$f^{(i)}_n(y) \xrightarrow{\mathcal{T}_\pm\mathcal{C}_\mp} \pm(P_y g^{(i)}_n)(y), \tag{5.7.15}$$

$$g^{(i)}_n(y) \xrightarrow{\mathcal{T}_\pm\mathcal{C}_\mp} \pm(P_y f^{(i)}_n)(y). \tag{5.7.16}$$

Therefore, the boundary vectors $\vec{F}^{(i)}_n$ and $\vec{G}^{(j)}_m$ are transformed as

$$\vec{F}^{(i)}_n \xrightarrow{\mathcal{T}_\pm\mathcal{C}_\mp} \mp(1_N \otimes i\sigma_2)\vec{G}^{(i)}_n, \tag{5.7.17}$$

$$\vec{G}^{(j)}_m \xrightarrow{\mathcal{T}_\pm\mathcal{C}_\mp} \pm(1_N \otimes i\sigma_2)\vec{F}^{(j)}_m, \tag{5.7.18}$$

and the following relations should be satisfied in order for $\mathcal{T}_\pm\mathcal{C}_\mp$ to be a symmetry:

$$(1_{2N} - U_\mathrm{B})(1_N \otimes i\sigma_2)\vec{G}^{(i)}_n = 0, \tag{5.7.19}$$

$$(1_{2N} + U_\mathrm{B})(1_N \otimes i\sigma_2)\vec{F}^{(j)}_n = 0. \tag{5.7.20}$$

Comparing these relations with the original boundary conditions leads to

$$\Gamma_- U_\mathrm{B} \Gamma_-^{-1} = -U_\mathrm{B}, \quad \Gamma_- \equiv 1_N \otimes \sigma_2. \tag{5.7.21}$$

Note that Γ_- is defined without the imaginary unit i to make the sign of the square positive. From the direct computation, Γ_- is unitary and we can find that Γ_- corresponds to the CS in the AZ symmetry classes. We can also confirm that Γ_- can be given by

$$\Gamma_- = -iT_+C_- \quad \text{or} \quad \Gamma_- = iT_-C_+. \tag{5.7.22}$$

5.8 Summary of correspondence to AZ symmetry class

Table 5.3 summarizes the transformations in our model corresponding to the AZ symmetry. It also shows how the matrix U_B, which specifies the boundary conditions, is restricted.

It should be noted that we assume only one of the same type symmetries such as $\mathcal{T}_+$ and $\mathcal{T}_-$ can be present so far. If both symmetries are present, Q_y also becomes the symmetry independently since Q_y can be given by their product. In this case, we consider the identification of the $(a+N/2)$-edge to a-edge ($a = 1, 2, \cdots, N/2$) by the symmetry Q_y with the eigenvalues $Q_y = +1$ or $Q_y = -1$, and then classify the boundary conditions of this reduced system. This identification effectively reduces the rose graph with N edges to the one with $N/2$ edges, then the same type symmetries such as $\mathcal{T}_+$ and $\mathcal{T}_-$ are trivially related with each other. For example, it is the same as regarding

Table 5.3: The transformation in our model and the correspondence to the AZ symmetries.

AZ symmetry	Transformation for $\Psi(x,y)$	Restriction for U_{B}
Time-reversal ($T^2=+1$)	$\Psi(x,y)\xrightarrow{\mathcal{T}_+} U_T\mathcal{K}\Psi(-x^0,x^i,y)$	$T_+U_{\mathrm{B}}T_+^{-1}=U_{\mathrm{B}}$ $T_+=\mathcal{K}$
Time-reversal ($T^2=-1$)	$\Psi(x,y)\xrightarrow{\mathcal{T}_-} Q_yU_T\mathcal{K}\Psi(-x^0,x^i,y)$	$T_-U_{\mathrm{B}}T_-^{-1}=U_{\mathrm{B}}$ $T_-=(i\sigma_2\otimes 1_N)\mathcal{K}$
Particle-hole ($C^2=+1$)	$\Psi(x,y)\xrightarrow{\mathcal{C}_+} Q_yP_yU_C\overline{\Psi}^{\top}(x,y)$	$C_+U_{\mathrm{B}}C_+^{-1}=-U_{\mathrm{B}}$ $C_+=(i\sigma_2\otimes 1_{N/2}\otimes i\sigma_2)\mathcal{K}$
Particle-hole ($C^2=-1$)	$\Psi(x,y)\xrightarrow{\mathcal{C}_-} P_yU_C\overline{\Psi}^{\top}(x,y)$	$C_-U_{\mathrm{B}}C_-^{-1}=-U_{\mathrm{B}}$ $C_-=(1_N\otimes i\sigma_2)\mathcal{K}$
Chiral	$\Psi(x,y)\xrightarrow{\mathcal{T}_\pm\mathcal{C}_\pm} \mp Q_yP_yU_TU_C^*\gamma^0\Psi(-x^0,x^i,y)$	$\Gamma_+U_{\mathrm{B}}\Gamma_+^{-1}=-U_{\mathrm{B}}$ $\Gamma_+=i\sigma_2\otimes 1_{N/2}\otimes i\sigma_2$
Chiral	$\Psi(x,y)\xrightarrow{\mathcal{T}_\pm\mathcal{C}_\mp} \pm P_yU_TU_C^*\gamma^0\Psi(-x^0,x^i,y)$	$\Gamma_-U_{\mathrm{B}}\Gamma_-^{-1}=-U_{\mathrm{B}}$ $\Gamma_-=1_N\otimes\sigma_2$

the S^1 as the interval by identifying it with the symmetry of Z_2. Under the Q_y transformation, the boundary vectors are transformed as (5.4.10) and (5.4.11), so the U_B can be written as

$$U_{\mathrm{B}}=\frac{1_2+\sigma_2}{2}\otimes u_{\mathrm{B}+}+\frac{1_2-\sigma_2}{2}\otimes u_{\mathrm{B}-} \tag{5.8.1}$$

in the present case, where $u_{\mathrm{B}\pm}$ are $N\times N$ Hermitian unitary matrices. This $u_{\mathrm{B}+}$ ($u_{\mathrm{B}-}$) specifies the boundary condition for the reduced rose graph with $N/2$ edges with $Q_y=+1$ ($Q_y=-1$) and corresponds to the irreducible blocks in the Hamiltonian for the gapped free-fermion system discussed in Sec. 5.2.

5.9 Index and zero modes in each symmetry class

The gapped free-fermion system is classified into 10 symmetric classes, each of which is characterized by nontrivial topological numbers of $\mathbb{Z}$, $\mathbb{Z}_2$ and $2\mathbb{Z}$ or a trivial topological number 0. The non-trivial topological number is the number of gapless modes that appear at the boundary of the system.

In the previous Section, we constructed the transformation corresponding to the AZ symmetric class in the case of our model. Unlike the original AZ classification, our model considers a classification of the matrix U_{B} that characterizes the boundary conditions. Here, we investigate what quantities can be obtained as topological numbers in our case of different classification objects. As a result, Table 5.4 is obtained. By comparing with the AZ classification of $d=0$ we find the following:

- The topological numbers $\mathbb{Z}$ and $2\mathbb{Z}$ are related to the Witten index.
- The topological number $\mathbb{Z}_2$ is related to even/odd parity of Dirac zero mode. This means that

Table 5.4: Tenfold classification of the boundary conditions in our model. The sign ± 1 in the column of T and C denote the presence of $T_\pm$ and $C_\pm$, respectively and also 1 in Γ indicates the presence of the chiral symmetry Γ_+ or Γ_-, while 0 means the absence of corresponding symmetries. We also describe the Witten index for the type$(2N-k,k)$ BC in each symmetry class, which is equivalent to the number of the chiral zero modes in our model. In addition, $\mathbb{Z}_2$ in the column of the $\mathbb{Z}_2$ index indicates that the number of massless 4d Dirac fields in module 2 is topologically nontrivial, while 0 means topologically trivial and the number of massless 4d Dirac fields can be zero by continuous deformations of parameters. These correspond to the topological numbers in Table 5.2 for the $d=0$ case.

Class	T	C	Γ	Classifying space of U_{B}	$d=0$	Δ_{W}	$\mathbb{Z}_2$ index
A	0	0	0	$C_0=\bigcup_{k=0}^{2N}\frac{U(2N)}{U(2N-k)\times U(k)}$	$\mathbb{Z}$	$N-k$	0
AIII	0	0	1	$C_1=U(N)$	0	0	0
AI	+1	0	0	$R_0=\bigcup_{k=0}^{2N}\frac{O(2N)}{O(2N-k)\times O(k)}$	$\mathbb{Z}$	$N-k$	0
BDI	+1	+1	1	$R_1=O(N)$	$\mathbb{Z}_2$	0	$\mathbb{Z}_2$
D	0	+1	0	$R_2=\frac{O(2N)}{U(N)}$	$\mathbb{Z}_2$	0	$\mathbb{Z}_2$
DIII	−1	+1	1	$R_3=\frac{U(N)}{Sp(N/2)}$	0	0	0
AII	−1	0	0	$R_4=\bigcup_{k=0}^{2N}\frac{Sp(N)}{Sp(N-k/2)\times Sp(k/2)}$	$2\mathbb{Z}$	$N-k$	0
CII	−1	−1	1	$R_5=Sp(N/2)$	0	0	0
C	0	−1	0	$R_6=\frac{Sp(N)}{U(N)}$	0	0	0
CI	+1	−1	1	$R_7=\frac{U(N)}{O(N)}$	0	0	0

there are an even number of Dirac zero modes and an odd number of classes, and they do not transfer to each other.

In the following, we discuss specifically for each class.

5.9.1 Witten index and classifying space

Here, let us discuss the Witten index and the classifying space for each symmetry class in our model. Furthermore we show the correspondence to the topological numbers $\mathbb{Z}$, $2\mathbb{Z}$ and the classifying spaces in the gapped free-fermion system. The $\mathbb{Z}_2$ index will be discussed in detail in the next Subsection.

5.9.1.1 Class A

Since the class A has no symmetries, there are no additional conditions for U_{B}. In general, a Hermitian matrix whose square equals 1 can be diagonalized by a unitary matrix and is shown in

$$U_{\mathrm{B}} = V \begin{pmatrix} 1_{2N-k} & \mathbf{0} \\ \mathbf{0} & -1_k \end{pmatrix} V^{\dagger}, \quad V \in U(2N) \quad (k = 0, 1, \cdots, 2N). \tag{5.9.1}$$

The Witten index is obtained once the matrix U_{B} is determined. Indeed, as discussed in Chap. 3, it can be obtained by subtracting the number of eigenvalues -1 from the number of intervals in the rose graph, N, i.e.,

$$\Delta_{\mathrm{W}} = N - k \quad (k = 0, 1, \cdots, 2N). \tag{5.9.2}$$

The matrix U_{B} in Eq. (5.9.1) is invariant under the transformation

$$V \to \begin{pmatrix} U_{2N-k} & \mathbf{0} \\ \mathbf{0} & U_k \end{pmatrix} V, \tag{5.9.3}$$

where U_{2N-k} is $2N-k$ dimensional unitary matrix and U_k is k dimensional unitary matrix. Thus, the parameter space of U_{B} in the case of type$(2N-k, k)$ boundary condition is given by the complex Grassmannian

$$\frac{U(2N)}{U(2N-k) \times U(k)} \quad (k = 0, 1, \cdots, 2N), \tag{5.9.4}$$

and the classifying space is given by

$$C_0 = \bigcup_{k=0}^{2N} \frac{U(2N)}{U(2N-k) \times U(k)}. \tag{5.9.5}$$

These result are shown in Table 5.4. This is also identical to the one for the 0d Hamiltonian in the gapped free-fermion system.

5.9.1.2 Class AIII

The class AIII has only the chiral symmetry which denotes Γ_+ or Γ_- given in Sec. 5.7.1 and 5.7.2. These operators satisfy

$$\{U_{\mathrm{B}}, \Gamma_{\pm}\} = 0, \quad \Gamma_{\pm}^2 = 1_{2N}. \tag{5.9.6}$$

The anti-commutation relation implies that the boundary vectors of the zero mode functions with the chiral operator $\Gamma_{\pm}\vec{F}_0^{(i)}$ ($\Gamma_{\pm}\vec{G}_0^{(j)}$) satisfy the boundary condition of $\vec{G}_0^{(i)}$ ($\vec{F}_0^{(j)}$). Therefore, in this class, $\vec{F}_0^{(i)}$ and $\vec{G}_0^{(j)}$ have the same degrees of degeneracy, i.e., the equal degrees of freedom for i and j. For this reason, the number of $+1$ and -1 eigenvalues of U_{B} is equal and diagonalized as

$$U_{\mathrm{B}} = U \begin{pmatrix} 1_N & 0 \\ 0 & -1_N \end{pmatrix} U^{\dagger} \quad U \in U(2N). \tag{5.9.7}$$

Once the diagonalized form is obtained, the Witten index can be calculated in the same way as for the class A, and the result is

$$\Delta_{\mathrm{W}} = 0. \tag{5.9.8}$$

As can be seen from the above discussion, the Witten index for a class with chiral symmetry is always zero.

Let us discuss the classifying space of U_{B}. To discuss Γ_+ and Γ_- simultaneously, we will drop the subscripts of the chiral symmetry operator and denote it by Γ. By changing to the appropriate basis, such as

$$U_{\mathrm{B}} \to \widetilde{U}_{\mathrm{B}} = \widetilde{V}^\dagger U_{\mathrm{B}} \widetilde{V}, \tag{5.9.9}$$

$$\Gamma \to \widetilde{\Gamma} = \widetilde{V}^\dagger \Gamma \widetilde{V}, \tag{5.9.10}$$

$$\vec{F}_n^{(i)} \to \widetilde{V}^\dagger \vec{F}_n^{(i)}, \tag{5.9.11}$$

$$\vec{G}_m^{(j)} \to \widetilde{V}^\dagger \vec{G}_m^{(j)} \quad (\widetilde{V} \in U(2N)), \tag{5.9.12}$$

the Γ can be taken to the diagonal form of $\widetilde{\Gamma} = \sigma_3 \otimes 1_N$. In this basis, $\widetilde{U}_{\mathrm{B}}$ is written as

$$\widetilde{U}_{\mathrm{B}} = \begin{pmatrix} 0 & u_{\mathrm{B}} \\ u_{\mathrm{B}}^\dagger & 0 \end{pmatrix}, \quad u_{\mathrm{B}} \in U(N) \tag{5.9.13}$$

from Eq. (5.9.6) and the conditions $U_{\mathrm{B}}^2 = 1_{2N}$ and $U_{\mathrm{B}}^\dagger = U_{\mathrm{B}}$. As a result, it can be found that the parameter space of U_{B} is specified by u_{B} and then the classifying space is given by

$$C_1 = U(N). \tag{5.9.14}$$

These result are shown in Table 5.4.

5.9.1.3 Class AI

The class AI has only the $\mathcal{T}_+$ symmetry and the additional condition for U_{B} is

$$T_+ U_{\mathrm{B}} T_+^{-1} = U_{\mathrm{B}}, \quad T_+ = \mathcal{K}. \tag{5.9.15}$$

This request implies that U_{B} is an orthogonal and symmetric matrix. Thus, in general, U_{B} can be diagonalized as

$$U_{\mathrm{B}} = R \begin{pmatrix} 1_{2N-k} & \mathbf{0} \\ \mathbf{0} & -1_k \end{pmatrix} R^\top, \quad R \in O(2N) \quad (k = 0, 1, \cdots, 2N). \tag{5.9.16}$$

The Witten index in this class is immediately computed as

$$\Delta_{\mathrm{W}} = N - k \quad (k = 0, 1, \cdots, 2N). \tag{5.9.17}$$

Since the matrix U_{B} in Eq. (5.9.15) is invariant under the transformation

$$R \to \begin{pmatrix} O_{2N-k} & \mathbf{0} \\ \mathbf{0} & O_k \end{pmatrix} R \quad (O_{2N-k} \in O(2N-k),\ O_k \in O(k)), \tag{5.9.18}$$

the classifying space of U_{B} is given by

$$R_0 = \bigcup_{k=0}^{2N} \frac{O(2N)}{O(2N-k) \times O(k)}. \tag{5.9.19}$$

These result are shown in Table 5.4.

5.9.1.4 Class BDI

The class BDI has the three symmetries $\mathcal{T}_+$, $\mathcal{C}_+$ and $\mathcal{T}_+\mathcal{C}_+$, and the additional conditions for U_B are

$$T_+ U_\mathrm{B} T_+^{-1} = U_\mathrm{B}, \qquad T_+ = \mathcal{K}, \tag{5.9.20}$$
$$C_+ U_\mathrm{B} C_+^{-1} = -U_\mathrm{B}, \qquad C_+ = (i\sigma_2 \otimes 1_{N/2} \otimes i\sigma_2)\mathcal{K}, \tag{5.9.21}$$
$$\Gamma_+ U_\mathrm{B} \Gamma_+^{-1} = -U_\mathrm{B}, \qquad \Gamma_+ = i\sigma_2 \otimes 1_{N/2} \otimes i\sigma_2. \tag{5.9.22}$$

From the same discussion in the class AIII, the degeneracies of $\vec{F}_0^{(i)}$ and $\vec{G}_0^{(j)}$ are equal to each other due to Γ_+ and the Witten index is given by

$$\Delta_\mathrm{W} = 0. \tag{5.9.23}$$

As we will discuss in the next Subsection, the quantity corresponding to the topological number of this class is not the Witten index but the even/odd parity of the number of Dirac zero modes.

Next, let us discuss the classifying space of U_B. Since C_+ is automatically symmetric if the conditions T_+ and Γ_+ are satisfied, we focus on T_+ and Γ_+ here. From Eq. (5.9.22), Γ_+ is the real symmetric matrix, thus, this can be diagonalized by a real orthogonal matrix. In particular, we consider the following basis

$$U_\mathrm{B} \to \widetilde{U}_\mathrm{B} = \widetilde{V}^\top U_\mathrm{B} \widetilde{V}, \tag{5.9.24}$$
$$\Gamma_+ \to \widetilde{\Gamma}_+ = \widetilde{V}^\top \Gamma_+ \widetilde{V}, \tag{5.9.25}$$
$$\vec{F}_n^{(i)} \to \widetilde{V}^\top \vec{F}_n^{(i)}, \tag{5.9.26}$$
$$\vec{G}_m^{(j)} \to \widetilde{V}^\top \vec{G}_m^{(j)}, \tag{5.9.27}$$

where $\widetilde{V}$ is the real orthogonal matrix given by

$$\widetilde{V} = \frac{1}{\sqrt{2}} \begin{pmatrix} 1_N & 1_{N/2} \otimes \sigma_1 \\ -1_{N/2} \otimes i\sigma_2 & 1_{N/2} \otimes \sigma_3 \end{pmatrix}. \tag{5.9.28}$$

In this basis, Γ_+ and T_+ can be written as

$$\begin{aligned}
\widetilde{\Gamma}_+ &= \widetilde{V}^\top \Gamma_+ \widetilde{V} \\
&= \frac{1}{(\sqrt{2})^2} \begin{pmatrix} 1_N & 1_{N/2} \otimes i\sigma_2 \\ 1_{N/2} \otimes \sigma_1 & 1_{N/2} \otimes \sigma_3 \end{pmatrix} \begin{pmatrix} 0 & 1_{N/2} \otimes i\sigma_2 \\ -1_{N/2} \otimes i\sigma_2 & 0 \end{pmatrix} \\
&\quad \times \begin{pmatrix} 1_N & 1_{N/2} \otimes \sigma_1 \\ -1_{N/2} \otimes i\sigma_2 & 1_{N/2} \otimes \sigma_3 \end{pmatrix} \\
&= \frac{1}{2} \begin{pmatrix} 1_{N/2} \otimes 1_2 & 1_{N/2} \otimes i\sigma_2 \\ -1_{N/2} \otimes \sigma_1 & -1_{N/2} \otimes \sigma_3 \end{pmatrix} \begin{pmatrix} 1_N & 1_{N/2} \otimes \sigma_1 \\ -1_{N/2} \otimes i\sigma_2 & 1_{N/2} \otimes \sigma_3 \end{pmatrix} \\
&= \begin{pmatrix} 1_N & 0 \\ 0 & -1_N \end{pmatrix} = \sigma_3 \otimes 1_N,
\end{aligned} \tag{5.9.29}$$

$$\begin{aligned}
\widetilde{T}_+ &= \widetilde{V}^\top T_+ \widetilde{V} \\
&= \widetilde{V}^\top \mathcal{K} \widetilde{V} \\
&= \mathcal{K}(\widetilde{V}^\top \widetilde{V}) = \mathcal{K}.
\end{aligned} \tag{5.9.30}$$

In addition, $\widetilde{U}_{\mathrm{B}} \equiv \widetilde{V}^{\top} U_{\mathrm{B}} \widetilde{V}$ is given by the real matrix and restricted to the form

$$\widetilde{U}_{\mathrm{B}} = \begin{pmatrix} 0 & u_{\mathrm{B}} \\ u_{\mathrm{B}}^{\top} & 0 \end{pmatrix}, \quad u_{\mathrm{B}} \in O(N) \tag{5.9.31}$$

by the conditions (5.9.20), (5.9.22) and $U_{\mathrm{B}}^{\dagger} = U_{\mathrm{B}}^{\top}$ and $U_{\mathrm{B}}^{\dagger} = U_{\mathrm{B}}$. As a result, it can be found that the parameter space of U_{B} is specified by $u_{\mathrm{B}} \in O(N)$ and then the classifying space is given by

$$R_1 = O(N). \tag{5.9.32}$$

These result are shown in Table 5.4.

5.9.1.5 Class D

The class D has only the C_+ symmetry, and the additional condition for U_{B} is

$$C_+ U_{\mathrm{B}} C_+^{-1} = -U_{\mathrm{B}}, \quad C_+ = (i\sigma_2 \otimes 1_{N/2} \otimes i\sigma_2)\mathcal{K}. \tag{5.9.33}$$

For the convenience of analysis, we chose the following basis:

$$U_{\mathrm{B}} \to \widetilde{U}_{\mathrm{B}} = \widetilde{V}^{\dagger} U_{\mathrm{B}} \widetilde{V}, \tag{5.9.34}$$

$$\vec{F}_n^{(i)} \to \widetilde{V}^{\dagger} \vec{F}_n^{(i)}, \quad \vec{G}_m^{(j)} \to \widetilde{V}^{\dagger} \vec{G}_m^{(j)}, \tag{5.9.35}$$

where $\widetilde{V}$ is defined by

$$\widetilde{V} = \frac{1}{\sqrt{2}} \begin{pmatrix} 1_N & 1_{N/2} \otimes i\sigma_1 \\ -1_{N/2} \otimes i\sigma_2 & 1_{N/2} \otimes i\sigma_3 \end{pmatrix}. \tag{5.9.36}$$

In this basis, C_+ can be written into a simple form such as

$$\begin{aligned}
\widetilde{C}_+ &= \widetilde{V}^{\dagger} C_+ \widetilde{V} \\
&\frac{1}{(\sqrt{2})^2} \begin{pmatrix} 1_N & 1_{N/2} \otimes i\sigma_2 \\ 1_{N/2} \otimes i\sigma_1 & 1_{N/2} \otimes i\sigma_3 \end{pmatrix} \left[\begin{pmatrix} 0 & 1_{N/2} \otimes i\sigma_2 \\ -1_{N/2} \otimes i\sigma_2 & 0 \end{pmatrix} \mathcal{K} \right] \begin{pmatrix} 1_N & 1_{N/2} \otimes i\sigma_1 \\ -1_{N/2} \otimes i\sigma_2 & 1_{N/2} \otimes i\sigma_3 \end{pmatrix} \\
&= \frac{1}{2} \begin{pmatrix} 1_{N/2} \otimes 1_2 & 1_{N/2} \otimes i\sigma_2 \\ -1_{N/2} \otimes i\sigma_1 & -1_{N/2} \otimes i\sigma_3 \end{pmatrix} \begin{pmatrix} 1_N & -1_{N/2} \otimes i\sigma_1 \\ -1_{N/2} \otimes i\sigma_2 & -1_{N/2} \otimes i\sigma_3 \end{pmatrix} \mathcal{K} \\
&= 1_{2N} \cdot \mathcal{K}.
\end{aligned} \tag{5.9.37}$$

From the conditions (5.9.33) and $U_{\mathrm{B}}^{\dagger} = U_{\mathrm{B}}$, $\widetilde{U}_{\mathrm{B}}$ ($\equiv \widetilde{V}^{\dagger} U_{\mathrm{B}} \widetilde{V}$) can be of the form

$$\widetilde{U}_{\mathrm{B}} = iA, \quad A^{\top} = -A, \tag{5.9.38}$$

where A is a $2N \times 2N$ antisymmetric real matrix. Since any pure imaginary antisymmetric matrix has the same number of positive and negative eigenvalues, the Witten index is given by

$$\Delta_{\mathrm{W}} = 0. \tag{5.9.39}$$

Alternatively, since this class satisfies $\{U_{\mathrm{B}}, C_+\} = 0$, we can also conclude that the Witten index is zero by repeating the same argument as for the class AIII. As we will discuss later, the quantity corresponding to the topological number of this class is the even/odd parity of the number of Dirac zero modes.

Let us calculate the classifying space in this class. From a general discussion of linear algebra, using a real orthogonal matrix R, we can bring the real antisymmetric matrix A satisfying $A^2 = -1_{2N}$ into a block off-diagonal form:

$$A = R\begin{pmatrix} 0 & 1_N \\ -1_N & 0 \end{pmatrix}R^\top, \quad R \in O(2N). \tag{5.9.40}$$

We want to find a transformation that keeps Eq. (5.9.40) invariant. Denoting this transformation by $R \to RR'$, then R' must be a subgroup of $O(2N)$ and satisfy

$$R'\begin{pmatrix} 0 & 1_N \\ -1_N & 0 \end{pmatrix}R'^\top = \begin{pmatrix} 0 & 1_N \\ -1_N & 0 \end{pmatrix}. \tag{5.9.41}$$

From Eq. (5.9.41), the matrix R' also belongs to the symplectic group. Therefore, the determinant of R' should be $+1$, i.e., R' is at least an element of $SO(2N)$. Indeed, we obtain

$$\mathrm{Pf}\left(R'\begin{pmatrix} 0 & 1_N \\ -1_N & 0 \end{pmatrix}R'\right) = \det(R') \cdot \mathrm{Pf}\begin{pmatrix} 0 & 1_N \\ -1_N & 0 \end{pmatrix} \tag{5.9.42}$$

from the properties of the Pfaffian. Furthermore, substituting Eq. (5.9.41) into the left-hand side of the above equation, we can confirm that $\det R' = +1$. In general, the element of $SO(2N)$ can be expressed as

$$R' = \exp\{1_2 \otimes X_0 + \sigma_2 \otimes X_2\}, \tag{5.9.43}$$

where X_0 is an antisymmetric real matrix and X_2 is a symmetric pure imaginary matrix. Since by using the unitary matrix

$$G_2 = \frac{1}{\sqrt{2}}\begin{pmatrix} 1 & -i \\ 1 & i \end{pmatrix}, \quad G_2^\dagger G_2 = G_2 G_2^\dagger = 1_2, \tag{5.9.44}$$

σ_2 can be replaced by $G_2^\dagger \sigma_3 G_2$, the matrixR' is rewritten as

$$\begin{aligned} R' &= (G_2^\dagger \otimes 1_N)\exp\{1_2 \otimes X_0 + \sigma_3 \otimes X_2\}(G_2 \otimes 1_N) \\ &= (G_2^\dagger \otimes 1_N)\begin{pmatrix} \exp(X_0 + X_2) & 0 \\ 0 & \exp(X_0 - X_2) \end{pmatrix}(G_2 \otimes 1_N) \\ &\equiv (G_2^\dagger \otimes 1_N)\begin{pmatrix} r & 0 \\ 0 & r^* \end{pmatrix}(G_2 \otimes 1_N) \quad (r \equiv \exp(X_0 + X_2)). \end{aligned} \tag{5.9.45}$$

Here, r is a unitary matrix because it satisfies $r^\dagger r = 1_N$. Now we have obtained the redundancy of Eq. (5.9.40), and we can divide them and find that the classifying space is

$$R_2 = \frac{O(2N)}{U(N)}. \tag{5.9.46}$$

These result are shown in Table 5.4.

5.9.1.6 Class DIII

The class DIII has the three symmetries $\mathcal{T}_-$, $\mathcal{C}_+$ and $\mathcal{T}_-\mathcal{C}_+$, and the additional conditions for U_{B} are

$$T_- U_{\mathrm{B}} T_-^{-1} = U_{\mathrm{B}}, \qquad T_- = (i\sigma_2 \otimes 1_N)\mathcal{K}, \tag{5.9.47}$$

$$C_+ U_{\mathrm{B}} C_+^{-1} = -U_{\mathrm{B}}, \qquad C_+ = (i\sigma_2 \otimes 1_{N/2} \otimes i\sigma_2)\mathcal{K}, \tag{5.9.48}$$

$$\Gamma_- U_{\mathrm{B}} \Gamma_-^{-1} = -U_{\mathrm{B}}, \qquad \Gamma_- = 1_N \otimes \sigma_2. \tag{5.9.49}$$

If CS is preserved, the degeneracy of $\vec{F}_0^{(i)}$ and $\vec{G}_0^{(j)}$ are equal to each other, i.e., the Witten index in this class is

$$\Delta_{\mathrm{W}} = 0. \tag{5.9.50}$$

Since C_+ is automatically symmetric if the conditions T_- and Γ_- $(= T_- C_+)$ are satisfied, we focus on T_- and Γ_- in the following.

Let us calculate the classifying space in this class. For the convenience of analysis, we chose the following basis:

$$U_{\mathrm{B}} \to \widetilde{U}_{\mathrm{B}} = \widetilde{V}^\dagger U_{\mathrm{B}} \widetilde{V}, \tag{5.9.51}$$

$$\vec{F}_n^{(i)} \to \widetilde{V}^\dagger \vec{F}_n^{(i)}, \quad \vec{G}_m^{(j)} \to \widetilde{V}^\dagger \vec{G}_m^{(j)}, \tag{5.9.52}$$

$$\widetilde{V} = W_{N\leftrightarrow 2} \frac{1}{\sqrt{2}} \begin{pmatrix} 1_N & 1_N \\ i1_N & -i1_N \end{pmatrix}, \tag{5.9.53}$$

where $W_{n_a \leftrightarrow n_b}$ is a real orthogonal matrix which exchanges the order of the direct product of an $n_a \times n_a$ matrix A and an $n_b \times n_b$ matrix B such that

$$W_{n_a\leftrightarrow n_b}^\top (A \otimes B) W_{n_a\leftrightarrow n_b} = B \otimes A, \tag{5.9.54}$$

$$W_{n_a\leftrightarrow n_b} = \sum_{i,\alpha} (\vec{e}_i \otimes \vec{E}_\alpha)(\vec{E}_\alpha^\top \otimes \vec{e}_i^\top), \tag{5.9.55}$$

$$\vec{e}_i^\top = (\underbrace{0, \cdots, 0}_{i-1}, 1, 0, \cdots, 0)^\top, \tag{5.9.56}$$

$$\vec{E}_\alpha^\top = (\underbrace{0, \cdots, 0}_{\alpha-1}, 1, 0, \cdots, 0)^\top \quad (i = 1, \cdots, n_a,\ \alpha = 1, \cdots, n_b). \tag{5.9.57}$$

In this basis, $\widetilde{\Gamma}_-$ and $\widetilde{T}_-$ are written as

$$\begin{aligned}
\widetilde{\Gamma}_- &= \widetilde{V}^\dagger \Gamma_- \widetilde{V} \\
&= \frac{1}{(\sqrt{2})^2} \begin{pmatrix} 1_N & -i1_N \\ 1_N & i1_N \end{pmatrix} \underbrace{W_{N\leftrightarrow 2}^\top \left[1_N \otimes \sigma_2\right] W_{N\leftrightarrow 2}}_{=\sigma_2 \otimes 1_N} \begin{pmatrix} 1_N & 1_N \\ i1_N & -i1_N \end{pmatrix} \\
&= \frac{1}{2} \begin{pmatrix} 1_N & -i1_N \\ 1_N & i1_N \end{pmatrix} \begin{pmatrix} 0 & -i1_N \\ i1_N & 0 \end{pmatrix} \begin{pmatrix} 1_N & 1_N \\ i1_N & -i1_N \end{pmatrix} \\
&= \frac{1}{2} \begin{pmatrix} 1_N & -i1_N \\ -1_N & -i1_N \end{pmatrix} \begin{pmatrix} 1_N & 1_N \\ i1_N & -i1_N \end{pmatrix} \\
&= \sigma_3 \otimes 1_N,
\end{aligned} \tag{5.9.58}$$

$$
\begin{aligned}
\widetilde{T}_- &= \widetilde{V}^\dagger T_- \widetilde{V} \\
&= \frac{1}{(\sqrt{2})^2}\begin{pmatrix} 1_N & -i1_N \\ 1_N & i1_N \end{pmatrix} \underbrace{W_{N\leftrightarrow 2}^\top \left[(i\sigma_2\otimes 1_{N/2}\otimes 1_2)\mathcal{K}\right] W_{N\leftrightarrow 2}}_{=(1_2\otimes i\sigma_2\otimes 1_{N/2})\mathcal{K}} \begin{pmatrix} 1_N & 1_N \\ i1_N & -i1_N \end{pmatrix} \\
&= \frac{1}{2}\begin{pmatrix} 1_N & -i1_N \\ 1_N & i1_N \end{pmatrix}\begin{pmatrix} i\sigma_2\otimes 1_{N/2} & 0 \\ 0 & i\sigma_2\otimes 1_{N/2} \end{pmatrix}\begin{pmatrix} 1_N & 1_N \\ -i1_N & i1_N \end{pmatrix}\mathcal{K} \\
&= \frac{1}{2}\begin{pmatrix} i\sigma_2\otimes 1_{N/2} & \sigma_2\otimes 1_{N/2} \\ i\sigma_2\otimes 1_{N/2} & -\sigma_2\otimes 1_{N/2} \end{pmatrix}\begin{pmatrix} 1_N & 1_N \\ -i1_N & i1_N \end{pmatrix}\mathcal{K} \\
&= \begin{pmatrix} 0 & (i\sigma_2\otimes 1_{N/2})\mathcal{K} \\ (i\sigma_2\otimes 1_{N/2})\mathcal{K} & 0 \end{pmatrix}.
\end{aligned} \tag{5.9.59}
$$

From the conditions (5.9.47), (5.9.49), $U_{\mathrm{B}}^2 = 1_{2N}$ and $U_{\mathrm{B}}^\dagger = U_{\mathrm{B}}$, we can obtain the block off-diagonalized form

$$
\widetilde{U}_{\mathrm{B}} = \begin{pmatrix} 0 & u_{\mathrm{B}} \\ u_{\mathrm{B}}^\dagger & 0 \end{pmatrix}, \quad u_{\mathrm{B}}u_{\mathrm{B}}^\dagger = 1_N, \quad (\sigma_2\otimes 1_{N/2})u_{\mathrm{B}}^\top(\sigma_2\otimes 1_{N/2}) = u_{\mathrm{B}}. \tag{5.9.60}
$$

Since u_{B} is an $N\times N$ unitary matrix, it can be diagonalized as

$$
\begin{aligned}
&u_{\mathrm{B}} = v^\dagger u_{\mathrm{d}} v, \quad u_{\mathrm{d}} = \begin{pmatrix} e^{i\alpha_1} & & 0 \\ & \ddots & \\ 0 & & e^{i\alpha_N} \end{pmatrix}, \\
&v \in U(N), \quad \alpha_i \in \mathbb{R} \quad (i = 1, 2, \cdots, N).
\end{aligned} \tag{5.9.61}
$$

Substituting the first equation in (5.9.61) into the third equation in (5.9.60) with $J_y \equiv \sigma_2\otimes 1_{N/2}$, we can obtain the relation

$$
(vJ_yv^\top)u_{\mathrm{d}} = u_{\mathrm{d}}(vJ_yv^\top), \tag{5.9.62}
$$

or equivalently

$$
(vJ_yv^\top)_{ij}(u_{\mathrm{d}})_{jj} = (u_{\mathrm{d}})_{ii}(vJ_yv^\top)_{ij} \quad (i, j = 1, 2, \cdots, N), \tag{5.9.63}
$$

where i and j denote the indices of the matrix elements and are not summed up. If $(vJ_yv^\top)_{ij} \neq 0$, one can obtain $(u_{\mathrm{d}})_{ii} = (u_{\mathrm{d}})_{jj}$ from the above equations. By dividing both sides of the Eq. (5.9.63) by $u_{\mathrm{d}}^{1/2}$, we can also obtain the following relation:

$$
(vJ_yv^\top)_{ij}\sqrt{(u_{\mathrm{d}})_{jj}} = \sqrt{(u_{\mathrm{d}})_{ii}}(vJ_yv^\top)_{ij}. \tag{5.9.64}
$$

With this relation, u_{B} can be rewritten as

$$
\begin{aligned}
u_{\mathrm{B}} &= J_y u_{\mathrm{B}}^\top J_y \\
&= J_y (v^\dagger u_{\mathrm{d}} v)^\top J_y \\
&= \underbrace{J_y v^\top u_{\mathrm{d}}^{1/2}}_{v^\dagger u_{\mathrm{d}}^{1/2}(vJ_yv^\top)} u_{\mathrm{d}}^{1/2} v^* J_y \\
&= v^\dagger u_{\mathrm{d}}^{1/2} v \cdot J_y \cdot v^\top u_{\mathrm{d}}^{1/2} v^* \cdot J_y \\
&= w^\top J_y w J_y,
\end{aligned} \tag{5.9.65}
$$

where w is defined by $w \equiv v^\top u_{\mathrm{d}}^{1/2} v^*$. By definition, w is an $N \times N$ unitary matrix and specifies the parameter space of u_{B}. We can find that u_{B} is invariant by the transformation

$$\omega \to g\omega \quad (g^\dagger g = 1_N, \quad g^\top J_y g = J_y). \tag{5.9.66}$$

Now, since g is an element of the symplectic group $Sp(N/2)$ itself, the classifying space of U_{B} is obtained by excluding the degrees of freedom of this transformation and becomes

$$R_3 = \frac{U(N)}{Sp(N/2)}. \tag{5.9.67}$$

These result are shown in Table 5.4.

5.9.1.7 Class AII

The class AII has only the $\mathcal{T}_-$ symmetry. The restriction for U_{B} is

$$T_- U_{\mathrm{B}} T_-^{-1} = U_{\mathrm{B}}, \quad T_- = (i\sigma_2 \otimes 1_N)\mathcal{K}. \tag{5.9.68}$$

Let $\vec{F}^{(i)}$ and $\vec{G}^{(j)}$ $(i, j = 1, 2, \cdots)$ be orthonormal eigenvectors with $U_{\mathrm{B}} = +1$ and $U_{\mathrm{B}} = -1$, respectively. From the above condition, the vectors $\vec{F}^{(i)}$ and $T_-\vec{F}^{(i)}$ (with the same index i) have the same eigenvalues $U_{\mathrm{B}} = +1$. Furthermore, they are orthogonal to each other from the direct calculation,

$$\begin{aligned}
&\vec{F}^{(i)\dagger}(T_-\vec{F}^{(i)}) \\
&= \left(f_n^{(i)*}(L_0+\varepsilon), f_n^{(i)*}(L_1-\varepsilon), \cdots, f_n^{(i)*}(L_N-\varepsilon)\right)\begin{pmatrix} 0 & 1_N \cdot \mathcal{K} \\ -1_N \cdot \mathcal{K} & 0 \end{pmatrix}\begin{pmatrix} f_n^{(i)}(L_0+\varepsilon) \\ f_n^{(i)}(L_1-\varepsilon) \\ \vdots \\ f_n^{(i)}(L_N-\varepsilon) \end{pmatrix} \\
&= \left(-f_n^{(i)*}(L_{N/2}+\varepsilon), \cdots, -f_n^{(i)*}(L_N-\varepsilon), |\, f_n^{(i)*}(L_0+\varepsilon), \cdots, f_n^{(i)*}(L_{N/2}-\varepsilon)\right)\begin{pmatrix} f_n^{(i)*}(L_0+\varepsilon) \\ f_n^{(i)*}(L_1-\varepsilon) \\ \vdots \\ f_n^{(i)*}(L_N-\varepsilon) \end{pmatrix} \\
&= \left[-f_n^{(i)*}(L_{N/2}+\varepsilon)f_n^{(i)*}(L_0+\varepsilon) - \cdots - f_n^{(i)*}(L_N-\varepsilon)f_n^{(i)*}(L_{N/2}-\varepsilon)\right]\mathcal{K} \\
&\quad + \left[f_n^{(i)*}(L_0+\varepsilon)f_n^{(i)*}(L_{N/2}+\varepsilon) + \cdots + f_n^{(i)*}(L_{N/2}-\varepsilon)f_n^{(i)*}(L_N-\varepsilon)\right]\mathcal{K} \\
&= 0.
\end{aligned} \tag{5.9.69}$$

If we have a boundary vector $\vec{F}^{(j)}$ $(j \neq i)$ which is orthogonal with $\vec{F}^{(i)}$ and $T_-\vec{F}^{(i)}$, $T_-\vec{F}^{(j)}$ is also orthogonal with them. Therefore, the number of the eigenvalue $U_{\mathrm{B}} = +1$ is even in this class. The same is true for the case of $\vec{G}^{(j)}$ and $T_-\vec{G}^{(j)}$, and the number of the eigenvalue $U_{\mathrm{B}} = -1$ is also even. Therefore, in the type$(2N-k, k)$ BC, the number k should be even. It should be noted that N is also even for the Q_y transformation in T_- to be well-defied. Thus, the Witten index in this class is given by an even number:

$$\Delta_{\mathrm{W}} = N - k \quad (k = 0, 2, 4, \cdots, N, \quad N : \text{even}). \tag{5.9.70}$$

This corresponds to the topological number $2\mathbb{Z}$.

For the convenience of calculating the parameter space of U_{B}, we rewrite U_{B} as

$$U_{\mathrm{B}} = V\begin{pmatrix} 1_{(2N-k)/2} & & & 0 \\ & -1_{k/2} & & \\ & & 1_{(2N-k)/2} & \\ 0 & & & -1_{k/2} \end{pmatrix}V^{\dagger}, \tag{5.9.71}$$

where the $2N \times 2N$ matrix V is a unitary matrix defined by

$$V = \left(\vec{F}^{(1)}, \cdots, \vec{F}^{(\frac{2N-k}{2})}, \vec{G}^{(1)}, \cdots, \vec{G}^{(\frac{k}{2})}, -T_{-}\vec{F}^{(1)}, \cdots, -T_{-}\vec{F}^{(\frac{2N-k}{2})}, -T_{-}\vec{G}^{(1)}, \cdots - T_{-}, \vec{G}^{(\frac{k}{2})}\right). \tag{5.9.72}$$

The matrix V is divided into $N \times N$ submatrices and denoted as

$$V = \begin{pmatrix} A & -B^* \\ B & A^* \end{pmatrix}. \tag{5.9.73}$$

Note that since $V^{\dagger}V = 1_{2N}$ and $VV^{\dagger} = 1_{2N}$, A and B must satisfy

$$\begin{cases} A^{\dagger}A + B^{\dagger}B = 1_N, \\ B^{\top}B^* + A^{\top}A^* = 1_N, \\ AA^{\dagger} + B^*B^{\top} = 1_N, \\ BB^{\dagger} + A^*A^{\top} = 1_N, \end{cases} \qquad \begin{cases} -A^{\dagger}B^* + B^{\dagger}A^* = 0, \\ -B^{\top}A + A^{\top}B = 0, \\ AB^{\dagger} - B^*A^{\top} = 0, \\ BA^{\dagger} - A^*B^{\top} = 0. \end{cases} \tag{5.9.74}$$

Now, the matrix V satisfies

$$\begin{aligned} V^{\top}\begin{pmatrix} 0 & 1_N \\ -1_N & 0 \end{pmatrix}V &= \begin{pmatrix} A^{\top} & B^{\top} \\ -B^{\dagger} & A^{\dagger} \end{pmatrix}\begin{pmatrix} 0 & 1_N \\ -1_N & 0 \end{pmatrix}\begin{pmatrix} A & -B^* \\ B & A^* \end{pmatrix} \\ &= \begin{pmatrix} -B^{\top} & A^{\top} \\ -A^{\dagger} & -B^{\dagger} \end{pmatrix}\begin{pmatrix} A & -B^* \\ B & A^* \end{pmatrix} \\ &= \begin{pmatrix} -B^{\top}A + A^{\top}B & B^{\top}B^* + A^{\top}A^* \\ -A^{\dagger}A - B^{\dagger}B & A^{\dagger}B^* - B^{\dagger}A^* \end{pmatrix} \\ &= \begin{pmatrix} 0 & 1_N \\ -1_N & 0 \end{pmatrix}. \end{aligned} \tag{5.9.75}$$

Thus V is an element of the symplectic group $Sp(N)$. However, there is redundancy in this V. Let

$$g_i = \begin{pmatrix} A_i & -B_i^* \\ B_i & A_i^* \end{pmatrix} \tag{5.9.76}$$

be an element of $Sp(i)$ and we consider the $2N \times 2N$ matrix g which belongs to $Sp((2N-k)/2) \times Sp(k/2)$ such as

$$g = \begin{pmatrix} A_{(2N-k)/2} & 0 & -B^*_{(2N-k)2} & 0 \\ 0 & A_{k/2} & 0 & -B^*_{k/2} \\ B_{(2N-k)/2} & 0 & A^*_{(2N-k)2} & 0 \\ 0 & B_{k/2} & 0 & A^*_{k/2} \end{pmatrix} \in Sp\left(\frac{2k-N}{2}\right) \times Sp\left(\frac{k}{2}\right). \tag{5.9.77}$$

Then we find that U_{B} is invariant by the replacement $V \to Vg$. Indeed, one can get a relation

$$
\begin{aligned}
& g\begin{pmatrix} 1_{(2N-k)/2} & & & 0 \\ & -1_{k/2} & & \\ & & 1_{(2N-k)/2} & \\ 0 & & & -1_{k/2} \end{pmatrix} g^{\dagger} \\
&= \left(\begin{array}{cc|cc} A_{(2N-k)/2} & 0 & -B^*_{(2N-k)2} & 0 \\ 0 & A_{k/2} & 0 & -B^*_{k/2} \\ \hline B_{(2N-k)/2} & 0 & A^*_{(2N-k)2} & 0 \\ 0 & B_{k/2} & 0 & A^*_{k/2} \end{array}\right) \begin{pmatrix} 1_{(2N-k)/2} & & & 0 \\ & -1_{k/2} & & \\ & & 1_{(2N-k)/2} & \\ 0 & & & -1_{k/2} \end{pmatrix} \\
&\quad \times \left(\begin{array}{cc|cc} A^{\dagger}_{(2N-k)/2} & 0 & B^{\dagger}_{(2N-k)2} & 0 \\ 0 & A^{\dagger}_{k/2} & 0 & B^{\dagger}_{k/2} \\ \hline -B^{\top}_{(2N-k)/2} & 0 & A^{\top}_{(2N-k)2} & 0 \\ 0 & -B^{\top}_{k/2} & 0 & A^{\top}_{k/2} \end{array}\right) \\
&= \left(\begin{array}{cc|cc} A_{(2N-k)/2} & 0 & -B^*_{(2N-k)2} & 0 \\ 0 & -A_{k/2} & 0 & B^*_{k/2} \\ \hline B_{(2N-k)/2} & 0 & A^*_{(2N-k)2} & 0 \\ 0 & -B_{k/2} & 0 & -A^*_{k/2} \end{array}\right) \left(\begin{array}{cc|cc} A^{\dagger}_{(2N-k)/2} & 0 & B^{\dagger}_{(2N-k)2} & 0 \\ 0 & A^{\dagger}_{k/2} & 0 & B^{\dagger}_{k/2} \\ \hline -B^{\top}_{(2N-k)/2} & 0 & A^{\top}_{(2N-k)2} & 0 \\ 0 & -B^{\top}_{k/2} & 0 & A^{\top}_{k/2} \end{array}\right) \\
&\equiv \begin{pmatrix} U_{11} & 0 \\ 0 & U_{22} \end{pmatrix},
\end{aligned} \tag{5.9.78}
$$

where

$$
U_{11} = \begin{pmatrix} A_{(2N-k)/2}A^{\dagger}_{(2N-k)/2} + B^*_{(2N-k)2}B^{\top}_{(2N-k)/2} & 0 \\ 0 & -A_{k/2}A^{\dagger}_{k/2} - B^*_{k/2}B^{\top}_{k/2} \end{pmatrix} = \begin{pmatrix} 1_{(2N-k)/2} & 0 \\ 0 & -1_k \end{pmatrix}, \tag{5.9.79}
$$

$$
U_{22} = \begin{pmatrix} B_{(2N-k)/2}B^{\dagger}_{(2N-k)2} + A^*_{(2N-k)2}A^{\top}_{(2N-k)2} & 0 \\ 0 & -B_{k/2}B^{\dagger}_{k/2} - A^*_{k/2}A^{\top}_{k/2} \end{pmatrix} = \begin{pmatrix} 1_{(2N-k)/2} & 0 \\ 0 & -1_k \end{pmatrix}. \tag{5.9.80}
$$

Therefore, the classifying space of U_{B} is given by the coset space

$$
R_4 = \bigcup_{k=0}^{2N} \frac{Sp(N)}{Sp(N-k/2) \times Sp(k/2)} \quad (N, k : \text{even}). \tag{5.9.81}
$$

These result are shown in Table 5.4.

5.9.1.8 Class CII

The class CII has the three symmetries, $\mathcal{T}_-$, $\mathcal{C}_-$ and $\mathcal{T}_-\mathcal{C}_-$. The conditions which U_{B} should satisfy are

$$
T_- U_{\mathrm{B}} T_-^{-1} = U_{\mathrm{B}}, \qquad T_- = (i\sigma_2 \otimes 1_N)\mathcal{K}, \tag{5.9.82}
$$

$$
C_- U_{\mathrm{B}} C_-^{-1} = -U_{\mathrm{B}}, \qquad C_- = (1_N \otimes i\sigma_2)\mathcal{K}, \tag{5.9.83}
$$

$$
\Gamma_+ U_{\mathrm{B}} \Gamma_+^{-1} = -U_{\mathrm{B}}, \qquad \Gamma_+ = i\sigma_2 \otimes 1_{N/2} \otimes i\sigma_2. \tag{5.9.84}
$$

Since the CS is present, the Witten index in this class is

$$\Delta_{\mathrm{W}} = 0. \tag{5.9.85}$$

Since C_- is automatically symmetric if the conditions T_- and Γ_+ ($= T_-C_-$) are satisfied, we focus on T_- and Γ_+ in the following.

For the convenience in analyzing the classifying space, we change the basis as

$$U_{\mathrm{B}} \to \widetilde{U}_{\mathrm{B}} = \widetilde{V}^{\top} U_{\mathrm{B}} \widetilde{V}, \tag{5.9.86}$$
$$\vec{F}_n^{(i)} \to \widetilde{V}^{\top} \vec{F}_n^{(i)}, \quad \vec{G}_m^{(j)} \to \widetilde{V}^{\top} \vec{G}_m^{(j)}, \tag{5.9.87}$$
$$\widetilde{V} = \frac{1}{\sqrt{2}} \begin{pmatrix} 1_{N/2} \otimes \sigma_3 & -1_{N/2} \otimes i\sigma_2 \\ 1_{N/2} \otimes \sigma_1 & 1_N \end{pmatrix} (1_2 \otimes W_{N/2\leftrightarrow 2}), \tag{5.9.88}$$

where the matrix $W_{N/2\leftrightarrow 2}$ is defined by (5.9.54)–(5.9.57), which exchanges the order of the direct product of an $(N/2) \times (N/2)$ matrix A and an 2×2 matrix B. In this basis, $\widetilde{\Gamma}_+$ and $\widetilde{T}_-$ are rewritten as

$$\begin{aligned}
\widetilde{\Gamma}_+ &= \widetilde{V}^{\top} \Gamma_+ \widetilde{V} \\
&= \frac{1}{(\sqrt{2})^2} (1_2 \otimes W_{N/2\leftrightarrow 2}^{\top}) \begin{pmatrix} 1_{N/2} \otimes \sigma_3 & 1_{N/2} \otimes \sigma_1 \\ 1_{N/2} \otimes i\sigma_2 & 1_N \end{pmatrix} \begin{pmatrix} 0 & 1_{N/2} \otimes i\sigma_2 \\ -1_{N/2} \otimes i\sigma_2 & 0 \end{pmatrix} \\
&\quad \times \begin{pmatrix} 1_{N/2} \otimes \sigma_3 & -1_{N/2} \otimes i\sigma_2 \\ 1_{N/2} \otimes \sigma_1 & 1_N \end{pmatrix} (1_2 \otimes W_{N/2\leftrightarrow 2}) \\
&= (1_2 \otimes W_{N/2\leftrightarrow 2}^{\top})(\sigma_3 \otimes 1_{N/2} \otimes 1_2)(1_2 \otimes W_{N/2\leftrightarrow 2}) \\
&= \sigma_3 \otimes 1_N,
\end{aligned} \tag{5.9.89}$$

$$\begin{aligned}
\widetilde{T}_- &= \widetilde{V}^{\top} T_- \widetilde{V} \\
&= \frac{1}{(\sqrt{2})^2} (1_2 \otimes W_{N/2\leftrightarrow 2}^{\top}) \begin{pmatrix} 1_{N/2} \otimes \sigma_3 & 1_{N/2} \otimes \sigma_1 \\ 1_{N/2} \otimes i\sigma_2 & 1_N \end{pmatrix} \begin{pmatrix} 0 & 1_N \mathcal{K} \\ -1_N \mathcal{K} & 0 \end{pmatrix} \\
&\quad \times \begin{pmatrix} 1_{N/2} \otimes \sigma_3 & -1_{N/2} \otimes i\sigma_2 \\ 1_{N/2} \otimes \sigma_1 & 1_N \end{pmatrix} (1_2 \otimes W_{N/2\leftrightarrow 2}) \\
&= (1_2 \otimes W_{N/2\leftrightarrow 2}^{\top})(1_2 \otimes 1_{N/2} \otimes i\sigma_2)(1_2 \otimes W_{N/2\leftrightarrow 2}) \mathcal{K} \\
&= 1_2 \otimes \underbrace{\left[W_{N/2\leftrightarrow 2}^{\top} (1_{N/2} \otimes i\sigma_2) W_{N/2\leftrightarrow 2} \right]}_{= i\sigma_2 \otimes 1_{N/2}} \mathcal{K} \\
&= \begin{pmatrix} (i\sigma_2 \otimes 1_{N/2})\mathcal{K} & 0 \\ 0 & (i\sigma_2 \otimes 1_{N/2})\mathcal{K} \end{pmatrix}.
\end{aligned} \tag{5.9.90}$$

From the conditions (5.9.82), (5.9.84) and $U_{\mathrm{B}}^2 = 1_{2N}$, matrix $\widetilde{U}_{\mathrm{B}}$ is given by

$$\widetilde{U}_{\mathrm{B}} = \begin{pmatrix} 0 & u_{\mathrm{B}} \\ u_{\mathrm{B}}^{\dagger} & 0 \end{pmatrix} \tag{5.9.91}$$

with the conditions

$$u_{\mathrm{B}} u_{\mathrm{B}}^{\dagger} = 1_N, \quad u_{\mathrm{B}}^{\top} (\sigma_2 \otimes 1_{N/2}) u_{\mathrm{B}} = \sigma_2 \otimes 1_{N/2}. \tag{5.9.92}$$

These relations means that the matrix u_{B} is an element of the symplectic group $Sp(N/2)$. Therefore, the classifying space of U_{B} is obtained by

$$R_5 = Sp(N/2). \tag{5.9.93}$$

These result are shown in Table 5.4.

5.9.1.9 Class C

The class C has only the C_- symmetry. The restriction for U_{B} is

$$C_- U_{\mathrm{B}} C_-^{-1} = -U_{\mathrm{B}}, \quad C_- = (1_N \otimes i\sigma_2)\mathcal{K}. \tag{5.9.94}$$

Since the anticommutation relation $\{U_{\mathrm{B}}, C_-\} = 0$ is satisfied, there are as many eigenvectors $C_-\vec{F}^{(i)}$ with eigenvalue -1 as there are eigenvectors $\vec{F}^{(i)}$ with eigenvalue $+1$. As a result, the number of $+1$ and -1 eigenvalues of U_{B} is equal. Thus, the Witten index in this class is obtained by

$$\Delta_{\mathrm{W}} = 0. \tag{5.9.95}$$

Let us calculate the parameter space of U_{B}. For convenience, we take the new basis as

$$U_{\mathrm{B}} \to \widetilde{U}_{\mathrm{B}} = \widetilde{V}^{\top} U_{\mathrm{B}} \widetilde{V}, \tag{5.9.96}$$
$$\vec{F}_n^{(i)} \to \widetilde{V}^{\top} \vec{F}_n^{(i)}, \quad \vec{G}_m^{(j)} \to \widetilde{V}^{\top} \vec{G}_m^{(j)}, \tag{5.9.97}$$
$$\widetilde{V} = W_{N\leftrightarrow 2}. \tag{5.9.98}$$

In this basis, $\widetilde{C}_-$ is rewritten as

$$\begin{aligned}\widetilde{C}_- &= \widetilde{V}^{\top} C_- \widetilde{V} \\ &= W_{N\leftrightarrow 2}^{\top} \left[(1_N \otimes i\sigma_2)\mathcal{K}\right] W_{N\leftrightarrow 2} \\ &= \underbrace{W_{N\leftrightarrow 2}^{\top}(1_N \otimes i\sigma_2) W_{N\leftrightarrow 2}}_{=i\sigma_2\otimes 1_N} \mathcal{K} \\ &= (i\sigma_2 \otimes 1_N)\mathcal{K}.\end{aligned} \tag{5.9.99}$$

On the other hand, by using the redundancy of V, the matrix can be taken as

$$V = \left(\widetilde{V}\vec{F}^{(1)}, \cdots, \widetilde{V}\vec{F}^{(N)}, -C_-\widetilde{V}\vec{F}^{(1)}, \cdots, -C_-\widetilde{V}\vec{F}^{(N)}\right), \tag{5.9.100}$$

then we can diagonalized the matrix $\widetilde{U}_{\mathrm{B}}$ $(= \widetilde{V}^{\top} U_{\mathrm{B}} \widetilde{V})$ as

$$\widetilde{U}_{\mathrm{B}} = V \begin{pmatrix} 1_N & 0 \\ 0 & -1_N \end{pmatrix} V^{\dagger}. \tag{5.9.101}$$

As in the class AII, the matrix V is divided into the $N \times N$ submatrices and denoted as

$$V = \begin{pmatrix} A & -B^* \\ B & A^* \end{pmatrix}, \tag{5.9.102}$$

where A and B satisfy

$$\begin{cases} A^\dagger A + B^\dagger B = 1_N, \\ B^\top B^* + A^\top A^* = 1_N, \\ AA^\dagger + B^* B^\top = 1_N, \\ BB^\dagger + A^* A^\top = 1_N, \end{cases} \qquad \begin{cases} -A^\dagger B^* + B^\dagger A^* = 0, \\ -B^\top A + A^\top B = 0, \\ AB^\dagger - B^* A^\top = 0, \\ BA^\dagger - A^* B^\top = 0. \end{cases} \tag{5.9.103}$$

Now, the matrix V satisfies

$$V^\top \begin{pmatrix} 0 & 1_N \\ -1_N & 0 \end{pmatrix} V = \begin{pmatrix} 0 & 1_N \\ -1_N & 0 \end{pmatrix}, \tag{5.9.104}$$

thus V is an element of the symplectic group $Sp(N)$. Furthermore, Eq. (5.9.101) is invariant under the transformation

$$V \to V \begin{pmatrix} U & 0 \\ 0 & U^* \end{pmatrix}, \qquad U \in U(N). \tag{5.9.105}$$

Therefore, the classifying space of U_B is given by

$$R_6 = \frac{Sp(N)}{U(N)} \tag{5.9.106}$$

with this degree of freedom removed. These result are shown in Table 5.4.

5.9.1.10 Class CI

The class CI has the three symmetries, $\mathcal{T}_+$, C_- and $\mathcal{T}_+ C_-$. The restrictions for U_B are

$$T_+ U_\mathrm{B} T_+^{-1} = U_\mathrm{B}, \qquad T_+ = \mathcal{K}, \tag{5.9.107}$$

$$C_- U_\mathrm{B} C_-^{-1} = -U_\mathrm{B}, \qquad C_- = (1_N \otimes i\sigma_2)\mathcal{K}, \tag{5.9.108}$$

$$\Gamma_- U_\mathrm{B} \Gamma_-^{-1} = -U_\mathrm{B}, \qquad \Gamma_- = 1_N \otimes \sigma_2. \tag{5.9.109}$$

If the CS is preserved, the degeneracy of $\vec{F}_0^{(i)}$ and $\vec{G}_0^{(j)}$ are equal to each other, i.e., the Witten index in this class is

$$\Delta_\mathrm{W} = 0. \tag{5.9.110}$$

Let us calculate the classifying space in this class. For the convenience of analysis, we chose the following basis:

$$U_\mathrm{B} \to \widetilde{U}_\mathrm{B} = \widetilde{V}^\dagger U_\mathrm{B} \widetilde{V}, \tag{5.9.111}$$

$$\vec{F}_n^{(i)} \to \widetilde{V}^\dagger \vec{F}_n^{(i)}, \quad \vec{G}_m^{(j)} \to \widetilde{V}^\dagger \vec{G}_m^{(j)}, \tag{5.9.112}$$

$$\widetilde{V} = \frac{1}{\sqrt{2}} W_{N\leftrightarrow 2} \begin{pmatrix} 1_N & 1_N \\ i1_N & -i1_N \end{pmatrix}, \tag{5.9.113}$$

where $W_{N\leftrightarrow 2}$ is a real orthogonal matrix that exchange the order of the direct product of an $N\times N$ matrix A and a 2×2 matrix B. In this basis, $\widetilde{\Gamma}_-$ and $\widetilde{T}_+$ are rewritten as

$$\begin{aligned}
\widetilde{\Gamma}_- &= \widetilde{V}^\dagger \Gamma_- \widetilde{V} \\
&= \sigma_3 \otimes 1_N \quad (\because (5.9.60)),
\end{aligned} \tag{5.9.114}$$

$$\begin{aligned}
\widetilde{T}_+ &= \widetilde{V}^\dagger T_+ \widetilde{V} \\
&= \frac{1}{(\sqrt{2})^2}\begin{pmatrix} 1_N & -i1_N \\ 1_N & i1_N \end{pmatrix} \underbrace{W_{N\leftrightarrow 2}^\top \mathcal{K} W_{N\leftrightarrow 2}}_{=\mathcal{K}} \begin{pmatrix} 1_N & 1_N \\ i1_N & -i1_N \end{pmatrix} \\
&= \frac{1}{2}\begin{pmatrix} 1_N & -i1_N \\ 1_N & i1_N \end{pmatrix}\begin{pmatrix} 1_N & 1_N \\ -i1_N & i1_N \end{pmatrix}\mathcal{K} \\
&= \begin{pmatrix} 0 & 1_N\cdot\mathcal{K} \\ 1_N\cdot\mathcal{K} & 0 \end{pmatrix},
\end{aligned} \tag{5.9.115}$$

From the conditions (5.9.107), (5.9.109), $U_\mathrm{B}^2 = 1_{2N}$ and $U_\mathrm{B}^\dagger = U_\mathrm{B}$, we can obtain the block off-diagonalized form:

$$\widetilde{U}_\mathrm{B} = \begin{pmatrix} 0 & u_\mathrm{B} \\ u_\mathrm{B}^\dagger & 0 \end{pmatrix}, \quad u_\mathrm{B} u_\mathrm{B}^\dagger = 1_N, \quad u_\mathrm{B}^\top = u_\mathrm{B}. \tag{5.9.116}$$

Since u_B is a unitary matrix, it can be diagonalized, using the unitary matrix v, as

$$\begin{aligned}
&u_\mathrm{B} = v^\dagger u_\mathrm{d} v, \quad u_\mathrm{d} = \begin{pmatrix} e^{i\alpha_1} & & 0 \\ & \ddots & \\ 0 & & e^{i\alpha_N} \end{pmatrix}, \\
&v \in U(N), \quad \alpha_i \in \mathbb{R} \quad (i = 1, 2, \cdots, N)
\end{aligned} \tag{5.9.117}$$

We repeat the same analysis as for the class DIII. Substituting the first equation in (5.9.117) into the third equation in (5.9.116) and multiplying v from the left of both sides by $v^\top$ from the right of both sides, we can obtain

$$(vv^\top)u_\mathrm{d} = u_\mathrm{d}(vv^\top). \tag{5.9.118}$$

Or, if expressed in terms of components, we can obtain

$$(vv^\top)_{ij}(u_\mathrm{d})_{jj} = (u_\mathrm{d})_{ii}(vv^\top)_{ij}, \tag{5.9.119}$$

where i, j denote the indices of the matrix elements and are not summed up. If $(vJ_y v^\top)_{ij} \neq 0$, one can obtain $(u_\mathrm{d})_{ii} = (u_\mathrm{d})_{jj}$ from the above equations. By dividing both sides of the Eq. (5.9.119) by $u_\mathrm{d}^{1/2}$, we can also obtain the following relation:

$$(vv^\top)_{ij}\sqrt{(u_\mathrm{d})_{jj}} = \sqrt{(u_\mathrm{d})_{ii}}(vv^\top)_{ij}. \tag{5.9.120}$$

With this relation, u_B can be rewritten as

$$\begin{aligned}
u_\mathrm{B} &= u_\mathrm{B}^\top \\
&= (v^\dagger u_\mathrm{d} v)^\top \\
&= v^\top u_\mathrm{d}^{1/2}\cdot u_\mathrm{d}^{1/2} v^* \\
&= v^\top u_\mathrm{d}^{1/2} \underbrace{v^* v^\top}_{=1_N} u_\mathrm{d}^{1/2} v^* \\
&= w^\top w,
\end{aligned} \tag{5.9.121}$$

where w is defined by $w \equiv v^{\top} u_{\rm d}^{1/2} v^{*}$ and satisfies $w^{\dagger} w = 1_N$. Thus, we find that $u_{\rm B}$ can be characterized by $U(N)$. However, Eq. (5.9.121) is invariant under the transformation

$$\omega \to g\omega, \quad g \in O(N). \tag{5.9.122}$$

Therefore, we can obtain the classifying space of $U_{\rm B}$ as

$$R_5 = \frac{U(N)}{O(N)}. \tag{5.9.123}$$

These result are shown in Table 5.4.

5.9.2 $\mathbb{Z}_2$ index

The topological number of the class BDI and class D is known as $\mathbb{Z}_2$ in the AZ symmetry class. In this Subsection, we show that $\mathbb{Z}_2$ index is given by the even/odd parity of the number of Dirac zero modes, not the Witten index in our model.

The key to understand this index is the existence of C_+ symmetry. Under the C_+ transformation, the mode functions are transformed as

$$f_n^{(i)}(y) \xrightarrow{C_+} f_n^{C_+(i)}(y) = Q_y P_y g_n^{(i)*}(y), \tag{5.9.124}$$

$$g_n^{(i)}(y) \xrightarrow{C_+} g_n^{C_+(i)}(y) = Q_y P_y f_n^{(i)*}(y). \tag{5.9.125}$$

For the convenience of discussion, we introduce the two-component vector $\Phi_n^{(i)}(y) \equiv (f_n^{(i)}(y), g_n^{(i)}(y))^{\top}$ and denote the C_+ transformation as

$$\Phi_n^{(i)}(y) \xrightarrow{C_+} \Phi_n^{C_+(i)}(y) = \begin{pmatrix} Q_y P_y \mathcal{K} g_n^{(i)}(y) \\ Q_y P_y \mathcal{K} f_n^{(i)}(y) \end{pmatrix} = \sigma_1 Q_y P_y \mathcal{K} \Phi_n^{(i)}(y). \tag{5.9.126}$$

The eigenequations and supersymmetric relations can be written in this notation as

$$\widehat{H}\Phi_n^{(i)}(y) = m_n^2 \Phi_n^{(i)}(y), \quad \widehat{H} \equiv \begin{pmatrix} \partial_y^2 + M^2 & 0 \\ 0 & \partial_y^2 + M^2 \end{pmatrix}, \tag{5.9.127}$$

$$\widehat{Q}\Phi_n^{(i)}(y) = m_n \Phi_n^{(i)}(y), \quad \widehat{Q} \equiv \begin{pmatrix} 0 & -\partial_y + M \\ \partial_y + M & 0 \end{pmatrix}. \tag{5.9.128}$$

Now we can show that $\Phi_n^{C_+(i)}$ and $\Phi_n^{(i)}$ have in the same eigenvalue with respect to $\widehat{Q}$:

$$\begin{aligned} \widehat{Q}\Phi_n^{C_+(i)}(y) &= \widehat{Q}\sigma_1 Q_y P_y \mathcal{K} \Phi_n^{(i)}(y) \\ &= \sigma_1 Q_y P_y \mathcal{K} \widehat{Q} \Phi_n^{(i)}(y) \\ &\qquad (\because [\widehat{Q}, \sigma_1 P_y] = [\widehat{Q}, P_y] = [\widehat{Q}, \mathcal{K}] = 0) \\ &= \sigma_1 Q_y P_y \mathcal{K} \cdot m_n \Phi_n^{(i)}(y) \\ &= m_n \Phi_n^{C_+(i)}(y). \end{aligned} \tag{5.9.129}$$

On the other hand, it can also be shown that these are mutually orthogonal vectors, i.e., $\langle\Phi_n^{(i)}|\Phi_n^{C_+(i)}\rangle = 0$. Indeed, it can be shown from direct calculations such that

$$
\begin{aligned}
\langle\Phi_n^{(i)}|\Phi_n^{C_+(i)}\rangle &= \langle\Phi_n^{(i)}|\sigma_1 Q_y P_y \mathcal{K}\Phi_n^{(i)}\rangle \\
&= \langle P_y Q_y \sigma_1 \Phi_n^{(i)}|\mathcal{K}\Phi_n^{(i)}\rangle \quad (\because Q_y, P_y : \text{Hermitian op.}) \\
&= \langle \sigma_1 Q_y P_y \Phi_n^{(i)}|\mathcal{K}\Phi_n^{(i)}\rangle \quad (\because [Q_y, P_y] = 0) \\
&= \sum_{a=1}^{N}\int_{L_{a-1}+\varepsilon}^{L_a-\varepsilon} dy\,(\sigma_1 Q_y P_y \Phi_n^{(i)})^\dagger \Phi_n^{(i)*} \\
&= \sum_{a=1}^{N}\int_{L_{a-1}+\varepsilon}^{L_a-\varepsilon} dy\,(-\sigma_1 Q_y P_y \Phi_n^{(i)*})^\top \Phi_n^{(i)*} \quad (\because Q_y^* = -Q_y) \\
&= \sum_{a=1}^{N}\int_{L_{a-1}+\varepsilon}^{L_a-\varepsilon} dy\,\Phi_n^{(i)\dagger}(-\sigma_1 Q_y P_y \Phi_n^{(i)*}) \quad (\because \text{overall transposition}) \\
&= -\langle\Phi_n^{(i)}|\Phi_n^{C_+(i)}\rangle \\
&\Longrightarrow \langle\Phi_n^{(i)}|\Phi_n^{C_+(i)}\rangle = 0.
\end{aligned}
\tag{5.9.130}
$$

From the above calculation, we can find that for every $\Phi_n^{(i)}\,(i = 1,2,\cdots)$, the C_+-transformed $\Phi_n^{C_+(i)}\,(i = 1,2,\cdots)$ is degenerate as an independent eigenstate with the same eigenvalue. This implies that $\Phi_n^{C_+(i)}$ must satisfy the same boundary conditions as $\Phi_n^{(i)}$. The above discussion is also true for $\sigma_3\Phi_n^{(i)}(y)$, which has $-m_n$ as the eigenvalues of $\widehat{Q}$. Hence, we conclude that the massive modes ($m_n \neq 0$) are degenerated by a factor of 4 due to the C_+ symmetry.

In general, moving the parameters of the boundary conditions changes the mass spectrum. The even/odd parity of the number of Dirac zero modes is invariant because a massive mode must have degeneracy in multiples of 4. Fig. 5.4 illustrates this situation.

It should be emphasized that Q_y in the C_+ symmetry essentially contributes to the degeneracy, while it does not occur in other symmetries $\mathcal{T}_-$ or chiral transformations involving Q_y. This is because the $\mathcal{T}_-$ symmetry leads to the twofold degeneracy of not only the massive modes but also massless modes (is known as the Kramers degeneracy). In other words, the Kramers degeneracy breaks $\mathbb{Z}_2$ index. As a result, only classes with the C_+ symmetry without $\mathcal{T}_-$, i.e., the class BDI and the class D, can obtain a nontrivial $\mathbb{Z}_2$ index.

In the following, we specifically confirm that the $\mathbb{Z}_2$ index is topologically invariant in the case of class D and class BDI, and that $\mathbb{Z}_2$ is obtained as a discontinuity in the classification space. In addition, we explain in detail that the $\mathbb{Z}_2$ index is trivial due to the symmetry of $\mathcal{T}_-$.

5.9.2.1 Class D

The class D has only the C_+ symmetry. In this class, from the discussion in Subsec. 5.9.1.5, the matrix U_B can be written as follows:

$$
U_\mathrm{B} = \widetilde{V}R\begin{pmatrix} 0 & i1_N \\ -i1_N & 0 \end{pmatrix}R^\top\widetilde{V}^\dagger, \quad R \in O(2N),
\tag{5.9.131}
$$

where

$$
\widetilde{V} = \frac{1}{\sqrt{2}}\begin{pmatrix} 1_N & 1_{N/2}\otimes i\sigma_1 \\ -1_{N/2}\otimes i\sigma_2 & 1_{N/2}\otimes i\sigma_3 \end{pmatrix}.
\tag{5.9.132}
$$

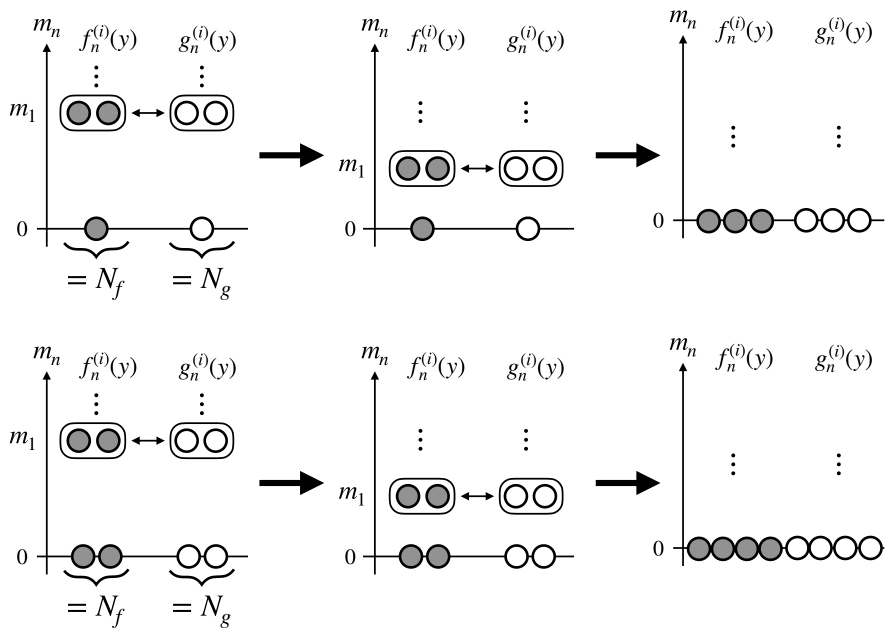

Figure 5.4: The Figures represent the change in the number of zero modes under continuous deformations of parameters with the symmetry C_+. Comparing the top three Figures with the bottom three Figures, we can see that the number of massless Dirac fields $N_{\rm D}\,(\equiv (N_f + N_g)/2)$ mod 2 is invariant.

Furthermore, the classifying space is given by $R_2 = O(2N)/U(N)$ and has two connected regions labeled by $\det R = \pm 1$. The symmetry of C_+ requires the massive modes to degenerate to a multiple of 4, and the resulting even/odd parity in the number of Dirac zero modes is a topological invariant.

In the following, we show that the equation

$$\det R = (-1)^{N_{\rm D}} \tag{5.9.133}$$

can be obtained, where $N_{\rm D}$ is defined by $N_{\rm D} \equiv (N_f + N_g)/2$. This relation implies that $N_{\rm D} = 0\,(\mathrm{mod}\,2)$ for the parameter space of the boundary condition with $\det R = +1$ and $N_{\rm D} = 1\,(\mathrm{mod}\,2)$ for the parameter space of the boundary condition with $\det R = -1$. Therefore, we can find that this index corresponds to the topological number $\mathbb{Z}_2$ of the 0-th homotopy group of the classifying space.

To confirm the result (5.9.133), it is enough to calculate a simple example since this index is invariant by continuous deformations of parameters. As an example, we take the matrix R as

$$R = \begin{pmatrix} 1_m \otimes \sigma_3 & & & \\ & 1_{N-2m} & & \\ & & 1_{2m} & \\ & & & 1_{N-2m} \end{pmatrix} \quad (m = 0, 1, \cdots, N/2). \tag{5.9.134}$$

Note that $\det R = (-1)^m$. Substituting (5.9.134) into Eq. (5.9.131), U_{B} is written as

$$U_{\mathrm{B}} = \left(\begin{array}{cc|cc} 0_{2m} & & 1_{2m} & \\ & 1_{N/2-m} \otimes \sigma_1 & & 0_{N-2m} \\ \hline 1_{2m} & & 0_{2m} & \\ & 0_{N-2m} & & 1_{N/2-m} \otimes \sigma_1 \end{array}\right). \tag{5.9.135}$$

Then the boundary conditions for zero modes are given by

$$\left(\begin{array}{cc|cc} 1_{2m} & & -1_{2m} & \\ & 1_{N/2-m} \otimes (1_2 - \sigma_1) & & 0_{N-2m} \\ \hline -1_{2m} & & 1_{2m} & \\ & 0_{N-2m} & & 1_{N/2-m} \otimes (1_2 - \sigma_1) \end{array}\right) \begin{pmatrix} A_1^{(i)} e^{-M(L_0+\varepsilon)} \\ A_1^{(i)} e^{-M(L_1-\varepsilon)} \\ \vdots \\ A_N^{(i)} e^{-M(L_{N-1}+\varepsilon)} \\ A_N^{(i)} e^{-M(L_N+\varepsilon)} \end{pmatrix} = 0, \tag{5.9.136}$$

$$\left(\begin{array}{cc|cc} 1_{2m} & & 1_{2m} & \\ & 1_{N/2-m} \otimes (1_2 + \sigma_1) & & 0_{N-2m} \\ \hline 1_{2m} & & 1_{2m} & \\ & 0_{N-2m} & & 1_{N/2-m} \otimes (1_2 + \sigma_1) \end{array}\right) \begin{pmatrix} B_1^{(j)} e^{M(L_0+\varepsilon)} \\ -B_1^{(j)} e^{M(L_1-\varepsilon)} \\ \vdots \\ B_N^{(j)} e^{M(L_{N-1}+\varepsilon)} \\ -B_N^{(j)} e^{M(L_N+\varepsilon)} \end{pmatrix} = 0, \tag{5.9.137}$$

where the $A_a^{(i)}$, $B_a^{(j)}$ $(a = 1, 2, \cdots, N)$ are the coefficients of zero modes $f_0^{(i)}$, $g_0^{(j)}$. Rewriting the above boundary conditions, we obtain

$$A_1^{(i)} = A_{N/2+1}^{(i)} e^{M(L_0 - L_{N/2})}, \cdots, A_m^{(i)} = A_{N/2+m}^{(i)} e^{M(L_{m-1} - L_{N/2+m-1})}, \tag{5.9.138}$$

$$B_1^{(j)} = -B_{N/2+1}^{(j)} e^{-M(L_0 - L_{N/2})}, \cdots, B_m^{(j)} = -B_{N/2+m}^{(j)} e^{-M(L_{m-1} - L_{N/2+m-1})}. \tag{5.9.139}$$

For $M \neq 0$, the independent coefficients are $A_1^{(i)}, A_2^{(i)}, \cdots, A_m^{(i)}$ and $B_1^{(i)}, B_2^{(i)}, \cdots, B_m^{(i)}$, so we found that there are m independent zero-mode functions, respectively. Therefore, $N_{\mathrm{D}} = m$ for the case of $M \neq 0$ and we can find that the result (5.9.133) is satisfied. We also mention that for $M = 0$ case we obtain $N_{\mathrm{D}} = N - m$ Dirac zero modes. Consequently, the result (5.9.133) is also satisfied since N is even in this class.

5.9.2.2 Class BDI

The class BDI has the three symmetries $\mathcal{T}_+$, $\mathcal{C}_+$ and chiral $\mathcal{T}_+\mathcal{C}_+$. In this class, from the discussion in Subsec. 5.9.1.5, the matrix U_{B} can be written as follows:

$$U_{\mathrm{B}} = \widetilde{V}_{\mathrm{BDI}} \begin{pmatrix} 0 & u_{\mathrm{B}} \\ u_{\mathrm{B}}^{\top} & 0 \end{pmatrix} \widetilde{V}_{\mathrm{BDI}}^{\top}, \quad u_{\mathrm{B}} \in O(N), \tag{5.9.140}$$

where to avoid confusion with Eq. (5.9.132), we denote

$$\widetilde{V}_{\mathrm{BDI}} = \frac{1}{\sqrt{2}} \begin{pmatrix} 1_N & 1_{N/2} \otimes \sigma_1 \\ -1_{N/2} \otimes i\sigma_2 & 1_{N/2} \otimes \sigma_3 \end{pmatrix} \tag{5.9.141}$$

with the subscript BDI. Now, if we restrict R as

$$R = \begin{pmatrix} u_{\mathrm{B}} & 0 \\ 0 & 1_N \end{pmatrix}, \quad u_{\mathrm{B}} \in O(N) \tag{5.9.142}$$

in Eq. (5.9.131) and , U_{B} is written

$$\begin{aligned}
U_{\mathrm{B}} &= \widetilde{V} R \begin{pmatrix} 0 & i1_N \\ -i1_N & 0 \end{pmatrix} R^\top \widetilde{V}^\dagger \\
&\to \frac{1}{\sqrt{2}} \begin{pmatrix} 1_N & 1_{N/2} \otimes i\sigma_1 \\ -1_{N/2} \otimes i\sigma_2 & 1_{N/2} \otimes i\sigma_3 \end{pmatrix} \begin{pmatrix} u_{\mathrm{B}} & 0 \\ 0 & 1_N \end{pmatrix} \begin{pmatrix} 0 & i1_N \\ -i1_N & 0 \end{pmatrix} \begin{pmatrix} u_{\mathrm{B}}^\top & 0 \\ 0 & 1_N \end{pmatrix} \\
&\quad \times \frac{1}{\sqrt{2}} \begin{pmatrix} 1_N & 1_{N/2} \otimes i\sigma_2 \\ -1_{N/2} \otimes i\sigma_1 & -1_{N/2} \otimes i\sigma_3 \end{pmatrix} \\
&= \frac{1}{\sqrt{2}} \begin{pmatrix} 1_N & 1_{N/2} \otimes i\sigma_1 \\ -1_{N/2} \otimes i\sigma_2 & 1_{N/2} \otimes i\sigma_3 \end{pmatrix} \begin{pmatrix} 0 & iu_{\mathrm{B}} \\ -iu_{\mathrm{B}}^\top & 0 \end{pmatrix} \frac{1}{\sqrt{2}} \begin{pmatrix} 1_N & 1_{N/2} \otimes i\sigma_2 \\ -1_{N/2} \otimes i\sigma_1 & -1_{N/2} \otimes i\sigma_3 \end{pmatrix} \\
&= \frac{1}{\sqrt{2}} \begin{pmatrix} 1_N & 1_{N/2} \otimes i\sigma_1 \\ -1_{N/2} \otimes i\sigma_2 & 1_{N/2} \otimes i\sigma_3 \end{pmatrix} \left[-\begin{pmatrix} 1 & 0 \\ 0 & i \end{pmatrix} \begin{pmatrix} 0 & u_{\mathrm{B}} \\ u_{\mathrm{B}}^\top & 0 \end{pmatrix} \begin{pmatrix} 1 & 0 \\ 0 & -i \end{pmatrix} \right] \frac{1}{\sqrt{2}} \begin{pmatrix} 1_N & 1_{N/2} \otimes i\sigma_2 \\ -1_{N/2} \otimes i\sigma_1 & -1_{N/2} \otimes i\sigma_3 \end{pmatrix} \\
&= -\widetilde{V}_{\mathrm{BDI}} \begin{pmatrix} 0 & u_{\mathrm{B}} \\ u_{\mathrm{B}}^\top & 0 \end{pmatrix} \widetilde{V}_{\mathrm{BDI}}^\top.
\end{aligned} \tag{5.9.143}$$

Therefore, repeating the argument below Eq. (5.9.131), we can obtain the relation

$$\begin{aligned}
(-1)^{N_{\mathrm{D}}} &= \det(-u_{\mathrm{B}}) \\
&= (-1)^N \det u_{\mathrm{B}} \\
&= \det u_{\mathrm{B}} \quad (\because N = \text{even}).
\end{aligned} \tag{5.9.144}$$

In other words, the classifying space in this class is $O(N)$ specified by the matrix u_{B} and divided into two spaces by $\det u_{\mathrm{B}} = +1$ and $\det u_{\mathrm{B}} = -1$ disconnected with each other. Indeed, we can see that the number of Dirac zero modes also corresponds to the topological number $\mathbb{Z}_2$ of the 0-th homotopy group of the classifying space in the class BDI.

5.10 Summary and discussion

In this chapter, we studied a Dirac fermion on a 5-dimensional (5d) spacetime with 1d extra dimension of the quantum graph. A unique feature of this model is that the extra-dimensional directions can generally take on a variety of boundary conditions. We showed that the boundary conditions of the quantum graphs are classified into ten symmetry classes according to the presence or absence of time-reversal, charge conjugation, and extra-spatial symmetries of 5d fermions. These classifications were based on the similarity to AZ symmetries for $(1+0)$-d gapped free-fermion system, which is classified according to time-reversal, particle-hole symmetry and chiral symmetry. A Hermitian matrix U_{B} specifying the boundary conditions corresponds to a 0d Hamiltonian H of gapped free fermion systems. The 0d Hamiltonian means that H has no dependence of momentum $\boldsymbol{k}$ and is a constant Hermitian matrix. We also showed that the constraints for U_{B} originating from symmetries of 5d fermions are the same as those for the 0d Hamiltonian with AZ symmetries. As a result, we could introduce topological numbers for the boundary conditions in the same manner as those of 0d topological insulators and superconductors such that

- The topological numbers $\mathbb{Z}$ and $2\mathbb{Z}$ are related to the Witten index;
- The topological number $\mathbb{Z}_2$ is related to even/odd parity of Dirac zero mode.

The topological numbers is known as the number of edge modes from bulk-boundary correspondence in the condensed matter physics. Importantly, the topological numbers in our model coincide with the number of KK 4d chiral or Dirac fermions localized at the vertex of quantum graphs, which would be a generalization of the bulk-boundary correspondence for gapped free-fermion systems.

We studied the application of quantum graphs as an extra dimension to the phenomenological models in Chap. 3. In order to explain the flavor structure of the Standard Model, a boundary condition with the Witten index $\Delta_{\mathrm{W}} = \pm 3$ is required. From this, our classification implies that class A with no symmetries or class AI with the time-reversal symmetry is preferable for realizing the fermion flavor structure in the Standard Model. However, in order to discuss phenomenological models quantitatively, it is necessary to add gauge fields and scalar fields as matter contents. Since the boundary conditions that do not violate gauge symmetry are generally more restrictive than those of free-fermion systems, it should be discussed whether this study can be applied naively. This issue will be addressed in further work.

The key point in the classification of the boundary conditions for the 5d fermions is the existence of chiral spinors in four dimensions. The Hermiticity of the boundary matrix U_{B} originates from the independence of the left and right-handed chiral fields under the 4d Lorentz invariance. We expect that the same discussion works for general odd d-dimensional cases since chiral spinors exist in $d-1$ dimensions. In contrast, for even d-dimensions case, we cannot apply the same discussions. In fact, the matrix for the boundary conditions is not generally Hermitian in even dimensions (See e.g.,[29]). We leave the extension of our results to other spacetime dimensions as a future problem. In particular, the investigations for lower dimensions would be important from the viewpoint of condensed matter physics.

We are also interested in the correspondence to SPT phases in other dimensions, i.e., the Hamiltonian H has momentum dependence. In this dissertation, we have discussed the relation between the boundary conditions for quantum graphs and $(1+0)$-d SPT phases for gapped free-fermion systems, assuming that the 4d spacetime and the extra dimension are factorized, and the boundary conditions on the extra space do not have a 4d momentum dependence. However, if we consider the boundary conditions depending on the 4d momentum (or equivalently the 4d derivative) such that

$$U_{\mathrm{B}}(k) = V(k)\begin{pmatrix} 1_{2N-k} & 0 \\ 0 & -1_k \end{pmatrix} V^\dagger(k) \quad (V(k) \in U(2N)),$$

the boundary condition matrix would be regarded as a higher dimensional Hamiltonian, and thus we may obtain the correspondence to SPT phases in other dimensions.

Another future direction is the effect of interactions. In our study, we have considered free fermions on quantum graphs. However, by considering interactions and also quantum corrections, the boundary conditions would be changed, and breakdowns of the topological phases may occur, which affects low-energy physics. For the topological matter side, it has been known that SPT phases of gapped free-fermion systems may break down by interactions preserving symmetries (see e.g., [48–54]). For example, the $\mathbb{Z}$ classification of class BDI for 1d topological superconductor reduces to the $\mathbb{Z}_8$ classification if quartic interactions are present. We are interested in whether a similar breakdown occurs in the topological classification of boundary conditions. It is also known that interacting SPT phases in bulk can be characterized by perturbative and/or non-perturbative anomalies on boundary [55–59]. This is described by an anomaly inflow. Thus, it could be interesting to consider the boundary conditions from the viewpoint of anomalies.

Chapter 6

Summary and discussion

In this dissertation, we consider Dirac fermions on a five-dimensional (5d) spacetime with a quantum graph as a 1d extra dimension and study their boundary dependence. Especially, using a master graph consisting of N loops and a single vertex (called the rose graph), as a quantum graph, we investigate the topological structure of the boundary conditions.

The extra-dimensional model is usually decomposed into a 4d part and an extra-dimensional part. In doing the above, the extra-dimensional direction is expanded by the complete set of mass eigenfunctions of the 4d field, which is called Kaluza–Klein (KK) expansion or decomposition. The information on the boundary conditions of quantum graphs appears as a 4d theory through mode functions in the extra-dimensional direction. The behavior of the zero mass states, or KK zero modes, then describes a 4d low-energy effective theory.

In Chap. 2, through a simple quantum graph example, we explained how to derive boundary conditions from current conservation conditions on the graph. An important feature of the resulting boundary conditions is that they are expressions that include parameter degrees of freedom. Fixing the parameters determines certain boundary conditions, which can be the well-known Dirichlet BC, Neumann BC, and periodic BC, but also various other boundary conditions.

In Chap. 3, we derived the boundary conditions that Dirac fermions on a 5d spacetime with quantum graph as an extra dimension must satisfy by using the computational methods of the previous Chapter. Furthermore, the degeneracy of the KK zero mode was systematically evaluated under each of the boundary conditions. The boundary condition can be characterized by a $2N$ dimensional unitary Hermitian matrix U_{B} with $U_{\mathrm{B}}^2 = 1_{2N}$, and it is revealed that the difference between the number of right- and left-handed chiral fermions is $\Delta_{\mathrm{W}} = N - k$, which is known as the Witten index, for boundary conditions of k with the number of eigenvalues -1. A remarkable feature is that Δ_{W} is invariant under continuous deformation of boundary conditions that do not change k, which is a topological quantity in this sense.

We also discussed strategies for applying our model to theories beyond the Standard Model. There are several clarifications of the flavor structure of fermions using extra-dimensional models. Our extra-dimensional model has the potential to simultaneously explain the number of generations, the mass hierarchy of fermions, and the origin of flavor mixing and CP phases. Future work will involve quantitative evaluations for full setups involving gauge and scalar fields.

In Chap. 4, we focused on zero mode and studied the Berry's connection in the parameter space of boundary conditions. It is shown that the structure of the ADHM construction is similar to the boundary conditions of the quantum graph, which allows us to construct instanton solutions as

Berry's connections. The point that zero modes on the quantum graph can in general have multiple degeneracies and the parameter-dependent nature of the boundary conditions play a major role in these results.

Instanton solutions as the Berry's connections are constructible for a restricted parameter space. We will investigate whether these limitations can become feedback to the phenomenological model construction. This is also future study. Another future study is to construct monopole solutions as the Berry's connections for our model. The Nahm construction method is known as a method for constructing general monopole solutions. Using this one, it is shown that the $SU(2)$ BPS monopole can be constructed for simple quantum graphs [12]. The similar strategy is expected to be used to construct systematic monopole solutions for our setup, which is a more general quantum graph model.

In Chap. 5, we have identified a nontrivial correspondence between the classification of $(1+0)$-d gapped free-fermion systems and the classification of boundary condition U_{B}. The former classification is known as the Altland–Zirnbauer symmetry classes, which are classified into 10 classes corresponding to whether time-reversal symmetry, particle hole symmetry and chiral symmetry is present or absent. In our model, we found the existence of time-reversal symmetry, charge-conjugate symmetry, and extra-spatial symmetries of 5d fermions as the corresponding symmetries. Furthermore, each class classified in the AZ symmetric class is characterized by a topological number. The correspondences in our setup are also revealed as follows: (a) the $\mathbb{Z}$ and $2\mathbb{Z}$ topological numbers corresponds to the Witten index; (b) the $\mathbb{Z}_2$ topological number corresponds to the even/odd parity of Dirac zero mode. These quantities would be regarded as a generalization of the bulk-boundary correspondence.

With reference to the advanced work in topological insulators and superconductors, there are several things to discuss in the case of our model. For example, we discuss the SPT phase counterparts in dimensions different from the $(1+0)$-dimension in our model. Furthermore, we investigate what our class of boundary conditions corresponding to the SPT phase would be if the interaction were taken into account. We also investigate whether fermions have a correspondence with the AZ symmetries in a different dimension of spacetime than 5d.

Through this dissertation, we have studied various aspects of quantum graphs. Boundary conditions are a very important element in physics. The quantum graphs reveal nontrivial relationships between different fields of physics through the degrees of freedom of their boundary conditions. Thus, we believe that pushing forward the future study discussed above will have an impact on physics at various energy scales and reveal new connections between them.

Appendix A

Details of Calculation

A.1 ’t Hooft instanton

The normalized solution is

$$V_{[2+2k]\times[2]} = \frac{1}{\sqrt{\phi}}\begin{pmatrix} \mathbf{1}_{[2]\times[2]} \\ -\left(\bar{e}_\mu \otimes \left(x_\mu \mathbf{1} - T_\mu\right)\right)^{-1} S^\dagger \end{pmatrix}, \tag{A.1.1}$$

where

$$\left(\bar{e}_\mu \otimes \left(x_\mu \mathbf{1} - T_\mu\right)\right)^{-1} = e_\mu \otimes \begin{pmatrix} \frac{(x-b^1)_\mu}{(x-b^1)^2} & & & \mathbf{0} \\ & \frac{(x-b^2)_\mu}{(x-b^2)^2} & & \\ & & \ddots & \\ \mathbf{0} & & & \frac{(x-b^k)_\mu}{(x-b^k)^2} \end{pmatrix}_{[k]\times[k]}, \tag{A.1.2}$$

$$\phi = 1 + \sum_{i=1}^{k} \frac{\rho_i^2}{(x-b^i)^2}. \tag{A.1.3}$$

By using the relations

$$\frac{1}{\sqrt{\phi}}\partial_\mu \frac{1}{\sqrt{\phi}} = \partial_\mu \frac{1}{2\phi}, \tag{A.1.4}$$

$$\bar{e}_\alpha e_\beta (x-b_i)^\alpha (x-b_i)^\beta = (x-b_i)^2, \tag{A.1.5}$$

we can calculate as

$$\begin{aligned}(\mathcal{A}_\mu)_{[2]\times[2]} &= V^\dagger \partial_\mu V \\ &= 1_2 \frac{1}{\sqrt{\phi}}\partial_\mu \frac{1}{\sqrt{\phi}} + \bar{e}_\alpha e_\beta \frac{1}{\sqrt{\phi}} \sum_{i=1}^{k} \rho_i^2 \frac{(x-b_i)^\alpha}{(x-b_i)^2} \partial_\mu \left(\frac{1}{\sqrt{\phi}} \frac{(x-b_i)^\beta}{(x-b_i)^2}\right) \\ &= 1_2 \frac{1}{\sqrt{\phi}}\partial_\mu \frac{1}{\sqrt{\phi}} + \bar{e}_\alpha e_\beta \frac{1}{\sqrt{\phi}}\partial_\mu \frac{1}{\sqrt{\phi}} \sum_{i=1}^{k} \rho_i^2 \frac{(x-b_i)^\alpha (x-b_i)^\beta}{(x-b_i)^4}\end{aligned}$$

$$
\begin{aligned}
&+ \bar{e}_\alpha e_\beta \frac{1}{\phi} \sum_{i=1}^{k} \rho_i^2 \frac{(x-b_i)^\alpha}{(x-b_i)^2} \partial_\mu \left(\frac{(x-b_i)^\beta}{(x-b_i)^2} \right) \\
&= 1_2 \partial_\mu \frac{1}{2\phi} + 1_2 \partial_\mu \frac{1}{2\phi} \sum_{i=1}^{k} \frac{\rho_i^2}{(x-b_i)^2} + \bar{e}_\alpha e_\beta \frac{1}{\phi} \sum_{i=1}^{k} \rho_i^2 \frac{(x-b_i)^\alpha}{(x-b_i)^2} \partial_\mu \left(\frac{1}{\sqrt{\phi}} \frac{(x-b_i)^\beta}{(x-b_i)^2} \right).
\end{aligned} \tag{A.1.6}
$$

Then, using Eq. (A.1.5) again, it can be rewritten as follows.

$$
\begin{aligned}
& 1_2 \phi \partial_\mu \frac{1}{2\phi} + \bar{e}_\alpha e_\beta \frac{1}{\phi} \sum_{i=1}^{k} \rho_i^2 \frac{(x-b_i)^\alpha}{(x-b_i)^2} \partial_\mu \left(\frac{1}{\sqrt{\phi}} \frac{(x-b_i)^\beta}{(x-b_i)^2} \right) \\
&= 1_2 \phi \partial_\mu \frac{1}{2\phi} + \bar{e}_\alpha e_\beta \frac{1}{\phi} \sum_{i=1}^{k} \rho_i^2 \frac{(x-b_i)^\alpha}{(x-b_i)^4} \left(\delta_{\mu\beta} - 2 \frac{(x-b_i)_\mu (x-b_i)^\beta}{(x-b_i)^2} \right) \\
&= 1_2 \phi \partial_\mu \frac{1}{2\phi} + \bar{e}_\alpha e_\mu \frac{1}{\phi} \sum_{i=1}^{k} \rho_i^2 \frac{(x-b_i)^\alpha}{(x-b_i)^4} - 2 \frac{1}{\phi} \sum_{i=1}^{k} \rho_i^2 \frac{(x-b_i)_\mu}{(x-b_i)^4}
\end{aligned} \tag{A.1.7}
$$

Finally, applying $\bar{e}_\alpha e_\mu = \delta_{\mu\alpha} + i\eta^{(+)}_{\mu\alpha}$ and organizing equation, we obtain

$$
\begin{aligned}
(\mathcal{A}_\mu)_{[2]\times[2]} &= 1_2 \phi \partial_\mu \frac{1}{2\phi} + \bar{e}_\alpha e_\mu \frac{1}{\phi} \sum_{i=1}^{k} \rho_i^2 \frac{(x-b_i)^\alpha}{(x-b_i)^4} - 2 \frac{1}{\phi} \sum_{i=1}^{k} \rho_i^2 \frac{(x-b_i)_\mu}{(x-b_i)^4} \\
&= 1_2 \phi \partial_\mu \frac{1}{2\phi} + (\delta_{\mu\alpha} 1_2 + i\eta^{(+)}_{\mu\alpha}) \frac{1}{\phi} \sum_{i=1}^{k} \rho_i^2 \frac{(x-b_i)^\alpha}{(x-b_i)^4} - 2 \frac{1}{\phi} \sum_{i=1}^{k} \rho_i^2 \frac{(x-b_i)_\mu}{(x-b_i)^4} \\
&= 1_2 \phi \partial_\mu \frac{1}{2\phi} - 1_2 \frac{1}{\phi} \underbrace{\sum_{i=1}^{k} \rho_i^2 \frac{(x-b_i)_\mu}{(x-b_i)^4}}_{=-(1/2)\partial_\mu \phi} + i\eta^{(+)}_{\mu\alpha} \frac{1}{\phi} \sum_{i=1}^{k} \rho_i^2 \frac{(x-b_i)^\alpha}{(x-b_i)^4} \\
&= 1_2 \frac{1}{2} \left(\phi \partial_\mu \frac{1}{\phi} + \frac{1}{\phi} \partial_\mu \phi \right) + i\eta^{(+)}_{\mu\alpha} \frac{1}{\phi} \sum_{i=1}^{k} \rho_i^2 \frac{(x-b_i)^\alpha}{(x-b_i)^4} \\
&= -i\eta^{(+)}_{\mu\alpha} \frac{\sum_{i=1}^{k} \rho_i^2 \frac{(x-b_i)^\alpha}{(x-b_i)^2}}{1 + \sum_{i=1}^{k} \frac{\rho_i^2}{(x-b_i)^2}}.
\end{aligned} \tag{A.1.8}
$$

Appendix B

Structure of the ADHM construction

The ADHM construction method is proposed by Atiyah, Drinfeld, Hitchin and Manin in 1978 [22]. It is possible to construct arbitrary instanton solutions by using a one-to-one correspondence between the moduli space of instantons and the moduli space of matrices, called ADHM data. In this Appendix, we review the reasons why instantons can be constructed using the ADHM construction method and the structure behind them.

This Appendix is organized as follows: In Secs. B.1 and B.2, we explain each settings. These correspond to the two ends "Instatnon" and "ADHM data" in Fig. B.1. In Sec. B.3, starting from the ADHM data, we show that the instantons are constructed via the zero-dimensional (0d) Dirac equation. Conversely, Sec. B.4 shows that the ADHM data is constructed starting from instanton. In Sec. B.5, to check the completeness of the ADHM construction, we start from the ADHM data, reconstruct the ADHM data via instantons, and prove that they are consistent. In Sec. B.6, starting from the instanton, we construct the instanton via the ADHM data to show consistency.

This Appendix refers to I. Ueba's unpublished note and M. Hamanaka's review paper in Japanese[1].

B.1 Instanton side settings

Instantons are gauge field configurations that make the Yang–Mills action finite, defined on four-dimension (4d) Euclidean spacetime. This action is given by

$$S = -\frac{1}{2g^2}\int d^4x\,\mathrm{Tr}F_{\mu\nu}F_{\mu\nu} = \frac{1}{4g^2}\int d^4x\,F^a_{\mu\nu}F^a_{\mu\nu}, \tag{B.1.1}$$

$$F_{\mu\nu} = \partial_\mu A_\nu - \partial_\nu A_\mu + [A_\mu, A_\nu], \tag{B.1.2}$$

where the generators of the gauge group are defined by

$$[T^a, T^b] = i f_{abc} T^c, \quad \mathrm{Tr}\,T^aT^b = \frac{1}{2}\delta^{ab}, \tag{B.1.3}$$

and the gauge field $A_\mu(x)$ and the field strength $F_{\mu\nu}(x)$ are represented by

$$F_{\mu\nu} = F^a_{\mu\nu}(iT^a), \quad A_\mu = A^a_\mu(iT^a), \tag{B.1.4}$$

$$F^a_{\mu\nu} = \partial_\mu A^a_\nu - \partial_\nu A^a_\mu - f_{abc}A^b_\mu A^c_\nu. \tag{B.1.5}$$

[1]DOI: https://doi.org/10.24532/soken.106.1_1

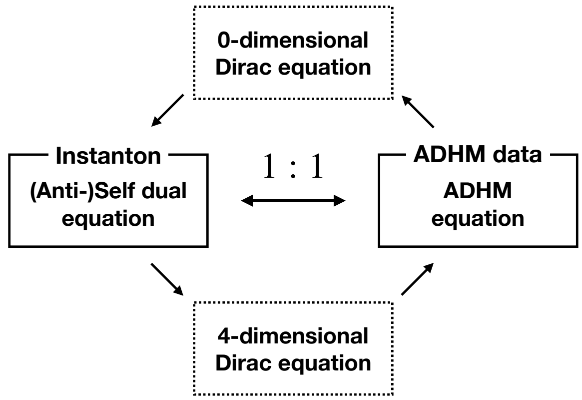

Figure B.1: Schematic diagram showing the relationship between the ADHM data and instantons. The specific one-to-one correspondence is given via the 0- or 4-dimensional massless Dirac equation.

Under gauge transformations, the gauge field and the field strength are transformed as

$$A_\mu(x) \to A'_\mu(x) = g(x)A_\mu(x)g^{-1}(x) + g(x)\partial_\mu g^{-1}(x), \tag{B.1.6}$$

$$F_{\mu\nu}(x) \to F'_{\mu\nu}(x) = g(x)F_{\mu\nu}(x)g^{-1}(x), \tag{B.1.7}$$

where $g(x) \in SU(N)$. The Yang–Mills action is invariant under the above gauge transformations. The equation of motion (called the Yang–Mills equation)

$$D_\mu F_{\mu\nu} = \partial_\mu F_{\mu\nu} + [A_\mu, F_{\mu\nu}] = 0 \tag{B.1.8}$$

that the gauge field must satisfy is derived from the action. Instantons are characterized by a topological charge called the instanton number:

$$|Q| = -\frac{1}{16\pi^2}\int d^4x \,\mathrm{Tr}\,(F_{\mu\nu}\widetilde{F}_{\mu\nu}) \in \mathbb{Z}, \tag{B.1.9}$$

where the gauge filed is satisfied the pure gauge $A_\mu(x) \approx g^{-1}(x)\partial_\mu g(x)$ (or $F_{\mu\nu} \approx 0$) at infinity to take a finite value. In this appendix, we shall consider anti-instantons whose instanton number is $-k$.

4d Dirac operator Here, we define a Dirac operator on the instanton side required for the ADHM construction method:

$$\mathcal{D} = e^\mu \otimes D_\mu = e^\mu \otimes (\partial_\mu + A_\mu), \tag{B.1.10}$$

$$\overline{\mathcal{D}} = \bar{e}_\mu \otimes D_\mu = -\mathcal{D}^\dagger, \tag{B.1.11}$$

where e_μ is the 2d representation of a quaternion defined as

$$e_\mu = (-i\sigma_i, 1), \quad \bar{e}_\mu = (i\sigma_i, 1). \tag{B.1.12}$$

These operators are the off-diagonal components of the Dirac operator $\gamma^\mu D_\mu$ in the chiral representation.

Formulas satisfied by e_μ and $\bar{e}_\mu$ are obtained

$$\bar{e}_\mu e_\nu = \delta_{\mu\nu} + i\eta^{(+)}_{\mu\nu}, \qquad e_\mu \bar{e}_\nu = \delta_{\mu\nu} + i\eta^{(-)}_{\mu\nu}, \tag{B.1.13}$$

$$e_\mu \bar{e}_\nu + e_\nu \bar{e}_\mu = 2\delta_{\mu\nu}, \qquad \bar{e}_\mu e_\nu + \bar{e}_\nu e_\mu = 2\delta_{\mu\nu}, \tag{B.1.14}$$

$$e_\mu \bar{e}_\nu e_\mu = -2e_\nu, \qquad \bar{e}_\mu e_\nu \bar{e}_\mu = -2\bar{e}_\nu, \tag{B.1.15}$$

where $\eta^{(\pm)}_{\mu\nu}$ is known as 't Hooft matrix and defined by

$$\eta^{(\pm)}_{\mu\nu} = \eta^{a(\pm)}_{\mu\nu}\sigma_a, \tag{B.1.16}$$

$$\eta^{a(\pm)}_{\mu\nu} = \epsilon_{a\mu\nu 4} \pm (\delta_{a\mu}\delta_{\nu 4} - \delta_{a\nu}\delta_{\mu 4}) \quad (a = 1, 2, 3). \tag{B.1.17}$$

The useful formulas that appear in this Appendix can be summarized as shown in

$$\begin{aligned}\eta^{(\pm)}_{\mu\nu}\eta^{(\pm)}_{\lambda\rho} &= (\delta_{\mu\lambda}\delta_{\nu\rho} - \delta_{\mu\rho}\delta_{\nu\lambda} \pm \epsilon_{\mu\nu\lambda\rho}) \cdot 1 \\ &\quad + i\left(\delta_{\mu\lambda}\eta^{(\pm)}_{\nu\rho} - \delta_{\mu\rho}\eta^{(\pm)}_{\nu\lambda} + \delta_{\nu\rho}\eta^{(\pm)}_{\mu\lambda} - \delta_{\nu\lambda}\eta^{(\pm)}_{\mu\rho}\right),\end{aligned} \tag{B.1.18}$$

$$\left[\eta^{(\pm)}_{\mu\nu}, \eta^{(\pm)}_{\lambda\rho}\right] = 2i\left(\delta_{\mu\lambda}\eta^{(\pm)}_{\nu\rho} - \delta_{\nu\lambda}\eta^{(\pm)}_{\mu\rho} + \delta_{\mu\rho}\eta^{(\pm)}_{\lambda\nu} - \delta_{\nu\rho}\eta^{(\pm)}_{\lambda\mu}\right), \tag{B.1.19}$$

$$\epsilon_{\mu\nu\lambda\rho}\eta^{(\pm)}_{\sigma\rho} = \pm\left(\delta_{\mu\sigma}\eta^{(\pm)}_{\nu\lambda} + \delta_{\lambda\sigma}\eta^{(\pm)}_{\mu\nu} + \delta_{\nu\sigma}\eta^{(\pm)}_{\lambda\mu}\right), \tag{B.1.20}$$

$$\mathrm{Tr}\,\eta^{(\pm)}_{\mu\nu}\eta^{(\pm)}_{\lambda\rho} = 2\left(\delta_{\mu\lambda}\delta_{\nu\rho} - \delta_{\mu\rho}\delta_{\nu\lambda} \pm \epsilon_{\mu\nu\lambda\rho}\right), \tag{B.1.21}$$

$$\mathrm{Tr}\,\eta^{(\pm)}_{\mu\nu}\eta^{(\pm)}_{\mu\rho} = 6\delta_{\nu\rho}, \tag{B.1.22}$$

$$\mathrm{Tr}\,\eta^{(\pm)}_{\mu\nu}\eta^{(\pm)}_{\mu\nu} = 24, \tag{B.1.23}$$

$$\begin{aligned}\eta^{i(\pm)}_{\mu\nu}\eta^{j(\pm)}_{\lambda\rho} &= (\delta_{\mu\lambda}\delta_{\nu\rho} - \delta_{\mu\rho}\delta_{\nu\lambda} \pm \epsilon_{\mu\nu\lambda\rho})\delta_{ij} \\ &\quad + \frac{1}{2}\epsilon_{ijk}\left(\delta_{\mu\lambda}\eta^{k(\pm)}_{\nu\rho} - \delta_{\mu\rho}\eta^{k(\pm)}_{\nu\lambda} + \delta_{\nu\rho}\eta^{k(\pm)}_{\mu\lambda} - \delta_{\nu\lambda}\eta^{k(\pm)}_{\mu\rho}\right),\end{aligned} \tag{B.1.24}$$

$$\eta^{i(\pm)}_{\mu\nu}\eta^{j(\pm)}_{\mu\rho} = \delta_{\nu\rho}\delta_{ij} + \epsilon_{ijk}\eta^{k(\pm)}_{\nu\rho}, \tag{B.1.25}$$

$$\eta^{a(-)}_{\mu\nu} = -\frac{i}{2}\mathrm{Tr}\,\sigma^a \bar{e}_\mu e_\nu, \tag{B.1.26}$$

$$\eta^{a(-)}_{\mu\nu} = -\frac{i}{2}\mathrm{Tr}\,\sigma^a e_\mu \bar{e}_\nu. \tag{B.1.27}$$

Anti-self dual equation The anti-self duality of the gauge field, $\widetilde{F}_{\mu\nu} = -F_{\mu\nu}$, can then be defined using the Dirac operators. That is, the square $\overline{\mathcal{D}}\mathcal{D}$ of the Dirac operator is commutative with the Pauli matrix σ_i , which is a necessary and sufficient condition for the gauge field to be anti-self dual.

Indeed, $\overline{\mathcal{D}}\mathcal{D}$ is written down as

$$\begin{aligned}
\overline{\mathcal{D}}\mathcal{D} &= (\bar{e}_\mu e_\nu) \otimes (D_\mu D_\nu) \\
&= \delta_{\mu\nu} \otimes (D_\mu D_\nu) + \frac{i}{2}\eta^{(+)}_{\mu\nu} \otimes [D_\mu, D_\nu] \quad (\because\ \bar{e}_\mu e_\nu = \delta_{\mu\nu} + i\eta^{(+)}_{\mu\nu}) \\
&= 1_2 \otimes D^2 + \frac{i}{2}\eta^{(+)}_{\mu\nu} \otimes F_{\mu\nu} \quad (\because\ [D_\mu, D_\nu] = F_{\mu\nu}) \\
&= 1_2 \otimes D^2 + \frac{i}{4}\eta^{(+)}_{\mu\nu} \otimes F_{\mu\nu} + \frac{i}{4}\eta^{(+)}_{\mu\nu} \otimes F_{\mu\nu} \\
&= 1_2 \otimes D^2 + \frac{i}{4}\eta^{(+)}_{\mu\nu} \otimes F_{\mu\nu} + \frac{i}{4} \cdot \left(\frac{1}{2}\epsilon_{\mu\nu\rho\sigma}\eta^{(+)}_{\rho\sigma}\right) \otimes F_{\mu\nu} \quad (\because\ (1/2)\epsilon_{\mu\nu\rho\sigma}\eta^{(+)}_{\rho\sigma} = \eta^{(+)}_{\mu\nu}) \\
&= 1_2 \otimes D^2 + \frac{i}{4}\eta^{(+)i}_{\mu\nu}\sigma_i \otimes (F_{\mu\nu} + \widetilde{F}_{\mu\nu}).
\end{aligned} \tag{B.1.28}$$

Therefore, the request to commute with the Pauli matrix leads to

$$\begin{aligned}
&F_{12} = -F_{34}, \quad F_{13} = F_{24}, \quad F_{14} = -F_{23} \\
&\Longleftrightarrow F_{\mu\nu} = -\widetilde{F}_{\mu\nu}.
\end{aligned} \tag{B.1.29}$$

We suppose that A_μ satisfies the pure gauge at infinity.

Invertibility of D^2 We require that $D^2\,(= D_\mu D_\mu)$ is invertible, or there exists Green's function $G(x)$:

$$D_x^2 G(x,y) = -\delta^4(x-y), \quad G(x,y) \simeq O(r^{-2}) \quad (r \to \infty). \tag{B.1.30}$$

4d Dirac equation A 4d massless Dirac equation is given by

$$\bar{e}_\mu D_\mu \psi(x) = 0, \tag{B.1.31}$$

where $\psi(x)$ is the normalized 2-components spinor. By using the index theorem, it is proofed that the number of Dirac zero modes is k.

Indeed, let the number of normalized solutions $\psi_\pm(x)$, which are satisfied

$$\bar{e}_\mu D_\mu \psi_+(x) = 0, \quad e_\mu D_\mu \psi_-(x) = 0, \tag{B.1.32}$$

be defined by $n_\pm$ respectively. Then, by using the index theorem, the relation

$$n_+ - n_- = \frac{1}{16\pi^2}\int d^4x\, \mathrm{Tr}\, F_{\mu\nu}\widetilde{F}_{\mu\nu} = -Q\,(=k) \tag{B.1.33}$$

is satisfied. On the other hand, if the anti-self dual equation is satisfied, from $(\bar{e}_\mu \otimes D_\mu)(e_\nu \otimes D_\mu) = D^2$, we can obtain

$$\begin{aligned}
&0 = (\bar{e}_\mu \otimes D_\mu)(e_\nu \otimes D_\mu)\psi_-(x) = D^2\psi_-(x) \\
&\Longrightarrow 0 = \int d^4x\, \psi_-^\dagger(x)(-D^2)\psi_-(x) = \int d^4x\, |D_\mu\psi_-(x)|^2 \\
&\Longrightarrow D_\mu\psi_-(x) = 0.
\end{aligned} \tag{B.1.34}$$

Since the equation

$$\begin{aligned} 0 &= D_\mu \psi_-(x) - D_\mu \psi_-(x) \quad (\because \text{(B.1.34)}) \\ &= [D_\mu, D_\nu]\psi_-(x) \\ &= F_{\mu\nu}\psi_-(x) \end{aligned} \tag{B.1.35}$$

is satisfied from Eq. (B.1.34) and $F_{\mu\nu} \neq 0$, the solution of the Eq. (B.1.34) is $\psi_-(x) = 0$. Therefore, we can conclude that the number of $\psi_-(x)$ is zero, i.e., $n_- = 0$, and $n_+ = k$ from Eq. (B.1.34).

Normalization condition For the convenience in the following discussion, the $2N \times k$ matrix with k independent $\psi_{-,i}$ $(i = 1, 2, \cdots, k)$ components is again defined as

$$\psi(x) \equiv (\psi_{+,1}, \psi_{+,2}, \cdots, \psi_{+,k})^\top. \tag{B.1.36}$$

This matrix is satisfied the normalization condition

$$\int d^4x\, \psi^\dagger(x)\psi(x) = 1_k, \tag{B.1.37}$$

where $\psi^\dagger\psi$ is assumed to be smooth over the entire region. Note that $\psi(x)$ behaves asymptotically as $\psi \sim \mathcal{O}(r^{-3})$ if $r \to \infty$ [60, 61].

Completeness The completeness is denoted as

$$\psi(x)\psi^\dagger(x) - \mathcal{D}_x G(x,y)\overleftarrow{\mathcal{D}}_y = \delta^4(x-y), \tag{B.1.38}$$

where

$$\overleftarrow{\mathcal{D}} = \bar{e}_\mu \overleftarrow{D}_\mu = \bar{e}_\mu(-\overleftarrow{\partial}_\mu + A_\mu). \tag{B.1.39}$$

$\psi(x)\psi^\dagger(x)$ and $-\mathcal{D}_x G(x,y)\overleftarrow{\mathcal{D}}_y$ correspond to the projection operators to the zero mode and the massive mode, respectively.

We show that the completeness relation is given by Eq. (B.1.38). First, we consider the equation

$$\gamma_\mu D_\mu \Psi_{\pm,n}(x) = \lambda_n \Psi_{\mp,n}(x), \tag{B.1.40}$$

where $\Psi_{\pm,n}(x)$ is the orthonormal 4-components chiral spinor, n represent the mode label and A_μ is anti-seld dual. In the chiral representation, this equation is written as

$$\begin{pmatrix} 0 & e_\mu D_\mu \\ \bar{e}_\mu D_\mu & 0 \end{pmatrix}\begin{pmatrix} \psi_{+,n} \\ 0 \end{pmatrix} = \lambda_n \begin{pmatrix} 0 \\ \psi_{-,n} \end{pmatrix}, \quad \begin{pmatrix} 0 & e_\mu D_\mu \\ \bar{e}_\mu D_\mu & 0 \end{pmatrix}\begin{pmatrix} 0 \\ \psi_{-,n} \end{pmatrix} = \lambda_n \begin{pmatrix} \psi_{+,n} \\ 0 \end{pmatrix}, \tag{B.1.41}$$

$$\Psi_{+,n} = \begin{pmatrix} \psi_{+,n} \\ 0 \end{pmatrix}, \quad \Psi_{-,n} = \begin{pmatrix} 0 \\ \psi_{-,n} \end{pmatrix}. \tag{B.1.42}$$

If we let $-\gamma_\mu D_\mu$ act on the both sides of Eq. (B.1.40), we obtain

$$-(\gamma_\mu D_\mu)^2 \Psi_{\pm,n}(x) = -\lambda_n^2 \Psi_{\pm,n}(x). \tag{B.1.43}$$

Since $\gamma_\mu D_\mu$ is anti-Hermitian and $-(\gamma_\mu D_\mu)^2$ is Hermitian, the eigenvalue $-\lambda_n^2$ is a real number greater than or equal to zero.

Next, we consider Green's function $S(x,y)$ of $\gamma_\mu D_\mu$. If the zero mode exists, $S(x,y)$ is defined as

$$\gamma_\mu D_\mu^x S(x,y) = -\delta^4(x-y) + \sum \Psi_{+,0}(x)\Psi_{+,0}^\dagger(x), \tag{B.1.44}$$

where the summation means adding with respect to the zero mode. The above equation in chiral representation is

$$S(x,y) = \begin{pmatrix} 0 & s(x,y) \\ \bar{s}(x,y) & 0 \end{pmatrix}, \tag{B.1.45}$$

$$\begin{pmatrix} 0 & e_\mu D_\mu^x \\ \bar{e}_\mu D_\mu^x & 0 \end{pmatrix}\begin{pmatrix} 0 & s(x,y) \\ \bar{s}(x,y) & 0 \end{pmatrix} = -\delta^4(x-y) + \begin{pmatrix} \sum \psi_{+,0}(x)\psi_{+,0}(y) & 0 \\ 0 & 0 \end{pmatrix}. \tag{B.1.46}$$

Then, writing down each the components, we obtain

$$\overline{\mathcal{D}}_x s(x,y) = -\delta^4(x-y), \tag{B.1.47}$$

$$\mathcal{D}_x \bar{s}(x,y) = -\delta^4(x-y) + \sum \psi_{+,0}(x)\psi_{+,0}^\dagger(y). \tag{B.1.48}$$

Since $\overline{\mathcal{D}}\mathcal{D} = D^2$ and $D^2 G(x,y) = -\delta^4(x-y)$, we show that the relation

$$s(x,y) = \mathcal{D}_x G(x,y) \tag{B.1.49}$$

is satisfied from Eq. (B.1.47). Furthermore, multiplying both sides of Eq. (B.1.47) by $\int d^4x\, G^\dagger(x,z)$ from the left, we obtain

$$\begin{aligned}(\text{LHS}) &= \int d^4x\, G^\dagger(x,z)\overline{\mathcal{D}}_x s(x,y) \overset{(\text{B.1.49})}{=} \int d^4x\, G^\dagger(x,z)\overline{\mathcal{D}}_x\mathcal{D}_x G(x,y) \\ &= \int d^4x\, [\underbrace{\overline{\mathcal{D}}_x\mathcal{D}_x G(x,z)}_{=-\delta^4(x-z)}]^\dagger G(x,y) = -G(z,y),\end{aligned} \tag{B.1.50}$$

$$\begin{aligned}(\text{RHS}) &= -\int d^4x\, G^\dagger(x,z)\delta^4(x-y) \\ &= -G^\dagger(y,z).\end{aligned} \tag{B.1.51}$$

Therefore, we find $G^\dagger(x,y) = G(y,x)$. On the other hand, multiplying both sides of Eq. (B.1.48) by $\int d^4x\, s^\dagger(x,z)$ from the left, we obtain

$$\begin{aligned}(\text{LHS}) &= \int d^4x\, s^\dagger(x,z)\mathcal{D}_x\bar{s}(x,y) \overset{(\text{B.1.49})}{=} \int d^4x\, [\mathcal{D}_x G(x,z)]^\dagger \mathcal{D}_x\bar{s}(x,y) \\ &= -\int d^4x\, [\underbrace{\overline{\mathcal{D}}_x\mathcal{D}_x G(x,z)}_{=-\delta^4(x-z)}]^\dagger \bar{s}(x,y) = \bar{s}(z,y),\end{aligned} \tag{B.1.52}$$

$$\begin{aligned}(\text{RHS}) &= \int d^4x\, s^\dagger(x,z)\left(-\delta^4(x-y) + \sum \psi_{+,0}(x)\psi_{+,0}(y)\right) \\ &\overset{(\text{B.1.49})}{=} -s^\dagger(y,z) + \sum \int d^4x\, [\mathcal{D}_x G(x,z)]^\dagger \psi_{+,0}(x)\psi_{+,0}(y)\end{aligned}$$

Table B.1: The correspondence between instanton side and ADHM data side

Instanton side	ADHM data side
4d Dirac operator $\mathcal{D}$	0d Dirac operator Δ
Anti-self dual equation	ADHM equation
invertibility of $D^2\ (= D_\mu D_\mu)$	invertibility of $\Delta^\dagger\Delta$
4d Dirac equation $\bar{e}_\mu D_\mu \psi = 0$	0d Dirac equation $\Delta^\dagger V = 0$
normalization condition: $\int d^4x\, \psi^\dagger(x)\psi(x) = 1$	normalization condition: $V^\dagger V = 1$
completeness: $\psi(x)\psi^\dagger(x) - \mathcal{D}_x G(x,y)\overleftarrow{\mathcal{D}}_y = \delta^4(x-y)$	completeness: $VV^\dagger + \Delta f \Delta^\dagger = 1$
moduli space $\mathcal{M}^{\text{inst}}_{N,k}$	moduli space $\mathcal{M}^{\text{ADHM}}_{N,k}$

$$
\begin{aligned}
&= -s^\dagger(y,z) + \sum \int d^4x\, G^\dagger(x,z) \cdot \underbrace{\overline{\mathcal{D}}_x \psi_{+,0}(x)}_{=0} \psi_{+,0}(y) \\
&= -s^\dagger(y,z).
\end{aligned} \tag{B.1.53}
$$

Therefore, we find the relation

$$
\bar{s}(x,y) = -s^\dagger(y,x) \overset{\text{(B.1.49)}}{=} -(\mathcal{D}_x G(y,x))^\dagger = G(x,y)\overleftarrow{\mathcal{D}}_y. \tag{B.1.54}
$$

From the above results, if we substitute Eq. (B.1.54) into Eq. (B.1.48), we obtain

$$
\mathcal{D}_x G(x,y)\overleftarrow{\mathcal{D}}_y = -\delta^4(x-y) + \sum \psi_{+,0}(x)\psi^\dagger_{+,0}(y). \tag{B.1.55}
$$

Expressed using the matrix $\psi(x) \equiv (\psi_{+,1}, \cdots, \psi_{+,k})^\top$, it is none other than Eq. (B.1.38).

Moduli space The dimension of the moduli space of instantons with instanton number $-k$ is known to be

$$
\dim \mathcal{M}^{\text{inst}}_{N,k} = \begin{cases} 4Nk - N^2 - 1 & (N \leq 2k) \\ 4k^2 + 1 & (N > 2k) \end{cases} \tag{B.1.56}
$$

from the index theorem.

B.2 ADHM data side settings

In parallel with the settings on the instanton side, the settings on the ADHM data side are described in turn. The correspondence is summarized in Table B.1.

In this chapter, the settings on the ADHM data side are described for each of them.

0d Dirac operator First, we introduce the 0d Dirac operator $\Delta(x)$, which is represented by the matrix without derivatives, as

$$
\Delta(x) = C \cdot (e_\mu \otimes x^\mu) 1_k - D(x) = \begin{pmatrix} S_{[N]\times[2k]} \\ e_\mu \otimes (x^\mu 1_k - T^\mu_{[k]\times[k]}) \end{pmatrix}_{[N+2k]\times[2k]}, \tag{B.2.1}
$$

$$
\Delta^\dagger(x) = \begin{pmatrix} S^\dagger_{[2k]\times[N]} & \bar{e}_\mu \otimes (x^\mu 1_k - T^\mu_{[k]\times[k]}) \end{pmatrix}_{[2k]\times[N+2k]}, \tag{B.2.2}
$$

where the matrices C and $D(x)$ are represented by

$$C = \begin{pmatrix} 0_{[N]\times[2k]} \\ 1_{2k} \end{pmatrix}_{[N+2k]\times[2k]}, \tag{B.2.3}$$

$$D = \begin{pmatrix} -S_{[N]\times[2k]} \\ T_{[2k]\times[2k]} \end{pmatrix}_{[N+2k]\times[2k]} = \begin{pmatrix} -S_{[N]\times[2k]} \\ e_\mu \otimes T^\mu_{[k]\times[k]} \end{pmatrix} = \begin{pmatrix} -I^\dagger_{[N]\times[k]} & -J_{[N]\times[k]} \\ T^4 - iT^3 & -(T^2 + iT^1) \\ T^2 - iT^1 & T^4 + iT^3 \end{pmatrix}. \tag{B.2.4}$$

The matrix $D(x)$ is called the ADHM data. The matrices $I^\dagger$, J are a complex constant matrix and T^μ is a $k \times k$ constant Hermitian matrix. The matrix C can be taken to be a complex matrix in general, but here it is in what is called the standard form with gauge fixing.

ADHM equation On the instanton side, the requirement that $\overline{\mathcal{D}}\mathcal{D}$ be commutative with the Pauli matrix led to the anti-self dual equation. Correspondingly, we define the ADHM equation by requiring that $\Delta^\dagger\Delta$ be commutative with the Pauli matrix. To simplify the notation, we introduce the new letters

$$I^1 = \frac{1}{2}(J^\dagger I^\dagger + IJ), \quad I^2 = \frac{1}{2}(J^\dagger I^\dagger - IJ), \tag{B.2.5}$$

$$I^3 = \frac{i}{2}(II^\dagger - J^\dagger J), \quad I^4 = \frac{1}{2}(II^\dagger + J^\dagger J). \tag{B.2.6}$$

By using these notations, $\Delta^\dagger\Delta$ can be rewritten as

$$\begin{aligned}
\Delta^\dagger\Delta &= S^\dagger S + \bar{e}_\mu e_\nu \otimes (x^\mu - T^\mu)(x^\nu - T^\nu) \\
&= S^\dagger S + (\delta_{\mu\nu} + i\eta^{(+)}_{\mu\nu}) \otimes (x^\mu - T^\mu)(x^\nu - T^\nu) \\
&\quad (\because \bar{e}_\mu e_\nu = \delta_{\mu\nu} + i\eta^{(+)}_{\mu\nu}) \\
&= S^\dagger S + 1_2 \otimes (x^\mu - T^\mu)^2 + i\eta^{(+)}_{\mu\nu} \otimes T^\mu T^\nu \\
&= (-i\sigma_i \otimes I^i + 1_2 \otimes I^4) + 1_2 \otimes (x^\mu - T^\mu)^2 + i\sigma_i \otimes \eta^{(+)i}_{\mu\nu} T^\mu T^\nu \\
&= (-i\sigma_i \otimes I^i + 1_2 \otimes I^4) + 1_2 \otimes (x^\mu - T^\mu)^2 + i\sigma_i \otimes \left(\frac{1}{2}\epsilon_{ijk}[T^j, T^k] + [T^i, T^4]\right) \\
&\quad (\because \eta^{(+)i}_{\mu\nu} = \epsilon_{i\mu\nu4} + \delta_{i\mu}\delta_{\nu4} - \delta_{i\nu}\delta_{\mu4}) \\
&= 1_2 \otimes \left(I^4 + (x^\mu - T^\mu)^2\right) + i\sigma_i \otimes \left(-I^i + \frac{1}{2}\epsilon_{ijk}[T^j, T^k] + [T^i, T^4]\right).
\end{aligned} \tag{B.2.7}$$

Therefore, for the right-hand side of the above equation to exchange with $\Delta^\dagger\Delta$, the relations

$$\frac{1}{2}\epsilon_{ijk}[T^j, T^k] + [T^i, T^4] - I^i = 0 \quad (i, j, k = 1, 2, 3) \tag{B.2.8}$$

must hold. These equations are called the ADHM equations. If we write down each component independently, we obtain

$$[T^1, T^2] + [T^3, T^4] - \frac{i}{2}(II^\dagger - J^\dagger J) = 0, \tag{B.2.9}$$

$$[T^1, T^3] - [T^2, T^4] - \frac{1}{2}(IJ - J^\dagger I^\dagger) = 0, \tag{B.2.10}$$

$$[T^1, T^4] + [T^2, T^3] - \frac{1}{2}(IJ + J^\dagger I^\dagger) = 0. \tag{B.2.11}$$

In some literature, the ADHM equation in complex representation is used. In such cases, the coordinates are denoted by

$$x^\mu \otimes e_\mu = \begin{pmatrix} x^4 - ix^3 & -(x^2 + ix^1) \\ x^2 - ix^1 & x^4 + ix^3 \end{pmatrix} = \begin{pmatrix} \bar{z}_2 & -z_1 \\ \bar{z}_1 & z_2 \end{pmatrix} \tag{B.2.12}$$

and the ADHM data by

$$D = \begin{pmatrix} -I^\dagger & -J \\ T^4 - iT^3 & -(T^2 + iT^1) \\ T^2 - iT^1 & T^4 + iT^3 \end{pmatrix} = \begin{pmatrix} -I^\dagger_{[N]\times[k]} & -J_{[N]\times[k]} \\ B_2^\dagger & -B_1 \\ B_1^\dagger & B_2 \end{pmatrix}. \tag{B.2.13}$$

The ADHM equation is then written as

$$(\mu_{\mathrm{R}} :=) \quad [B_1, B_1^\dagger] + [B_2, B_2^\dagger] + II^\dagger - J^\dagger J = 0, \tag{B.2.14}$$

$$(\mu_{\mathrm{C}} :=) \quad [B_1, B_2] + IJ = 0. \tag{B.2.15}$$

The left-hand sides in complex representation are often written as $\mu_{\mathrm{R}}, \mu_{\mathrm{C}}$, respectively.

If the ADHM equation is satisfied, $\Delta^\dagger\Delta$ is written as

$$\Delta^\dagger\Delta = 1_2 \otimes \square_{[k]\times[k]}, \tag{B.2.16}$$

$$\square_{[k]\times[k]} = \left(\frac{1}{2}(II^\dagger + J^\dagger J) + (T^\mu)^2 - T^\mu x_\mu + x^2 1_k\right). \tag{B.2.17}$$

Invertibility of operator $\square_{[k]\times[k]}$ The requirement of the invertibility of $\square_{[k]\times[k]}$ for any x is denoted as

$$\square_{[k]\times[k]} f_{[k]\times[k]} = 1_k, \quad f_{[k]\times[k]} \sim O(r^{-2}) \quad (r \to \infty). \tag{B.2.18}$$

This requirement is the necessary and sufficient condition of the condition which Δ is full rank.

We show that the invertibility of $\square_{[k]\times[k]}$ is the necessary and sufficient condition of the condition which Δ is full rank. First, using the singular value decomposition, Δ is written as

$$\Delta_{[N+2k]\times[2k]} = U_{[N+2k]\times[N+2k]} \Sigma_{[N+2k]\times[2k]} V^\dagger_{[2k]\times[2k]}, \tag{B.2.19}$$

where U is a $N + 2k$ dimensional unitary matrix and V is a $2k$ dimensional unitary matrix, and Σ is the matrix composed by square root of positive eigenvalue of $\Delta^\dagger\Delta$ such as

$$\Sigma_{[N+2k]\times[2k]} = \left(\begin{array}{ccc|c} \sigma_1 & & & \\ & \ddots & & 0 \\ & & \sigma_r & \\ \hline & 0 & & 0 \end{array}\right) \quad (0 \leq r \leq 2k). \tag{B.2.20}$$

Now, if $\square_{[k]\times[k]}$ is invertible, then $\det \Delta^\dagger\Delta \neq 0$ holds. Therefore, all eigenvalues of $\Delta^\dagger\Delta$ are nonzero, and $r = 2k$, i.e., Δ must be full rank. Conversely, if Δ has full rank, then $r = 2k$ holds. Therefore, all eigenvalues of $\Delta^\dagger\Delta$ must be nonzero, and there exists an inverse matrix of $\Delta^\dagger\Delta$.

The transformation of ADHM datas Gauge transformations of the ADHM data are introduced as follows

$$I \to R^\dagger I Q^\dagger, \quad J \to QJR, \quad T^\mu \to R^\dagger T^\mu R, \tag{B.2.21}$$

where $Q \in SU(N)$ and $R \in U(k)$. Under this transformation, the 0d Dirac operator Δ, the constant matrix C and the ADHM data D are transformed as

$$\Delta \to \begin{pmatrix} Q_{[N]\times[N]} & & \\ & R^\dagger_{[k]\times[k]} & \\ & & R^\dagger_{[k]\times[k]} \end{pmatrix} \Delta_{[N]\times[k]} \begin{pmatrix} R_{[k]\times[k]} & \\ & R_{k]\times[k]} \end{pmatrix}, \tag{B.2.22}$$

$$C \to \begin{pmatrix} Q_{[N]\times[N]} & & \\ & R^\dagger_{[k]\times[k]} & \\ & & R^\dagger_{[k]\times[k]} \end{pmatrix} C_{[N]\times[k]} \begin{pmatrix} R_{[k]\times[k]} & \\ & R_{k]\times[k]} \end{pmatrix} = C, \tag{B.2.23}$$

$$D \to \begin{pmatrix} Q_{[N]\times[N]} & & \\ & R^\dagger_{[k]\times[k]} & \\ & & R^\dagger_{[k]\times[k]} \end{pmatrix} D_{[N]\times[k]} \begin{pmatrix} R_{[k]\times[k]} & \\ & R_{k]\times[k]} \end{pmatrix}. \tag{B.2.24}$$

Note that, the constant matrix C is invariant under the above gauge transformation. Furthermore, the ADHM equations are also invariant under the gauge transformation:

$$\begin{aligned} &\frac{1}{2}\epsilon_{ijk}[T^j, T^k] + [T^i, T^4] - T^i = 0 \\ &\to R^\dagger \left(\frac{1}{2}\epsilon_{ijk}[T^j, T^k] + [T^i, T^4] - T^i \right) R = 0. \end{aligned} \tag{B.2.25}$$

The gauge transformation of the ADHM data is more generally given as

$$\Delta \to Q_{[N+2k]\times[N+2k]} \Delta \begin{pmatrix} \mathcal{R}_{[k]\times[k]} & \\ & \mathcal{R}_{[k]\times[k]} \end{pmatrix} \quad (Q \in U(N+2k), \quad \mathcal{R} \in GL(k, \mathbb{C})). \tag{B.2.26}$$

In Eq. (B.2.3), using the degrees of freedom of this transformation, we convert the matrix C to the standard form. In the following, the matrix C will be discussed only in its the standard form, as in Eq. (B.2.3), but it can also be a general complex matrix by using a gauge transformations (B.2.26).

0d Dirac equation We define the 0d Dirac equation as

$$\Delta^\dagger_{[2k]\times[N+2k]} V_{[N+2k]\times[N]} = 0, \tag{B.2.27}$$

where V is a normalized Dirac zero mode. For the computational convenience, V is represented as

$$V_{[N+2k]\times[N]} = \begin{pmatrix} u_{[N]\times[N]} \\ v_{[2k]\times[N]} \end{pmatrix} = \begin{pmatrix} u_{[N]\times[N]} \\ v_{1[k]\times[N]} \\ v_{2[k]\times[N]} \end{pmatrix}, \tag{B.2.28}$$

$$v_{[2k]\times[N]} = C^\dagger_{[2k]\times[N+2k]} V_{[N+2k]\times[N]}. \tag{B.2.29}$$

Normalization condition The Dirac zero mode is satisfied the normalization condition

$$V^\dagger_{[N]\times[N+2k]} V_{[N+2k]\times[N]} = 1_N. \tag{B.2.30}$$

Completeness relation The completeness relation of the Dirac zero mode is given by

$$VV^\dagger + \Delta f \Delta^\dagger = 1_{N+2k}. \tag{B.2.31}$$

We show that this condition is a completeness relation. First, we introduce $W_{[N+2k]\times[N+2k]} = (\Delta\ V)$. Since Δ and V are invertible, W has also an inverse matrix W^{-1}. Then, using the invertibility of $\Delta^\dagger\Delta$ and the normalization condition, we can calculate

$$\begin{aligned}
1_{N+2k} &= W(W^\dagger W)^{-1}W^\dagger = W\begin{pmatrix}\Delta^\dagger\Delta & \Delta^\dagger V\\ V^\dagger\Delta & V^\dagger V\end{pmatrix}^{-1} W^\dagger\\
&= W\begin{pmatrix}\Delta^\dagger\Delta & 0\\ 0 & V^\dagger V\end{pmatrix}^{-1} W^\dagger \quad (\because \text{(B.2.27)} : \Delta^\dagger V = V^\dagger\Delta = 0)\\
&= W\begin{pmatrix}1_2\otimes f_{[k]\times[k]} & 0\\ 0 & 1_N\end{pmatrix}^{-1} W^\dagger\\
&\quad (\because \Delta^\dagger\Delta \text{ is invertible, noramalization condition})\\
&= VV^\dagger + \Delta f\Delta^\dagger.
\end{aligned} \tag{B.2.32}$$

This result is the completeness relation itself.

Moduli space The moduli space of the ADHM data $\mathcal{M}^{\mathrm{ADHM}}_{N,k}$ is defined as the set of equivalence classes that identify the transitions in the gauge transformation. If we specifically compute the dimension of this space, we find that it coincides with the dimension of instanton's moduli space:

$$\dim \mathcal{M}^{\mathrm{ADHM}}_{N,k} = \dim \mathcal{M}^{\mathrm{inst}}_{N,k} = \begin{cases}4Nk - N^2 + 1 & (N \le 2k),\\ 4k^2 + 1 & (N > 2k).\end{cases} \tag{B.2.33}$$

In the case of $N \le 2k$, we find

$$\begin{aligned}
\dim \mathcal{M}^{\mathrm{ADHM}}_{N,k} &= (\text{Complex DoF}) \times (\text{Number of } D \text{ components}) - (\text{Hermiticity of } T^\mu)\\
&\quad - (\text{ADHM eq.}) - (\text{DoF of } \mathcal{Q}) - (\text{DoF of } \mathcal{R})\\
&= 2 \times [2k(N+2k)] - 4k^2 - 3k^2 - (N^2 - 1) - k^2\\
&= 4Nk - N^2 + 1.
\end{aligned} \tag{B.2.34}$$

On the other hand, in the case of $N > 2k$, it is not the same as Eq. (B.2.34). We need to add an extra drawn $U(N-2k)$ degree of freedom (DoF). Thus, we conclude that the dimension of moduli space is given by

$$\begin{aligned}
\dim \mathcal{M}^{\mathrm{ADHM}}_{N,k} &= (4Nk - N^2 + 1) + (N-2k)^2\\
&= 4k^2 + 1 \quad (N > 2k).
\end{aligned} \tag{B.2.35}$$

In the following, we explain that an extra $SU(N-2k)$ degrees of freedom are drawn.

We focus on the submatrix $S_{[N+2k]\times[2k]}$ of the ADHM data

$$D = \begin{pmatrix}-S_{[N]\times[2k]}\\ e_\mu \otimes T^\mu_{[k]\times[k]}\end{pmatrix}. \tag{B.2.36}$$

Since we are considering the case $N > 2k$, each of the N columns of S can be represented by $2k\,(< N)$ linear combinations. Let $\vec{e}_i\,(i = 1, 2, \cdots, 2k)$ be bases. Then, S is written as

$$S_{[N]\times[2k]} = (\vec{s}_1, \vec{s}_2, \cdots, \vec{s}_{2k}), \quad \vec{s}_i = \sum_{j=1}^{2k} a_{ij}\vec{e}_j \quad (a_{ij} \in \mathbb{C}). \tag{B.2.37}$$

Under the gauge transformations, S is transformed as

$$S_{[N]\times[2k]} \to Q_{[N]\times[N]} S_{[N]\times[2k]} \begin{pmatrix} R_{[k]\times[k]} & \\ & R_{[k]\times[k]} \end{pmatrix}. \tag{B.2.38}$$

Here, for example, Q is decomposed as

$$Q_{[N]\times[N]} = Q'_{[N]\times[N]} \begin{pmatrix} \vec{e}^{\,\dagger}_{2k+1} \\ \vdots \\ \vec{e}^{\,\dagger}_N \\ * \\ \vdots \\ * \end{pmatrix} \quad (Q'_{[N]\times[N]} \in SU(N),\ * : \text{appropriate vectors}). \tag{B.2.39}$$

Then, since each column of S is represented by a linear combination of $\vec{e}_i\,(i = 1, 2, \cdots, 2k)$, we obtain

$$\begin{aligned} S_{[N]\times[2k]} &\to Q_{[N]\times[N]} S_{[N]\times[2k]} \begin{pmatrix} R_{[k]\times[k]} & \\ & R_{[k]\times[k]} \end{pmatrix} \\ &= Q'_{[N]\times[N]} \begin{pmatrix} \vec{e}^{\,\dagger}_{2k+1} \\ \vdots \\ \vec{e}^{\,\dagger}_N \\ * \\ \vdots \\ * \end{pmatrix} (\vec{s}_1, \vec{s}_2, \cdots, \vec{s}_{2k}) \begin{pmatrix} R_{[k]\times[k]} & \\ & R_{[k]\times[k]} \end{pmatrix} \\ &= Q'_{[N]\times[N]} \begin{pmatrix} \vec{0}^{\dagger} \\ \vdots \\ \vec{0}^{\dagger} \\ * \\ \vdots \\ * \end{pmatrix} \begin{pmatrix} R_{[k]\times[k]} & \\ & R_{[k]\times[k]} \end{pmatrix}. \end{aligned} \tag{B.2.40}$$

This means that the upper left $(N-2k)\times(N-2k)$ submatrix of Q' does not contribute to the gauge transformation. Thus, the intrinsic degrees of freedom of the gauge transformation with matrix Q is the $SU(N)$ degrees of freedom minus the $U(N-2K)$ degrees of freedom. We have now confirmed that the dimension of the moduli space for $N > 2k$ is given by Eq. (B.2.35).

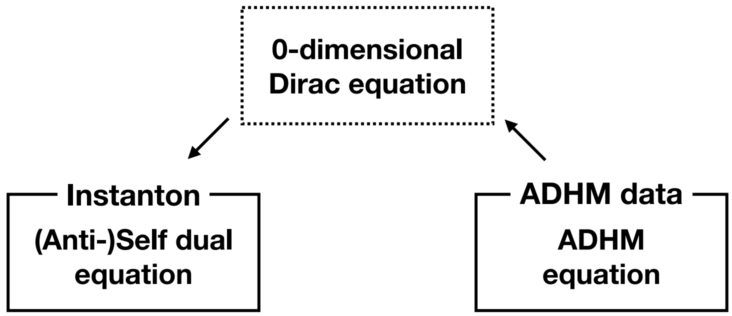

Figure B.2: Schematic diagram showing the relationship ADHM data → instanton.

B.3 ADHM data → Instanton

In this Section, we proof the relation ADHM data → instanton. In other words, we verify that $A_\mu\,(= V^\dagger \partial_\mu V)$ constructed by the ADHM construction method is the expected instanton solutions.

In the following, we use the notations

$$e_\mu \otimes 1_k \to e_\mu, \quad 1_2 \otimes f_{[k]\times[k]} \to f, \tag{B.3.1}$$

for simplicity.

The gauge field is constructed with the ADHM data as

$$(A_\mu)_{[N]\times[N]} = V^\dagger_{[N]\times[N+2k]} \partial_\mu V_{[N+2k]\times[N]}. \tag{B.3.2}$$

Form the normalization condition $V^\dagger V = 1_N$, A_μ is an anti-Hermitian matrix.

Useful formulas:

$$\begin{aligned}
\partial_\mu f &= -f(\partial_\mu f^{-1})f, && \text{(B.3.3)}\\
e_\mu \Delta^\dagger C e_\mu &= -2C^\dagger \Delta, && \text{(B.3.4)}\\
D_\mu V^\dagger &= V^\dagger \partial_\mu (V^\dagger V) = -V^\dagger C f e_\mu \Delta^\dagger, && \text{(B.3.5)}\\
D^2 V^\dagger &= -4V^\dagger C f C^\dagger, && \text{(B.3.6)}\\
D^2 u^\dagger &= 0, && \text{(B.3.7)}\\
\mathrm{Tr}\, F_{\mu\nu}F_{\mu\nu} &= -\partial^2\partial^2 \ln\det\, f_{[k]\times[k]}. && \text{(B.3.8)}
\end{aligned}$$

- Proof of Eq. (B.3.3): Since $f^{-1}f = 1$, we can calculate the following

$$\partial_\mu(f^{-1}f) = 0 \Longrightarrow (\partial_\mu f^{-1})f + f^{-1}\partial_\mu f = 0 \overset{\times f}{\Longrightarrow} f(\partial_\mu f^{-1})f + \partial_\mu f = 0. \tag{B.3.9}$$

- Proof of Eq. (B.3.4): From the equation

$$\begin{aligned}
\Delta^\dagger C &= \begin{pmatrix} S^\dagger_{[2k]\times[N]} & \bar{e}_\mu \otimes (x^\mu 1_k - T^\mu_{[k]\times[k]}) \end{pmatrix} \begin{pmatrix} 0_{[N]\times[2k]} \\ 1_{2k} \end{pmatrix}\\
&= \bar{e}_\mu \otimes (x^\mu 1_k - T^\mu_{[k]\times[k]}),
\end{aligned} \tag{B.3.10}$$

we can show

$$\begin{aligned}
e_\mu \Delta^\dagger C e_\mu &= (e_\mu \otimes 1_k)\left(\bar{e}_\nu \otimes (x^\nu 1_k - T^\nu_{[k]\times[k]})\right)(e_\mu \otimes 1_k) \\
&= e_\mu \bar{e}_\nu e_\mu \otimes (x^\nu 1_k - T^\nu_{[k]\times[k]}) \\
&= -2e_\nu \otimes (x^\nu 1_k - T^\nu_{[k]\times[k]}) \quad (\because\ e_\mu \bar{e}_\nu e_\mu = -2e_\nu) \\
&= -2C^\dagger \Delta.
\end{aligned} \tag{B.3.11}$$

- Proof of Eq. (B.3.5): By direct calculating, we can obtain

$$\begin{aligned}
D_\mu V^\dagger &= (\partial_\mu + A_\mu)V^\dagger = (\partial_\mu + V^\dagger \partial_\mu V)V^\dagger \quad (\because\ A_\mu = V^\dagger \partial_\mu V) \\
&= (V^\dagger V)\partial_\mu V^\dagger + V^\dagger(\partial_\mu V)V^\dagger \quad (\because\ V^\dagger V = 1) \\
&= V^\dagger \partial_\mu (VV^\dagger).
\end{aligned} \tag{B.3.12}$$

Furthermore, differentiating both sides of the completeness relation (B.2.31), we obtain

$$\begin{aligned}
\partial_\mu(VV^\dagger) &= -\partial_\mu(\Delta f \Delta^\dagger) \\
&= -(\partial_\mu \Delta) f \Delta^\dagger - \Delta \partial_\mu (f\Delta^\dagger) \\
&= -C \cdot e_\nu (\partial_\mu x_\nu) f \Delta^\dagger - \Delta \partial_\mu (f\Delta^\dagger) \\
&= -Ce_\mu f \Delta^\dagger - \Delta \partial_\mu (f \Delta^\dagger).
\end{aligned} \tag{B.3.13}$$

Therefore, multiplying $V^\dagger$ from the left of both sides and using the Dirac equation $V^\dagger \Delta = 0$,

$$V^\dagger \partial_\mu (VV^\dagger) = -V^\dagger C f e_\mu \Delta^\dagger \tag{B.3.14}$$

is obtained.

- Proof of Eq. (B.3.6): From Eq. (B.3.5), we can calculate as

$$\begin{aligned}
D^2 V^\dagger &= -D_\mu D_\mu V^\dagger \\
&\overset{(\because (\text{B.3.5}))}{=} -D_\mu (V^\dagger C f e_\mu \Delta^\dagger) \\
&= -\underbrace{(D_\mu V^\dagger)}_{-V^\dagger C f e_\mu \Delta^\dagger} C f e_\mu \Delta^\dagger - V^\dagger C e_\mu \underbrace{(\partial_\mu f)}_{-f\partial_\mu(\Delta^\dagger \Delta) f} \Delta^\dagger - V^\dagger C e_\mu f \underbrace{(\partial_\mu \Delta^\dagger)}_{\bar{e}_\mu C^\dagger} \\
&= V^\dagger C f e_\mu \Delta^\dagger \cdot C f e_\mu \Delta^\dagger + V^\dagger C e_\mu \cdot f \partial_\mu(\Delta^\dagger \Delta) f \cdot \Delta^\dagger - V^\dagger C e_\mu f \bar{e}_\mu C^\dagger \\
&= -V^\dagger[-Cf \underbrace{e_\mu \Delta^\dagger C e_\mu}_{-2C^\dagger \Delta} f \Delta^\dagger - Ce_\mu f \underbrace{(\partial_\mu \Delta^\dagger)}_{\bar{e}_\mu C^\dagger} \Delta f \Delta^\dagger - C e_\mu f \Delta^\dagger \underbrace{(\partial_\mu \Delta)}_{Ce_\mu} f\Delta^\dagger + C f e_\mu \bar{e}_\mu C^\dagger] \\
&= -V^\dagger[2CfC^\dagger \Delta f \Delta^\dagger - Cf \underbrace{e_\mu \bar{e}_\mu}_{=4} C^\dagger \Delta f \Delta^\dagger - Cf \underbrace{e_\mu \Delta^\dagger C e_\mu}_{-2C^\dagger \Delta} f\Delta^\dagger + Cf \underbrace{e_\mu \bar{e}_\mu}_{=4} C^\dagger] \\
&= -V^\dagger[\cancel{2CfC^\dagger \Delta f \Delta^\dagger} - \cancel{4CfC^\dagger \Delta f \Delta^\dagger} + \cancel{2CfC^\dagger \Delta f \Delta^\dagger} + 4CfC^\dagger] \\
&= -4V^\dagger C f C^\dagger.
\end{aligned} \tag{B.3.15}$$

- Proof of Eq. (B.3.7): Since the matrix u is defined by

$$V_{[N+2k]\times[N]} = \begin{pmatrix} u_{[N]\times[N]} \\ v_{[2k]\times[N]} \end{pmatrix}, \tag{B.3.16}$$

we can show

$$V^\dagger \begin{pmatrix} 1_N \\ 0_{[2k]\times[N]} \end{pmatrix} = \begin{pmatrix} u^\dagger_{[N]\times[N]} & v^\dagger_{[N]\times[2k]} \end{pmatrix} \begin{pmatrix} 1_N \\ 0_{[2k]\times[N]} \end{pmatrix} = u^\dagger_{[N]\times[N]}, \tag{B.3.17}$$

$$C^\dagger \begin{pmatrix} 1_N \\ 0_{[2k]\times[N]} \end{pmatrix} = (0_{[2k]\times[N]} \; 1_{2k}) \begin{pmatrix} 1_N \\ 0_{[2k]\times[N]} \end{pmatrix} = 0. \tag{B.3.18}$$

Therefore, multiplying $(1_N^\top \; 0^\top_{[N]\times[2k]})^\top$ from the right on both sides of Eq. (B.3.6), we obtain

$$\begin{aligned} D^2 V^\dagger \begin{pmatrix} 1_N \\ 0_{[2k]\times[N]} \end{pmatrix} &= -4V^\dagger C f C^\dagger \begin{pmatrix} 1_N \\ 0_{[2k]\times[N]} \end{pmatrix} \\ \to D^2 u^\dagger &= 0. \end{aligned} \tag{B.3.19}$$

- Proof of Eq. (B.3.8): See refs [62, 63].

We verify that the $A_\mu \, (= V^\dagger \partial_\mu V)$ constructed by the ADHM construction method is expected instanton solutions. In the following, we check in turn that the gauge group is $SU(N)$, that it is the pure gauge at infinity, that it satisfies the anti-self dual equation, that the instanton number is $-k$, and that D^2 is invertible.

B.3.1 Gauge group

Under the gauge transformations

$$V \to V g(x) \quad (g(x) \in U(N)), \tag{B.3.20}$$

A_μ is transformed as

$$\begin{aligned} A_\mu &\to A'_\mu \\ &= (Vg(x))^\dagger \, \partial_\mu \, (Vg(x)) \\ &= g^\dagger(x) V^\dagger (\partial_\mu V) g(x) + g^\dagger(x) \underbrace{V^\dagger V}_{=1} \partial_\mu g(x) \\ &= g^\dagger(x) V^\dagger (\partial_\mu V) g(x) + g^\dagger(x) \partial_\mu g(x) \\ &= g^\dagger(x) A_\mu g(x) + g^\dagger(x) \partial_\mu g(x). \end{aligned} \tag{B.3.21}$$

Therefore, A_μ is a gauge field of $U(N)$. Of course, the 0d Dirac equation and the normalization condition for V are invariant under the gauge transformations.

The A_μ is not traceless in general, but can be made into a traceless $SU(N)$ gauge field by using $U(1)$ degrees of freedom. This is confirmed in the following.

On the ADHM side, the field strength is given by

$$\begin{aligned}
F &= dA + A \wedge A \\
&= d(V^\dagger dV) + (V^\dagger dV) \wedge (V^\dagger dV) \\
&= dV^\dagger \wedge dV + (-dV^\dagger V) \wedge (V^\dagger dV) \\
&= dV^\dagger \underbrace{(1 - VV^\dagger)}_{\Delta f \Delta^\dagger\ (\because (\text{B.2.31}))} \wedge dV \\
&= dV^\dagger (\Delta f \Delta^\dagger) \wedge dV \\
&= V^\dagger \underbrace{(d\Delta)}_{Ce} f \wedge \underbrace{(d\Delta^\dagger)}_{\bar{e}C^\dagger} V \\
&\quad (\because 0 = d(V^\dagger \Delta) = (dV^\dagger)\Delta + V^\dagger(d\Delta)) \\
&= V^\dagger C e_\mu dx^\mu f \wedge dx^\nu \bar{e}_\nu C^\dagger V \\
&= V^\dagger C dx^\mu f \wedge dx^\nu \underbrace{e_\mu \bar{e}_\nu}_{\delta_{\mu\nu} + i\eta^{(-)}_{\mu\nu}} C^\dagger V \\
&= iV^\dagger C f \eta^{(-)}_{\mu\nu} C^\dagger V dx^\mu \wedge dx^\nu,
\end{aligned} \tag{B.3.22}$$

or expressed in terms of components

$$F_{\mu\nu} = 2iV^\dagger C f \eta^{(-)}_{\mu\nu} C^\dagger V = 2iV^\dagger C(\eta^{(-)}_{\mu\nu} \otimes f)C^\dagger V. \tag{B.3.23}$$

It can be verified that $\mathrm{Tr}\, F_{\mu\nu} = 0$ holds as follows.

$$\begin{aligned}
\mathrm{Tr}\, F_{\mu\nu} &= 2i\mathrm{Tr}\,[V^\dagger C(\eta^{(-)}_{\mu\nu} \otimes f)C^\dagger V] \\
&= 2i\mathrm{Tr}\,[(\eta^{(-)}_{\mu\nu} \otimes f)C^\dagger \underbrace{V \cdot V^\dagger}_{1 - \Delta f \Delta^\dagger} C] \quad (\because \mathrm{Tr}\, AB = \mathrm{Tr}\, BA) \\
&= 2i\mathrm{Tr}\,[(\eta^{(-)}_{\mu\nu} \otimes f)C^\dagger \{1 - \Delta(1_2 \otimes f)\Delta^\dagger\} C] \\
&= 2i\mathrm{Tr}\,[\eta^{(-)}_{\mu\nu} \otimes f - (\eta^{(-)}_{\mu\nu} \otimes f)C^\dagger \Delta(1_2 \otimes f)\Delta^\dagger C] \\
&= 2i\mathrm{Tr}\,[\eta^{(-)}_{\mu\nu} \otimes f - \eta^{(-)}_{\mu\nu} e_\lambda \bar{e}_\rho \otimes f(x^\lambda - T^\lambda) f(x^\rho - T^\rho)] \\
&\quad (\because C^\dagger \Delta = e_\mu \otimes (x^\mu - T^\mu),\ \Delta^\dagger C = \bar{e}_\mu \otimes (x^\mu - T^\mu)) \\
&= 2i\Big[\underbrace{\mathrm{Tr}\, \eta^{(-)}_{\mu\nu}}_{=0} \cdot \mathrm{Tr}\, f - \mathrm{Tr}\,(\eta^{(-)}_{\mu\nu} e_\lambda \bar{e}_\rho) \cdot \mathrm{Tr}\,\{f(x^\lambda - T^\lambda) f(x^\rho - T^\rho)\}\Big] \\
&\quad (\because \mathrm{Tr}\, A \otimes B = \mathrm{Tr}\, A \cdot \mathrm{Tr}\, B) \\
&= -2i\mathrm{Tr}\,(\eta^{(-)}_{\mu\nu} e_\lambda \bar{e}_\rho) \cdot \mathrm{Tr}\,[f(x^\lambda - T^\lambda) f(x^\rho - T^\rho)] \\
&= -i\mathrm{Tr}\,(\eta^{(-)}_{\mu\nu} e_\lambda \bar{e}_\rho) \cdot \mathrm{Tr}\,[f(x^\lambda - T^\lambda) f(x^\rho - T^\rho) + f(x^\rho - T^\rho) f(x^\lambda - T^\lambda)] \\
&\quad (\because \mathrm{Tr}\, AB = \mathrm{Tr}\, BA) \\
&= -\frac{i}{2}\mathrm{Tr}\,[\eta^{(-)}_{\mu\nu} \underbrace{(e_\lambda \bar{e}_\rho + e_\rho \bar{e}_\lambda)}_{2\delta_{\lambda\rho}}] \cdot \mathrm{Tr}\,[f(x^\lambda - T^\lambda) f(x^\rho - T^\rho) + f(x^\rho - T^\rho) f(x^\lambda - T^\lambda)] \\
&= -2i \underbrace{\mathrm{Tr}\, \eta^{(-)}_{\mu\nu}}_{=0} \cdot \mathrm{Tr}\,[f(x^\lambda - T^\lambda) f(x^\rho - T^\rho)] \\
&= 0
\end{aligned} \tag{B.3.24}$$

B.3.2 Pure gauge condition

We consider the zero mode

$$V = \begin{pmatrix} u_{[N]\times[N]} \\ v_{[2k]\times[N]} \end{pmatrix}. \tag{B.3.25}$$

Now considering the condition $\Delta^\dagger \sim x^\mu \bar{e}_\mu C^\dagger$ at $r \to \infty$, we can find

$$0 = \Delta^\dagger V \Longrightarrow 0 = x^\mu \bar{e}_\mu C^\dagger V = x^\mu \bar{e}_\mu v \tag{B.3.26}$$

i.e., $v \sim 0$ if $r \to \infty$.

Since V is satisfied the normalization condition

$$1_N = V^\dagger V = u^\dagger u + v^\dagger v, \tag{B.3.27}$$

we can obtain

$$u^\dagger u \sim 1_N \quad (r \to \infty). \tag{B.3.28}$$

This relation show that u is an element of $SU(N)$. Thus, we can conclude that A_μ is the pure gauge at infinity:

$$A_\mu = V^\dagger \partial_\mu V \sim u^\dagger \partial_\mu u \quad (r \to \infty). \tag{B.3.29}$$

B.3.3 Anti-self duality of $F_{\mu\nu}$

Since the 't Hooft's η symbol is antisymmetric with respect to the subscripts, the field strength

$$F_{\mu\nu} = 2iV^\dagger C f \eta^{(-)}_{\mu\nu} C^\dagger V \tag{B.3.30}$$

is also anti-self dual.

B.3.4 Instanton number

Since the relation

$$\mathrm{Tr}\, F_{\mu\nu} F_{\mu\nu} = -\mathrm{Tr}\, F_{\mu\nu} \widetilde{F}_{\mu\nu} \overset{(\because (\text{B.3.8}))}{=} -\partial^2 \partial^2 \ln \det\, f_{[k]\times[k]} \tag{B.3.31}$$

is satisfied, we can obtain

$$\begin{aligned} Q &= -\frac{1}{16\pi^2} \int dx^4\, \mathrm{Tr}\, F_{\mu\nu} \widetilde{F}_{\mu\nu} \\ &= -\frac{1}{16\pi^2} \int dx^4\, \partial^2 \partial^2 \ln \det f_{[k]\times[k]} \\ &= -\frac{1}{16\pi^2} \int dS_\mu\, \partial_\mu \partial^2 \ln \det f_{[k]\times[k]} \\ &= -\frac{1}{16\pi^2} \int dS_\mu\, \partial_\mu \partial^2 \mathrm{Tr}\, \ln f_{[k]\times[k]} \quad (\because \ln \det A = \mathrm{Tr}\, \ln A). \end{aligned} \tag{B.3.32}$$

Now, since $f \sim r^{-2} \cdot 1_k\,(r \to \infty)$ from Eq. (B.2.18), we can calculate as

$$
\begin{aligned}
Q &= -\frac{1}{16\pi^2}\int dS_\mu\, \partial_\mu \partial^2 \mathrm{Tr}\ \ln f_{[k]\times[k]} \\
&= -\frac{1}{16\pi^2}\int dS_\mu\, \partial_\mu \partial^2 \mathrm{Tr}\ \ln (r^{-2} 1_k) \\
&= \frac{k}{16\pi^2}\int dS_\mu\, \partial_\mu \partial^2 \mathrm{Tr}\ \ln r^2 \\
&= \frac{k}{16\pi^2}\int d\Omega\, r^3 \frac{x_\mu}{r} \partial_\mu \partial^2 \ln r^2 \\
&= -\frac{k}{16\pi^2}\int d\Omega\, r^3 \frac{x_\mu}{r} \frac{8 x_\mu}{r^4} \\
&\quad \left(\because\ \partial_\mu \partial^2 \ln r^2 = \partial_\mu \partial_\nu \left(\frac{2x_\nu}{r^2}\right) = \partial_\mu \left(\frac{2\delta_{\nu\nu}}{r^2} - 2x_\nu \frac{2x_\nu}{r^4}\right) = \partial_\mu \frac{4}{r^2} = -\frac{8x_\mu}{r^4}\right) \\
&= -\frac{k}{2\pi^2} \underbrace{\int d\Omega}_{=2\pi^2} \\
&= -k,
\end{aligned}
\tag{B.3.33}
$$

where we use the result that the surface area of a 3d sphere of radius 1 is $2\pi^2$. Therefore, it is confirmed that the instantons constructed by the ADHM construction method have instanton number $-k$.

B.3.5 Invertibility of D^2

The invertibility of D^2 is concluded from the existence of the Green's function

$$
G(x, y) = \frac{1}{4\pi^2} \frac{V_x^\dagger V_y}{(x-y)^2}. \tag{B.3.34}
$$

We show from the direct calculation that this function is the Green's function of D^2. Calculating D^2 acting on $G(x, y)$, we obtain

$$
\begin{aligned}
D_x^2 G(x,y) &= \frac{1}{4\pi^2} D_\mu^x \left(\partial_\mu^x \frac{1}{(x-y)^2} \cdot V_x^\dagger V_y + \frac{1}{(x-y)^2} \cdot D_\mu^x V_x^\dagger V_y\right) \\
&= \frac{1}{4\pi^2} \cdot \underbrace{\partial_x^2 \frac{1}{(x-y)^2}}_{-4\pi^2 \delta^4(x-y)} \cdot V_x^\dagger V_y + \frac{1}{4\pi^2} \cdot 2\partial_\mu^x \frac{1}{(x-y)^2} \cdot D_\mu^x V_x^\dagger V_y + \frac{1}{4\pi^2} \frac{1}{(x-y)^2} \cdot D_x^2 V_x^\dagger V_y \\
&= -\delta^4(x-y) V_x^\dagger V_y + \frac{1}{4\pi^2} \cdot 2\partial_\mu^x \frac{1}{(x-y)^2} \cdot D_\mu^x V_x^\dagger V_y + \frac{1}{4\pi^2} \frac{1}{(x-y)^2} \cdot D_x^2 V_x^\dagger V_y \\
&= -\delta^4(x-y) + \frac{1}{4\pi^2} \left[2\partial_\mu^x \frac{1}{(x-y)^2} \cdot D_\mu^x V_x^\dagger V_y + \frac{1}{(x-y)^2} \cdot D_x^2 V_x^\dagger V_y\right] \\
&\quad (\because\ \delta^4(x-y) V_x^\dagger V_y = \delta^4(x-y) V_x^\dagger V_x = \delta^4(x-y)).
\end{aligned}
\tag{B.3.35}
$$

Furthermore, the terms two and three of the above equation are calculated as

$$
\begin{aligned}
&2\partial^x_\mu \frac{1}{(x-y)^2} \cdot D^x_\mu V^\dagger_x V_y + \frac{1}{(x-y)^2} \cdot D^2_x V^\dagger_x V_y \\
&= \frac{4(x-y)_\mu}{(x-y)^4}(-V^\dagger_x C f_x e_\mu \Delta^\dagger_x)V_y + \frac{1}{(x-y)^2}(-4V^\dagger_x C f_x C^\dagger)V_y \quad (\because \text{(B.3.5)}, \text{(B.3.6)}) \\
&= -\frac{4}{(x-y)^2} V^\dagger_x C f_x \left[\frac{(x-y)_\mu}{(x-y)^2} e_\mu \Delta^\dagger_x + C^\dagger\right] V_y \\
&= -\frac{4}{(x-y)^2} V^\dagger_x C f_x \left[\frac{(x-y)_\mu}{(x-y)^2} e_\mu [\Delta^\dagger_y - \bar{e}_\nu (x-y)^\nu C^\dagger] + C^\dagger\right] V_y \\
&\quad (\because \Delta^\dagger_x = \bar{e}_\nu x^\nu C^\dagger - D^\dagger = \Delta^\dagger_y - \bar{e}_\nu (x-y)^\nu C^\dagger) \\
&= -\frac{4}{(x-y)^2} V^\dagger_x C f_x \left[-\frac{(x-y)_\mu}{(x-y)^2} e_\mu \bar{e}_\nu (x-y)^\nu + 1\right] C^\dagger V_y \quad (\because \Delta^\dagger_y V_y = 0) \\
&= -\frac{4}{(x-y)^2} V^\dagger_x C f_x \left[-\frac{(x-y)_\mu (x-y)_\nu}{(x-y)^2}(\delta_{\mu\nu} + i\eta^{(-)}_{\mu\nu}) + 1\right] C^\dagger V_y \quad (\because e_\mu \bar{e}_\nu = \delta_{\mu\nu} + i\eta^{(-)}_{\mu\nu}) \\
&= -\frac{4}{(x-y)^2} V^\dagger_x C f_x \left[-\frac{(x-y)_\mu (x-y)_\nu}{(x-y)^2}\delta_{\mu\nu} + 1\right] C^\dagger V_y \quad (\because \eta^{(-)}_{\mu\nu} = -\eta^{(-)}_{\nu\mu}) \\
&= -\frac{4}{(x-y)^2} V^\dagger_x C f_x \left[-1 + 1\right] C^\dagger V_y \\
&= 0.
\end{aligned}
\tag{B.3.36}
$$

Therefore, we can show $G(x,y)$ is the Green's function of D^2 since relation $D^2_x G(x,y) = -\delta^4(x-y)$ is satisfied.

B.4 Instanton → ADHM data

Here, we start with the $SU(N)$ instantons and construct the corresponding ADHM datas $S_{[N]\times[2k]}$, $T^\mu_{[k]\times[k]}$. Then we check in turn that

- S is a $N \times 2k$ matrix and T^μ is a $k \times k$ Hermitian matrix,
- S and T^μ satisfy the ADHM equation,
- $\Delta^\dagger \Delta$ is invertible.

B.4.1 Constructing the ADHM data from instanton

First, we construct ADHM datas form instanton. We consider

$$\widetilde{\psi}_{[N]\times[2k]} \equiv \psi^\top_{[N]\times[2k]} \cdot (e_2 \otimes 1_k), \tag{B.4.1}$$

where $\psi^\top$ means to take the transposition with respect to the spinor subscript. At infinity, the relation

$$\widetilde{\psi}_{[N]\times[2k]} \equiv \psi^\top_{[N]\times[2k]} \cdot (e_2 \otimes 1_k) \sim \frac{g_{[N]\times[N]} S_{[N]\times[2k]} (\bar{e}_\mu \otimes 1_k) x_\mu}{\pi r^4} + O(r^{-4}) \tag{B.4.2}$$

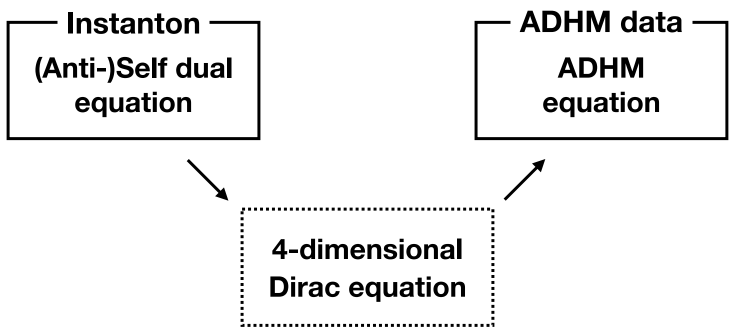

Figure B.3: Schematic diagram showing the relationship instanton → ADHM data.

is satisfied, where g is a $SU(N)$ matrix appearing in the gauge field at infinity, $A_\mu \sim g\partial_\mu g^{-1}$ $(r \to \infty)$. Since S is constructed as the above equation, we find that S is a $N \times 2k$ matrix. On the other hand, T_μ is constructed as

$$T_\mu = \int d^4x\, \psi^\dagger_{[k]\times[2N]} x_\mu \psi_{[2N]\times[k]}. \tag{B.4.3}$$

Therefore, T_μ is a $k \times k$ Hermitian matrix.

We consider the transformations

$$g \to gQ, \quad \psi \to \psi R \quad (Q \in SU(N),\, R \in U(k)). \tag{B.4.4}$$

Under these transformations,

$$\text{(4d Dirac eq.)} : \bar{e}_\mu D_\mu \psi = 0, \tag{B.4.5}$$

$$\text{(Normalization condition)} : \int dx^4\, \psi^\dagger \psi = 1_k, \tag{B.4.6}$$

$$\text{(Completeness relation)} : \psi(x)\psi^\dagger(x) - \mathcal{D}_x G(x,y) \overleftarrow{\mathcal{D}}_y = \delta^4(x-y), \tag{B.4.7}$$

are invariant. These transformations are nothing but the transformation of ADHM datas:

$$I \to R^\dagger I Q^\dagger, \quad J \to QJR, \quad T^\mu \to R^\dagger T^\mu R. \tag{B.4.8}$$

B.4.2 Satisfying the ADHM equation

Next, we show that the ADHM data constructed by the ADHM construction is satisfied the ADHM equation. Specifically, we show that the constructed S and T^μ satisfy

$$\mathrm{Tr}_2\,(\sigma^i T^\dagger T) = \mathrm{Tr}_2\,(\sigma^i S^\dagger S) \quad \left(\Longleftrightarrow \mathrm{Tr}_2\left(\sigma^i (S^\dagger S + T^\dagger T)\right) = 0\right). \tag{B.4.9}$$

First, by using the relation $\mathrm{Tr}\,(\sigma^i \bar{e}_\mu e_\nu) = 2i\eta^{i(+)}_{\mu\nu}$, we can rewritten as

$$\mathrm{Tr}_2\,(\sigma^i T^\dagger T) = \mathrm{Tr}_2\,(\sigma^i \bar{e}_\mu e_\nu) T^\mu T^\nu = 2i\eta^{i(+)} T^\mu T^\nu. \tag{B.4.10}$$

Now, $T^\mu T^\nu$ is given by

$$T^\mu T^\nu = \int d^4x\, x^\mu \psi^\dagger(x)\psi(x) \cdot \int d^4y\, y^\nu \psi^\dagger(y)\psi(y). \tag{B.4.11}$$

To perform the above integration, we first restrict the integral region to $|x| \le R_x$, $|y| \le R_y$ and finally take the limits $R_y \to \infty$ and $R_x \to \infty$ in that order:

$$\begin{aligned} T^\mu T^\nu &= \lim_{R_x\to\infty}\lim_{R_y\to\infty} \int_{|x|\le R_x} d^4x\, x^\mu \psi^\dagger(x)\psi(x) \cdot \int_{|y|\le R_y} d^4y\, y^\nu \psi^\dagger(y)\psi(y) \\ &= \lim_{R_x\to\infty}\lim_{R_y\to\infty} \int_{|x|\le R_x} d^4x \int_{|y|\le R_y} d^4y\, x^\mu y^\nu \cdot \psi^\dagger(x)\psi(x) \cdot \psi^\dagger(y)\psi(y). \end{aligned} \tag{B.4.12}$$

By using the completeness relation (B.4.7) and integration by parts, we can calculate as

$$\begin{aligned} T^\mu T^\nu &= \lim_{R_x\to\infty}\lim_{R_y\to\infty} \int_{|x|\le R_x} d^4x \int_{|y|\le R_y} d^4y\, x^\mu y^\nu \cdot \psi^\dagger(x) \left[\mathcal{D}_x G(x,y)\overleftarrow{\overline{\mathcal{D}}}_y + \delta^4(x-y)\right]\psi(y) \\ &= \lim_{R_x\to\infty}\lim_{R_y\to\infty} \int_{|x|\le R_x} d^4x\, (x^\mu x^\nu)\psi^\dagger(x)\psi(x) \\ &\quad + \lim_{R_x\to\infty}\lim_{R_y\to\infty} \int_{|x|\le R_x} d^4x \int_{|y|\le R_y} d^4y\, x^\mu y^\nu \cdot \psi^\dagger(x) \left[\mathcal{D}_x G(x,y)\overleftarrow{\overline{\mathcal{D}}}_y\right]\psi(y) \\ &\overset{\text{for } x}{=} \lim_{R_x\to\infty}\lim_{R_y\to\infty} \int_{|x|\le R_x} d^4x\, (x^\mu x^\nu)\psi^\dagger(x)\psi(x) \\ &\quad + \lim_{R_x\to\infty}\lim_{R_y\to\infty} \int_{|x|\le R_x} d^4x \int_{|y|\le R_y} d^4y\, \left(x^\mu \psi^\dagger(x)\right) \overleftarrow{\overline{\mathcal{D}}}_x G(x,y)\overleftarrow{\overline{\mathcal{D}}}_y (y^\nu\psi(y)) \\ &\quad + \lim_{R_x\to\infty}\lim_{R_y\to\infty} \int_{|x|\le R_x} dS_\lambda \int_{|y|\le R_y} d^4y\, x^\mu \psi^\dagger(x) \left[e_\lambda G(x,y)\overleftarrow{\overline{\mathcal{D}}}_y\right] y^\nu\psi(y). \end{aligned} \tag{B.4.13}$$

Then integrating by parts with respect to y, we can obtain

$$\begin{aligned} \text{(B.4.13)} &\overset{\text{for } y}{=} \lim_{R_x\to\infty}\lim_{R_y\to\infty} \int_{|x|\le R_x} d^4x\, (x^\mu x^\nu)\psi^\dagger(x)\psi(x) \\ &\quad + \lim_{R_x\to\infty}\lim_{R_y\to\infty} \int_{|x|\le R_x} d^4x \int_{|y|\le R_y} d^4y\, \left(x^\mu \psi^\dagger(x)\right) \overleftarrow{\overline{\mathcal{D}}}_x G(x,y)\overrightarrow{\overline{\mathcal{D}}}_y (y^\nu\psi(y)) \\ &\quad - \lim_{R_x\to\infty}\lim_{R_y\to\infty} \int_{|x|\le R_x} d^4x \int_{|y|\le R_y} dS_\lambda\, \left(x^\mu \psi^\dagger(x)\right) \overleftarrow{\overline{\mathcal{D}}}_x G(x,y)\bar{e}_\lambda (y^\nu\psi(y)) \\ &\quad + \lim_{R_x\to\infty}\lim_{R_y\to\infty} \int_{|x|\le R_x} dS_\lambda \int_{|y|\le R_y} d^4y\, x^\mu \psi^\dagger(x) \left[e_\lambda G(x,y)\overrightarrow{\overline{\mathcal{D}}}_y\right] (y^\nu\psi(y)) \\ &\quad - \lim_{R_x\to\infty}\lim_{R_y\to\infty} \int_{|x|\le R_x} dS_\lambda \int_{|y|\le R_y} dS_\rho\, x^\mu \psi^\dagger(x) \left[e_\lambda G(x,y)\bar{e}_\rho\right] y^\nu\psi(y). \end{aligned} \tag{B.4.14}$$

Finally, by using the relations $\overline{\mathcal{D}}\psi = 0$ and $\psi^\dagger \overleftarrow{\overline{\mathcal{D}}} = -(\overline{\mathcal{D}}\psi)^\dagger = 0$, we can obtain

$$\text{(B.4.14)} = \lim_{R_x\to\infty}\lim_{R_y\to\infty}\int_{|x|\leq R_x} d^4x\,(x^\mu x^\nu)\psi^\dagger(x)\psi(x) \tag{B.4.15}$$

$$-\lim_{R_x\to\infty}\lim_{R_y\to\infty}\int_{|x|\leq R_x} d^4x\int_{|y|\leq R_y} d^4y\,\psi^\dagger(x)e_\mu\bar{e}_\nu G(x,y)\psi(y) \tag{B.4.16}$$

$$+\lim_{R_x\to\infty}\lim_{R_y\to\infty}\int_{|x|\leq R_x} d^4x\int_{|y|\leq R_y} dS_\lambda\,\psi^\dagger(x)e_\mu\bar{e}_\lambda G(x,y)y^\nu\psi(y) \tag{B.4.17}$$

$$+\lim_{R_x\to\infty}\lim_{R_y\to\infty}\int_{|x|\leq R_x} dS_\lambda\int_{|y|\leq R_y} d^4y\,x^\mu\psi^\dagger(x)e_\lambda\bar{e}_\nu G(x,y)\psi(y) \tag{B.4.18}$$

$$+\lim_{R_x\to\infty}\lim_{R_y\to\infty}\int_{|x|\leq R_x} dS_\lambda\int_{|y|\leq R_y} dS_\rho\,x^\mu\psi^\dagger(x)e_\lambda\bar{e}_\rho G(x,y)y^\nu\psi(y). \tag{B.4.19}$$

Next, evaluate each of Eq. (B.4.15) to Eq. (B.4.19). The first term (B.4.15) eventually vanishes because it becomes zero when we take the contraction with $\eta^{i(+)}_{\mu\nu}$. From the relation

$$\begin{aligned}
\eta^{(i)(+)}_{\mu\nu}e_\mu\bar{e}_\nu &= \eta^{i(+)}_{\mu\nu}\cdot\frac{1}{2}(e_\mu\bar{e}_\nu - e_\nu\bar{e}_\mu)\\
&= \frac{1}{2}\left(\frac{i}{2}\epsilon_{\mu\nu\lambda\rho}\eta^{i(+)}_{\lambda\rho}\right)\eta^{(-)}_{\mu\nu}\\
&= -\frac{1}{2}\eta^{i(+)}_{\lambda\rho}\eta^{(-)}_{\lambda\rho}\quad\left(\because\ \frac{i}{2}\epsilon_{\mu\nu\lambda\rho}\eta^{i(+)}_{\lambda\rho} = \eta^{i(+)}_{\mu\nu}\right)\\
&\Longrightarrow \eta^{i(+)}_{\mu\nu}e_\mu\bar{e}_\nu = 0,
\end{aligned} \tag{B.4.20}$$

the second term (B.4.16) is also vanished by taking the contraction with $\eta^{i(+)}_{\mu\nu}$. By taking the limit $R_y \to \infty$, we obtain

$$dS_\rho \sim O(R_y^3),\quad G(x,y)\sim O(R_y^{-2}),\quad \psi(y)\sim O(R_y). \tag{B.4.21}$$

Consequently, we can calculate as

$$\lim_{R_y\to\infty}\int_{|y|\leq R_y} dS_\rho\,G(x,y)y^\nu\psi(y) \sim \lim_{R_y\to\infty} O(R_y^{-1}) = 0, \tag{B.4.22}$$

i.e., the terms (B.4.17), (B.4.19) are vanished. As a result, we only need to focus on the term (B.4.18) when we calculate Eq. (B.4.10).

Taking the transpose with respect to the spinor indices, we can write Eq. (B.4.12) as

$$\begin{aligned}
T^\mu T^\nu &= \lim_{R_x\to\infty}\lim_{R_y\to\infty}\int_{|x|\leq R_x} dS_\lambda\int_{|y|\leq R_y} d^4y\,x^\mu\psi^\dagger(x)(e_\lambda\otimes 1_N)G(x,y)(\bar{e}_\nu\otimes 1_N)\psi(y) + (\text{other terms})\\
&= \lim_{R_x\to\infty}\lim_{R_y\to\infty}\int_{|x|\leq R_x} dS_\lambda\int_{|y|\leq R_y} d^4y\,x^\mu\mathrm{Tr}_2\left[(e_\lambda^\top\otimes 1_k)(\psi^\top(x))^\dagger G(x,y)\psi^\top(y)(\bar{e}_\nu^\top\otimes 1_k)\right] + (\text{other terms})\\
&= \lim_{R_x\to\infty}\lim_{R_y\to\infty}\int_{|x|\leq R_x} dS_\lambda\int_{|y|\leq R_y} d^4y\,x^\mu\mathrm{Tr}_2\left[\bar{e}_2e_\lambda^\top e_2\cdot\bar{e}_2(\psi^\top(x))^\dagger G(x,y)\psi^\top(y)e_2\cdot e_2\bar{e}_\nu^\top e_2)\right] + (\text{other terms})\\
&\quad (\because\ e_2e_2 = \bar{e}_2\bar{e}_2 = -1_2,\ e_2\bar{e}_2 = \bar{e}_2e_2 = 1_2)\\
&= \lim_{R_x\to\infty}\lim_{R_y\to\infty}\int_{|x|\leq R_x} dS_\lambda\int_{|y|\leq R_y} d^4y\,x^\mu\mathrm{Tr}_2\left[\bar{e}_\lambda\widetilde{\psi}^\dagger(x)G(x,y)\widetilde{\psi}(y)e_\nu\right] + (\text{other terms})\\
&\quad (\because\ \sigma_2e_\lambda^\top\sigma_2 = \bar{e}_\lambda,\ \sigma_2\bar{e}_\nu^\top\sigma_2 = e_\nu,\ \psi^\top e_2 = \widetilde{\psi})
\end{aligned} \tag{B.4.23}$$

Here, we consider the solution $\widetilde{\chi}(x)$ that satisfies the relation

$$D^2\widetilde{\chi}(x) = -4\pi\widetilde{\psi}(x), \quad \widetilde{\chi}(x) \sim 0 \quad (r \to \infty). \tag{B.4.24}$$

Since this solution is given by

$$\widetilde{\chi}(x) = 4\pi \int d^4y\, G(x,y)\widetilde{\psi}(y), \tag{B.4.25}$$

its behavior at infinity is calculated as

$$\widetilde{\chi}(x) \sim -\frac{gS\,\bar{e}_\mu x_\mu}{r^2} \quad (r \to \infty). \tag{B.4.26}$$

Indeed, we can directly verify this result from the following.

$$\begin{aligned}
D_x^2\widetilde{\chi}(x) &= -4\pi\widetilde{\psi}(x) \\
&\overset{r\to\infty}{\sim} -(\partial_\mu^x + g\partial_\mu^x g^{-1})(\partial_\mu^x + g\partial_\mu^x g^{-1})\frac{gS\,\bar{e}_\nu x_\nu}{r^2} \quad (\because (\text{B.4.2})) \\
&= -gS\,\bar{e}_\nu \partial_x^2 \frac{x_\nu}{r^2} \\
&= -gS\,\bar{e}_\nu \partial_\mu^x \left(\frac{\delta_{\mu\nu}}{r^2} - 2\frac{x_\nu x_\mu}{r^4}\right) \\
&= -gS\,\bar{e}_\nu \left(-2\frac{\delta_{\mu\nu}x_\mu}{r^4} - 2\frac{\delta_{\nu\mu}x_\nu + x_\nu\delta_{\mu\mu}}{r^4} + 8\frac{x_\nu x_\mu x_\mu}{r^6}\right) \\
&- gS\,\bar{e}_\nu \left(-2\frac{x_\nu}{r^4} - 10\frac{x_\nu}{r^4} + 8\frac{x_\nu}{r^4}\right) \\
&= -4\pi \cdot \underbrace{\left(-\frac{gS\,\bar{e}_\nu x_\nu}{\pi r^4}\right)}_{\sim\widetilde{\psi}(x)}
\end{aligned} \tag{B.4.27}$$

From the above discussion and the fact that the y-integral is finite, Eq. (B.4.23) can be written by

$$\begin{aligned}
T^\mu T^\nu &= \lim_{R_x\to\infty}\lim_{R_y\to\infty}\int_{|x|\le R_x} dS_\lambda \int_{|y|\le R_y} d^4y\, x^\mu \mathrm{Tr}_2\left[\bar{e}_\lambda \widetilde{\psi}^\dagger(x)G(x,y)\widetilde{\psi}(y)e_\nu\right] + (\text{other terms}) \\
&= -\lim_{R_x\to\infty}\frac{1}{4\pi}\int_{|x|\le R_x} dS_\lambda\, x^\mu \mathrm{Tr}_2\left[\bar{e}_\lambda \widetilde{\psi}^\dagger(x)\widetilde{\chi}(x)e_\nu\right] + (\text{other terms}) \\
&= \lim_{R_x\to\infty}\frac{1}{4\pi}\int_{|x|\le R_x} dS_\lambda\, x^\mu \mathrm{Tr}_2\left[\bar{e}_\lambda \frac{e_\alpha x_\alpha S^\dagger g^\dagger}{\pi r^4}\cdot\frac{gS\,\bar{e}_\beta x_\beta}{r^2}e_\nu\right] + (\text{other terms}) \\
&= \frac{1}{4\pi}\lim_{R_x\to\infty}\int_{|x|\le R_x} d\Omega\,\frac{x_\alpha x_\mu}{r}r^3\cdot\frac{x_\alpha x_\beta}{\pi r^6}\mathrm{Tr}_2\left[\bar{e}_\lambda e_\alpha S^\dagger S\,\bar{e}_\beta e_\nu\right] + (\text{other terms}) \\
&= \frac{1}{4\pi}\lim_{R_x\to\infty}\int_{|x|\le R_x} d\Omega\,\frac{x_\mu x_\beta}{\pi r^2}\mathrm{Tr}_2\left[S^\dagger S\,\bar{e}_\beta e_\nu\right] + (\text{other terms}) \\
&\quad (\because \bar{e}_\lambda e_\alpha = \delta_{\lambda\alpha} + i\eta^{(+)}_{\lambda\alpha}) \\
&= \frac{1}{8}\mathrm{Tr}_2\left[S^\dagger S(\delta_{\mu\nu} + i\eta^{(+)}_{\mu\nu})\right] + (\text{other terms}).
\end{aligned} \tag{B.4.28}$$

Therefore, we conclude that Eq. (B.4.2) is given by

$$\begin{aligned}
\mathrm{Tr}_2\,(\sigma_i T^\dagger T) &= 2i\eta^{i(+)}_{\mu\nu} T^\mu T^\nu \\
&= 2i\eta^{i(+)}_{\mu\nu}\cdot\frac{1}{8}\mathrm{Tr}_2\left[S^\dagger S\,(\cancel{\delta_{\mu\nu}} + i\eta^{(+)}_{\mu\nu})\right] + \underbrace{2i\eta^{i(+)}_{\mu\nu}\cdot(\text{other terms})}_{=0} \\
&= -\frac{1}{4}\underbrace{\eta^{i(+)}_{\mu\nu}\eta^{j(+)}_{\mu\nu}}_{4\delta_{ij}}\mathrm{Tr}_2\left[S^\dagger S\sigma^j\right] \\
&= -\mathrm{Tr}_2\left[\sigma^i S^\dagger S\right].
\end{aligned} \tag{B.4.29}$$

This equation means that the ADHM equation is satisfied.

B.4.3 Invertibility of $\Delta^\dagger\Delta$

We confirm that $\Delta^\dagger\Delta$ is invertible. Since the ADHM equation is satisfied, we can obtain

$$\Delta^\dagger\Delta = 1_2\otimes\Box_{[k]\times[k]}, \tag{B.4.30}$$

$$\begin{aligned}
\Box_{[k]\times[k]} &= \frac{1}{2}\mathrm{Tr}(D^\dagger D) - 2T^\mu x_\mu + x^2 \\
&= \frac{1}{2}(II^\dagger + J^\dagger J) + T^\mu T^\mu - 2T^\mu x_\mu + x^2.
\end{aligned} \tag{B.4.31}$$

Since $\Box_{[k]\times[k]} \sim x^2$ $(r\to\infty)$ is satisfied, there exist the inverse matrix $f\sim 1/x^2$ in the region of $r\to\infty$ and $\Delta^\dagger\Delta$ is invertible.

On the other hand, it can be shown that in a finite region of r, $\Delta^\dagger\Delta$ must be invertible in order to be consistent with the assumption that $\psi^\dagger\psi$ is smooth over the entire region. In the following, we show it using proof by contradiction. Suppose that $\Delta^\dagger\Delta$ is not invertible in a finite region of r. Then, there exists at least the one vector ξ with zero eigenvalues such that

$$\Box_{[k]\times[k]}(y)\cdot\xi = 0, \quad \xi^\dagger\xi = 1. \tag{B.4.32}$$

From the relation

$$0 = \begin{pmatrix}\xi\\ \xi\end{pmatrix}^\dagger \Delta^\dagger\Delta\begin{pmatrix}\xi\\ \xi\end{pmatrix} = \left|\Delta\begin{pmatrix}\xi\\ \xi\end{pmatrix}\right|^2, \tag{B.4.33}$$

if $\Delta^\dagger\Delta$ is not invertible at the point $x^\mu = y^\mu$, we obtain

$$\Delta(y)\begin{pmatrix}\xi\\ \xi\end{pmatrix} = 0, \quad \Delta(y) = \begin{pmatrix} S_{[N]\times[2k]} \\ e_\mu\otimes(y^\mu 1_k - T^\mu_{[k]\times[k]})\end{pmatrix} = \begin{pmatrix} I^\dagger_{[N]\times k]} & J_{[N]\times[k]} \\ \multicolumn{2}{c}{e_\mu\otimes(y^\mu 1_k - T^\mu_{[k]\times[k]})}\end{pmatrix}, \tag{B.4.34}$$

$$\Longrightarrow I^\dagger\xi = 0, \quad J\xi = 0, \quad (y^\mu - T^\mu)\xi = 0. \tag{B.4.35}$$

In this case, by using the ADHM transformations with ξ

$$I\to R^\dagger I Q^\dagger, \quad J\to QJR, \quad T^\mu\to R^\dagger T^\mu R, \tag{B.4.36}$$

$$Q\in SU(N), \quad R = (\xi, *, \cdots, *)\in U(k), \tag{B.4.37}$$

the matrices $I^\dagger$, J and T^μ are transformed as

$$I^\dagger = \begin{pmatrix} 0 & & & \\ \vdots & * & \cdots & * \\ 0 & & & \end{pmatrix}, \quad J = \begin{pmatrix} 0 & & & \\ \vdots & * & \cdots & * \\ 0 & & & \end{pmatrix}, \quad T^\mu = \begin{pmatrix} y^\mu & 0 & \cdots & 0 \\ 0 & & & \\ \vdots & * & \cdots & * \\ 0 & & & \end{pmatrix}, \tag{B.4.38}$$

where $*$ is an appropriate k component vector. In the basis, $\square_{[k]\times[k]}$ is given by

$$\begin{aligned} \square_{[k]\times[k]} &= \frac{1}{2}(II^\dagger + J^\dagger J) + T^\mu T^\mu - T^\mu x_\mu + x^2 \\ &= \begin{pmatrix} y^2 - 2y^\mu x^\mu + x^2 & 0 & \cdots & 0 \\ 0 & & & \\ \vdots & * & \cdots & * \\ 0 & & & \end{pmatrix} \\ &= \begin{pmatrix} (x-y)^2 & 0 & \cdots & 0 \\ 0 & & & \\ \vdots & * & \cdots & * \\ 0 & & & \end{pmatrix}. \end{aligned} \tag{B.4.39}$$

Therefore, we conclude that the component $(1,1)$ of the inverse matrix f is given by $f_{1,1} = 1/(x-y)^2$ at a point away from $x^\mu = y^\mu$, on the other hand, $f_{1,1}$ is singular at the point $x^\mu = y^\mu$. Now, if formula

$$\psi^\dagger(x)\psi(x) = -\frac{1}{4\pi^2}\partial^2 f_{[k]\times[k]} \tag{B.4.40}$$

used in the Sec. B.3 holds[2], then if $f_{[k]\times[k]}$ is singular at $x^\mu = y^\mu$, then $\psi^\dagger\psi$ is also singular. Consequently, this means the contradiction with the assumption that $\psi^\dagger\psi$ is smooth over the entire region. In other words, we proof that ξ is not existed and $\Delta^\dagger\Delta$ is invertible.

B.5 Completeness: ADHM data → Instanton → ADHM data

In this Section, we proof the completeness as follows:

1. We compose a 0d Dirac zero-mode V to the 4d Dirac zero-mode $\psi(x)$ and check that $\psi(x)$ satisfies the Dirac equation,

2. check that $\psi(x)$ is normalized.

3. We confirm that the ADHM data constructed using ψ is equivalent to the original ADHM data.

[2] It is a claim that can be used only when the "uniqueness: instatnon → ADHM data → isntanton" is shown. Therefore, we assume that such uniqueness, which we will prove in the Sec. B.6, holds.

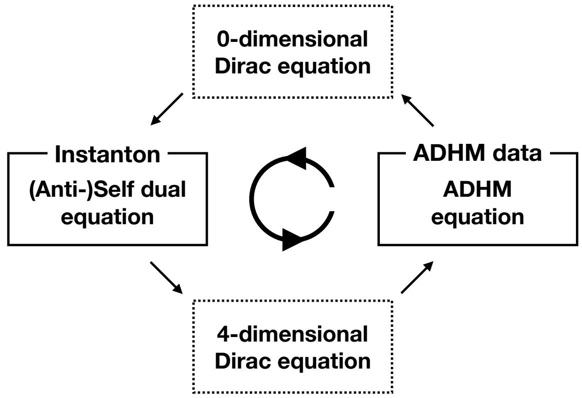

Figure B.4: Schematic diagram showing the completeness: ADHM data → instanton → ADHM data.

B.5.1 Constructing ψ from V

First, we construct a 4d Dirac zero mode with the ADHM datas. Using the solution V of the 0d Dirac equation and the ADHM data f, the 4d Dirac zero mode can be constructed as

$$\widetilde{\psi} = \frac{1}{\pi} V^\dagger C f. \tag{B.5.1}$$

We verify that this solution actually satisfies the 4d Dirac equation

$$\bar{e}_\mu D_\mu \widetilde{\psi}(x) = 0. \tag{B.5.2}$$

Taking the transpose with respect to the spinor in the Dirac equation, we obtain

$$0 = D_\mu \psi^\top \bar{e}_\mu^\top = -D_\mu \psi^\top e_2 \cdot e_2 \bar{e}_\mu^\top. \tag{B.5.3}$$

Furthermore, multiplying by e_2 from the right of both sides yields

$$0 = -D_\mu \underbrace{\psi^\top e_2}_{=\widetilde{\psi}} \cdot \underbrace{e_2 \bar{e}_\mu^\top e_2}_{=-e_\mu} = D_\mu \widetilde{\psi} e_\mu. \tag{B.5.4}$$

Thus, $D_\mu \widetilde{\psi} e_\mu = 0$ is equivalent to the original Dirac equation. By using the formulas (B.3.3)–(B.3.5), we can show that $\widetilde{\psi}$ constructed as Eq. (B.5.1) is satisfied the Dirac equation:

$$\begin{aligned}
D_\mu \widetilde{\psi} e_\mu &= \frac{1}{\pi} D_\mu (V^\dagger C f) e_\mu \\
&= \frac{1}{\pi} (D_\mu V^\dagger C f + V^\dagger C \partial_\mu f) e_\mu \\
&= \frac{1}{\pi} (-V^\dagger C f e_\mu \Delta^\dagger) C f e_\mu + \frac{1}{\pi} V^\dagger C [-f \partial_\mu (\Delta^\dagger \Delta) f] e_\mu \quad (\because \text{(B.3.5), (B.3.3)}) \\
&= -\frac{1}{\pi} V^\dagger C f \underbrace{e_\mu \Delta^\dagger C e_\mu}_{-2C^\dagger \Delta\, (\because \text{(B.3.4)})} f - \frac{1}{\pi} V^\dagger C f e_\mu \underbrace{(\partial_\mu \Delta^\dagger)}_{\bar{e}_\mu C^\dagger} \Delta f - \frac{1}{\pi} V^\dagger C f e_\mu \Delta^\dagger \underbrace{(\partial_\mu \Delta)}_{C e_\mu} f
\end{aligned}$$

$$
\begin{aligned}
&= \frac{2}{\pi}V^\dagger CfC^\dagger\Delta f - \frac{1}{\pi}V^\dagger Cf \underbrace{e_\mu\bar{e}_\mu}_{=4} C^\dagger\Delta f - \frac{1}{\pi}V^\dagger Cf \underbrace{e_\mu\Delta^\dagger Ce_\mu}_{-2C^\dagger\Delta\,(\because(\text{B.3.4}))} f \\
&= \frac{2}{\pi}V^\dagger CfC^\dagger\Delta f - \frac{4}{\pi}V^\dagger CfC^\dagger\Delta f + \frac{2}{\pi}V^\dagger CfC^\dagger\Delta f \\
&= 0.
\end{aligned}
\tag{B.5.5}
$$

From the above, it is shown that the 4d Dirac zero mode can be constructed as Eq. (B.5.1).

B.5.2 Satisfying the normalization condition

It is shown that the 4d Dirac zero mode constructed above is normalized. First, the relation

$$\psi^\dagger\psi = -\frac{1}{4\pi^2}\partial^2 f_{[k]\times[k]} \tag{B.5.6}$$

is satisfied. Indeed, we can calculate as follows:

$$
\begin{aligned}
(\text{RHS}) &= \psi^\dagger\psi \\
&= \mathrm{Tr}_2\left[(\psi^\dagger)^\top\psi^\top\right] \\
&= \mathrm{Tr}_2\left[\bar{e}_2(\psi^\dagger)^\top\psi^\top e_2\right] \\
&= \mathrm{Tr}_2\left[\widetilde{\psi}^\dagger\widetilde{\psi}\right] \\
&= \frac{1}{\pi^2}\mathrm{Tr}_2\left[fC^\dagger VV^\dagger Cf\right] \quad (\because \widetilde{\psi} = V^\dagger Cf/\pi),
\end{aligned}
\tag{B.5.7}
$$

$$
\begin{aligned}
(\text{LHS}) &= -\frac{1}{4\pi^2}\partial^2 f_{[k]\times[k]} \\
&= -\frac{1}{8\pi^2}\partial^2\mathrm{Tr}_2\left[1_2\otimes f_{[k]\times[k]}\right] \\
&= \frac{1}{4\pi^2}\mathrm{Tr}_2\left[f\bar{e}_\mu C^\dagger VV^\dagger Ce_\mu f\right] \\
&\quad (\because \partial^2 f = -2f\bar{e}_\mu C^\dagger VV^\dagger Ce_\mu f) \\
&= \frac{1}{4\pi^2}\mathrm{Tr}_2\,[\underbrace{e_\mu\bar{e}_\mu}_{=4} fC^\dagger VV^\dagger Cf] \\
&= \frac{1}{\pi^2}\mathrm{Tr}_2\left[fC^\dagger VV^\dagger Cf\right].
\end{aligned}
\tag{B.5.8}
$$

Furthermore, if $r \to \infty$, $f_{[k]\times[k]}$ behaves as

$$
\begin{aligned}
f_{[k]\times[k]} &= \Box^{-1}_{[k]\times[k]} \\
&= \left(\frac{1}{2}\mathrm{Tr}_2(D^\dagger D) - 2T^\mu x_\mu + x^2\right)^{-1} \\
&= \frac{1_k}{r^2}\left(1 - \frac{2T^\mu x_\mu}{r^2} + \frac{\mathrm{Tr}_2(D^\dagger D)}{2r^2}\right)^{-1} \\
&\sim \frac{1_k}{r^2} + \frac{2T^\mu x_\mu}{r^4} - \frac{\mathrm{Tr}_2(D^\dagger D)}{2r^4} + \frac{4(T^\mu x_\mu)}{r^6}
\end{aligned}
$$

$$-\frac{T^\mu x_\mu \mathrm{Tr}_2(D^\dagger D) + \mathrm{Tr}_2(D^\dagger D) T^\mu x_\mu}{r^6} + \frac{(\mathrm{Tr}_2(D^\dagger D))^2}{4r^6} + \cdots . \tag{B.5.9}$$

Therefore, we can proof that ψ is normalized such that

$$\begin{aligned}
\int d^4x\, \psi^\dagger(x)\psi(x) &\overset{(\text{B.5.1})}{=} -\frac{1}{4\pi^2}\int d^4x\, \partial^2 f_{[k]\times[k]} \\
&= -\frac{1}{4\pi^2}\lim_{r\to\infty}\int d\Omega\, \frac{x_\mu}{r} r^3 \partial_\mu f_{[k]\times[k]} \\
&\overset{(\text{B.5.9})}{=} -\frac{1}{4\pi^2}\lim_{r\to\infty}\int d\Omega\, \frac{x_\mu}{r} r^3 \partial_\mu \left(\frac{1_k}{r^2} + O(r^{-3})\right) \\
&= -\frac{1}{4\pi^2}\lim_{r\to\infty}\int d\Omega\, \frac{x_\mu}{r} r^3 \left(-\frac{2x_\mu}{r^4}\cdot 1_k + O(r^{-4})\right) \\
&= \frac{1}{2\pi^2}\cdot 1_k \underbrace{\int d\Omega}_{2\pi^2} \\
&= 1_k.
\end{aligned} \tag{B.5.10}$$

B.5.3 Equivalence to the original ADHM data

We show that the ADHM data constructed using ψ is regarded as the original ADHM data. T^μ is constructed as follows:

$$\begin{aligned}
T'^\mu &= \int d^4x\, \psi^\dagger x_\mu \psi \\
&= -\frac{1}{4\pi^2}\int d^4x\, x_\mu \partial^2 f \quad (\because\ \psi^\dagger\psi = -\partial^2 f_{[k]\times[k]}/4\pi^2) \\
&= -\frac{1}{4\pi^2}\int d^4x\, [\partial_\nu(x_\mu\partial_\nu f) - \delta_{\mu\nu}\partial_\nu f] \\
&= -\frac{1}{4\pi^2}\lim_{r\to\infty}\int d\Omega\, \frac{x_\nu}{r} r^3 [x_\mu \partial_\nu f - \delta_{\mu\nu} f] \\
&= -\frac{1}{4\pi^2}\lim_{r\to\infty}\int d\Omega\, \frac{x_\nu}{r} r^3 \left[x_\mu\partial_\nu\left(\frac{1}{r^2} + \frac{2T^\lambda x_\lambda}{r^4} + O(r^{-4})\right) - \delta_{\mu\nu}\left(\frac{1}{r^2} + \frac{2T^\lambda x_\lambda}{r^4} + O(r^{-4})\right)\right] \\
&\quad (\because\ (\text{B.5.9})) \\
&= -\frac{1}{4\pi^2}\lim_{r\to\infty}\int d\Omega\, \frac{x_\nu}{r} r^3 \left[x_\mu\left(-\frac{2x^\nu}{r^4} + \frac{2T^\nu}{r^4} - \frac{8T^\lambda x_\lambda x_\nu}{r^6}\right) - \delta_{\mu\nu}\left(\frac{1}{r^2} + \frac{2T^\lambda x_\lambda}{r^4}\right)\right] \\
&= -\frac{1}{4\pi^2}\lim_{r\to\infty}\int d\Omega\, \left[-2x_\mu + \frac{2T^\nu x_\nu x_\mu}{r^2} - \frac{8T^\lambda x_\lambda x_\mu}{r^2} - x_\mu - \frac{2T^\lambda x_\lambda x_\mu}{r^2}\right] \\
&= -\frac{1}{4\pi^2}\lim_{r\to\infty}\int d\Omega\, \left[-3x_\mu - \frac{8T^\lambda x_\lambda x_\mu}{r^2}\right].
\end{aligned} \tag{B.5.11}$$

Now, considering the transformability under the Lorentz transformation, we obtain

$$\int d\Omega\, x_\mu = 0, \qquad \int d\Omega\, x_\lambda x_\mu = \frac{\pi^2}{2}\delta_{\lambda\mu} r^2. \tag{B.5.12}$$

Thus, we can obtain

$$
\begin{aligned}
T'^{\mu} &= -\frac{1}{4\pi^2}\lim_{r\to\infty}\int d\Omega\left[-3x_\mu - \frac{8T^\lambda x_\lambda x_\mu}{r^2}\right] \\
&= -\frac{1}{4\pi^2}\lim_{r\to\infty}\left(-8T^\lambda\cdot\frac{\pi^2}{2}\delta_{\lambda\mu}\right) \\
&= T^\mu,
\end{aligned}
\tag{B.5.13}
$$

i.e., T'^{μ} is consistent with original the ADHM data T^μ.

Next, we show that S' is consistent with original S. Firs, if $r\to\infty$, $\widetilde{\psi}$ behaves as

$$
\widetilde{\psi}_{[N]\times[2k]} \sim \frac{g_{[N]\times[N]}S'_{[N]\times[2k]}(\bar{e}_\mu\otimes 1_k)x_\mu}{\pi r^4} + O(r^{-4}) \quad (r\to\infty)
\tag{B.5.14}
$$

from Eq. (B.4.2). On the other hand, the 4d Dirac zero mode $\widetilde{\psi}$ can be written as

$$
\widetilde{\psi} = \frac{1}{\pi}V^\dagger C f
\tag{B.5.15}
$$

from Eq. (B.5.1). Now, multiplying by $e_\nu x_\nu$ from the left of both sides of the 0d Dirac equation, $\Delta^\dagger V = 0$, yields

$$
\begin{aligned}
0 &= e_\nu x_\nu \Delta^\dagger V \\
&= (\underbrace{e_\nu\bar{e}_\mu x_\nu x_\mu}_{r^2}C^\dagger - e_\nu x_\nu D^\dagger)V \quad (\because \Delta^\dagger = \bar{e}_\mu x_\mu C^\dagger - D^\dagger) \\
&= (r^2 C^\dagger - e_\nu x_\nu D^\dagger)V.
\end{aligned}
\tag{B.5.16}
$$

For the above equation to hold, the equations

$$
C^\dagger V = \frac{e_\nu x_\nu D^\dagger}{r^2}V, \quad V^\dagger C = V^\dagger\frac{D\bar{e}_\nu x_\nu}{r^2} \quad (r\neq 0)
\tag{B.5.17}
$$

must satisfy. As a result, $\widetilde{\psi}$ is also written by

$$
\widetilde{\psi} = \frac{1}{\pi}V^\dagger C f = V^\dagger\frac{D\bar{e}_\nu x_\nu}{\pi r^2}f.
\tag{B.5.18}
$$

Now recalling that D is given as

$$
D_{[N+2k]\times[2k]} = \begin{pmatrix} -S_{[N]\times[2k]} \\ e_\mu\otimes T^\mu_{[k]\times[k]} \end{pmatrix}_{[N+2k]\times[2k]},
\tag{B.5.19}
$$

$v\sim 0$ and u behaves as an element of $SU(N)$ at infinity, we obtain

$$
\begin{aligned}
V^\dagger_{[N]\times[N+2k]} &= \begin{pmatrix} u^\dagger_{[N]\times[N]} & v^\dagger_{[N]\times[2k]} \end{pmatrix} \sim \begin{pmatrix} g_{[N]\times[N]} & 0_{[N]\times[2k]} \end{pmatrix} \quad (r\to\infty), \\
f_{[2k]\times[2k]} &\sim \frac{1_{2k}}{r^2},
\end{aligned}
\tag{B.5.20}
$$

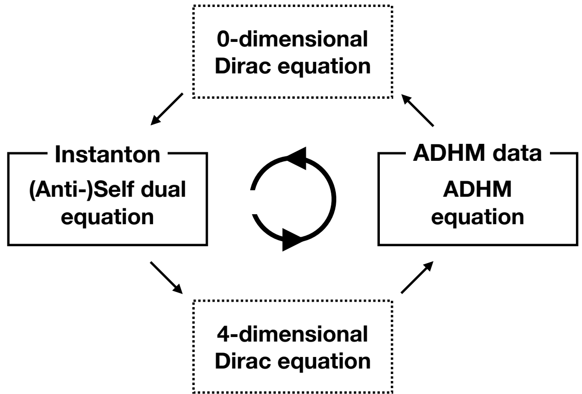

Figure B.5: Schematic diagram showing the uniqueness: instanton → ADHM data → instanton.

where $g \in SU(N)$. Therefore, Eq. (B.5.18) is written as

$$\begin{aligned}
\widetilde{\psi} &= V^{\dagger} \frac{D\bar{e}_{\nu} x_{\nu}}{\pi r^2} f \\
&\sim \left(g_{[N]\times[N]} \; 0_{[N]\times[2k]} \right) \begin{pmatrix} -S_{[N]\times[2k]} \\ e_{\mu} \otimes T^{\mu}_{[k]\times[k]} \end{pmatrix} \frac{\bar{e}_{\nu} x_{\nu}}{\pi r^4} \qquad (r \to \infty) \\
&= -\frac{gS\,\bar{e}_{\nu} x_{\nu}}{\pi r^4}.
\end{aligned} \tag{B.5.21}$$

The S is defined through Eq. (B.4.2), indicating that the above equation is also defined through a similar expression, i.e., we can show that S' is consistent with original S.

In the above, it was shown that the ADHM data starting from the ADHM data and reconstructed via instantons is consistent with the original one. This correspondence is shown as Fig. B.4 .

B.6 Uniqueness: Instaton → ADHM data → Instanton

In this Section, we proof the completeness as follows:

1. We compose the 4d Dirac zero-mode $\psi(x)$ to the 0d Dirac zero-mode V,
2. check that V satisfies the Dirac equation,
3. check that V is normalized.
4. We confirm that the instanton constructed using V is equivalent to the original instanton.

B.6.1 Constructing V from ψ

To construct the 0d Dirac zero mode from the 4d Dirac zero mode, we consider the solutions $\widetilde{\tau}$ and $\widetilde{\chi}$ that satisfy

$$D^2\widetilde{\tau} = 0, \quad \widetilde{\tau} \sim g(x) \quad (r \to \infty), \tag{B.6.1}$$

$$D^2\widetilde{\chi} = -4\pi\widetilde{\psi}, \quad \widetilde{\chi} \sim -\frac{gS\,\bar{e}_\mu x_\mu}{r^2} \quad (r \to \infty). \tag{B.6.2}$$

The $\widetilde{\chi}$ is the same solution introduced in Eqs. (B.4.24)–(B.4.26). Note that $\widetilde{\tau}$ consists of a sequence of N independent column vectors that are covariantly constant at infinity ($D_\mu\widetilde{\tau} \sim O(r^{-3})$ at $r \to \infty$) and are newly introduced to correspond to Eq. (B.3.25).

Here, we can construct the 0d Dirac zero mode as

$$V = \begin{pmatrix} \widetilde{\tau}^\dagger_{[N]\times[N]} \\ \widetilde{\chi}^\dagger_{[2k]\times[N]} \end{pmatrix}, \tag{B.6.3}$$

where each components are satisfied the equations

$$D_\mu\widetilde{\tau} = -\pi\widetilde{\psi}e_\mu S^\dagger, \tag{B.6.4}$$

$$D_\mu\widetilde{\chi} = -\pi\widetilde{\psi}e_\mu\bar{e}_\nu(x_\nu - T_\nu). \tag{B.6.5}$$

Indeed, these equations are confirmed as follows. From Eq. (B.6.1) and $D_\mu\widetilde{\psi}e_\mu = 0$, which is equivalent to the 4d Dirac equation, there exists a certain constant matrix $L_{[2k]\times[N]}$ satisfying

$$D_\mu\widetilde{\tau} = \widetilde{\psi}e_\mu L. \tag{B.6.6}$$

Then, multiplying by $\bar{e}_\mu\widetilde{\psi}^\dagger$ from the left of both sides, we obtain

$$\begin{aligned}
(\mathrm{RHS}) &= \int d^4x\,\bar{e}_\mu\widetilde{\psi}^\dagger\widetilde{\psi}e_\mu L \\
&= \int d^4x\,(\bar{e}_\mu)^\alpha_\beta\widetilde{\psi}^\dagger_\alpha\widetilde{\psi}^\beta(e_\mu)^\gamma_\beta L_\gamma \\
&= 2\int d^4x\,\delta^\gamma_\delta\delta^\alpha_\beta\widetilde{\psi}^\dagger_\alpha\widetilde{\psi}^\beta L_\gamma \quad (\because (\bar{e}_\mu)^\alpha_\beta(e_\mu)^\gamma_\beta = 2\delta^\gamma_\beta\delta^\alpha_\beta) \\
&= 2\int d^4x\,\widetilde{\psi}^\dagger_\alpha\widetilde{\psi}^\alpha L_\delta \\
&= 2\int d^4x\,\mathrm{Tr}_2\left[\widetilde{\psi}^\dagger\widetilde{\psi}\right]L_\delta \\
&= 2\cdot 1_k L_\delta \\
&\quad \left(\because \int d^4x\,\mathrm{Tr}_2\left[\widetilde{\psi}\widetilde{\psi}\right] = 1_k\right) \\
&= 2L,
\end{aligned} \tag{B.6.7}$$

$$
\begin{aligned}
(\text{LHS}) &= \int d^4x\, \bar{e}_\mu \widetilde{\psi}^\dagger D_\mu \widetilde{\tau} \\
&= \int dS_\mu\, \bar{e}_\mu \widetilde{\psi}^\dagger \widetilde{\tau} + \int d^4x\, \underbrace{\bar{e}_\mu \widetilde{\psi}^\dagger \overleftarrow{D}_\mu}_{=0} \widetilde{\tau} \quad (\because \overleftarrow{D}_\mu = -\overleftarrow{\partial}_\mu + A_\mu) \\
&= \int dS_\mu\, \bar{e}_\mu \widetilde{\psi}^\dagger \widetilde{\tau} \\
&\sim -\frac{1}{\pi} S^\dagger \int d\Omega\, \frac{x_\mu}{r} r^3 \cdot \bar{e}_\mu \frac{-x_\nu e_\nu S^\dagger g^\dagger}{\pi r^4} \cdot g \quad (\because (\text{B.4.2}), (\text{B.6.2})) \\
&= -\frac{1}{\pi} S^\dagger \int d\Omega \quad (\because x_\mu x_\nu \bar{e}_\mu e_\nu = r^2) \\
&= -2\pi S^\dagger \quad \left(\because \int d\Omega = 2\pi^2\right).
\end{aligned} \tag{B.6.8}
$$

Therefore, we can obtain $L = -\pi S^\dagger$ and conclude that the equation

$$
D_\mu \widetilde{\tau} = \widetilde{\psi} e_\mu L = -\pi \widetilde{\psi} e_\mu S^\dagger \tag{B.6.9}
$$

is satisfied. The second Eq. (B.6.5) is also confirmed. From Eq. (B.6.2), there exists a certain constant matrix $M_{[2k]\times[2k]}$ satisfying

$$
D_\mu \widetilde{\chi} + \pi \widetilde{\psi} e_\mu \bar{e}_\nu x_\nu = \widetilde{\psi} e_\mu M. \tag{B.6.10}
$$

Then, multiplying by $\bar{e}_\mu \widetilde{\psi}^\dagger$ from the left of both sides, we obtain

$$
(\text{RHS}) = 2M, \tag{B.6.11}
$$

$$
\begin{aligned}
(\text{LHS}) &= \int d^4x\, \bar{e}_\mu \widetilde{\psi}^\dagger (D_\mu \widetilde{\chi} + \pi \widetilde{\psi} e_\mu \bar{e}_\nu x_\nu) \\
&= \int dS_\mu\, \bar{e}_\mu \widetilde{\psi}^\dagger \widetilde{\chi} + \int d^4x\, \bar{e}_\mu \widetilde{\psi}^\dagger \overleftarrow{D}_\mu \widetilde{\chi} \\
&\quad + \pi \int d^4x\, \bar{e}_\mu \widetilde{\psi}^\dagger \widetilde{\psi} e_\mu x_\nu \quad (\because \overleftarrow{D}_\mu = \overleftarrow{\partial}_\mu + A_\mu) \\
&= \int dS_\mu\, \bar{e}_\mu \widetilde{\psi}^\dagger \widetilde{\chi} + 2\pi \bar{e}_\nu \underbrace{\int d^4x\, \psi^\dagger x_\nu \psi}_{T^\nu} \\
&\sim \int d\Omega\, \frac{x_\mu}{r} r^3 \cdot \bar{e}_\mu \frac{-x_\nu e_\nu S^\dagger g^\dagger}{\pi r^4} \cdot \frac{-gS\, \bar{e}_\lambda x_\lambda}{r^2} + 2\pi T^\dagger \\
&\quad (\because (\text{B.4.2}), (\text{B.6.2}), (\text{B.4.3})) \\
&= \underbrace{\int d\Omega\, x_\mu x_\nu x_\lambda \bar{e}_\mu e_\nu \frac{S^\dagger S}{\pi r^4} \bar{e}_\lambda}_{=O(r^{-1})\sim 0\ (r\to\infty)} + 2\pi T^\dagger \\
&= 2\pi T^\dagger.
\end{aligned} \tag{B.6.12}
$$

Thus, we obtain $M = \pi T^\dagger$ $(= \pi\bar{e}_\mu T^\mu)$ and conclude

$$\begin{aligned} D_\mu\widetilde{\chi} &= -\pi\widetilde{\psi}e_\mu\bar{e}_\nu x_\nu + \widetilde{\psi}e_\mu M \\ &= -\pi\widetilde{\psi}e_\mu\bar{e}_\nu x_\nu + \pi\widetilde{\psi}e_\mu\bar{e}_\nu T^\nu \\ &= \pi\widetilde{\psi}e_\mu\bar{e}_\nu(x_\nu - T_\nu). \end{aligned} \tag{B.6.13}$$

Eqs. (B.6.4) and (B.6.5) can be written in a single equation such that

$$D_\mu V^\dagger = -\pi\widetilde{\psi}e_\mu\Delta^\dagger \tag{B.6.14}$$

by using the 0d Dirac operator

$$\Delta^\dagger_{[2k]\times[N+2k]}(x) = \left(S^\dagger_{[2k]\times[N]}\ \bar{e}_\mu \otimes (x_\mu 1_k - T^\mu_{[k]\times[k]})\right). \tag{B.6.15}$$

B.6.2 Satisfying the 0d Dirac equation

We show that the constructed V satisfies the 0d Dirac equation. Introducing $\Theta = V^\dagger\Delta$ for convenience, we show from the direct computation that

$$\begin{aligned} D_\mu\Theta &= \underbrace{D_\mu V^\dagger}_{-\pi\widetilde{\psi}e_\mu\Delta^\dagger}\ \Delta \\ &= -\pi\widetilde{\psi}e_\mu\Delta^\dagger\Delta + V^\dagger C e_\mu, \end{aligned} \tag{B.6.16}$$

$$\begin{aligned} D^2\Theta &= -\pi\underbrace{D_\mu\widetilde{\psi}e_\mu}_{=0}\Delta^\dagger\Delta - \pi\widetilde{\psi}e_\mu\partial_\mu(\Delta^\dagger\Delta) + \underbrace{D_\mu V^\dagger}_{-\pi\widetilde{\psi}e_\mu\Delta^\dagger}\ Ce_\mu \\ &= -\pi\widetilde{\psi}e_\mu\partial_\mu(\Delta^\dagger\Delta) - 2\pi\widetilde{\psi}e_\mu\Delta^\dagger Ce_\mu \\ &= -\pi\widetilde{\psi}\underbrace{e_\mu\bar{e}_\mu}_{=4}C^\dagger\Delta - 2\pi\widetilde{\psi}\underbrace{e_\mu\Delta^\dagger Ce_\mu}_{-2C^\dagger\Delta\ (\because(\text{B.3.3}))} \\ &= -4\pi\widetilde{\psi}C^\dagger\Delta + 4\pi\widetilde{\psi}C^\dagger\Delta \\ &= 0. \end{aligned} \tag{B.6.17}$$

Furthermore, Θ behaves as

$$\begin{aligned} \Theta &= \widetilde{\tau}S + \widetilde{\chi}e_\mu(x-T)_\mu \\ &\sim gS - \frac{gS\,\bar{e}_\mu x_\mu}{r^2}e_\nu(x-T)_\nu \quad (r\to\infty) \\ &= \frac{gS\,\bar{e}_\mu x_\mu}{r^2}e_\nu T_\nu \\ &= O(r^{-1}) \end{aligned} \tag{B.6.18}$$

if $r \to \infty$.

For a function $\rho(x)$, the solution $\phi(x)$ of

$$D^2\phi(x) = \rho(x) \tag{B.6.19}$$

that goes to zero at infinity is given by

$$\phi(x) = \int d^4x\, G(x,y)\rho(y) \tag{B.6.20}$$

using the Green's function from the invertibility of D^2. Now, from Eq. (B.6.18), $\Theta\,(=\Delta^\dagger V)$ has the same property as $\phi(x)$, so it can be expressed as

$$\Theta = \int d^4x\, G(x,y)\rho(y). \tag{B.6.21}$$

In addition to, from Eq. (B.6.17) we show that it corresponds to the case where $\rho(x) = 0$. Therefore, we can conclude that

$$\Theta = 0. \tag{B.6.22}$$

This is nothing but the 0d Dirac equation.

B.6.3 Satisfying the normalization condition

We show that the constructed V satisfies the normalization condition. Introducing $\Xi = V^\dagger V$ for convenience, we show from the direct computation that

$$\begin{aligned} D_\mu \Xi &= \partial_\mu \Xi + [A_\mu, \Xi] \\ &= \partial_\mu (V^\dagger V) + A_\mu V^\dagger V - V^\dagger V A_\mu \\ &= (D_\mu V^\dagger) V + V^\dagger (D_\mu V^\dagger)^\dagger \\ &= -\pi \widetilde{\psi} e_\mu \underbrace{\Delta^\dagger V}_{=0} - \pi \underbrace{V^\dagger \Delta}_{=0} \bar{e}_\mu \widetilde{\psi}^\dagger \quad (\because D_\mu V^\dagger = -\pi \widetilde{\psi} e_\mu \Delta^\dagger) \\ &= 0. \end{aligned} \tag{B.6.23}$$

Since Ξ is an $N \times N$ Hermitian matrix, it can be expanded in terms of identity matrix and $SU(N)$ generators and multiplied as

$$\Xi(x) = \Xi^0(x) 1_N + \Xi^\alpha(x) T^\alpha, \tag{B.6.24}$$

where $\alpha = 1, 2, \cdots, N^2 - 1$ and Ξ^0, Ξ^α are real function. Then, multiplying by Ξ from the right of both sides of Eq. (B.6.23), we obtain

$$\begin{aligned} \mathrm{Tr}\,(\Xi \partial_\mu \Xi) &= \frac{1}{2} \partial_\mu \mathrm{Tr}\,\Xi^2 = 0 \\ &\Longrightarrow (\Xi^0)^2 + (\Xi^\alpha)^2 = \text{const.} \end{aligned} \tag{B.6.25}$$

$$\Longrightarrow \Xi^0, \Xi^\alpha = \text{const.}, \tag{B.6.26}$$

i.e., we find that Ξ is a constant matrix. Furthermore, examining the behavior of Ξ at infinity yields

$$\begin{aligned} \Xi &= (\widetilde{\tau}\, \widetilde{\chi}) \begin{pmatrix} \widetilde{\tau}^\dagger \\ \widetilde{\chi}^\dagger \end{pmatrix} \\ &= \widetilde{\tau}\widetilde{\tau}^\dagger + \widetilde{\chi}\widetilde{\chi}^\dagger \\ &\sim g g^\dagger + \underbrace{\frac{g S \bar{e}_\mu x_\mu}{r^2} \cdot \frac{x_\nu e_\nu S^\dagger g^\dagger}{r^2}}_{=O(r^{-2})} \\ &\sim 1_N. \end{aligned} \tag{B.6.27}$$

This means that the 0d Dirac zero mode V is normalized.

B.6.4 Equivalence to the original ADHM data

Finally, we confirm that the instantons composed using V is consistent with the original ones. This can be shown from direct calculations as follows:

$$
\begin{aligned}
A'_\mu &= V^\dagger \partial_\mu V \\
&= V^\dagger (\partial_\mu V - V A_\mu) + V^\dagger V A_\mu \\
&= V^\dagger (\underbrace{D_\mu V^\dagger}_{-\pi \widetilde{\psi} e_\mu \Delta^\dagger})^\dagger + A_\mu \quad (\because V^\dagger V = 1) \\
&= -\pi \underbrace{V^\dagger \Delta}_{=0} \bar{e}_\mu \widetilde{\psi}^\dagger + A_\mu \\
&= A_\mu .
\end{aligned}
\tag{B.6.28}
$$

In the above, it was shown that the instantons starting from the instanton and reconstructed via the ADHM data are consistent with the original one. This correspondence is shown as Fig. B.5.

Appendix C

Topological insulator and superconductor

Topological insulators are a type of insulator, which is also called band insulator, described by band theory. The name is derived from the fact that its state of electron is characterized by a topological number. A topology of the band insulator is described as follows. A whole set of Hamiltonians for an electron in the band insulator can be viewed as a space with a corresponding structure once the symmetry of the system is determined. For a point in this space, the Hamiltonian draws a closed curve or surface when parameters in the Hamiltonian are varied periodically, e.g., from $-p$ to p for the electron wavenumber k. A number of windings of this closed curve corresponds to the topological number for the band insulator. A closed-curved Hamiltonian with a non-zero topological number gives a topological insulator. This topological number does not change as long as the band gap does not close, even if the parameters of the system are continuously deformed.

An important feature of topological insulators is that there are always a number of bound states on their surfaces corresponding to the topological number. Surface bound states appear in the band gap as shown in Fig. C.1 and have an energy dispersion connecting the valence band and conduction band. Since the energy dispersion of surface states are nearly linear, the surface states can be approximately regarded as massless Dirac particles. In general, at the interface between two insulators with different topological numbers, a number of bound states corresponding to the difference in topological numbers will appear. Therefore, the surface state of the topological insulator is considered to be a state of electron bounded at the interface with the vacuum with topological number zero.

Topological superconductors are superconducting versions of topological insulators. In other word, topological superconductors (or topological superfluids) are superconductors (or superfluids) in which the quasiparticle excitation spectrum in the bulk has a full gap, but a gapless Andreev bound state is stable on the surface.

In this Appendix, we will present a theory that classifies topological insulators and superconductors based on symmetry. In Chap. 5, we have classified the boundary conditions of quantum graphs based on symmetries, and showed that the classification has some nontrivial correspondences with the Altlatnd–Zirnbauer classification. The purpose of this Appendix is to provide an understanding of well-known examples of the classification on the condensed matter physics side through some concrete examples.

We refer to A. Furusaki's review paper in Japanese[1] and review paper [64] as references.

[1]DOI: https://doi.org/10.1380/jsssj.32.209

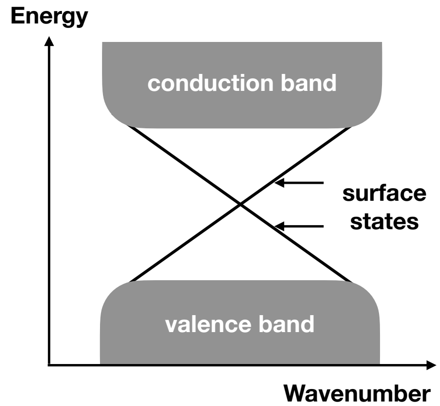

Figure C.1: Energy dispersion of a topological insulator.

C.1 Classification of Hamiltonians based on symmetry

C.1.1 Time-reversal symmetry

Time-reversal transformations T converts the Hamiltonian to $T^{-1}HT$, where T is an anti-unitary operator and generally satisfies $T^2 = +1$ or $T^2 = -1$. The former corresponds to an integer spin and the latter to a half-integer spin. For example, the Hamiltonian H for a spin zero particle has time-reversal symmetry if H can be written in a real symmetric matrix such that

$$T^{-1}HT = H^* = H \tag{C.1.1}$$

with respect to the appropriate basis. In this case, we can write $T = K$ using the complex conjugate operator K, and $T^2 = +1$. On the other hand, the time-reversal symmetry for particles of spin-1/2 (generally half-integer) is

$$i\sigma_y H^*(-i\sigma_y) = H, \tag{C.1.2}$$

using the Pauli matrix acting in the spin space. This means taking $T = -i\sigma_y K$ and satisfying $T^2 = -1$. The T reverses the spin direction but does not change the energy. Therefore, all energy eigenstates are doubly degenerate, and the two states are linked by the time reversal. This is called Kramers degeneracy. Note that, if the system is rotationally symmetric in the spin space, the Hamiltonian can be block diagonalized for each spin quantum number, even for particles with non-zero spin. Then, it can be discussed in the same way as for the spin zero particle.

From the above discussion, general systems can be classified into three cases depending on the transformation of the Hamiltonian concerning for to the time-reversal. (i) Invariant under time-reversal transformation satisfying $T^2 = +1$, (ii) invariant under time-reversal transformation satisfying $T^2 = -1$, and (iii) no time-reversal symmetry.

C.1.2 Particle-hole symmetry

Quasiparticle excitations in superconductors are quantum mechanical superpositions of electrons and holes, which is called Bogoliubov quasiparticles. Topological superconductors are topological insulators with respect to Bogoliubov quasiparticles. That is, there is a gap in the excitation spectrum of Bogoliubov quasiparticles in the bulk, and a bound state of quasiparticles, which is called the Andreev bound state, exists on the surface of the superconductor. The Hamiltonian of the BCS mean-field theory of superconductivity is generally given by

$$\begin{aligned} H_{\mathrm{BCS}} &= \sum_{\alpha,\beta}\left(h_{\alpha\beta}c_\alpha^\dagger c_\beta + \frac{1}{2}\Delta_{\alpha\beta}c_\alpha^\dagger c_\beta^\dagger + \frac{1}{2}\Delta_{\alpha\beta}^* c_\beta c_\alpha\right) \\ &= \frac{1}{2}\sum_{\alpha,\beta}\begin{pmatrix} c_\alpha^\dagger & c_\alpha \end{pmatrix}\begin{pmatrix} h_{\alpha\beta} & \Delta_{\alpha\beta} \\ -\Delta_{\alpha\beta}^* & -h_{\alpha\beta}^* \end{pmatrix}\begin{pmatrix} c_\beta \\ c_\beta^\dagger \end{pmatrix}, \end{aligned} \tag{C.1.3}$$

where h is a one-electron Hamiltonian and α, β are the lattice points and spin degrees of freedom collectively, and c_α ($c_\alpha^\dagger$) is a annihilation (creation) operator of the state α. Δ is the superconducting order parameter, which satisfies $\Delta_{\alpha\beta} = -\Delta_{\beta\alpha}$ due to the Fermi statistics of the electrons. Let

$$H = \begin{pmatrix} h & \Delta \\ -\Delta^* & -h^* \end{pmatrix} \tag{C.1.4}$$

denote the Bogoliubov–de Gennes (BdG) Hamiltonian matrix, then

$$\tau_x H^* \tau_x = \begin{pmatrix} 0 & 1 \\ 1 & 0 \end{pmatrix}\begin{pmatrix} h & \Delta \\ -\Delta^* & -h^* \end{pmatrix}\begin{pmatrix} 0 & 1 \\ 1 & 0 \end{pmatrix} = -H \tag{C.1.5}$$

holds. We assume that the BdG Hamiltonian has particle-hole symmetry when it is transformed as $C^{-1}HC = -H$ by the particle-hole transformation C, as in the above equation. The particle-hole transformation exchange electrons and holes and is an anti-unitary transformation, as is the time-reversal T. The transformation of Eq. (C.1.5) corresponds to taking $C = \tau_x K$, and $C^2 = +1$. Given an eigenstate ψ with eigenvalue E of H, the eigenstate with eigenvalue $-E$ is also immediately obtained as $C^{-1}\psi = \tau_x\psi^*$, so the eigenvalues of the BdG Hamiltonian appear in pairs $(+E, -E)$. On the other hand, an interesting possibility arises for the $E = 0$ eigenstates. That is, if ψ and $\tau_x\psi^*$ coincide, the eigenstates of $E = 0$ are the so-called Majorana states, in which the electron and the the hole as an antiparticle of the electron are identical.

If a Cooper pair is spin-singlet and rotationally symmetric in the spin space, the mean-field Hamiltonian is given by

$$\begin{aligned} \widetilde{H}_{\mathrm{BCS}} &= \sum_{a,b}\left[\widetilde{h}_{ab}\left(c_{a\uparrow}^\dagger c_{b\uparrow} + c_{a\downarrow}^\dagger c_{b\downarrow}\right) + \widetilde{\Delta}_{ab}c_{a\uparrow}^\dagger c_{b\downarrow}^\dagger + \widetilde{\Delta}_{ba}^* c_{b\downarrow}c_{a\uparrow}\right] \\ &= \sum_{a,b}\begin{pmatrix} c_{a\uparrow}^\dagger & c_{a\downarrow} \end{pmatrix}\begin{pmatrix} \widetilde{h}_{ab} & \widetilde{\Delta}_{ba} \\ \widetilde{\Delta}_{ba}^* & -\widetilde{h}_{ba} \end{pmatrix}\begin{pmatrix} c_{b\uparrow} \\ c_{b\downarrow}^\dagger \end{pmatrix}, \end{aligned} \tag{C.1.6}$$

where $\widetilde{\Delta}_{ab} = +\widetilde{\Delta}_{ba}$. Let

$$\widetilde{H} = \begin{pmatrix} \widetilde{h} & \widetilde{\Delta} \\ \widetilde{\Delta}^* & -\widetilde{h}^\top \end{pmatrix} \tag{C.1.7}$$

denote the BdG Hamiltonian matrix, then

$$(i\tau_y)\widetilde{H}^*(-i\tau_y) = \begin{pmatrix} 0 & 1 \\ -1 & 0 \end{pmatrix}\begin{pmatrix} \widetilde{h} & \widetilde{\Delta} \\ \widetilde{\Delta}^* & -\widetilde{h}^\top \end{pmatrix}\begin{pmatrix} 0 & -1 \\ 1 & 0 \end{pmatrix} = -\widetilde{H} \tag{C.1.8}$$

holds. In this case, the particle-hole symmetry is defined by $C = -i\tau_y K$ and satisfied $C^2 = -1$.

For the particle-hole transformation, general free-fermion systems can also be classified into three cases. The three cases are (i) a superconductor (superfluid) with $C^2 = +1$, (ii) a superconductor (superfluid) with $C^2 = -1$, and (iii) a normal conduction state with no particle-hole symmetry.

C.1.3 Chiral symmetry

We consider a time-reversal symmetric superconductor. Then, the composite transformation Γ of the time-reversal transformation T and the particle-hole transformation C acts the Hamiltonian as

$$\begin{aligned}(TC)^{-1}H(TC) &= C^{-1}T^{-1}HTC \\ &= C^{-1}HC \\ &= -H,\end{aligned} \tag{C.1.9}$$

so H is anti-commutate with Γ. Thus, a system is regarded as having chiral symmetry when there exists a unitary matrix that is anti-commuting with the Hamiltonian. A system with T and C symmetry necessarily has the chiral symmetry, but the its inversion does not necessarily hold. For example, we consider a tight-binding model on a lattice with an AB sublattice structure where only the jump integral between different sublattice points is nonzero. A Hamiltonian for this model is given by

$$H = \begin{pmatrix} 0 & h_{AB} \\ h_{AB}^\dagger & 0 \end{pmatrix}. \tag{C.1.10}$$

Since this H is satisfied

$$\begin{pmatrix} 1 & 0 \\ 0 & -1 \end{pmatrix}\begin{pmatrix} 0 & h_{AB} \\ h_{AB}^\dagger & 0 \end{pmatrix}\begin{pmatrix} 1 & 0 \\ 0 & -1 \end{pmatrix} = -\begin{pmatrix} 0 & h_{AB} \\ h_{AB}^\dagger & 0 \end{pmatrix}, \tag{C.1.11}$$

this system has the chiral symmetry regardless of whether T or C is symmetry. In general, the Hamiltonian of a chiral symmetric model takes a form where only the off-diagonal blocks have matrix elements, as in Eq. (C.1.10) on the appropriate basis. As in the case of the particle-hole transformation, the wave function $\Gamma\psi$ with eigenvalue $-E$ is immediately obtained from the wave function ψ with eigenvalue E of the chiral symmetric Hamiltonian.

C.1.4 Symmetry classes of Hamiltonians

To summarize the above discussion, the free-fermion Hamiltonians can be classified into ten different classes depending on the presence or absence of time-reversal symmetry, particle-hole symmetry, and chiral symmetry. Note that classes with both T and C symmetry have Γ at the same time, and conversely there are classes with no T and C symmetry but only Γ symmetry. The classification table is summarized in Table C.1.

The symbols A, AI, etc. in Table C.1 are borrowed from the symbols of symmetric spaces isomorphic to the set of time evolution operators $\exp(-iHt/\hbar)$ consisting of Hamiltonians belonging to each symmetry class, which are derived from those used by E. Cartan in his classification of symmetric spaces. The ± 1 in the T and C columns are the values of T^2 and C^2, on the other hand, 0 indicates no symmetry. 1 or 0 in the Γ column corresponds to the presence or absence of the chiral symmetry.

Table C.1: Symmetry classes of free fermion Hamiltonians. T, C, Γ stand for time-reversal, particle-hole, and chiral symmetries, respectively. The value of time-reversal operator T squared and that of particle-hole transformation C squared are shown in the third and fourth columns. In the fifth column "0" and "1" indicate the absence and presence of chiral symmetry, respectively.

	Symmetry classes	T	C	Γ
Wigner–	A (unitary)	0	0	0
Dyson	AI (orthogonal)	+1	0	0
classes	AII (symplectic)	−1	0	0
Chiral	AIII (chiral unitary)	0	0	1
symmetry	BDI (chiral orthogonal)	+1	+1	1
classes	CII (chiral symplectic)	−1	−1	1
	D	0	+1	0
BdG	C	0	−1	0
classes	DIII	−1	+1	1
	CI	+1	−1	1

The classification in Table C.1 was completed by A. Altland and M. R. Zirnbauer from their study of random matrix theory in mesoscopic superconductor systems. The random matrix theory was originally developed by E. Wigner and F. J. Dyson in the 1950s and 1960s in the study of highly excited states of atomic nuclei, and at that time, three symmetry classes were discussed (see the Wigner–Dyson class in Table C.1). Classes A, AI, and AII are symmetry classes called unitary, orthogonal, and symplectic classes, respectively, corresponding to what are known as universality classes in Anderson localization studies of irregular electron systems. The Hamiltonians of class A and AI are the sets of Hermitian and real symmetric matrices, respectively. In the early 1990s, in connection with the study of chiral symmetry breaking based on quantum chromodynamics, a random matrix theory for the Dirac Hamiltonian was conceived and three chiral symmetry classes were introduced. They are the three symmetry classes of the Wigner–Dyson classes with the chiral symmetry. Later, four classes of superconductivity were added to complete the classification. Since classes C and CI have $C^2 = -1$ particle-hole symmetry, the systems are symmetry in spin space, corresponding to a singlet pairing superconducting (superfluid) system. Classes D and DIII are other superconducting (superfluid) systems, such as triplet-pairing superconductors and superconductors without parity symmetry, some of which have been found in recent years. Furthermore, classes DIII and CI have time-reversal symmetry (the sign of T^2 is opposite), but class D and C are not symmetry in time-reversal.

C.1.5 Classification table for topological insulators and superconductors

For each symmetry class in Table C.1, we summarize whether the band insulator or full-gap superconductor is a topological insulator or superconductor (see Table C.2). The d means the dimension of the space. The symbols "0", "$\mathbb{Z}$", and "$\mathbb{Z}_2$" in the table indicate that the topological phase cannot be a topological phase, that there can be a topological phase characterized by an integer topological number, and that there can be a topological phase characterized by a 0 or 1 topological number, respectively. Examples of each non-trivial topological insulator or topological superconductor are

Table C.2: Classification of topological insulators and superconductors for 10 symmetry classes in spatial dimensions $d = 1, 2, 3$. The symbols $\mathbb{Z}$ ($\mathbb{Z}_2$) indicate that topological insulators or superconductors with an integer (binary) topological number can be present. The symbol 0 implies that no topological state can appear.

	Symmetry classes	$d = 1$	$d = 2$	$d = 3$
Wigner–Dyson classes	A (unitary)	0	$\mathbb{Z}$	0
	AI (orthogonal)	0	0	0
	AII (symplectic)	0	$\mathbb{Z}_2$	$\mathbb{Z}_2$
Chiral symmetry classes	AIII (chiral unitary)	$\mathbb{Z}$	0	$\mathbb{Z}$
	BDI (chiral orthogonal)	$\mathbb{Z}$	0	0
	CII (chiral symplectic)	$\mathbb{Z}$	0	$\mathbb{Z}_2$
BdG classes	D	$\mathbb{Z}_2$	$\mathbb{Z}$	0
	C	0	$\mathbb{Z}$	0
	DIII	$\mathbb{Z}_2$	$\mathbb{Z}_2$	$\mathbb{Z}$
	CI	0	0	$\mathbb{Z}$

presented in the next section.

Several derivation methods are known, the Anderson delocalization of boundary states [23], the K-theory method [24], and the Dirac Hamiltonian-based classification method [25].

C.2 Some examples of topological insulators

We briefly review some examples of topological insulators. In particular, examples belonging to the following classes are presented (see Tables C.1 and C.2).

1. The 1d class AIII: only chiral symmetry exists and the topological number is $\mathbb{Z}$.

2. The 2d class A: there is no symmetry and the topological number is $\mathbb{Z}$.

3. The 2d class AII: only time-reversal symmetry satisfying $T^2 = -1$ exists and the topological number is $\mathbb{Z}_2$.

C.2.1 The 1d class AIII polyacetylene

We consider a 1d tight-binding model for polyacetylene (see Fig. C.2). A Hamiltonian is given by

$$H = -t \sum_j \left[(1+\delta) c^\dagger_{j,\mathrm{A}} c_{j,\mathrm{B}} + (1-\delta) c^\dagger_{j+1,\mathrm{A}} c_{j,\mathrm{B}} + \mathrm{h.c.} \right], \tag{C.2.1}$$

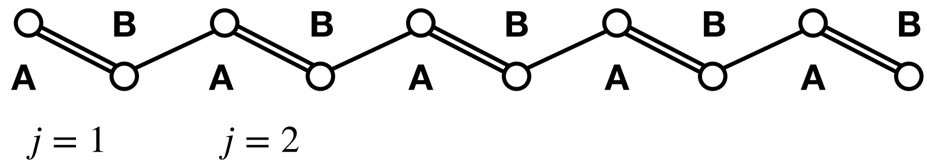

Figure C.2: Schematic picture of a 1d tight-binding model with bond dimerization.

where spin degrees of freedom are not considered for simplicity and j is the index of the unit cell. Fourier transformation for j yields the Hamiltonian matrix in wavenumber space (k-space) as

$$\begin{aligned} H(k) &= -t\begin{pmatrix} 0 & 1+\delta+(1-\delta)e^{-ik} \\ 1+\delta+(1-\delta)e^{ik} & 0 \end{pmatrix} \\ &= -t\boldsymbol{d}(k)\cdot\boldsymbol{\sigma} \\ &= -t\,|\boldsymbol{d}(k)|\begin{pmatrix} 0 & q \\ q^* & 0 \end{pmatrix}, \end{aligned} \tag{C.2.2}$$

where $\boldsymbol{d}(k)$ is defined by

$$\boldsymbol{d}(k) = \Big(1+\delta-(1-\delta)\cos k,\ (1-\delta)\sin k,\ 0\Big) \tag{C.2.3}$$

and q is a complex number whose absolute value is one. The Hamiltonian $H(k)$ is satisfied

$$H^*(-k) = H(k), \quad \sigma_z H(k)\sigma_z = -H(k). \tag{C.2.4}$$

Therefore this system belongs to the class BDI. Since an energy eigenvalue for this system is $\pm t|\boldsymbol{d}(k)|$, it is a band insulator if $|\delta| \leq 1$.

We consider a system with a finite length ($j = 1, 2, \cdots, n$). When $d = 1$, the Hamiltonian

$$H = -t\sum_{j=1}^{n}\Big[(1+\delta)c^\dagger_{j,\mathrm{A}}c_{j,\mathrm{B}} + (1-\delta)c^\dagger_{j+1,\mathrm{A}}c_{j,\mathrm{B}} + \mathrm{h.c.}\Big] \tag{C.2.5}$$

is isolated at each unit cell and is a trivial insulator occupying a bonding orbital per unit cell. On the other hand, when $d = -1$, the lattice points at both ends (A for $j = 1$ and B for $j = n$) are isolated and become zero-energy states. The other lattice points pair up with the A and B lattice points of the neighboring unit cell to form bonding orbitals. In other words, for $d = -1$, the bulk is an insulator and the edges are topological insulators with zero-energy states. Although we have considered two extreme cases, in fact, when $d > 0$, it is a trivial insulator, and when $d < 0$, it is a topological insulator.

The number that characterizes this topological insulator is

$$\Gamma = \frac{1}{2\pi i}\int_{-\pi}^{\pi} dk\,\frac{\partial_k q}{q} \tag{C.2.6}$$

that the complex number q circumnavigates the origin in the complex plane. In the case of $\delta < 0$, as the wavenumber varies from $-\pi$ to π, the trajectory of q circles around the origin $k = 0$.

Consequently, we obtain $\Gamma = 1$ and conclude that this system is regarded as nontrivial topological insulator. On the other hand, in the case of $\delta > 0$, the trajectory of q does not enclose the origin in the complex plane. Therefore, we obtain $\Gamma = 0$.

C.2.2 2d topological insulators

C.2.2.1 The 2d class A integer quantum Hall system

As an example of a 2d class A (unitary) topological insulator, we consider the Dirac Hamiltonian

$$\begin{aligned} H(\boldsymbol{k}) &= k_x\sigma_x + k_y\sigma_y + m\sigma_z \\ &= \begin{pmatrix} m & k_x - ik_y \\ k_x + ik_y & -m \end{pmatrix}. \end{aligned} \tag{C.2.7}$$

This Hamiltonian is known as a system that shows the integer quantum Hall effect. The system is transformed as

$$\sigma_y H^*(-\boldsymbol{k})\sigma_y = k_x\sigma_x + k_y\sigma_y - m\sigma_z \tag{C.2.8}$$

under time-reversal symmetry for a spin-1/2 particle. Therefore, it can be seen that the mass term breaks the symmetry. It is also an insulator with an energy eigenvalue of $\pm\lambda = \pm\sqrt{k_x^2 + k_y^2 + m^2}$ and a band gap of $2|m|$.

Let us calculate the topological number of this band insulator. The eigenvector for the eigenvalue $-\lambda$ of the Hamiltonian (C.2.7) is $|\boldsymbol{k}\rangle$. Berry's connections and Berry's curvatures are defined as

$$A_\mu(k_x, k_y) = -i\langle \boldsymbol{k}|\partial_\mu|\boldsymbol{k}\rangle \quad (\mu = k_x, k_y), \tag{C.2.9}$$

$$F(k_x, k_y) = \frac{\partial A_y}{\partial k_x} - \frac{\partial A_x}{\partial k_y}, \tag{C.2.10}$$

respectively. The topological number N is given by the magnetic flux penetrating the two-dimensional k-plane and is calculated as

$$N = \frac{1}{2\pi}\int dk_x dk_y\, F(k_x, k_y) = \frac{m}{2|m|}. \tag{C.2.11}$$

This means that the topological number N depends on the mass m. Furthermore, N is a topological invariant, which is called the Chern number. Since the Hall conductivity is given by $\sigma_{xy} = -e^2N/\hbar$ from the Kubo formula, it is equal to the topological number in units of quantum conductance $e^2/\hbar$. This phenomenon is exactly the integer Hall effect.

We consider the case where $m < 0$ in the region $x > 0$ and $m > 0$ in the region $x < 0$. In this case, there exists a state of motion in the $-y$ direction, bounded at the boundary ($x = 0$) where the sign of the mass m changes. Indeed, the Hamiltonian

$$H(x, y) = -i(\partial_x\sigma_x + \partial_y\sigma_y) + m(x)\sigma_z \tag{C.2.12}$$

in real space representation has eigenstate

$$|k_y\rangle = \zeta \exp\left[ik_y y - \frac{1}{c}\sigma_y \int_0^x dx'\, m(x')\right]\begin{pmatrix} \exp(i\pi/4) \\ \exp(-i\pi/4) \end{pmatrix} \tag{C.2.13}$$

localized near $x = 0$, where ζ is a normalization constant. This state is in the band gap with a linear energy dispersion $E = -k_y$ and corresponds to the edge state of the integer quantum Hall system moving in one direction. If the sign of the mass is reversed, the direction of motion is in the $+y$ direction. In other words, the sign of the mass plays a role like the direction of the magnetic field in the integer quantum Hall effect.

C.2.2.2 The 2d class AII quantum spin Hall system

In the 2d class AII, there exists a topological insulator with topological number $\mathbb{Z}_2$. It is known as the quantum spin Hall insulator. It consists of a combination of an up (↑) state and a down (↓) state that exhibit integer quantum Hall effects in a magnetic field. Individually, they break the time-reversal symmetry, but by combining the two state, the whole system has time-reversal symmetry. In this case, there are edge states of up-spin electrons and down-spin electrons moving in opposite directions along the edge of the system, which are called helical edge states. These states are connected each other under the time-reversal transformation. In particular, it is known that for k points in the Brillouin zone invariant under time reversal such as $k = (0, 0)$, $(\pi, 0)$, the Kramers degeneracy is stable under arbitrary perturbations without evaporating the degeneracy as long as the time-reversal symmetry is preserved. Therefore, the helical edge states are stable even when spin-orbit interactions are applied to flip the spin direction, and a pair of Kramers degenerate helical edge states always remain when there are an odd number of helical edge states. This fact implies that quantum spin hall system has $\mathbb{Z}_2$ topological number. Although we have presented a 2d example here, insulators with $\mathbb{Z}_2$ topological numbers exist in 3d as well. In that case, an odd number of massless Dirac particles appear as bound states on the 2d surface.

C.3 Some examples of topological superconductor

We briefly review some examples of topological superconductors. In particular, examples belonging to the following classes are presented (see Tables C.1 and C.2).

1. The 1d class D: only particle-hole symmetry satisfying $C^2 = +1$ exists and the topological number is $\mathbb{Z}_2$.

2. The 2d class D: different dimensions, but same as above.

3. The 3d class DIII: there are three symmetries, time-reversal symmetry satisfying $T^2 = -1$, particle-hole symmetry satisfying $C^2 = +1$, and chiral symmetry exists, and the topological number is $\mathbb{Z}$.

C.3.1 The 1d class D p-wave superconductor

We consider a 1d p-wave superconductor. A Hamiltonian is given by

$$
\begin{aligned}
H &= \sum_j \left[-t(c_j^\dagger c_{j+1} + c_{j+1}^\dagger c_j) - \mu c_j^\dagger c_j + \Delta c_j^\dagger c_{j+1}^\dagger + \Delta^* c_{j+1} c_j \right] \\
&= \int_{-\pi}^{\pi} dk \begin{pmatrix} a_k^\dagger & a_{-k} \end{pmatrix} \begin{pmatrix} -t\cos k - (\mu/2) & i\Delta \sin k \\ -i\Delta^* \sin k & t\cos k + (\mu/2) \end{pmatrix} \begin{pmatrix} a_k \\ a_{-k}^\dagger \end{pmatrix},
\end{aligned}
\tag{C.3.1}
$$

where a_k is Fourier transform of the fermion annihilation operator c_j at lattice point j. We denote $H(k)$ for the 2×2 matrix of the BdG Hamiltonian in Eq. (C.3.1). Since then $H(k)$ is satisfied

$$\tau_x H^*(-k)\tau_x = -H(k), \tag{C.3.2}$$

this model has particle-hole symmetry satisfying $C^2 = +1$. Consequently, this model belongs to the class D. The energy eigenvalue of the BdG quasiparticle is

$$E(k) = \pm\sqrt{(t\cos k + \mu/2)^2 + |\Delta|^2 \sin^2 k}, \tag{C.3.3}$$

and the gap is open unless $\mu = 2t$.

Let the operators $\gamma_{j,1}$ and $\gamma_{j,2}$ of the two Majorana particles be defined as

$$\gamma_{j,1} = e^{-i\theta/2}c_j + e^{i\theta/2}c_j^\dagger, \quad \gamma_{j,2} = -ie^{-i\theta/2}c_j + ie^{i\theta/2}c_j^\dagger \tag{C.3.4}$$

with the fermion creation and annihilation operators $c_j^\dagger$ and c_j, where θ is is the phase of the superconducting order parameter Δ. From the definition, the Majorana operators are satisfied $\gamma^\dagger = \gamma$ and

$$\{\gamma_{j,a}, \gamma_{i,b}\} = 2\delta_{j,i}\delta_{a,b}. \tag{C.3.5}$$

By using these facts, BdG Hamiltonian is written as

$$H = \frac{i}{2}\sum_j \left[-\mu\gamma_{j,1}\gamma_{j,2} - (|\Delta| + t)\gamma_{j,1}\gamma_{j+1,2} - (|\Delta| - t)\gamma_{j,2}\gamma_{j+1,1}\right]. \tag{C.3.6}$$

For a system of finite length ($j = 1, 2, \cdots, n$) with ends, we consider the following two extreme cases. (a) When $\Delta = t = 0$, the ground state of Eq. (C.3.1) is the $c_j^\dagger c_j = 1$ state and a topologically trivial insulator with an excitation gap $\mu\,(> 0)$. (b) If $t = -|\Delta| < 0$ and $\mu = 0$, $\gamma_{1,1}$ and $\gamma_{n,2}$ are isolated and a zero-energy Majorana state appears localized at their edge lattice points. This is a unique phenomenon for topological superconductors. In general, not only in extreme cases, a p-wave superconductor in Eq. (C.3.1) is a topological superconductor if the chemical potential μ is in the superconducting state in the band when normal conduction, i.e., $2|t| > |\mu|$ and $|\Delta| > 0$.

C.3.2 The 2d class D chiral p-wave superconductor

A typical example of a 2d topological superconductor is a chiral p-wave superconducting state in which the Cooper pair has $p_x + ip_y$ symmetry. Note that, chiral here means that all Cooper pairs rotate in the same direction with orbital angular momentum 1, which has nothing to do with the chiral symmetry. Neglecting spin degrees of freedom for simplicity, the BdG Hamiltonian in continuous space is given by

$$H(k) = \begin{pmatrix} k^2/2m - \mu & |\Delta|/k_F \cdot (k_x - ik_y) \\ |\Delta|/k_F \cdot (k_x + ik_y) & -k^2/2m + \mu \end{pmatrix}. \tag{C.3.7}$$

Since the Cooper pair is turning in one direction with orbital angular momentum 1, the time-reversal symmetry is spontaneously broken. Therefore, this model belongs to the class D. Since this system is essentially the same as the Hamiltonian (C.2.7), the topological numbers can be calculated in the same way as Eq. (C.2.11). Furthermore, at the edge of the superconductor or at the interface between regions with different signs of m, there exists a gapless edge state corresponding to Eq. (C.2.13) exist. The field operator for edge states can be expanded as

$$\begin{pmatrix} \psi(x,y) \\ \psi^\dagger(x,y) \end{pmatrix} = \int_{k_y>0} dk_y \left(a_{k_y} |k_y\rangle + a^\dagger_{k_y} \tau_x |k_y\rangle^* \right), \tag{C.3.8}$$

where a_{k_y} is an annihilation operator for quasiparticles and $|k_y\rangle$ is defined by Eq. (C.2.13). Each of the components can be written as

$$\psi(x,y) = \int_{k_y>0} dk_y\, \zeta \left(a_{k_y} \exp\left[ik_y y - \frac{1}{c}\sigma_y \int_0^x dx'\, m(x') \right] + a^\dagger_{k_y} \exp\left[-ik_y y + \frac{1}{c}\sigma_y \int_0^x dx'\, m(x') \right] \right) e^{i\pi/4}, \tag{C.3.9}$$

$$\psi^\dagger(x,y) = \int_{k_y>0} dk_y\, \zeta \left(a_{k_y} \exp\left[ik_y y - \frac{1}{c}\sigma_y \int_0^x dx'\, m(x') \right] + a^\dagger_{k_y} \exp\left[-ik_y y + \frac{1}{c}\sigma_y \int_0^x dx'\, m(x') \right] \right) e^{-i\pi/4}. \tag{C.3.10}$$

Therefore, edge states are regarded as the Majorana particles since the relation $\psi(x,y) = i\psi^\dagger(x,y)$ is satisfied from the above. The direction of moving of the edge state is reversed for the $p_x - ip_y$ state.

A system in which the up- and down-spin particles are each in the chiral p-wave superconducting state is also a topological superconductor, and a similar state is thought to be realized in the superconducting phase of Sr_2RUO_4 and in a 2d thin film of ^{3}He-A. The system in which an s-wave superconductor is attached to the 2d surface of a 3d $\mathbb{Z}_2$ topological insulator and a superconducting gap is induced in the surface Dirac electrons is equivalent to the Hamiltonian of Eq. (C.3.7), and Majorana states appear at the edge and in the magnetic flux.

C.3.3 The 3d class DIII ^{3}He-B

In the context of the B phase of superfluid ^{3}He, several 3d class DIII topological superconductors have been discovered. Here, we consider the Balian–Werthamer state of the B phase of superfluid ^{3}He. The BdG Hamiltonian is given by

$$H = \frac{1}{2} \sum_k \Psi^\dagger(k) H(k) \Psi(k), \quad \Psi^\dagger = (\psi^\dagger_\uparrow, \psi^\dagger_\downarrow, \psi_\uparrow, \psi_\downarrow), \tag{C.3.11}$$

where $\psi_{\uparrow,\downarrow}$ are annihilation operator for ^{3}He and the Hamiltonian matrix $H(k)$ is defined by

$$H(k) = \begin{pmatrix} \xi(k) & \Delta(k) \\ \Delta^\dagger(k) & -\xi(k) \end{pmatrix}, \quad \xi(k) = \frac{k^2}{2m} - \mu, \quad \Delta(k) = \Delta_0 i\sigma_2 \boldsymbol{k} \cdot \boldsymbol{\sigma}. \tag{C.3.12}$$

Since the Hamiltonian $H(k)$ is satisfied

$$\tau_x H^\top(-k) \tau_x = -H(k), \quad \sigma_y H^*(-k) \sigma_y = H(k), \tag{C.3.13}$$

this system belongs to class DIII.

The topological number for the BdG Hamiltonian (C.3.12) is given by

$$\nu[q] = \frac{1}{2}(\operatorname{sgn}\mu + 1). \tag{C.3.14}$$

Hence, for $\mu > 0$ a topological superfluid is realized. When terminated by a surface, topological superfluids support a topologically stable surface Andreev bound state (Majorana cone).

Bibliography

[1] V. Kostrykin and R. Schrader, "Kirchoff's rule for quantum wires," *J. Phys.* **A32** (1999) 595–630.

[2] C. Texier and G. Montambaux, "Scattering theory on graphs," *J. Phys. A* **34** no. 47, (Nov, 2001) 10307–10326.

[3] J. Boman and P. Kurasov, "Symmetries of quantum graphs and the inverse scattering problem," *Advances in Applied Mathematics* **35** no. 1, (2005) 58–70.

[4] Y. Fujimoto, K. Konno, T. Nagasawa, and R. Takahashi, "Quantum Reflection and Transmission in Ring Systems with Double Y-Junctions: Occurrence of Perfect Reflection," *J. Phys. A* **53** no. 15, (2020) 155302, `arXiv:1812.05749 [quant-ph]`.

[5] T. Kottos and U. Smilansky, "Quantum chaos on graphs," *Phys. Rev. Lett.* **79** (Dec, 1997) 4794–4797.

[6] S. Gnutzmann, J. Keating, and F. Piotet, "Eigenfunction statistics on quantum graphs," *Annals of Physics* **325** no. 12, (2010) 2595–2640.

[7] T. Nagasawa, M. Sakamoto, and K. Takenaga, "Supersymmetry and discrete transformations on S^1 with point singularities," *Phys. Lett. B* **583** (2004) 357–363, `arXiv:hep-th/0311043`.

[8] T. Nagasawa, M. Sakamoto, and K. Takenaga, "Extended supersymmetry and its reduction on a circle with point singularities," *J. Phys. A* **38** (2005) 8053–8082, `arXiv:hep-th/0505132`.

[9] S. Ohya, "Parasupersymmetry in Quantum Graphs," *Annals Phys.* **331** (2013) 299–312, `arXiv:1210.7801 [hep-th]`.

[10] S. Ohya, "Non-Abelian Monopole in the Parameter Space of Point-like Interactions," *Annals Phys.* **351** (2014) 900–913, `arXiv:1406.4857 [hep-th]`.

[11] S. Ohya, "BPS Monopole in the Space of Boundary Conditions," *J. Phys.* **A48** no. 50, (2015) 505401, `arXiv:1506.04738 [hep-th]`.

[12] S. Ohya, "Models for the BPS Berry Connection," *Mod. Phys. Lett. A* **36** no. 02, (2020) 2150007, `arXiv:2009.01553 [hep-th]`.

[13] A. Bechinger and G. Seidl, "Resonant Dirac leptogenesis on throats," *Phys. Rev.* **D81** (2010) 065015, `arXiv:0907.4341 [hep-ph]`.

[14] S. Abel and J. Barnard, "Strong coupling, discrete symmetry and flavour," *JHEP* **08** (2010) 039, arXiv:1005.1668 [hep-ph].

[15] Y. Fujimoto, T. Nagasawa, K. Nishiwaki, and M. Sakamoto, "Quark mass hierarchy and mixing via geometry of extra dimension with point interactions," *PTEP* **2013** (2013) 023B07, arXiv:1209.5150 [hep-ph].

[16] Y. Fujimoto, K. Nishiwaki, and M. Sakamoto, "*CP* phase from twisted Higgs vacuum expectation value in extra dimension," *Phys. Rev.* **D88** no. 11, (2013) 115007, arXiv:1301.7253 [hep-ph].

[17] Y. Fujimoto, K. Nishiwaki, M. Sakamoto, and R. Takahashi, "Realization of lepton masses and mixing angles from point interactions in an extra dimension," *JHEP* **10** (2014) 191, arXiv:1405.5872 [hep-ph].

[18] Y. Fujimoto, T. Miura, K. Nishiwaki, and M. Sakamoto, "Dynamical generation of fermion mass hierarchy in an extra dimension," *Phys. Rev.* **D97** no. 11, (2018) 115039, arXiv:1709.05693 [hep-th].

[19] F. Nortier, "Large star/rose extra dimension with small leaves/petals," *Int. J. Mod. Phys. A* **35** no. 30, (2020) 2050182, arXiv:2001.07102 [hep-ph].

[20] M. Kobayashi and T. Maskawa, "CP Violation in the Renormalizable Theory of Weak Interaction," *Prog. Theor. Phys.* **49** (1973) 652–657.

[21] T. Cheon, T. Fulop, and I. Tsutsui, "Symmetry, duality and anholonomy of point interactions in one-dimension," *Annals Phys.* **294** (2001) 1–23, arXiv:quant-ph/0008123.

[22] M. F. Atiyah, N. J. Hitchin, V. G. Drinfeld, and Y. I. Manin, "Construction of Instantons," *Phys. Lett. A* **65** (1978) 185–187.

[23] A. Schnyder, S. Ryu, A. Furusaki, and A. Ludwig, "Classification of topological insulators and superconductors in three spatial dimensions," *Phys. Rev. B* **78** no. 19, (2008) 195125, arXiv:0803.2786 [cond-mat.mes-hall].

[24] A. Kitaev, "Periodic table for topological insulators and superconductors," *AIP Conf. Proc.* **1134** no. 1, (2009) 22–30, arXiv:0901.2686 [cond-mat.mes-hall].

[25] S. Ryu, A. P. Schnyder, A. Furusaki, and A. W. W. Ludwig, "Topological insulators and superconductors: Tenfold way and dimensional hierarchy," *New J. Phys.* **12** (2010) 065010, arXiv:0912.2157 [cond-mat.mes-hall].

[26] G. Y. Cho, K. Shiozaki, S. Ryu, and A. W. W. Ludwig, "Relationship between Symmetry Protected Topological Phases and Boundary Conformal Field Theories via the Entanglement Spectrum," *J. Phys. A* **50** no. 30, (2017) 304002, arXiv:1606.06402 [cond-mat.str-el].

[27] B. Han, A. Tiwari, C.-T. Hsieh, and S. Ryu, "Boundary conformal field theory and symmetry protected topological phases in $2 + 1$ dimensions," *Phys. Rev. B* **96** no. 12, (2017) 125105, arXiv:1704.01193 [cond-mat.str-el].

[28] Y. Fujimoto, T. Inoue, M. Sakamoto, K. Takenaga, and I. Ueba, "5d Dirac fermion on quantum graph," *J. Phys. A* **52** no. 45, (2019) 455401, arXiv:1904.12458 [hep-th].

[29] T. Inoue, M. Sakamoto, and I. Ueba, "Instantons and Berry's connections on quantum graph," *J. Phys. A* **54** no. 35, (2021) 355301, arXiv:2104.02311 [hep-th].

[30] T. Inoue, M. Sakamoto, M. Sato, and I. Ueba, "Correspondence of topological classification between quantum graph extra dimension and topological matter," *Phys. Rev. D* **106** no. 8, (2022) 085006, arXiv:2204.03834 [hep-th].

[31] Y. Fujimoto, T. Nagasawa, S. Ohya, and M. Sakamoto, "Phase Structure of Gauge Theories on an Interval," *Prog. Theor. Phys.* **126** (2011) 841–854, arXiv:1108.1976 [hep-th].

[32] E. Witten, "Dynamical Breaking of Supersymmetry," *Nucl. Phys.* **B188** (1981) 513.

[33] M. V. Libanov and S. V. Troitsky, "Three fermionic generations on a topological defect in extra dimensions," *Nucl. Phys.* **B599** (2001) 319–333, arXiv:hep-ph/0011095 [hep-ph].

[34] J. M. Frere, M. V. Libanov, and S. V. Troitsky, "Three generations on a local vortex in extra dimensions," *Phys. Lett.* **B512** (2001) 169–173, arXiv:hep-ph/0012306 [hep-ph].

[35] R. Blumenhagen, L. Goerlich, B. Kors, and D. Lust, "Noncommutative compactifications of type I strings on tori with magnetic background flux," *JHEP* **10** (2000) 006, arXiv:hep-th/0007024 [hep-th].

[36] R. Blumenhagen, B. Kors, and D. Lust, "Type I strings with F flux and B flux," *JHEP* **02** (2001) 030, arXiv:hep-th/0012156 [hep-th].

[37] D. Cremades, L. E. Ibanez, and F. Marchesano, "Computing Yukawa couplings from magnetized extra dimensions," *JHEP* **05** (2004) 079, arXiv:hep-th/0404229 [hep-th].

[38] H. Abe, T. Kobayashi, and H. Ohki, "Magnetized orbifold models," *JHEP* **09** (2008) 043, arXiv:0806.4748 [hep-th].

[39] H. Abe, K.-S. Choi, T. Kobayashi, and H. Ohki, "Three generation magnetized orbifold models," *Nucl.Phys.* **B814** (2009) 265–292, arXiv:0812.3534 [hep-th].

[40] T. Appelquist, H.-C. Cheng, and B. A. Dobrescu, "Bounds on universal extra dimensions," *Phys. Rev. D* **64** (2001) 035002, arXiv:hep-ph/0012100.

[41] A. A. Belavin, A. M. Polyakov, A. S. Schwartz, and Y. S. Tyupkin, "Pseudoparticle Solutions of the Yang-Mills Equations," *Phys. Lett. B* **59** (1975) 85–87.

[42] A. Nakamula, S. Sasaki, and K. Takesue, "ADHM Construction of (Anti-)Self-dual Instantons in Eight Dimensions," *Nucl. Phys. B* **910** (2016) 199–224, arXiv:1604.01893 [hep-th].

[43] K. Takesue, "ADHM Construction of (Anti-)Self-dual Instantons in 4n Dimensions," *JHEP* **07** (2017) 110, arXiv:1706.03518 [hep-th].

[44] E. K. Loginov, "Octonionic instantons in eight dimensions," *Phys. Lett. B* **816** (2021) 136244, `arXiv:2003.09601 [hep-th]`.

[45] K. Wong, "Berry's connection, Kähler geometry and the Nahm construction of monopoles," *JHEP* **12** (2015) 147, `arXiv:1511.01052 [hep-th]`.

[46] K. Hashimoto and T. Kimura, "Topological Number of Edge States," *Phys. Rev. B* **93** no. 19, (2016) 195166, `arXiv:1602.05577 [cond-mat.mes-hall]`.

[47] A. Altland and M. R. Zirnbauer, "Nonstandard symmetry classes in mesoscopic normal-superconducting hybrid structures," *Phys. Rev. B* **55** (1997) 1142–1161, `arXiv:cond-mat/9602137`.

[48] L. Fidkowski and A. Kitaev, "Topological phases of fermions in one dimension," *Phys. Rev. B* **83** no. 7, (2011) 075103, `arXiv:1008.4138 [cond-mat.str-el]`.

[49] S. Ryu and S.-C. Zhang, "Interacting topological phases and modular invariance," *Phys. Rev. B* **85** (2012) 245132, `arXiv:1202.4484 [cond-mat.str-el]`.

[50] L. Fidkowski, X. Chen, and A. Vishwanath, "Non-Abelian Topological Order on the Surface of a 3D Topological Superconductor from an Exactly Solved Model," *Phys. Rev. X* **3** no. 4, (2013) 041016, `arXiv:1305.5851 [cond-mat.str-el]`.

[51] C. Wang and T. Senthil, "Interacting fermionic topological insulators/superconductors in three dimensions," *Phys. Rev. B* **89** no. 19, (2014) 195124, `arXiv:1401.1142 [cond-mat.str-el]`. [Erratum: Phys.Rev.B 91, 239902 (2015)].

[52] Y.-Z. You and C. Xu, "Symmetry Protected Topological States of Interacting Fermions and Bosons," *Phys. Rev. B* **90** no. 24, (2014) 245120, `arXiv:1409.0168 [cond-mat.str-el]`.

[53] T. Morimoto, A. Furusaki, and C. Mudry, "Breakdown of the topological classification $\mathbb{Z}$ for gapped phases of noninteracting fermions by quartic interactions," *Phys. Rev. B* **92** no. 12, (2015) 125104, `arXiv:1505.06341 [cond-mat.str-el]`.

[54] A. Kapustin, R. Thorngren, A. Turzillo, and Z. Wang, "Fermionic Symmetry Protected Topological Phases and Cobordisms," *JHEP* **12** (2015) 052, `arXiv:1406.7329 [cond-mat.str-el]`.

[55] E. Witten, "Fermion Path Integrals And Topological Phases," *Rev. Mod. Phys.* **88** no. 3, (2016) 035001, `arXiv:1508.04715 [cond-mat.mes-hall]`.

[56] S. Ryu, J. E. Moore, and A. W. W. Ludwig, "Electromagnetic and gravitational responses and anomalies in topological insulators and superconductors," *Phys. Rev. B* **85** (2012) 045104, `arXiv:1010.0936 [cond-mat.str-el]`.

[57] X.-G. Wen, "Classifying gauge anomalies through symmetry-protected trivial orders and classifying gravitational anomalies through topological orders," *Phys. Rev. D* **88** no. 4, (2013) 045013, `arXiv:1303.1803 [hep-th]`.

[58] C.-T. Hsieh, G. Y. Cho, and S. Ryu, "Global anomalies on the surface of fermionic symmetry-protected topological phases in (3+1) dimensions," *Phys. Rev. B* **93** no. 7, (2016) 075135, `arXiv:1503.01411 [cond-mat.str-el]`.

[59] E. Witten, "The "Parity" Anomaly On An Unorientable Manifold," *Phys. Rev. B* **94** no. 19, (2016) 195150, `arXiv:1605.02391 [hep-th]`.

[60] S. K. Donaldson and P. B. Kronheimer, *The geometry of four-manifolds*. Oxford mathematical monographs. Clarendon Press, 1990. `https://ci.nii.ac.jp/ncid/BA10797911`.

[61] B. Charbonneau, *Analytic aspects of periodic instantons*. PhD thesis, Massachusetts Institute of Technology, Dept. of Mathematics, 2004.

[62] E. Corrigan, P. Goddard, H. Osborn, and S. Templeton, "Zeta Function Regularization and Multi - Instanton Determinants," *Nucl. Phys. B* **159** (1979) 469–496.

[63] H. Osborn, "Calculation of Multi-Instanton Determinants," *Nucl. Phys. B* **159** (1979) 497–511.

[64] C.-K. Chiu, J. C. Y. Teo, A. P. Schnyder, and S. Ryu, "Classification of topological quantum matter with symmetries," *Rev. Mod. Phys.* **88** no. 3, (2016) 035005, `arXiv:1505.03535 [cond-mat.mes-hall]`.